Volume 49 February 1963 Number 2

Proceedings of the
National Academy of Sciences
of the United States of America

The Proceedings of the National Academy of Sciences

OFFICERS OF THE ACADEMY

FREDERICK SEITZ
President

J. A. STRATTON
Vice President

HARRISON S. BROWN
Foreign Secretary

HUGH L. DRYDEN
Home Secretary

L. V. BERKNER
Treasurer

EDITORIAL BOARD OF THE PROCEEDINGS

SAUNDERS MAC LANE
Chairman

HUGH L. DRYDEN, *Home Secretary*
L. V. BERKNER, *Treasurer*

HARRISON S. BROWN, *Foreign Secretary*
EDWIN B. WILSON, *Managing Editor*

S. CHANDRASEKHAR
THOMAS FRANCIS, JR.
DAVID R. GODDARD
G. EVELYN HUTCHINSON
ARTHUR KORNBERG
WILLARD F. LIBBY
J. R. PIERCE
S. S. STEVENS
FRANCIS J. TURNER

Subscription price is $17.50 for one year, $33.50 for two years, and $48.00 for three years. The price of a single issue beginning with volume 47 (1961), is $2.25; through volume 46 (1960), $1.50. Make all remittances payable to the National Academy of Sciences in U.S. currency or its equivalent.

Editorial correspondence should be addressed to the PROCEEDINGS OF THE NATIONAL ACADEMY OF SCIENCES, 2101 Constitution Avenue, Washington 25, D. C.

Business correspondence should be addressed to the Printing and Publishing Office, National Academy of Sciences, 2101 Constitution Ave., Washington 25, D. C.

Subscribers are requested to notify the Printing and Publishing Office of the Academy and their local postmaster immediately of change of address. Notices to the Academy should provide both the old and the new address.

Microfilms of complete volumes of this journal are available to regular subscribers only and may be obtained at the end of the volume year from University Microfilms, 313 N. First Street, Ann Arbor, Michigan.

Second-class postage paid at Easton, Pennsylvania.

PRINTED IN THE U. S. A.

THE PROCEEDINGS OF THE NATIONAL ACADEMY OF SCIENCES
is published monthly by
THE NATIONAL ACADEMY OF SCIENCES

Proceedings of the
NATIONAL ACADEMY OF SCIENCES

Volume 49 • Number 2 • February 15, 1963

*MECHANISMS UNDERLYING THE EQUILIBRIUM REACTIONS BETWEEN IONS AND ION-PAIRS IN SOLUTIONS OF ELECTROLYTES, II. THE EFFECT OF TEMPERATURE**

BY LAWRENCE C. KENAUSIS,† E. CHARLES EVERS,† AND CHARLES A. KRAUS‡

UNIVERSITY OF PENNSYLVANIA AND BROWN UNIVERSITY

Communicated December 12, 1962

The properties of electrolyte solutions are determined by the size, structure, and constitution of the ions of the electrolyte on the one hand and on the size, structure, and constitution of the solvent molecules on the other. The observed properties also depend on the independent variables: concentration, temperature, and pressure. Unless the dependence of the properties on the independent variables is known, it is not possible to determine how these properties may depend on the various constitutional factors of the electrolyte and solvent. Since most measurements are carried out at or near atmospheric pressure and the observed properties are not highly sensitive to this variable, pressure has little effect on most properties as ordinarily observed. However, the properties are quite sensitive to temperature and concentration, particularly the latter.

In the first paper of this series,[1] data were presented on the conductance, viscosity, and density of solutions of (n-amyl)$_4$NCNS in *p*-xylene at 52° from a concentration of about 1×10^{-4} *N* to the molten electrolyte. Data were also presented for solutions of (n-butyl)$_4$NCNS in benzene at 25° from a concentration of approximately 1×10^{-4} *N* up to the limit of solubility (2.05 *N*).[2] On the basis of these data and other data in the literature[2, 3] relating to solutions of the thiocyanate and other electrolytes in benzene at 25°, mechanisms underlying the equilibrium reactions between ions and ion-pairs have been proposed which account qualitatively for observations in *p*-xylene at 52° and in benzene at 25° at concentrations above as well as below the conductance minimum.

At concentrations below the conductance minimum, ion-pairs are formed by the interaction of oppositely charged ions due to Coulomb forces. These ion-pairs are dissociated by the impact of solvent molecules whose thermal energy is sufficiently great to do this. These mechanisms are in accord with the law of mass action as commonly accepted and account for the equilibrium between ions and ion-pairs in solvents of various dielectric constant.

At concentrations near and immediately above that of the conductance minimum, a new mechanism comes into play, as a result of which the ion-fraction, F_i, of electrolyte increases with increasing concentration of electrolyte, as shown by an increase in the equivalent conductance. Such an increase in the ion-fraction

may be accounted for by the micro-Wien effect resulting from the action of the ion fields on the ion-pair dipoles lying within these fields, leading to an increased dissociation of the ion dipoles.

In the preceding paper of this series,[1] the mechanism of the reactions underlying the equilibrium between ions and ion-pairs in ultra-concentrated solutions (where the molar ratio of solvent to electrolyte is less than unity) was touched upon but was not discussed in detail. In order to throw more light on these reactions as well as those occurring in more dilute solutions, we now present data on the conductance and viscosity of solutions of (n-amyl)$_4$NCNS in *p*-xylene at 90°. Temperature was controlled to ±0.015°; viscosities were measured using Cannon-Ubbelhode viscometers; densities were measured with a Westphal balance to a precision of ±0.0002 gm/cc. At 90°, the dielectric constant of *p*-xylene is 2.16 and differs little from that at 25° (2.22); the viscosity is 3.31 millipoise; the density is 0.7993 gm/cc.

The experimental results are presented in Table 1. Concentrations in gram equivalents per liter appear in Column 1; equivalent conductances, in Column 2; viscosities, in Column 3; and densities, in Column 4. Values of densities and the conductances above 10^{-2} *N* were interpolated from large-scale plots. Viscosities and

TABLE 1

TETRA-N-AMYLAMMONIUM THIOCYANATE IN *P*-XYLENE AT 52°

C	$\Lambda \times 10^1$	$\eta \times 10^1$ poise	*d*, gm/cc
2.474	6.815	5.446	0.8825
2.461	7.020	5.210	0.8823
2.443	7.294	4.904	0.8819
2.422	7.559	4.599	0.8813
2.390	8.010	4.160	0.8805
2.367	8.390	3.868	0.8799
2.331	8.867	3.486	0.8790
2.267	9.803	2.922	0.8772
2.235	10.40	2.628	0.8765
2.132	11.85	1.987	0.8738
2.074	12.70	1.716	0.8723
1.934	14.57	1.210	0.8684
1.712	16.39	0.7405	0.8620
1.461	17.06	0.4535	0.8541
1.212	15.38	0.2940	0.8457
0.8385	10.82	0.1781	0.8327
0.6464	6.599	0.1323	0.8253
$C \times 10^2$	$\Lambda \times 10^2$	$\times 10^2$ poise	*d*, gm/cc
46.84	46.62	9.23	0.8181
31.27	36.38	7.54	0.8124
14.49	21.15	5.17	0.0854
7.464	8.608	4.45	0.8024
3.969	3.769	3.91	0.8008
1.943	1.240	3.51	0.8001
$C \times 10^4$	$\Lambda \times 10^2$		
99.20	5.602		
77.97	4.620		
42.08	3.094		
17.58	2.018		
9.790	1.407		
7.281	1.417		
3.345	0.9979		
2.046	0.9052		
1.263	0.6580		
1.006	0.628		
0.815	0.509		
0.546	0.467		

TABLE 2

PROPERTIES OF MOLTEN TETRA-N-AMYLAMMONIUM THIOCYANATE

t °C	d, gm./cc	Λ	η poise	observed $\Lambda\eta$	calculated $\Lambda\eta$
52.00	0.9030	0.1229	3.234	0.3975	0.3984
60.00	0.8991	0.1876	2.103	0.3926	0.3921
70.00	0.8927	0.3021	1.279	0.3864	0.3847
80.00	0.8876	0.4624	0.8168	0.3777	0.3779
90.00	0.8825	0.6815	0.5446	0.3711	0.3716
100.00	0.8770	0.9581	0.3818	0.3658	0.3657
110.00	0.8721	1.312	0.2741	0.3596	0.3602

the conductances below 10^{-2} N were measured at the concentrations given in the table. Below a concentration of about 1×10^{-3} N, the densities and viscosities of the solutions are the same as that of the pure solvent within experimental error.

In Table 2 we have recorded the conductances, viscosities, and densities of molten (n-amyl)$_4$NCNS covering the temperature range from 52° to 110°. Temperatures appear in Column 1; densities, in Column 2; equivalent conductances, in Column 3; viscosities, in Column 4; and the products of conductance and viscosity, in Column 5. It will be noted that the equivalent conductance increases by approximately a factor of ten on going from 52°, where its value is 0.12, to 110°, where its value is 1.3. The viscosity on the other hand decreases by roughly a factor of ten in the same temperature range, going from a value of 3.2 poise at 52° to 0.27 poise at 110°. The result is that the change in the conductance-viscosity product for the fused electrolyte is relatively small, decreasing from a value of 0.40 at 52° to 0.36 at 110°. It was found that the temperature dependence of the conductance-viscosity product may be reproduced by the equation

$$\log \Lambda\eta = \frac{93.85}{T} - 0.6885$$

Recorded in Column 6 of Table 2 are values computed by this equation, which may be compared with the experimental values for the product recorded in Column 5. It may be noted further that a decrease in the conductance-viscosity product with increasing temperature appears to be a property characteristic of molten electrolytes. Thus, for sodium chloride,[4, 5] the product changes from a value of 1.96 at 818° to 1.67 at 880°; for potassium chloride,[4, 5] the value is 1.52 at 770° and 1.38 at 835°.

In Figure 1, Plot 1, is shown the conductance of (n-amyl)$_4$NCNS in p-xylene at 90°, corrected for the viscosity of the solution relative to that of the solvent. In plot 2 of Figure 1 are reproduced values of the corrected conductance at 52°. It will be noted that, at low concentrations, the ion-fraction, F_i, as determined from the corrected conductance and the limiting conductance of the electrolyte, Λ_0, as approximated by Walden's rule, $\Lambda\eta/\Lambda_0\eta_0$, is markedly higher at 90° than at 52°. This observation is a strong indication that the dissociation of ion-pairs to form ions is accomplished by the thermal impact of solvent molecules which possess the energy to do this.

While conductance measurements on (n-amyl)$_4$NCNS in p-xylene have not been carried out through the concentration of the minimum and below, measurements are available on the conductance of (iso-amyl)$_4$NI in benzene[6, 7] at 25° and 60°. For this electrolyte at concentrations below the minimum, the ion-fraction is markedly higher at the higher temperature, in accordance with the view that dissociation is

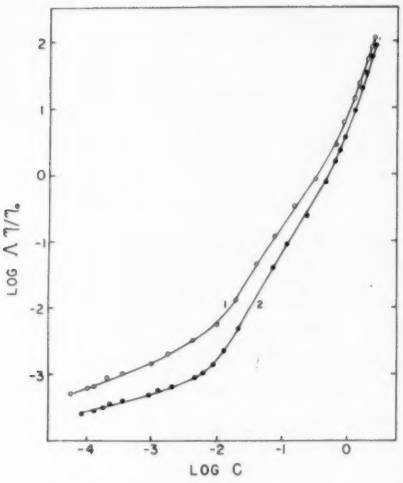

FIG. 1.—Corrected conductance of (n-amyl)$_4$NCNS in *p*-xylene at 90°, plot 1, and 52°, plot 2.

due to the impact of solvent molecules having sufficient energy. Specifically, the dissociation constant for (iso-amyl)$_4$-NI at 25° is 5×10^{-18}; at 60°, the value is 32.0×10^{-18}. Moreover, for this electrolyte in benzene the conductance above the minimum is also markedly higher at the higher temperature; again, this indicates that the dissociation of ion-pairs results from the impact of solvent molecules having the necessary energy. Obviously, since the ion-fraction increases markedly at concentrations above the minimum at both temperatures, the dissociation mechanism, while involving the impact of solvent molecules, must involve some factor other than that at concentrations below the minimum since the ion-fraction increases with increasing concentration. This observation lends support to the view that, at concentrations in the neighborhood of the conductance minimum and above, the dissociation process of ion-pairs involves the microscopic Wien effect referred to above and discussed in the earlier paper.

While the ion-fraction at concentrations below the minimum may be approximated fairly closely by dividing the equivalent conductance of the solution by the value of the limiting electrolyte conductance, Λ_0, which may be approximated fairly closely by means of Walden's rule, this method cannot be used for solutions at high concentrations, particularly for ultra-concentrated solutions. Since the molten electrolyte is completely dissociated into its ions and the ion-fraction therefore is unity, it would seem that a fairly close approximation to the correct ion-fraction for ultra-concentrated solutions may be obtained by dividing the conductance-viscosity product of the solution, $(\Lambda\eta)$, by that of the molten electrolyte, $(\Lambda\eta)_0$.

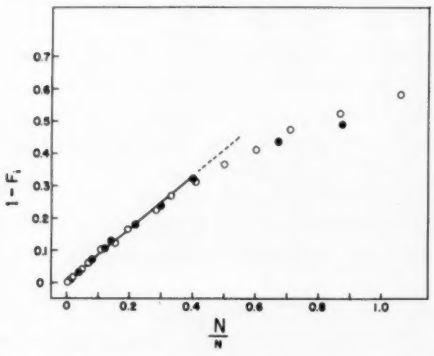

FIG. 2.—(n-amyl)$_4$NCNS in *p*-xylene at 52°, open circles, and 90°, black circles. Ion-pair fraction $(1 - F_i)$ versus molar ratio of solvent to electrolyte, N/n.

In Figure 2 are shown plots of the ion-pair fraction $(1\text{-}F_i)$, versus the molar ratio of solvent to electrolyte for the ultra-concentrated solutions of (n-amyl)$_4$NCNS in *p*-xylene at 52 and 90°. Values at 52° are shown by open circles; values at 90° are shown by black circles. It will be noted that up to a molar ratio of approximately 0.4, the ion-pair fraction, which is a measure of the

degree of association of the ions of the electrolyte in the solution, lies on the same straight line within experimental error at the two different temperatures. This coincidence of the data at the two temperatures is in accord with the view that the dissociation of ion-pairs in ultra-concentrated solutions is not due to the thermal impact of solvent molecules or ions of the electrolyte, and this indicates that the mechanism underlying the dissociation process in these solutions is quite different from those operating in the more dilute solutions.

It seems quite obvious that the formation of ion-pairs in ultra-concentrated solutions is due to the interaction of oppositely charged ions which are in the immediate neighborhood of a solvent molecule, since, up to a molar ratio of solvent to electrolyte of about 0.4, any one solvent molecule added to the solution produces as many ion-pairs as does another. As the molar ratio of solvent to electrolyte increases beyond 0.4, the ion-fraction of the electrolyte at the two temperatures begins to diverge, becoming temperature-dependent, as demanded by the reaction mechanisms proposed for the more dilute solutions.

The mechanism of the dissociation of an ion-pair in ultra-concentrated solutions to yield free ions is quite different from that in dilute solutions. If an ion-pair were introduced into a body of molten electrolyte, which is completely dissociated into its ions, it would not continue to exist as such because of the interaction of the fields of the surrounding ions on the dipolar-pair. These interactions are such that the force between the ions in the pairs is reduced to the point where the pair loses stability. However, in the presence of a nonpolar molecule, such as *p*-xylene, association of free ions to ion-pairs occurs when two oppositely charged ions come close to or in contact with the solvent molecule. Due to the presence of the solvent molecules, the symmetry of the field distribution about the ions is destroyed, leading to an increased Coulomb force acting between the ions. When an ion-pair wanders away from a solvent molecule into the body of the electrolyte solution, the symmetry of the fields is established and dissociation occurs.

The slope of the plot of the ion-fraction of electrolyte versus the molar ratio of solvent to electrolyte is characteristic of the size, structure, and constitution of the solvent molecules on the one hand and of the ions on the other. In ultra-concentrated solutions, it is possible therefore to investigate how the slope of the ion-fraction plot depends upon the constitution of the ions of the electrolyte on the one hand and of the solvent molecules on the other. According to existing data,[8, 9] it appears that, with increasing dielectric constant of the solvent, the slopes of the plot of ion-pair fraction versus the mole ratio of solvent to electrolyte decrease with increasing dielectric constant of the solvent medium. Since there is little meaning in speaking of the dielectric constant of the solvent in an ultra-concentrated solution, it is clear that the various constitutional factors of solvent and electrolyte determine the slopes. The effect of constitutional factors on the properties of ultra-concentrated solutions is now under investigation.

To summarize briefly: on the basis of the reaction mechanisms proposed in this and the preceding paper of this series, it is possible to account qualitatively for the phenomena that characterize solutions of electrolytes in benzene and *p*-xylene from high dilutions where the law of mass action is applicable to the molten electrolyte which is completely dissociated into free ions. How generally the mechanisms may

be applicable to solutions of electrolytes in solvents other than hydrocarbons remains to be investigated.

The authors gratefully acknowledge support of this work in part by the U.S. Atomic Energy Commission.

* Taken in part from a thesis presented by Lawrence C. Kenausis to the Graduate School, University of Pennsylvania, in partial fulfillment of the requirements for the degree of Doctor of Philosophy.

† John Harrison Laboratory of Chemistry, University of Pennsylvania, Philadelphia, Pennsylvania.

‡ Metcalf Research Laboratory, Brown University, Providence, Rhode Island.

[1] Kenausis, L. C., E. C. Evers, and C. A. Kraus, these PROCEEDINGS, **48**, 121 (1962).
[2] Strong, L. E., and C. A. Kraus, *J. Am. Chem. Soc.*, **72**, 166 (1950).
[3] Kraus, C. A., *J. Chem. Ed.*, **35**, 324 (1958).
[4] Goodwin, H., and R. Mailey, *Phys. Rev.*, **26**, 28 (1908).
[5] Harrap, B. S., and E. Haymann, *Trans. Faraday Soc.*, **51**, 259 (1955).
[6] Fuoss, R. M., and C. A. Kraus, *J. Am. Chem. Soc.*, **55**, 3614 (1932).
[7] Luder, W. F., P. B. Kraus, and C. A. Kraus, *J. Am. Chem. Soc.*, **58**, 255 (1936).
[8] Seward, R. P., *J. Am. Chem. Soc.*, **77**, 905 (1953).
[9] Seward, R. P., *J. Phys. Chem.*, **62**, 758 (1958).

---

*USE OF AN ULTRAMICROTOME FOR THE PREPARATION OF THIN SECTIONS OF SINGLE CRYSTALS FOR ABSORPTION SPECTROSCOPY**

BY ROBERT F. STEWART† AND NORMAN DAVIDSON

GATES AND CRELLIN LABORATORIES OF CHEMISTRY,‡ AND NORMAN W. CHURCH LABORATORY OF CHEMICAL BIOLOGY, CALIFORNIA INSTITUTE OF TECHNOLOGY

Communicated December 13, 1962

The polarized absorption spectra of single crystals are informative both as to the nature of the electronic transitions for an individual molecule and as to the effects on the spectra of the interactions between molecules with known relative orientation. Our particular interest has been the absorption spectra of single crystals of purines and pyrimidines, which are pertinent for an understanding of the absorption spectra of the nucleic acids and of the phenomenon of hypochromism.[1]

A major problem in such studies for electronic (or vibrational) transitions which are reasonably intense is the preparation of crystals in the shape of plates that are sufficiently thin so that the absorbance ($\log_{10} I_0/I$) is measurable. Thus, for a typical purine or pyrimidine crystal with a density corresponding to a molar concentration of about 10 mole liter^{-1} and a maximum decadic molar absorptivity of about 10^4 liter mole^{-1} cm^{-1}, the thickness should be about 10^{-5} cm.

In the past this technical problem has usually been solved by hunting and picking from a population of crystals obtained by crystallization or by sublimation, by crystallizing between two closely spaced plates, or occasionally by preparing a solid solution in a transparent host crystal. These techniques lack generality. It is not always possible to grow or find crystals that have the desired face development, that have a sufficiently large cross-sectional area, and that are sufficiently thin. It

is frequently not possible to find a transparent host crystal for the mixed crystal method.

We wish to describe a method for preparing thin sections of single crystals which we believe will work for a large number of organic crystals. Using a microtome and a diamond knife intended for thin sectioning of specimens for electron microscopy, suitable crystals with cross-sectional dimensions up to several hundred micra can be polished (or shaved) down to a thickness of 10^{-5} cm. The opposite faces of the crystal are maintained parallel by observing interference colors between crossed polarizers. This method works best for polishing soft organic crystals parallel to a cleavage plane, but in the one case tried it was possible to prepare a section 10^{-4} cm thick with faces perpendicular to the cleavage plane of a layer structure.

The microspectrophotometer used was such that a crystal with cross-sectional dimensions of about $100\ \mu \times 100\ \mu$ was needed. Our first idea was to mount a crystal in a methacrylate plastic and to slice a thin section by the same general technique used routinely in electron microscopy. This technique was tested with uracil, which has a structure in which the molecular planes are parallel to the cleavage plane (001) of the monoclinic crystal.[2] A stubby crystal about $200\ \mu \times 200\ \mu \times 50\ \mu$ (with the short axis parallel to the c-axis) was coated with polyvinyl alcohol (to promote adhesion to the methacrylate), imbedded in a methyl methacrylate-butyl methacrylate plastic, and then sectioned parallel to (001) at $0.25\ \mu$ increments with a diamond knife. The sections which were recovered had shattered into microcrystalline regions as revealed by ultraviolet absorption measurements and conoscopic observations. Presumably the crystal shatters because of the deformation suffered while being peeled off by the knife.

The same disappointing result was obtained upon attempting to section a 1-methylthymine crystal in the (102) plane (the plane of the molecules and the cleavage plane).[3] However, it was observed that the crystal face remaining on the methacrylate block after sectioning appeared to be optically polished.

It was then reasoned that, if the back face of the crystal were polished beforehand, it should be possible, by taking advantage of the small increments of advance of the microtome, to polish the front face down to the desired thickness.

The general features of the technique may be described as follows.[4] A methacrylate block was mounted in the microtome and cut with the knife, thus developing a plane parallel to the cutting plane of the knife. A natural face (A) of a crystal was then glued to the face of the plastic (using a few microliters of ethylene dichloride) maintaining parallelism to within $\pm 1°$. The opposite face (A′) of the crystal was polished with the microtome knife, down to a crystal thickness of 50–70 μ. The crystal was then cut away from the plastic with a razor blade. A thin ($\sim 5\ \mu$) polished layer of methacrylate coats one face of a fused quartz block. (This thin layer of plastic needs to be and is adequately transparent to ultraviolet light, provided redistilled monomer is used and no U-V absorbing catalyst is used for polymerization.) Face A′ was glued to the quartz block via this intermediate layer of plastic. The quartz block and crystal were mounted on the microtome in a device which included: (*a*) an adjustable chuck for changing the crystal orientation by a few degrees with a control of $\pm 1'$ of arc; (*b*) a 45° mirror on a steel block for sending polarized light through the crystal (Fig. 1). The crystal was then polished down to the desired thickness. The advance increment of the microtome should not

exceed $^1/_4\ \mu$ during this operation to avoid fracturing the crystal. Interference observations were used as an approximate measure of the thickness and to avoid wedge effects. The quartz block and crystal were removed and mounted in the spectrophotometer (which was also suitable for an accurate thickness measurement by a

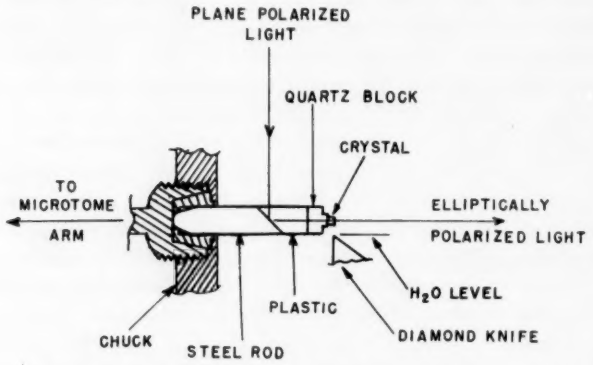

FIG. 1.—Schematic diagram of setup for final polishing of crystal, including the optical system for observation of thickness.

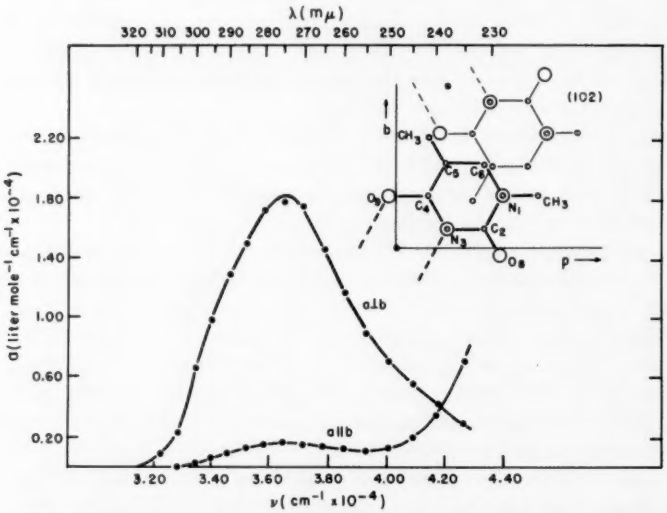

FIG. 2.—Polarized absorption spectra of 1-methylthymine in the (102) plane. Data for a $\perp$ b were obtained from a 0.1 μ section, a $\parallel$ b from a 0.5μ section. The inset figure shows two of the four molecules of the unit cell.[3] The other two, not shown, are hydrogen bonded to the ones which are shown, as indicated by the dotted lines, and are related to their hydrogen bonded partners by an inversion through the indicated centers of symmetry. The molecule drawn in light type is on a plane 3.38 Å below the molecule drawn in heavy type.

retardation method). Thus the thin fragile crystal section is supported by the quartz block during the optical measurements.

Figure 2 illustrates the results obtained from two 1-methylthymine crystals which were polished to thicknesses of 0.1 μ and 0.5 μ.

The problem of analyzing the effects of a wedge-shaped section on absorption for a microspectrophotometer with a circular specimen aperture is treated as follows. Assume that the crystal is oriented so that the plane of polarization is coincident with a principal direction. The angle of the wedge is α so that the thickness of the crystal at the point (r, θ) is $t = t_0 + \alpha r \cos\theta$ where t_0 is the crystal thickness at the center of the aperture. The transmission is

$$\frac{I}{I_0} = \frac{\int_0^a \int_0^{2\pi} e^{-K(t_0 + \alpha r \cos\Theta)} \, r d\theta dr}{\pi a^2}$$

where a is the radius of the aperture and K is an absorption cross section for the crystal in cm^{-1} along a principal direction.

Then

$$\frac{I}{I_0} = e^{-Kt_0}\left[\frac{2I_1(K\alpha a)}{K\alpha a}\right]$$

where I_1 is a hyperbolic Bessel function of the first kind. For $K\alpha a$ less than unity, the absorbance error is less than 0.05 absorbance units, which is about the limit of error for the microspectrophotometer. K is usually no more than $5 \times 10^{+5}$ cm^{-1} and a typical aperture radius is 2.5×10^{-3} cm. Thus the opposite faces should be parallel to within 0.001 radians or 4′ of arc.

Using an ultramicrotome for polishing crystals to thin sections has several advantages over the more conventional grinding techniques. The small advance increments of an ultramicrotome allow one to take off small sections and save the crystal from fractures or cleavages. This is then comparable to polishing crystals with very fine, hard powders. A trough, to which the diamond knife is mounted, is filled with water (or some other convenient solvent) up to the cutting edge of the knife. As the crystal is sectioned, the grains dissolve in the water and leave a clean, polished face on the crystal. The reproducible advance of the microtome makes it possible to take the crystal down to a thin section in a controlled manner. For the rather old Porter-Blum microtome which we used, the limiting thickness was about 10^{-5} cm. It is very likely that with the newer microtomes, a mechanical limit for a thin crystal section will be about 10^{-6} cm.

A disadvantage of the technique is the inefficient use of the diamond knife. For conventional microscopy, each section is useful; in our system, thousands of sections need to be made before the crystal is down to a useful thickness. We found that our knife[5] lasted for the polishing of two to three crystals.

The optical system used took advantage of the rather large birefringence of the purine and pyrimidine derivatives. The larger the birefringence, the more accurately can one cut a crystal to a desired thickness. If the birefringence is less than 0.02, this method is of marginal use for sectioning a crystal to a thickness less than 0.7 μ. However, ultraviolet absorbing crystals which have interesting dichroism usually have a birefringence larger than 0.02. A low birefringence poses another problem. Optical wedges can then only be observed for relatively large angles. For a typical cross section of 150 μ, the smallest wedge angle which can be observed for a birefringence of 0.02 is 0.007 radians. For crystals with low birefringence, one would probably have to set up a more elaborate optical system for observing

reflected interference fringes in order to know the crystal thickness and to avoid wedge effects while polishing.

All of the crystals which were studied in our polarized absorption experiments were layer structures. The cleavage planes were well defined and cutting along the cleavage plane posed no problem. One crystal, the hydrogen bonded complex of 9-methyladenine to 1-methylthymine,[3,6] had {001} and {100} as predominant forms. Both of these faces are perpendicular to the cleavage (and molecular) plane (010) and hence the crystal had a favorable morphology for sectioning in a direction perpendicular to the molecular layers. The crystal could be cut along the (100) to a section as thin as 1 μ without cleaving. This thickness was sufficient to determine the absorption in a direction perpendicular to the molecular layers.

Another sample of the hydrogen bonded complex of 9-methyl adenine and 1-methyl thymine was inadvertently polished at an angle of 5–10° with respect to the form {100}. In this case too, an optically polished plane was formed. Thus, it may not be necessary to cut parallel to any crystal plane.

As remarked above, the crystal sectioning technique described above took full advantage of the high birefringence which most purine and pyrimidine derivatives have. For the general problem of sectioning soft crystals the optical system would have to be improved. Reflected light from the crystal face can provide for long, optical lever arms which are needed for accurate orientation. A suitable goniometer device would eliminate the present necessity of having to polish a natural crystal face. We believe that with a sharp diamond knife and a microtome which has a small advance increment, one can cut soft crystals to thicknesses of the order of 0.1 μ.

Summary.—Sections of single crystals of organic substances with thicknesses down to 0.1 μ can be prepared by using a diamond knife and an ultramicrotome as a polishing tool. It is believed that this technique will be generally useful for preparing specimens for single crystal absorption spectroscopy.

We are indebted to Mr. William Schuelke for the design of the adjustable chuck. We are grateful to Dr. Karst Hoogsteen for advice and help as well as for permission to quote his crystal structure results.

* Research supported by grant AM-03907 from the U.S. Public Health Service, and by grant G-5908 from the National Science Foundation.

† National Institutes of Health Predoctoral Fellow.

‡ Contribution No. 2917.

[1] Rhodes, W., *J. Am. Chem. Soc.*, **83**, 3609 (1961); Tinoco, I., *ibid.*, **82**, 4785 (1960); *J. Chem. Phys.*, **34**, 1067 (1961).

[2] Parry, G. S., *Acta Cryst.*, **7**, 313 (1954); for preparing uracil crystals with a stubby habit, see Gilpin, V., and W. McCrone, *Anal. Chem.*, **22**, 368 (1950).

[3] Hoogsteen, K., *Acta Cryst.*, in press.

[4] Stewart, R., "Polarized absorption spectra of purines and pyrimidines," Ph.D. Thesis, California Institute of Technology, (1963). Practical details of our technique are described in this thesis.

[5] The diamond knife was a Type C I.V.I.C. knife purchased from the Instituto Venezolano De Investigaciones Cientificas. The angle of the knife was 55° with a cutting edge 1.2 mm long.

[6] Hoogsteen, K., *Acta Cryst.*, **12**, 822 (1959).

*CHANGES IN MOLECULAR WEIGHT OF DNA ACCOMPANYING MUTATIONS IN PHAGE**

By Elizabeth Burgi

GENETICS RESEARCH UNIT, CARNEGIE INSTITUTION OF WASHINGTON, COLD SPRING HARBOR, NEW YORK

Communicated by A. D. Hershey, December 13, 1962

Kellenberger *et al.*[1, 2] selected mutants of phage lambda characterized by altered buoyant densities in cesium chloride solutions. They obtained direct evidence that one of the mutants contains less DNA per particle than the wild-type phage.[3] In this paper we show that two of the mutants have lost different, non-overlapping segments of the parental DNA molecule.

Materials and Methods.—Four phage lines, obtained from J. Weigle, were studied. All were clear-plaque mutants of the following pertinent genotypes and densities: the parental type b^+ (1.508 gm/cm^3), the mutants *b2* (1.491) and *b5* (1.501), and the double-mutant recombinant *b2b5* (1.483). The density differences were confirmed with our stocks. The phages were grown in a synthetic medium[4] modified to contain 10 times the stated amount of $FeCl_3$ and 0.1 of the stated amounts of KCl and NaCl. An unbuffered medium of the same composition but lacking the tris (hydroxymethyl)aminomethane buffer is also referred to below. Its use caused the pH of the cultures to fall during growth and improved phage yields. *Escherichia coli*, strain W3110 (from J. Weigle), adapted to the buffered medium, was grown to 5×10^8 per ml, sedimented, washed and resuspended at 5×10^9 per ml in 0.01 *M* $MgSO_4$, and infected with 5 phage particles per cell. After 10 min the suspension was diluted 5-fold with 0.01 *M* $MgSO_4$ and recentrifuged. The pellet was resuspended (at time zero) in fresh buffered medium at 5×10^8 per ml, and the suspension was diluted 10 min later with an equal volume of unbuffered medium. Lysis ensued after aeration for two or three hr at 36°C. For preparation of labeled stocks, radiophosphate (1 mc/mg P) was added at time zero, or tritiated uridine (0.015 μM/ml, 3 mc/μM) 10 min later.

The lysate, containing nearly 10^{11} phage particles per ml, was brought to pH 7.2 and treated consecutively with deoxyribonuclease, ribonuclease, and pancreatin. Bacterial debris was removed by centrifugation with the aid of 0.5 mg of analytical grade Celite per ml of lysate, and the supernatant was passed through a 0.45 μ membrane filter supporting a thin layer of additional Celite. The phage particles in the filtrate were then sedimented, washed, and resuspended in dilute, buffered saline containing 0.1 mg/ml of gelatin.

DNA was extracted from the phage particles with phenol and sodium dodecylsulfate.[5] Differently labeled DNA's from phages of two genotypes were extracted from a mixture of the phages, not mixed after extraction. To prevent breakage of DNA when low concentrations (2 μg/ml) were extracted, the tubes were inclined at a low angle and rotated about their long axes at 60 rpm for 15 min, rather than shaken.[6] Extraction at low concentrations proved advantageous to avoid the aggregation to which lambda DNA is prone.[7] Phenol was removed by dialysis against 0.1 *M* NaCl.

DNA labeled with either P^{32} or H^3 showed about 2.5×10^5 disintegrations/μg-min.

Sedimentation of labeled DNA was observed in a density gradient of sucrose.[8] About 0.2 μg of DNA in 0.1 ml of 0.1 *M* saline was layered on 5 ml of the sucrose solution (in 0.1 *M* NaCl, 0.05 *M* PO_4, pH 6.7) and the tubes were spun cold at 28,100 rpm for 6 hr. Two-drop fractions were collected through a hole punctured in the bottom of each tube, and radioactivity was measured in a scintillation spectrometer as described elsewhere.[9]

Results and Discussion.—Phage particles, including those of lambda, are believed to contain single DNA molecules.[10] If the generalization is valid, changes in the

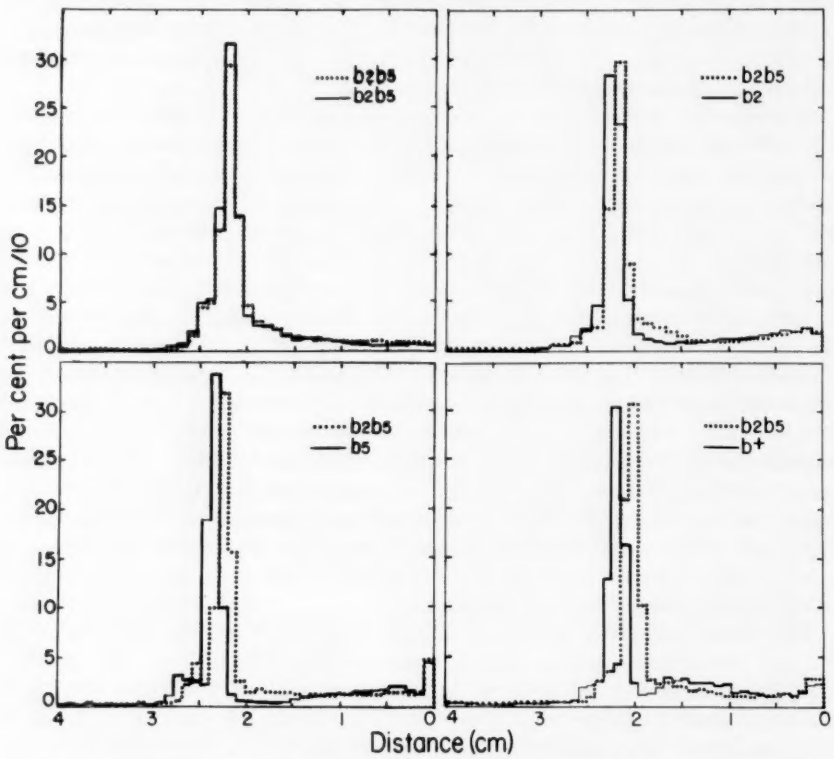

FIG. 1.—Zone sedimentation of differently labeled DNA's from pairs of mutant phages. Solid line, P^{32}; dotted line, H^3. Distance is measured from the meniscus.

DNA content of phage particles should be directly reflected in the molecular weights and sedimentation rates of their extracted DNA's. This expectation is confirmed by the results presented in Figure 1, which show that differently labeled DNA's from phage particles of different genotypes sediment at different rates in the same tube. The individual DNA's sediment as single, narrow bands, an evidence of the molecular homogeneity of each. Their sedimentation velocities increase in the same order as the densities of the phage particles: *b2b5*, *b2*, *b5*, b^+.

If the differences in sedimentation rate reflect differences in molecular length, a faster-sedimenting DNA should be more readily broken under shear than a slower

one.[11] Figure 2 presents the results of an experiment in which a mixture of differently labeled DNA's from phages b^+ and *b2b5* was partly broken by repeated aspiration through the orifice of a pipette. In the figure each DNA shows two sedimenting bands, one corresponding to the original material, the other moving more slowly as a result of breakage. The b^+ DNA has been broken to a greater extent than the *b2b5*. In other experiments we found by analysis of stirred solutions in the optical centrifuge that the unlabeled DNA's show the same difference in fragility. We conclude that at least two and probably all four of the DNA species studied here differ in both mass and length, as indicated by the differences in sedimentation rate.

We now ask whether or not the differences in molecular weight of the DNA's are quantitatively consistent with the differences in density of the phage particles. The relative distances through which two substances sediment in a density gradient of sucrose must be proportional to their relative sedimentation coefficients except as influenced by the increasing density and viscosity of the solution, and by the increasing centrifugal force, encountered by the particles as they move through the solution. Since the field and solvent effects tend to cancel each other, the deviation from proportionality must be slight when the difference in sedimentation rates is small. Accordingly, for structurally homologous DNA's,

$$\frac{D_2}{D_1} = \left(\frac{M_2}{M_1}\right)^k \qquad (1)$$

where D and M are the distances sedimented and the molecular weights of the sedimenting species 1 and 2,[12] and k will be nearly constant for ratios D_2/D_1 in the neighborhood of unity. The exponent k is 0.35 according to the data of Figure 2, which show that unbroken DNA sediments 1.27 times faster than broken DNA consisting of half-length fragments.[11]

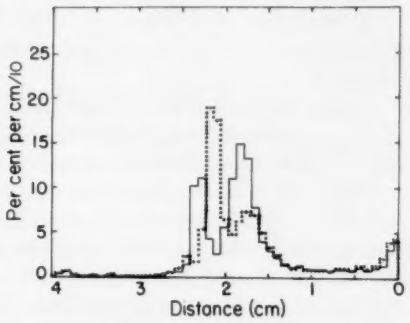

FIG. 2.—Zone sedimentation after partial breakage under shear of mixed DNA's of different sedimentation rate. Solid line, P^{32}-labeled b^+ DNA; dotted line, H^3-labeled *b2b5* DNA.

It will be noted that the estimate of k for equation (1) is lower than the values 0.51 and 0.55 given by Burgi and Hershey.[11] The difference reflects the fact, noticed by those authors, that k depends on the conditions of measurement of sedimentation coefficients for high molecular weight DNA's, a point now being investigated in this laboratory.

Relative molecular weights of DNA computed from the sedimentation rates using equation (1) with $k = 0.35$ are presented in Table 1. The results may be expressed as follows relative to the molecular weight of b^+ DNA taken as unity: *b5*, 0.925; *b2*, 0.849; *b2b5*, 0.793 to 0.810, where the latter range reflects errors of four independent measurements.

Weigle *et al.*[13] suggested a measurement of the DNA content of phage particles based on their buoyant densities in CsCl solutions. In this measurement the particles are assumed to be equivalent to simple mixtures of protein of density 1.30 and DNA of density 1.71. The method yields relative DNA contents per phage particle

TABLE 1

RELATIVE MOLECULAR WEIGHT OF DNA AND DNA CONTENT OF PHAGES OF DIFFERENT GENOTYPES

Phage pair	Relative molecular weight (equation 1) Expt. 1	Expt. 2	Relative DNA content (Weigle *et al.*[19])
b2/b2b5	1.07	...	1.08
b⁺/b5	...	1.08	1.07
b5/b2	...	1.09	1.10
b5/b2b5	1.16	1.14	1.19
b⁺/b2b5	1.24	...	1.28

Experiment 1 is shown in Figure 1; experiment 2 was similar except that H^3-labeled *b5* DNA was used.

as follows: for b^+ phage, 1.000; for *b5*, 0.934; for *b2*, 0.847; for *b2b5*, 0.783. The ratios of DNA contents for the phage pairs we studied are compared with the molecular weight ratios of DNA in Table 1. The comparison shows that the molecular weight changes of the DNA's nearly account for the different densities of the phage particles. The small discrepancy can be made to disappear by assigning a density of about 1.28 to DNA-less phage particles, or by assuming that the appropriate value of k in equation (1) is 0.32.

Kellenberger *et al.*[3] found by direct measurement of DNA content per plaque-forming particle that the *b2* mutant contained 18 per cent less DNA than the b^+ phage.

The consistency of these diverse measurements suggests that our molecular weight estimates are not far off, and that the DNA contents of phage mutants of the kind studied here can in fact be measured in terms of the phage particle densities.

Finally, it must be noted that the decreases in molecular weight of DNA attending the *b2* and *b5* mutations are within experimental error additive in the double mutant *b2b5*. We conclude, therefore, that each of the mutations was accompanied by the loss of a different segment of the DNA molecule, segments that do not overlap and that comprise together some 20 per cent of the original length of the molecule.

The mutations themselves occurred in widely separated regions of the phage chromosome.[2] This fact is consistent with the conclusion last stated if the losses of DNA have occurred at the sites of the mutations, an inference for which there is some evidence.[2] At any rate, the losses of segments of DNA molecules recognized here provide a plausible origin for the physiological effects of the mutations, and a model for a class of primary genetic deletions.

Summary.—DNA's from lambda phages of different genotypes sediment at increasing rates in the order *b2b5*, *b2*, *b5*, b^+, which is the same as the order of increasing densities of the phage particles. DNA from b^+ phage is more fragile than that from *b2b5*. The two mutations studied are therefore accompanied by characteristic reductions in the lengths of DNA molecules, reductions that are additive in the recombinant phage carrying both mutations.

The author wishes to thank A. D. Hershey for help and guidance in this work, George Streisinger for collaboration in early experiments along these lines, Jean Weigle for the phage and bacterial strains, and Laura Ingraham for her assistance.

* Aided by Grant C-2158 from the National Cancer Institute, U.S. Public Health Service.

[1] Kellenberger, G., M. L. Zichichi, and J. Weigle, *Nature*, **187**, 161 (1960).

[2] Kellenberger, G., M. L. Zichichi, and J. Weigle, these PROCEEDINGS, **47**, 869 (1961).

[3] Kellenberger, G., M. L. Zichichi, and J. Weigle, *J. Mol. Biol.*, **3**, 399 (1961).

[4] Hershey, A. D., *Virology*, **1**, 108 (1955).
[5] Mandell, J. D., and A. D. Hershey, *Analyt. Biochem.*, **1**, 66 (1960).
[6] Frankel, Fred, in preparation.
[7] Hershey, A. D., E. Burgi, and L. Ingraham, in preparation.
[8] Britten, R. J., and R. B. Roberts, *Science*, **131**, 32 (1960).
[9] Hershey, A. D., E. Goldberg, E. Burgi, and L. Ingraham, in preparation.
[10] Sinsheimer, R. L., *J. Molec. Biol.*, **1**, 43 (1959); Rubenstein, I., C. A. Thomas, Jr., and A. D. Hershey, these PROCEEDINGS, **47**, 1113 (1961); Davison, P. F., D. Freifelder, R. Hede, and C. Levinthal, these PROCEEDINGS, **47**, 1123 (1961); Hershey, A. D., E. Burgi, and L. Ingraham, *Biophys. J.*, **2**, 423 (1962); Kaiser, A. D., and D. S. Hogness, *J. Mol. Biol.*, **2**, 392 (1960).
[11] Burgi, E., and A. D. Hershey, *J. Mol. Biol.*, **3**, 458 (1961).
[12] Doty, P., B. B. McGill, and S. A. Rice, these PROCEEDINGS, **44**, 432 (1958).
[13] Weigle, J., M. Meselson, and K. Paigen, *J. Mol. Biol.*, **1**, 379 (1959).

APPARENT CYTOPLASMIC STERILITY IN DROSOPHILA PAULISTORUM

BY LEE EHRMAN*

THE ROCKEFELLER INSTITUTE

Communicated by Theodosius Dobzhansky, January 2, 1963

A hybrid inherits its chromosomes from both parents, but its cytoplasm mainly or exclusively from the mother. This may be expected to result in differences in the outcomes of the reciprocal crosses between a given pair of species or races. Differences between reciprocal crosses are indeed not uncommon,[1] but, at least in animals, most of them cannot be ascribed to influences emanating from the cytoplasm autonomously from the nuclear genes. In the first place, in organisms with separate sexes, the heterogametic sex is chromosomally not identical in the progenies of reciprocal crosses. Furthermore, certain characteristics of a progeny may be due to "maternal effects," i.e., to predetermination of the qualities of the egg cell by the chromosomal complement present in that cell before meiosis.[2] Laven[3] has, however, reported a thoroughly authentic case of hybrid sterility due to cytoplasmic differences in mosquitoes of the *Culex pipiens* species complex. A possible, but not certain, case of cytoplasmic sterility has been described in *Drosophila virilis* × *D. littoralis* hybrids by Patterson.[4] The purpose of the present communication is to report an apparently valid case of cytoplasmic hybrid sterility in *Drosophila paulistorum*.

D. paulistorum is a complex of at least six races or incipient species.[5, 6] Five of the races are difficult to intercross because of sexual isolation; when hybrid progenies are obtained they consist of fertile daughters and sterile sons. The sixth, Transitional race, produces fertile hybrids when crossed to at least one strain of every other race. Hybrids between different strains of the Transitional race are as a rule also fertile, but the case described below is an exception. The strains involved are Santa Marta (referred to below as "S") and Mesitas (referred to as "M"), both from Colombia, South America. The S strain is derived from flies collected in the Sierra Nevada de Santa Marta by Professors H. L. Carson and M. Wasserman; the M strain was collected at Mesitas, west of Bogotá, by Professor Alice Hunter of the Universidad de los Andes, Bogotá, Colombia. The S strain pro-

duces fertile hybrids with strains of Centro-American, Transitional, and Orinocan races.[5] The M strain yields fertile hybrids with the Bucaramanga, Buenaventura, and Palmira strains of the Transitional race, and the Angra and Tarapoto strains of the Andean-South Brazilian race (data of B. Spassky and the author).

All female hybrids between the M and S strains are fertile, but some of the male hybrids are fertile, while others are sterile. The genetic constitution of various male hybrids studied is represented symbolically in Figures 1–16. The cytoplasm derived from M mothers or grandmothers is represented by a continuous black circle, and that from S mothers by a dashed circular line; the Y chromosome of M is

FIGS. 1–16.—Genetic constitution of males of the Mesitas and Santa Marta strains and their hybrids. Black circle—M cytoplasm, dashed circle—S cytoplasm; Y chromosome of M strain shown in black, Y chromosome of S strain shown in white; M and S—genes of the M and S strains respectively.

shown as a black, and that of S as a white A-shaped figure. The letters M and S within the circles stand for the chromosomal genes of M and S (other than those in the Y chromosome).

The pure M males (Fig. 1) and pure S males (Fig. 2) are, of course, fertile. The cross M ♀ × S ♂ produces fertile sons (Fig. 3), while the cross S ♀ × M ♂ gives sterile sons (Fig. 10). The fertility or sterility of the males has in every case been diagnosed by repeated subculturing and by dissecting the mature males in physiological saline and checking for the presence of motile spermatozoa.

The M ♀ × S ♂ hybrid females, whose fertile brothers are represented in Figure 3, were backcrossed twice to pure M males; the male progenies of these backcrosses

were also fertile (Figs. 5, 6). Similar M♀ × S♂ hybrid females were backcrossed four times to pure S males; these backcrosses yielded exclusively sterile sons (Figs. 12, 13, 15, 16). Conversely, the S♀ × M♂ hybrid females, whose sterile brothers are shown in Figure 10, were backcrossed three times to pure S males, and gave quite fertile male progenies (Figs. 7–9). However, when S♀ × M♂ hybrid females were backcrossed to pure M males, they gave sterile sons (Fig. 11). An attempt to make a second backcross to M was made repeatedly, but without success, apparently because the MMS females with S-derived cytoplasm (sisters of the males in Fig. 11), refused to accept M males. It proved, therefore, impossible to test the fertility of males whose genotype is shown in Figure 14, which should have had a Y chromosome of the M strain, and mostly M genes in an S cytoplasm.

The above data are consistent with the hypothesis that the backcross males whose Y chromosome agrees in its strain origin with their cytoplasm are fertile, while an M cytoplasm with a Y chromosome of the S strain, or an S cytoplasm with a Y of the M strain, make the males sterile. The source of the chromosomes other than the Y seems to have little or no effects. There are, however, two facts which are not consistent with the hypothesis. First, the F_1 hybrid males from the cross M♀ × S♂ are fertile (Fig. 3), although they carry M cytoplasm and a Y chromosome of the S strain. Secondly, when these F_1 males were backcrossed to pure M females, they produced fertile sons which carried an S Y chromosome in M cytoplasm and a majority of M genes (Fig. 4). By analogy with the males of the constitutions shown in Figures 12, 13, 15, and 16, these males were expected to be sterile; however, males in Figure 4 differ from those in Figure 12 by having a majority of M, rather than of S genes. Therefore, some involvement of chromosomal genes other than those on the Y chromosome cannot be excluded.

However that may be, the sterility of the males in the hybrid progenies of the M and S strains of the Transitional race has a different genetic base from the sterility of the male hybrids between the races. As shown by Ehrman,[7] this hybrid male sterility is genic in origin, with a maternal effect, and with genes fostering this sterility distributed over all the chromosomes of the species karyotype. Thus, the sterility reported in the present article is unique in *D. paulistorum*.

Summary.—When crossed, the Mesitas and Santa Marta strains, both belonging to the Transitional race of *Drosophila paulistorum*, produce fertile female and some sterile male hybrids. A genetic analysis suggests that the sterility in this case is caused, chiefly if not exclusively, by interaction of the Y chromosome of one strain, with the cytoplasm of the other strain. If the Y and the cytoplasm come from the same strain, the male is fertile, while if their sources are different, the male is usually sterile.

* Supported, in part, by the Shirley Farr postdoctoral fellowship of the American Association of University Women.

[1] Ehrman, L., *Quarterly Review of Biology*, **37** (in press, 1962). See Table 2.

[2] Dobzhansky, Th., *genetics and the Origin of Species* (New York: Columbia University Press, 1951), p. 228.

[3] Laven, H., *Cold Spring Harbor Symposia on Quantitative Biology*, **24**, 166–173 (1959).

[4] Patterson, J. T., University of Texas Publication, No. 5204 (1952), pp. 7–19.

[5] Dobzhansky, Th., and B. Spassky, these PROCEEDINGS, **45**, 419–428 (1959).

[6] Dobzhansky, Th., and O. Pavlovsky, *Chromosoma*, **13**, 196–218 (1962).

[7] Ehrman, L., *Evolution*, **14**, 212–223 (1960).

*A DISCUSSION AND PROPOSALS CONCERNING FOSSIL DINOFLAGELLATES, HYSTRICHOSPHERES, AND ACRITARCHS, I**

By William R. Evitt

DEPARTMENT OF GEOLOGY, STANFORD UNIVERSITY

Communicated by Ernst Cloos, November 27, 1962

In 1961[1] I suggested that many post-Paleozoic organic microfossils that had been called hystrichospheres are really dinoflagellate cysts. Further extensive studies fully support that view. Although new findings and some revisions in details of the interpretations offered in 1961 await future publication, I feel it is appropriate now to propose several nomenclatural changes and taxonomic revisions affecting these fossils. That is the purpose of this paper, which includes (following certain background information): (1) an emendation of the dinoflagellate family Hystrichosphaeraceae, (2) proposal of three new dinoflagellate taxa: Hystrichosphaeridiaceae n. fam., Areoligeraceae n. fam., and *Achomosphaera* n. gen., (3) a recommendation that the term Hystrichosphaerida no longer be used and that its informal variations, such as hystrichosphere, be used cautiously, and (4) a proposal for a new informal group of microfossils of organic composition and unknown affinity to be known as acritarchs.

Note on Use of Botanical Code.—Downie *et al.*[2] recently proposed that fossil dinoflagellates and hystrichospheres (including acritarchs in the sense of this paper) be treated nomenclaturally under the Botanical Code. I have adopted this proposal (but without certain of their accessory suggestions regarding the erection of natural genera and form-genera) chiefly on the grounds (1) that, as algae, the dinoflagellates are nomenclaturally botanical entities, and (2) that the acritarchs, whose affinities are unknown (though they, too, probably include many fossil algae), should be treated under the same code as the dinoflagellates for purely practical reasons. However, this paper is not the place to discuss some of the knotty problems raised by transferring genera and families from the realm of the Zoological Code to that of the Botanical Code; for example, problems that devolve from the distinction between natural genera, organ-genera, and form-genera under the Botanical Code and the effect of this distinction on family names proposed originally under the Zoological Code. These and other problems are currently under extensive discussion in correspondence among interested co-workers. Slowly, workable solutions to them will emerge. For the present, I have simply used botanical family names in the same manner as zoological family names have been used in the past. Thus, Hystrichosphaeridae becomes Hystrichosphaeraceae, etc. This may not be the ideal procedure, but it seems at least a temporarily acceptable one that is consistent with stability in nomenclature, which is the spirit and purpose of nomenclatural codes.

Theca, Cyst and Test.—Currently incomplete research suggests that the fossilized remains of dinoflagellates possibly nowhere include the theca, if that term is used to designate only the external cellulose or cellulose-like covering of a motile dinoflagellate cell. Instead, the fossils seem to represent a layer of considerably more resistant material that formed inside the theca. Probably the structure formed by this resistant layer was functionally a cyst, but it will be referred to herein by the

less committal term *test*. The test appears to have contacted the theca over relatively larger and smaller areas in different genera and species. Tests that formed mainly in contact with or close to the inner surface of thecal plates seem to be represented by such obviously dinoflagellate-like fossils as have been commonly referred to the extant genus *Gonyaulax*. Tests that also formed within the theca, but that contacted it only by means of pillar-like supporting processes appear to be represented by superficially undinoflagellate-like fossils such as *Hystrichosphaera* and *Hystrichosphaeridium*. In genera of the last sort the pattern of thecal plates may not be directly observable, but only reflected by the number and distribution of surficial ridges and projecting processes. In other words, the fidelity with which the fossil test records morphological characteristics of the theca may depend chiefly upon the distance that separated the two structures, the fidelity decreasing with increasing separation. A virtually unbroken series of morphological types that collectively bridge the gap between the extreme examples just mentioned is rapidly being recognized among described genera of fossil dinoflagellates.

A test wall of at least two layers seems typical for fossil dinoflagellates, although it is not universal. The two layers that are discernible in many fossils customarily considered dinoflagellates (Eisenack[3]) are very likely homologous with the two layers noted in fossils like *Hystrichosphaera* and *Hystrichosphaeridium* (Klumpp,[4] Evitt[5]) that have traditionally been classified as hystrichospheres, separate from the dinoflagellates.

Hystrichosphaera, Hystrichosphaerida, and Hystrichospheres.—The history of the study of hystrichospheres to 1961 has been ably reviewed by Sarjeant.[6] Only a few details need concern us here.

In 1838, when Ehrenberg illustrated the first fossil dinoflagellates, he also figured some spiny organic microfossils from the Cretaceous of Germany and Poland, which he identified with the modern freshwater genus *Xanthidium*. He named one of the fossil species *Xanthidium furcatum*. Subsequent work showed that these objects, although unrelated to *Xanthidium*, are common fossils, and in 1933, O. Wetzel[7] proposed for them a new genus *Hystrichosphaera* (type species: *Xanthidium furcatum* Ehrbg.) and a new family, the Hystrichosphaeridae. In 1937 Deflandre[8] emended *Hystrichosphaera* by separating from it a second genus *Hystrichosphaeridium*, for whose type species he selected another of Ehrenberg's forms, *Xanthidium tubiferum*. In 1938 Eisenack[9] proposed a new order, the Hystrichosphaerida (= Hystrichosphaeridea auct.) for the Hystrichosphaeridae and a second family that he erected at the same time. Subsequent work of many authors (see Sarjeant[6]) has added to this order a complex of genera that have been referred to informally as "hystrichosphaerids," "hystrichospherids," or "hystrichospheres."

Thus, the nomenclatural history and current status of the three formal names, *Hystrichosphaera*, Hystrichosphaeridae and Hystrichosphaerida, and of their informal derivatives, "hystrichosphere," etc., are simple and clear. In addition, the morphology of the critical genus *Hystrichosphaera* is well known, especially through the detailed descriptions of Lejeune[10] and Deflandre,[8] supplemented by more recent observations (e.g., Evitt[1, 5]).

Much uncertainty and conflicting speculation have characterized attempts to determine the biological affinities of hystrichospheres. In conjunction with an extensive review of the evidence, Deflandre[11] concluded that they are not a single

biologic category, but probably a conglomeration of cysts, eggs, and entire shells representing many groups of organisms only remotely related. On the other hand, Eisenack[12] has argued for the "Einheitlichkeit der Hystrichosphaerideen." I follow Deflandre in believing that a great variety of biological entities is represented among the fossils that have been called hystrichospheres. Some of these fossils give no indication of being dinoflagellates, whereas many others seem, in fact, to be dinoflagellates, among them the genera *Hystrichosphaera* and *Hystrichosphaeridium*. I propose to consider these genera to be dinoflagellates.

Assignment of *Hystrichosphaera* to the Dinoflagellata means that the family Hystrichosphaeraceae (type genus *Hystrichosphaera*) is a family of dinoflagellates. Accordingly, the description of the family is emended below in a manner that will exclude those fossils formerly assigned to it which cannot be recognized as dinoflagellates, as well as certain other fossils that are dinoflagellates but which are herein assembled in a new family Areoligeraceae.

I also suggest that use of the name Hystrichosphaerida should be discontinued for two reasons: (1) The name is no longer appropriate for a group of nondinoflagellates, since the taxa upon which it was based (*Hystrichosphaera* and Hystrichosphaeridae) are here considered dinoflagellates. (2) Since the "dinoflagellate hystrichospheres" can be accommodated in the Peridiniales, there is no need for an ordinal grouping within the dinoflagellates to include the Hystrichosphaeraceae and for which the name Hystrichosphaerida (as Hystrichosphaerales) might be used.

By these changes the meaning of the informal term "hystrichosphere" also becomes modified and restricted. In the narrowest sense it now has the scope of a family (Hystrichosphaeraceae) instead of an order (Hystrichosphaerida). Cautious use of the term in a context that clearly associates it with the dinoflagellates seems advisable in order to avoid confusion with the nondinoflagellate, now "ex" hystrichospheres for which the informal name acritarchs is suggested and defined on a following page.

Descriptive Terminology.—The adjectives **sutural, intratabular,** and **nontabular** are used in the following pages with reference to contrasting arrangements of surface features (processes, ridges, etc.) on a dinoflagellate test. **Sutural** features rise from the lines or angles between polygonal fields and correspond in position to the sutures between thecal plates. **Intratabular** features occupy positions on the test that correspond to more or less of the central portions of thecal plates, rather than to the lines of separation between them. (The "plate-margin processes" and "plate-centered processes" of Evitt[1] are, respectively, sutural and intratabular.) For example, *Hystrichosphaera* (Fig. 1) possesses both sutural ridges and sutural processes, *Achomosphaera* (Fig. 2) has sutural processes only, and *Hystrichosphaeridium tubiferum* (Fig. 3) has intratabular processes. In *Hystrichosphaera* the simple reticulum of sutural ridges makes obvious the platelike fields that suggest a dinoflagellate tabulation. The arrangements of processes in the other two are not immediately apparent, but are decipherable and distinctive, according well with plausible patterns of thecal plates. **Process-groups** (i.e., multiple intratabular processes) also occur. The elements of a process-group may be arranged in one or more clusters, or in rows that surround more or less polygonal areas (as in *Areoligera*, Fig. 4), but these rows are not united in a single reticulum as in *Hystrichosphaera*.

Projecting surface features that are neither sutural nor intratabular are **nontabular**; that is, they are in random arrangement or the arrangement, if regular, has no apparent relation to a scheme of tabulation.

The term **sulcal notch** is applied to the commonly occurring re-entrant in the outline of an apical archeopyle on the ventral side of the test. The notch records the girdleward extension of the first apical plate in line with the sulcus, and inter-

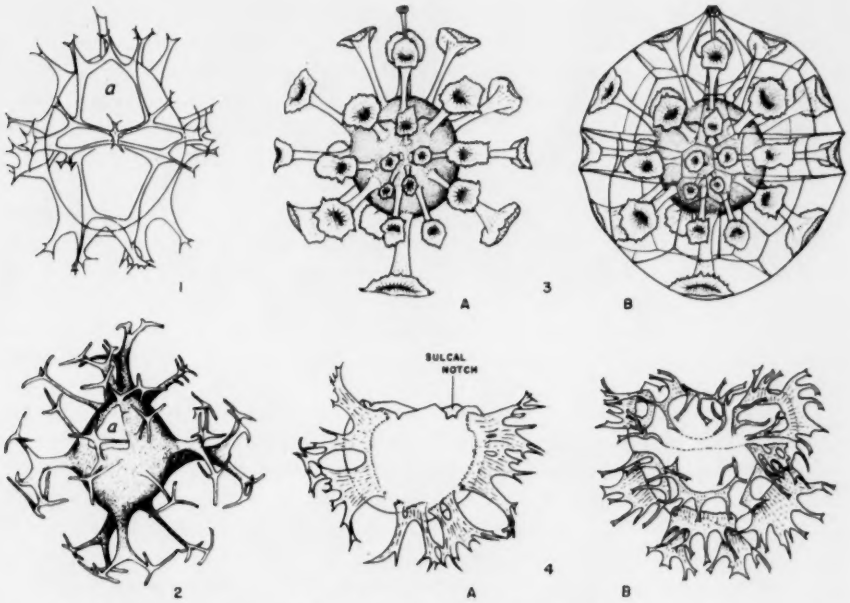

FIG. 1.—Sutural processes and sutural ridges in camera lucida drawing of *Hystrichosphaera* sp. from the Vincentown Formation (lower Eocene), New Jersey. Dorsal surface, about × 700. Note fusion of shafts of alternate pairs of girdle processes. *a*-precingular archeopyle.

FIG. 2.—Sutural processes without sutural ridges in *Achomosphaera ramulifera* (Defl.) n. comb. Holotype, after Deflandre,[8] pl. 11, fig. 6, from the Upper Cretaceous (probably Senonian), Paris; about × 450. Note fusion of alternate pairs of girdle processes and some near poles. *a*-precingular archeopyle.

FIG. 3.—Intratabular processes in *Hystrichosphaeridium tubiferum* (Ehrbg). A, reconstruction of test in ventral view, based on numerous specimens from the Redbank Formation (Maestrichtian), New Jersey; about × 500. B, inferred relationship between test and originally surrounding theca. Zigzag line on central body represents suture that forms archeopyle.

FIG. 4.—Intratabular process-groups and offset sulcal notch in camera lucida drawings of *Areoligera* cf. *A. senonensis* Lej.-Carp. from the Navesink Formation (Maestrichtian), New Jersey. Ventral views: A, ventral surface; B, dorsal surface par transparence; about × 350. Apical archeopyle is open and operculum not shown.

rupts the cycle of precingular plates. In members of the Areoloigeraceae (Fig. 4) this notch is conspicuously offset from the midline.

Central body refers to the compact central portion of a test from which the projecting structures (processes, septa, etc.) extend. **Capsule** is restricted to the innermost body formed by a multilayered wall. The capsule may fill all or only part of the central body, depending upon the extent to which their walls are in close contact. **Archeopyle** is used in the sense of Evitt.[1]

Systematics.—Many of the genera in the families discussed below require redescription and revision, but I do not feel this can yet be done effectively. Rather, it should wait until described species can be restudied to search for morphological characters not originally considered, and until additional undescribed forms can be studied and described.

Family HYSTRICHOSPHAERACEAE O. Wetzel 1933 emend.

Type genus: *Hystrichosphaera* O. Wetzel 1933,[7] emend. Deflandre 1937.[8]

Revised diagnosis: More or less radially or axially symmetrical dinoflagellate tests that consist of a spherical to ellipsoidal central body with basically spinelike sutural processes that may or may not be combined with low sutural ridges, folds, or membranous septa. The tips of processes may be free or interconnected by a network of trabeculae concentric to the central body. Archeopyle exclusively precingular.

Genera referable to the family: *Achomosphaera* Evitt n. gen., *Cannosphaeropsis* O. Wetzel 1933 (partim, including the type species *C. utinensis*), *Hystrichosphaera* O. Wetzel 1933, emend. Deflandre 1937, *Nematosphaeropsis* Deflandre & Cookson 1955, *Triblastula* O. Wetzel, 1933. *Hystrichokibotium* Klumpp 1953 is probably synonymous with *Hystrichosphaera*, comprising, I believe, specimens of that genus oriented so that the equatorial band of elongate platelike areas was not visible to the observer.

Discussion: The family is distinguished from Areoligeraceae by the uncompressed spherical to ellipsoidal shape and grossly radial or axial symmetry. It is distinguished from both Areoligeraceae and Hystrichosphaeridiaceae by restriction of projecting structures to sutural lines, and by the exclusively precingular archeopyle.

The wall is often distinctly two-layered: a generally thicker inner layer forms a simple spherical to ellipsoidal capsule; the outer layer forms the projecting structures and the external surface between their bases. The two layers may be in close contact over most of the surface (i.e., except under the projecting structures), or separated over large areas. The number of spinelike processes ranges from 2–3 to over 100. They may be solid or hollow, closed at the tips (usually) or open. Cavities of hollow processes do not communicate with the interior of the capsule. No major processes project from the central portions of the polygonal areas.

The distinctively furcate processes typical of *Hystrichospaera* (e.g., *H. furcata*)—trifurcate at the corners of reflected plates, bifurcate along their sides—occur repeatedly in the family. In *Achomosphaera* the processes stand isolated without sutural septa or ridges connecting their bases; hence, the fact that they are restricted in position to sutural lines is not obvious. In *Nematosphaeropsis*, the tips of processes are interconnected by tabeculae. In *Cannosphaeropsis* (as exemplified by the type species and a few others), complete processes may be greatly reduced: many lack bases and shafts and are represented only by characteristic pairs or triplets of short projections corresponding to the furcate tips, which branch from the trabecular network that envelops the central body. (Many species that have been referred to *Cannosphaeropsis* do not exhibit the basic features of the type species and must ultimately be accomodated elsewhere.) *Triblastula* lacks the *Hystrichosphaera*-like processes, but the sutural arrangement of ridges and processes is distinct in the equatorial region.

The tabulation reflected in the arrangement of ridges and processes that is most frequently encountered in the family is 3′, 0a, 5–6″, 6g, 5‴, 1p, 1⁗.

Genus ACHOMOSPHAERA n. gen.

Type species: *Achomosphaera ramulifera* (Deflandre) n. comb. = *Hystrichosphaeridium ramuliferum* Deflandre, 1937, pp. 74–75, pl. 15, figs. 5–6; pl. 17, fig. 10; Upper Cretaceous, France.

Description: Test consists of a spherical to ellipsoidal central body with precingular archeopyle and furcate, spinelike processes like those in *Hystrichosphaera* in both structure and distribution, but without sutural ridges or septa connecting their bases as in that genus. Tips of processes not interconnected. Wall two-layered; layers typically in close contact between bases of processes.

Discussion: Diagnostic characters are the precingular archeopyle and *Hystrichosphaera*-like processes, combined with an absence of sutural ridges or septa between process bases and an absence of trabeculae between process tips. Some of the equatorial processes reflecting the girdle are often large and double as in *Hystrichosphaera*. Processes at the poles may also be larger than ones between polar areas and equator. *Hystrichosphaera*, the most closely similar genus, and *Nematosphaeropsis* are distinguished by well-developed sutural ridges or septa, and *Nematosphaeropsis* has trabecular connections between process tips. Despite the lack of sutural ridges in *Achomosphaera*, the positional relationship of its processes to other features (e.g., poles, equator, archeopyle) shows that the processes are sutural.

Other species: No others have been described, but undescribed species of the genus have been observed in strata ranging from Albian to Lower Tertiary in age.

Family HYSTRICHOSPHAERIDIACEAE n. fam.

Type genus: *Hystrichosphaeridium* Deflandre 1937 emend. Eisenack 1958.[13]

Description: More or less radially or axially symmetrical dinoflagellate tests that consist of a spherical to ellipsoidal central body bearing from a few (but usually more than 15) to more than 50 basically conical to columnar or trumpet-shaped processes. Processes may be intratabular or nontabular, single or in groups. The tips of processes may be free or interconnected by trabeculae concentric to the central body. Archeopyles of several types occur, apical and precingular ones most commonly.

Genera referable to the family: *Hystrichokolpoma* Klumpp 1953, *Hystrichosphaeridium* Deflandre 1937 emend. Eisenack 1958, *Hystrichosphaerina* Alberti 1961, *Systematophora* Klement, 1960; probably *Polystephanephorus* Sarjeant 1961. In addition, some species that have been assigned to *Cannosphaeropsis* (e.g., *C. aemula* (Deflandre, 1947) and possibly *C. caulleryi* Deflandre 1938, *C. speciosa* Alberti 1961, and *C. urnaformis* Cookson 1953) represent the family.

Discussion: The family is distinguished from the Hystrichosphaeraceae by the intratabular or nontabular distribution of processes, from the Areoligeraceae by the uncompressed spherical to ellipsoidal shape, and from both by the variety of archeopyle types including precingular, apical, and epithecal ones.

The wall may be distinctly two-layered or only one layer may be recognizable. The processes may be solid or hollow and their substance may appear membranous, hyaline, or fibrous. The interiors of hollow processes do not communicate with the

interior of the capsule. Process tips may be open or closed, simple or compoundly divided, free or interconnected by trabeculae. A uniquely large or distinctively constructed process may mark either apical or antapical pole, or both. In species that exhibit a constant and decipherable process arrangement, all processes may be similar or some may be different; for example, the processes reflecting girdle and sulcal plates are often smaller and less complex than the pre- and postcingular processes, or they may be missing entirely.

The following are examples in which major processes or process-groups number less than 40 and are arranged in a constant and decipherable pattern: some species of *Hystrichosphaeridium* (including the type species *H. tubiferum*, Fig. 3), *Hystrichokolpoma*, *Systematophora*, *Hystrichosphaerina*, *Polystephanephorus*, and *Cannosphaeropsis* (partim, e.g., *C. aemula* (Deflandre)). The basic tabulation appears to be (1ap), 1–4′, 0a, 6″, 6g, 6s, 5‴, 1p, 1⁗.

Examples with more numerous, mostly nontabular processes (although alignment of girdle processes may be recognizable) are some species of *Hystrichosphaeridium*, and many species originally assigned to *Hystrichosphaeridium* but excluded from this genus by Eisenack's 1958 revision. These forms, which have no generic home among the dinoflagellates when *Baltisphaeridium* and *Micrhystridium* are considered acritarchs, include *H. hirsutum* (Ehrenberg), *H. horridum* Deflandre, *H. machaerophorum* Deflandre & Cookson, *H. striolatum* Deflandre, *H. ferox* Deflandre, and *H. flosculus* Deflandre.

New genera are needed here but their erection is beyond the scope of this paper.

* This paper draws upon research carried out while the author was employed by Jersey Production Research Company, Tulsa, Oklahoma. Their support of the research and permission to publish these remarks are gratefully acknowledged.

[1] Evitt, W. R., "Observations on fossil dinoflagellates," *Micropaleontology*, **7**, 385–420 (1961).

[2] Downie, Chas., G. L. Williams, and W. A. S. Sarjeant, "Classification of fossil microplankton," *Nature*, **192**, 471 (1961).

[3] Eisenack, Alfred, "Einige Erörterungen über fossile Dinoflagellaten nebst Übersicht über die zur Zeit bekannten Gattungen," *Neues Jahrb. Geol. Paläont., Abh.*, **112**, 281–324 (1961).

[4] Klumpp, Barbara, "Beitrag zur Kenntnis der Mikrofossilien des mittleren und oberen Eozän," *Palaecntographica, Abt., A.*, **103**, 377–406 (1953).

[5] Evitt, W. R., "Wall structure in hystrichospheres *Hystrichosphaera* and *Hystrichosphaeridium*," *Geol. Soc. Am., Sp. Paper* **68**, 172–173 (1962).

[6] Sarjeant, W. A. S., "The hystrichospheres—a review and discussion," *Grana Palynologica*, **2**, 101–111 (1961).

[7] Wetzel, Otto, "Die in organischer Substanz erhaltenen Mikrofossilien . . . . ," *Palaeontographica, Abt. A.*, **77**, 147–186, **78**, 1–110 (1933).

[8] Deflandre, Georges, "Microfossiles des silex crétacés, Deuxième partie, Flagellés incertae sedis, Hystrichosphaeridées, Sarcodinés, organismes divers," *Ann. Paléontologie*, **26**, 49–103 (1937).

[9] Eisenack, Alfred, "Hystrichosphaerideen und verwandte Formen im baltischen Silur," *Zs. Geschiebeforsch.*, **14**, 1–30 (1938).

[10] Lejeune, Maria, "L'étude microscopique des silex (Deuxième Note) Un fossile anciennement connu et pourtant méconnu: *Hystrichosphaera ramosa* Ehrbg.," *Soc. Géol. Belgique, Ann.*, **60**, 239–260 (1936).

[11] Deflandre, Georges, "Le problème des hystrichosphères, " *Inst. Océanogr. (Monaco), Bull.*, **918**, 1–23 (1947).

[12] Eisenack, Alfred, "Mikrofossilien aus Phosphoriten des samländischen Unteroligozäns und über die Einheitlichkeit der Hystrichosphaerideen," *Palaeontographica, Abt. A*, **105**, 49–95 (1954).

[13] Eisenack, Alfred, "Mikrofossilien aus dem norddeutschen Apt, nebst einigen Bemerkungen über fossile Dinoflagellaten," Neues Jahrb. Geol. Paläont., Abh., **106**, 383–422 (1958).

*THE PROGRAMMING OF HERPES VIRUS MULTIPLICATION IN DOUBLY-INFECTED AND IN PUROMYCIN-TREATED CELLS**

By Bernard Roizman

DEPARTMENT OF MICROBIOLOGY, THE JOHNS HOPKINS UNIVERSITY

Communicated by André Lwoff, December 20, 1962

For a given host, virus, and physiologic environment, the events which take place during infection at the cellular level are reproducible to a fine detail. This reproducibility is remarkable considering that within a short interval the virion becomes dismantled, the nucleic acid is transcribed, then duplicated, and new virions are assembled. Concomitantly the cell is phenotypically altered. At the present time the nature of known events is to some extent understood; what is largely unknown, however, is the mechanism by which each sequential event is ordered. For example, what determines the onset of the duplication of viral nucleic acid?

The objectives of our initial studies using HEp-2 cells and herpes simplex (HSV), a DNA virus, are to delineate specific events occurring during the infection, and to determine to what extent the experimental manipulation of one event exaggerates or inhibits the succeeding event. This paper describes the patterns of viral multiplication in cells treated with puromycin and in cells infected 3 hr apart with marked strains of HSV. It may be inferred from the results of these experiments that one and possibly more cycles of protein synthesis take place during the eclipse phase and that the duplication of viral DNA does not begin until some of the products of the eclipse phase reach a specific critical concentration in the host cell.

Materials and Methods.—Solutions and media: PBS-A: phosphate buffered saline[1] containing 0.2% bovine albumin (Fraction V, Armour). *PBS-AγG:* made by adding 0.4 ml of pooled human γ globulin (Lederle) to 100 ml of *PBS-A*. *MM-S:* maintenance medium for suspended cells contains 7.17 gm NaCl, 0.40 gm KCl, 0.20 gm $MgSO_4 \cdot 7H_2O$, 0.125 gm $NaH_2PO_4 \cdot H_2O$, 0.20 gm $CaCl_2$, 20 ml of 100× concentrate of amino acids,[2] 20 ml of 100× concentrate of vitamins,[2] 4.72 gm of tryptose phosphate broth powder (Difco), 3.0 gm glucose, 0.70 gm $NaHCO_3$, 0.60 gm glutamine, 20 mg of streptomycin sulfate, 2×10^4 units of penicillin G, and water to make 1.3 liters.

Viruses: The MP strain of HSV causes the formation of polykaryocytes in infected HEp-2 cell cultures; it is scored in terms of polykaryocyte-forming units (PoFU). The mP strain causes rounding and clumping of cells, and is scored in terms of microplaque-forming units. The properties of the two strains and procedures for their preparation and simultaneous scoring were reported elsewhere.[3, 4]

Experimental procedure: The method for infecting and suspending cells described by Lwoff and Lwoff[5] was modified to suit our needs. Approximately 10^6 HEp-2 cells in monolayer culture were washed with PBS-A and exposed to 2×10^6 PoFU of virus. The inoculated cultures were attached to an arm of a rotary shaker and submerged for 20 min in a 37°C water bath. At that time the inoculum was aspirated, the cells washed with PBS-A-γG, scraped off, separated from each other by vigorous pipetting and, after 2 cycles of centrifugation, suspended in sufficient MM-S to yield approximately 3×10^4 cells per ml. Ten-ml amounts of the cell suspension were added to siliconized Erlenmeyer flasks equipped with a gas-tight glass cap. The flasks were attached to an arm of a rotary shaker (60 rpm) and partially submerged in a 34°C water bath. At that time, and whenever opened subsequently, the flasks were thoroughly flushed with air containing 5 per cent CO_2. Drugs were added directly to the flasks. To withdraw the drugs, the cells were sedimented by centrifugation and resuspended in fresh MM-S. At times indicated in the text, samples consisting of half-milliliter amounts of cell suspensions were withdrawn and frozen at −60°C. Prior to assay the samples were frozen and thawed three times.

This procedure was modified for the experiments in which some cells were infected at 0 time with mP-HSV and 3 hr later with an equivalent amount of MP-HSV. In these experiments, the cells were suspended after they were superinfected.

The procedures outlined above were designed to fulfill two experimental requirements: (1) all or nearly all cells should be infected, and (2) the interval of exposure of cells to virus should be brief. It was determined that 10–20 per cent of input virus, i.e., 20–40 polykaryocyte or microplaque-forming units per cell were removed from the inoculum. However, allowance must be made for thermal inactivation, and for virus which adsorbed but did not penetrate into cells at the time that the cells were washed with antibody (PBS-A-γG).

The pattern of reproduction of MP-HSV in suspended HEp-2 cells has the following features: (1) Despite repeated washing with PBS-A-γG and MM-S, infected suspended cells yield infectious virus during the eclipse phase. Similar amounts of virus could be demonstrated in cell suspensions in which viral multiplication was prevented by phenethyl alcohol.[6] This residual, cell-associated virus fraction amounts to approximately 0.1 PoFU per cell and represents the base levels in the assays for newly formed virus. (2) New virus is first apparent 5–6 hr after infection. Since the process of infection and virus multiplication in a population of cells is at best only parasynchronous, the time at which an average of 1 PoFU per cell could be detected (6–7 hr) was arbitrarily designated as the end of the eclipse phase. (3) Virus multiplication appears to follow an exponential rate until about 13–15 hr after infection. Thereafter it tends to level off.

Two basic procedures were employed in the studies with puromycin dihydrochloride (N. B. Co.). First, puromycin was added immediately after infection or at other specified times, and allowed to react with cells for intervals ranging from 2–6 hr, i.e., during the eclipse phase only. Second, puromycin was added immediately after infection or at specified times and allowed to react for the remainder of the experiment. The final concentration of the drug was 5 μg/ml. The sensitivity of HSV multiplication to puromycin was as follows: No new progeny could be detected in cells suspended after infection in MM-S containing 10 or more μg of puromycin per ml. The yields from infected cells treated with 1 and with 3 μg/ml were 6 per cent and 0.6 per cent, respectively, of the yield obtained from untreated suspensions. With 5 μg/ml, in some experiments the base virus level doubled or tripled reaching 0.2 PoFU per cell; in others no newly formed virus could be detected.

Results.—HSV multiplication in cells exposed to puromycin during the eclipse phase: Puromycin added for any interval between 0 and 6 hr after infection prolonged the eclipse phase by an interval no less than the duration of exposure to the drug. However, once the multiplication began, the rate of reproduction of the virus was the same in both treated and untreated cell suspensions (Fig. 1 *A*).

Treatment with puromycin between 0 and 2 hr or between 4 and 6 hr after infection prolonged the eclipse by 2 hr. In accord with this formula, treatment between 0 and 4 hr or between 0 and 6 hr after infection prolonged the eclipse phase by 4 or 6 hr, respectively. Since in no experiment was the prolongation of the eclipse phase less than the duration of the treatment, it may be concluded that (1) puromycin affects events taking place during each of the three successive 2-hr intervals of the eclipse phase, (2) the events affected by puromycin cannot take place concurrently, that is, they are in an ordered sequence, and (3) processes inhibited by puromycin during the first and third interval resume at usual rates once the drug is withdrawn. Probably the most significant finding is that treatment with puromycin between 2 and 4 hr caused a 4-hr delay in the termination of the eclipse period. It seems likely that once the successive events of the first and second 2-hr intervals are interrupted, they cannot resume immediately and the events of the first 2-hr period must take place again. It could be that a product of the first 2-hr interval becomes diverted or degraded if it is not utilized for the synthesis of a product made at a later interval.

HSV multiplication in cells exposed to puromycin after the eclipse phase: Trivial yields were obtained from cells suspended after infection in MM-S containing 5 μg/ml of puromycin. Sizeable yields, however, could be obtained if the puromycin was added at 2, 4, and particularly 6 hr after infection (Fig. 1 *B*). In general the later the puromycin was added during the eclipse phase the sooner multiplication was detected, the greater the yield, and the higher the rate of apparent multiplication of the virus. The data support the findings reported in the preceding section that puromycin-sensitive events take place in each of the 2-hr intervals during the first 6 hr after infection.

Acceleration of the eclipse phase of the superinfecting virus in cells infected 3 hr apart with marked strains: Inhibition by puromycin of protein synthesis in mammalian cells has been demonstrated repeatedly.[7-11] However, there is no direct

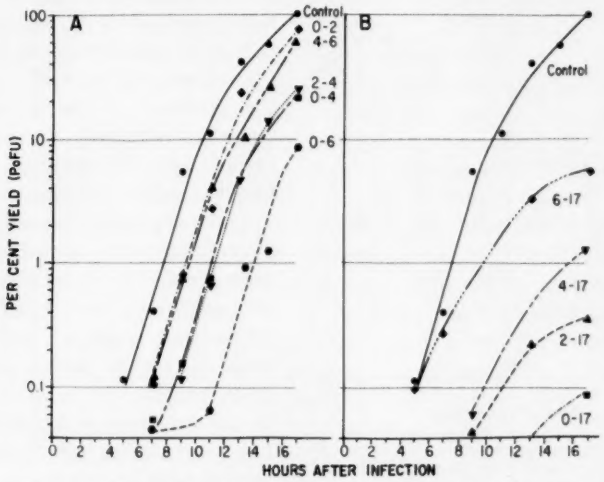

FIG. 1.—Effect of 5 μg/ml of puromycin dihydrochloride on multiplication of HSV. The first and second numbers on the right of each curve refer to the time of addition and removal of the drug, respectively, in hours after infection.

evidence that puromycin inhibits HSV protein synthesis during the eclipse phase or, in fact, that any other synthetic processes ordered by HSV and prerequisite to its multiplication take place during that phase. To determine whether the virus directs the synthesis of some product prerequisite to its multiplication, HEp-2 cells were infected first with mP virus (0 hr) and 3 hr later with MP virus. Controls consisted of cells infected with mP virus alone at 0 hr, cells infected with MP virus at 0 hr and cells infected with MP virus at 3 hr. The results of two experiments are summarized in Figure 2. It is evident that in cells infected at 0 time with mP virus, the duration of the eclipse phase of the superinfecting MP virus was reduced by 80–100 minutes in relation to that of appropriate controls. The remarkable feature of these experiments is that in the doubly-infected cells, the superinfecting MP virus followed the pattern of development of mP virus. The results indicate that (1) the synthesis of a product prerequisite to viral reproduction takes place during the eclipse phase, (2) the product is not an accretion of the

virus itself; it can serve either mP or MP virus, and (3) the eclipse phase is not an immutable interval; it can be reduced if the products of the eclipse phase are present in the cell at the time of infection.

Discussion.—Some speculative, but perhaps significant, aspects of this study emerge from considerations of the rates of apparent multiplication of HSV in cells treated with puromycin during the eclipse phase and during the phase of viral maturation. It is evident that the presence of the drug during any portion of the eclipse phase does not ultimately affect the subsequent rate of multiplication of the virus. However, virus matures at a reduced rate if puromycin is present during the phase of active multiplication.

The emphasis on "rate" of multiplication derives from the consideration of the factors that govern it. When all precursors are available, it may be deduced that (1) the apparent exponential rate of maturation of a DNA virus should reflect the exponential rate of duplication of the DNA, and (2) assuming the presence of the primer and of abundant substrates, the rate of duplication of the DNA should be a function of available polymerizing enzyme.

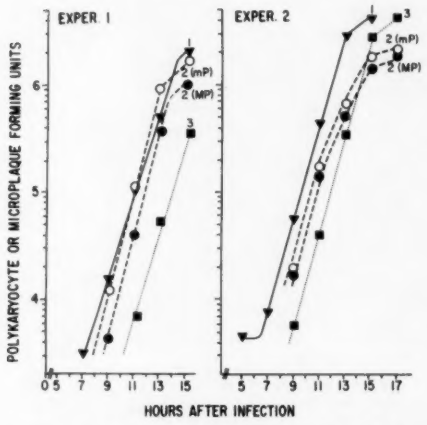

FIG. 2.—Viral multiplication in HEp-2 cells infected 3 hr apart with marked strains of HSV. (1) Cells infected at 0 hr with MP virus. (2) Cells infected with mP at 0 hr and MP at 3 hr. (3) Cells infected with MP at 3 hr. The pattern of multiplication of mP virus in cells singly infected at 0 hr coincided with mP virus development in the doubly-infected cells. Numbers on ordinate are exponents of 10.

These arguments cannot be used indiscriminantly to explain the data obtained in this study because the results are based on assays of infectious virions rather than assays of viral DNA. It could be argued that in cells exposed to puromycin at 6 hr DNA multiplied at the same rate as in untreated cells, but fewer virions were formed because the synthesis of capsomeric protein was inhibited. Since puromycin may act by stripping peptides off the ribosome before the protein is completed,[8-10] the small yield obtained in the presence of puromycin could be accounted for by assuming that the capsomeric protein is itself a polymer of small molecular weight proteins and that the synthesis of a small amount of the monomer was completed in the presence of the drug.

These arguments can be used to explain some features of viral development observed in cells treated with puromycin during the eclipse phase only. It could be asked why viral reproduction follows the same rate as the controls but only after a lag. Why does not reproduction begin at 6 hr at a reduced rate? The hypothesis that puromycin "freezes" all activities of the cell may be rejected because it is incompatible with the known effects of the drug and because puromycin-insensitive events in the eclipse phase of an animal virus have been described.[11] One plausible hypothesis is that the duplication of viral DNA does not begin until a specific event takes place. The probability of the completion of such an event would be a

function of the concentration of enzymes and precursors involved. Another way of stating this is that for a given physiologic state of the infected cell, critical concentrations of enzymes and precursors of DNA synthesis prevail in the cell at the time DNA duplication begins. If enzyme synthesis were arrested below this critical level, the specific event would be considerably delayed, and the rate of reproduction would be reduced.

There is no direct evidence to support this hypothesis and, moreover, very little is known concerning the requirements and determinants of the duplication of DNA of animal viruses. A considerable body of information has accumulated for DNA bacterial viruses. In bacteria infected with T-even phages the synthesis of proteins concerned with intermediary DNA metabolism begins almost immediately after infection and ends shortly after the onset of DNA synthesis.[12-14] In "nonpermissive" bacteria infected with certain amber mutants of phage T_4[14] and in bacteria exposed to irradiated phage[13-15] the synthesis of apparently functional early proteins may be exaggerated but duplication of DNA does not ensue. Of particular interest is the fact that the DNA polymerases obtained from uninfected and T_2-infected *E. coli* differ in functional as well as physical properties.[16] *In vitro* the "T_2" polymerase unlike the *E. coli* enzyme appears inert with native DNA and seems to react best with heat-collapsed or "single-stranded" DNA regardless of source. Moreover, the net amount of DNA synthesized by the T_2 polymerase does not exceed the amount of the primer added.[16, 17] The net amount of DNA synthesized by the *E. coli* polymerase may exceed 10- to 20-fold the amount of native or heat-collapsed DNA added as a primer.[18, 19] The problems involved have been stated.[14-16] To paraphrase, in the reproductive cycles of phage and animal viruses there are two intervals of transcription of DNA separated by a period of encapsidation and extracellular existence. Very likely some regulatory process or event determines the end of the last transcription interval and the beginning of duplication of DNA. The regulatory process could entail physical participation of the DNA itself or a physical modification of the enzyme molecules (tautomerization, monomerization, or polymerization). It seems likely, though not yet proved, that (1) termination of early protein synthesis and onset of duplication of DNA are interdependent, (2) the process terminating the last transcription period involves a physical modification of DNA, (3) the DNA is "primed" by a distinct, possibly labile, enzyme formed when other enzymes and precursors necessary for DNA synthesis attain critical concentrations.

The concept that a "critical concentration" and not just any small number of enzyme molecules sets off DNA duplication is based on the net duration of the eclipse phase and apparent rate of viral multiplication in cells exposed to puromycin for any interval during the first 6 hr after infection. It should be noted that two regulatory systems, one operating at the genetic level, the other at the level of the "enzyme molecules," have been postulated.[20] Alterations of the existing state in one system are triggered by "effectors" binding to products of regulatory genes; in the other system inhibitors or activators bind to allosteric sites of "enzyme molecules." Implicit in both systems are "critical concentrations" of the effectors and of the allosteric inhibitors or activators, respectively.

Finally, essentially similar considerations have led to the conclusion that the onset of poliovirus RNA duplication is triggered by a specific event.[21] It should

be noted that there is a striking correlation between cell volume and virus yields,[22] an observation which extends to multinucleated giant cells produced by X-irradiation.[23] Puromycin delays poliovirus reproduction if administered briefly during the eclipse phase.[24, 25] Moreover, following withdrawal of puromycin the rate of viral multiplication in treated and untreated cultures is the same.[25] It could follow that poliovirus reproduction follows an event actuated at critical concentrations of rate and yield-limiting enzymes or precursors. Interestingly enough a thermosensitive event occurring late in the eclipse phase of certain poliovirus mutants appears to determine subsequent rate of viral multiplication.[26] It has been tentatively concluded[21] that the thermosensitive event involves actuation of an RNA polymerase through polymerization of inactive protein monomers. This hypothetical polymerization could be determined by an alteration of the "milieu intérieur" of the infected cell or by some product synthesized late in the eclipse phase.

Summary.—Suspensions of HEp-2 cells infected with herpes simplex virus (HSV) were treated with puromycin during the eclipse phase and at various times during the reproductive cycle. Puromycin (5 μg/ml) treatment confined to the period of the eclipse prolongs the phase but does not alter the apparent rate of subsequent reproduction of the virus. Treatment between 0 and 2 hr, 2 and 4, or between 0 and 6 hr after infection causes equivalent delay in the termination of the eclipse phase. Treatment between 0 and 4 or between 2 and 4 hr after infection causes a 4-hr delay. Puromycin treatment beyond the end of the eclipse phase causes a decrease in the apparent rate of virus formation and decreases the yield.

The formation of a product prerequisite to viral reproduction could be inferred from an analysis of viral multiplication on HEp-2 cells infected 3 hr apart with two marked strains of HSV. The eclipse phase of the superinfecting virus was reduced. Moreover multiplication of the superinfecting virus followed the pattern of development of the first infecting virus rather than that of the homologous virus.

It is concluded that during the eclipse phase of HSV there is at least one and possibly more periods of synthesis of proteins required for the initiation of virus multiplication. It is tentatively inferred that the duplication of viral DNA does not commence until the precursors and enzymes required for its synthesis are present in the cell at a critical concentration.

I am indebted to André Lwoff for many invaluable discussions which have stimulated this work. I am also indebted to Miss V. L. Robinson for superb technical assistance.

* Aided by grants from the U.S. Public Health Service (CA-4204) and the National Science Foundation (G-23158).

[1] Dulbecco, R., and M. Vogt, *J. Exptl. Med.*, **99**, 167 (1954).

[2] Eagle, H., *J. Exptl. Med.*, **102**, 37 (1955).

[3] Roizman, B., and P. R. Roane, Jr., *Virology*, **15**, 75 (1961).

[4] Roizman, B., and P. R. Roane, Jr., *Virology*, **19**, in press (1963).

[5] Lwoff, A., and M. Lwoff, *Ann. Inst. Pasteur*, **98**, 173 (1960).

[6] Roizman, B., to be published.

[7] Lieberman, I., and P. Ove, these PROCEEDINGS, **45**, 867 (1959).

[8] Allen, E. H., and R. S. Schweet, *J. Biol. Chem.*, **237**, 760 (1962).

[9] Morris, A., S. Favelukes, R. Arlinghaus, and R. S. Schweet, *Biochem. & Biophys. Res. Commun.*, **7**, 326 (1962).

[10] Hultin, T., *Biochem. et Biophys. Acta*, **51**, 219 (1961).

[11] Wheelock, E. F., these PROCEEDINGS, **48**, 1358 (1962).

[12] Flaks, J. F., J. Lichtenstein, and S. S. Cohen, *J. Biol. Chem.*, **234**, 1507 (1959).
[13] Delihas, N., *Virology*, **13**, 242 (1961).
[14] Wiberg, J. S., M. L. Dirksen, R. H. Epstein, S. E. Luria, and J. M. Buchanan, these PROCEEDINGS, **48**, 293 (1962).
[15] Dirksen, M. L., J. S. Wiberg, J. F. Koerner, and J. M. Buchanan, these PROCEEDINGS, **46**, 1425 (1960).
[16] Aposhian, H. V., and A. Kornberg, *J. Biol. Chem.*, **237**, 519 (1962).
[17] Kornberg, A., in *Enzymatic Synthesis of DNA* (New York: John Wiley & Sons, Inc., 1961), pp. 98–100.
[18] Lehman, I. R., *J. Biol. Chem.*, **235**, 1479 (1960).
[19] Josse, J., and A. Kornberg, *J. Biol. Chem.*, **237**, 1968 (1962).
[20] Monod, J., and F. Jacob, *Cold Spring Harbor Symposia on Quantitative Biology*, vol. 26, 389 (1961).
[21] Lwoff, A., *Cold Spring Harbor Symposia on Quantitative Biology*, vol. 27, in press (1962).
[22] Dunnebacke, T. H., and H. B. Reaume, *Virology*, **6**, 8 (1958).
[23] Levine, S., *Nature*, **194**, 895 (1962).
[24] Levintow, L., M. M. Thorén, J. C. Darnell, Jr., and J. L. Hooper, *Virology*, **16**, 220 (1962).
[25] Lwoff, A., B. Roizman, and M. Lwoff, to be published.
[26] Lwoff, A., B. Roizman, and M. Lwoff, *C. R. Acad. Sci.* (Paris), **254**, 2462 (1962).

*STEPS IN THE NEOPLASTIC TRANSFORMATION OF HAMSTER EMBRYO CELLS BY POLYOMA VIRUS**

BY MARGUERITE VOGT AND RENATO DULBECCO

CALIFORNIA INSTITUTE OF TECHNOLOGY

Communicated December 10, 1962

Cultures of hamster embryo cells infected with polyoma virus undergo a characteristic transformation within several weeks after infection. The transformed cultures are constituted by highly atypical cells which have an abnormal morphology, grow rapidly *in vitro*, and give rise to progressively growing tumors when inoculated subcutaneously into the adult hamster.[1]

In the previous experiments, the transformed cells arose in mass cultures and their properties were only studied many cell generations after the original virus-cell interaction had taken place. The experiments to be reported in this communication were undertaken to get some information on the properties of transformed cells at earlier stages after infection with polyoma virus. The experiments show that the atypical cells are produced in two main steps; moreover, they reveal some new characteristics of the transformed cells which may contribute to a clarification of the mechanism of transformation.

Material and Methods.—The polyoma virus used was of the "large-plaque" type. Its origin and the preparation of its stocks have been described.[2] Tissue cultures of whole embryos of Golden hamsters were prepared according to a technique already described.[3]

A rich growth medium especially favorable for the cloning of mouse embryo cells (Weisberg, R., personal communication) and for the titration of polyoma-induced foci (Bayreuther, K., personal communication) was used for all experiments. It consisted of reinforced[4] Eagle's medium (40 pts), Puck's[5] nutrient solution N16 (40 pts), and medium NCTC 109 (4 pts); all ingredients were dissolved in Earle's saline containing 0.55 per cent glucose and 0.37 per cent $NaHCO_3$. This medium was further supplemented with 0.3 per cent Bacto tryptose phosphate broth (10 pts) and, unless stated differently, with 10 pts of fetal bovine serum.

Experimental procedure: Sets of secondary hamster embryo cultures, seeded with 8×10^5 cells per plate, were infected with polyoma virus: an aliquot of 0.1 ml of a virus suspension of a titer of 10^9 PFU/ml was distributed over the cells after removal of the fluid medium. Adsorption of the virus was allowed to proceed for 2 hr at 37°C in an incubator flushed with an adequate CO_2-air mixture; during this time, about 10 per cent of the input virus was adsorbed to the cells, as was shown by control experiments with purified, P^{32}-labeled, virus (unpublished). The cultures were washed three times with medium and overlaid with 5 ml of medium. The cultures were maintained under optimal growth conditions by three weekly fluid changes; the cells were transferred when the cell sheets became confluent.

At various times (2, 4, 9, 13, 16, and 24 days) after infection, single cultures of the sets were trypsinized and used to start a group of *sparse* subcultures. These cultures were seeded with 10^5 cells and grown for seven days in the presence of 20 per cent fetal bovine serum; thereafter, fluid changes were done with regular medium. The sparse subcultures were scanned on days 10 to 16 with a low-power inverted microscope for areas of high mitotic activity and/or abnormal morphology. At this time, the subcultures were mostly constituted by a confluent monolayer of cells showing almost no mitotic activity. Some cultures contained one or a few foci of cells of unusual morphology which grew in several layers and showed frequent mitoses. The cells of these foci were usually markedly refringent and fusiform in shape; they crisscrossed each other and sometimes piled up to form nodules or strands.

The number of foci obtained on sparse subcultures started within the first week after infection was about 10^{-5} of the cells plated; since the multiplicity of the adsorbed virus was 10–20, the efficiency of focus formation was about 10^{-6} that of plaque formation on mouse embryo cells.

A number of foci were picked from the sparse subcultures. To do so and to carry over the least amount of untransformed cells, small glass cylinders were used to isolate the foci from the surrounding cells.[6] The glass wells were filled with trypsin and the dispersed cells transferred to new petri dishes. In certain cases, the foci were aspirated with a capillary pipette to avoid the use of trypsin and transferred to petri dishes containing coverslips. The cell lines started from individual foci will be designated as *focal lines*. All focal lines derived from sparse subcultures started within the first two weeks after infection were isolated from cultures containing each a single focus. They can therefore be assumed to derive from a single transformed cell; however, the presence, at the outset, of a small proportion of contaminant nontransformed cells cannot be excluded.

The focal lines were maintained by a regular regime of fluid changes and transfers; where trypsin was to be avoided, the old coverslips were replaced at regular intervals by fresh coverslips which became repopulated by cells derived from the outgrowth surrounding the coverslips. Without exception, all focal lines could be maintained indefinitely in an actively growing state. The cells were characterized by their refringence, their high mitotic activity, and their capacity to form multilayered cell sheets with a crisscross pattern in dense cultures.

Two types of controls to the focal lines were done. One type consisted of lines started with cells from areas of the sparse subcultures outside of a focus = *nonfocal lines*. Usually, the cells from areas delimited by three glass cylinders were compounded to obtain enough cells to start each nonfocal line. These lines were constituted by cells with the characteristics of normal cells; they could not be maintained for more than a few passages.

The other type of control consisted in a repetition of the entire experimental procedure, as outlined, with the exception that the original sets of cultures were not infected with polyoma virus. In these control sets, no foci comparable to those of the infected sets were found in the sparse subcultures. Only a few areas of persistent mitotic activity but of normal morphology were seen. These areas were picked and *control lines* started. These lines could be maintained for only a few transfers. One exceptional line could be cultured for five transfers. This line consisted of very flat, transparent cells. It had other peculiar features to which we shall return.

Results.—The present investigation consisted in a study of the properties of the cells of the *focal* lines at various times after their isolation. The earliest observations were carried out at the second or third transfers when a sufficient number of cells were available. At this time, nontransformed cells which might have been picked with the focus when the line was started would have been considerably diluted

out owing to their limited growth ability, as demonstrated by the poor growth of control lines. The cells of the focal lines were characterized on the basis of the following properties: morphological types of the clones formed, efficiency of cloning, and transplantability into 20-day-old hamsters. The efficiency of cloning was measured by determining the proportion of cells capable of forming a clone of 200 or more cells after seven days of incubation in medium supplemented with 20 per cent fetal bovine serum (without feeder layer). The transplantability was determined by inoculating 5×10^6 cells from a trypsinized cell suspension subcutaneously into 20-day-old hamsters. The degree of transplantability was measured by the time required to form a tumor of the size of a walnut at the site of inoculation. The results of these determinations are summarized in Table 1. The following points should be emphasized.

The clones formed by the cells of the focal lines could be divided into two main morphological groups. One group consisted of "thin" clones in which the cells grew mainly in a single layer; at the early transfers, the thin clones had a very loose structure and were small in size (*ca.* 200 cells per clone); at later transfers, they became larger in size (1,000 and more cells) and showed a uniform crisscross-like pattern. All thin clones were clearly different from normal clones: the cells were refringent and randomly oriented. The thin clones were prevalent at the early transfers; their proportion decreased in later transfers. The second group of clones were "dense" clones, in which the cells piled up in many layers. The morphology of these dense clones was variable: some showed a uniform dense center, others had heavy strands, others nodules. These clones were absent or rare in early transfers and increased in proportion in later transfers.

Clones produced by cells from the nonfocal or control lines were of a strict monolayer type; the cells were thin and transparent and showed a regular arrangement. They were readily distinguishable from the thin clones just described. We can therefore conclude that both groups of clones formed by cells from focal lines were clones of transformed cells.

The efficiency of cloning of the cells of the focal lines at the early transfers was very similar to that of normal cells. At later transfers, this efficiency increased in parallel with the appearance of thin clones of large size and of dense clones.

The transplantability of the cells of the focal lines varied markedly from line to line, and within a given line, with the transfer number. In general, the transplantability was very low or absent at early transfers and increased with later transfers. The increase in transplantability proceeded at equal pace with the increase in the proportion of dense clones. These results suggested therefore that the highly transplantable cells were the same cells that gave rise to dense clones. This deduction was confirmed by comparing the transplantability of subcultures derived from eight clones of the thin type, obtained at later transfers when the clones formed were rather large, with that of subcultures of five dense clones. As shown in Table 2, the average time for developing a tumor of walnut size was 8.4 weeks for the cultures of the thin clones (2/35 animals did not develop any tumor) and 4.3 weeks for the cultures of dense clones (23/23 animals developed a tumor).

As to the relationship of the two types of cells present in the focal lines, two possibilities can be visualized: either the cells giving rise to dense clones are variants of the main cell type which forms thin clones or the two cell types originated in in-

TABLE 1

EFFICIENCY OF CLONING AND TRANSPLANTABILITY OF VARIOUS FOCAL LINES

Days after infection*	Focal line	Transfer	Efficiency of Cloning (%)†		Tumor of Walnut Size Within Weeks														No tumor ‡	Total number of animals§
			All clones	Dense clones	2	3	4	5	6	7	8	9	10	11	12	13	14	15		
2	26	tr9,10	4.0(277)**	0.2				1		3										4
	43	tr3,4	0.2(106)	0.0															2(12)	2
		tr12	3.5(278)	0.2									1		1					2
	61	tr9–11	13.0(104)	1.0			1	1	1	2										5
4	79	tr4	0.5(69)	0.0								2								2
		tr6,7	1.3(51)	0.03						3	1									4
		tr10					2													2
	80	tr3								1		1							1(9)	3
		tr7–10	1.4(115)	0.4			3	4												7
9	25	tr3				3														3
	27	tr3							1	1		1								3
	28	tr2,3	2.5(97)	0.4															3(12)	3
	29	tr3								1			1	1						3
		tr7–10	17.9(143)	4.1			4	1	1											6
	78	tr3–6							2	6										8
		tr7–8							4	1	1									6
13	30	tr2										1	1	1						3
		tr5–9	2.1(168)	0.2								2	1				1			4
16	18	tr2					1	3												4
		tr4–6				5														5
		tr7–9	6.6(397)	2.2	5															5
	42	tr2													1					3
		tr6	1.9(151)	0.1								1							2(12)	1
	45	tr2–4																	6(12)	6
		tr5–7																	5(13)	5
		tr8–9	9.0(74)	0.3									1		1	1		1		4
24	1	tr2,3	9.0(37)	0.0														1	1(13)	2
	2	tr9				3														3
	4	tr2,3	14.0(57)	2.0				2	1		1	1								5
		tr9					3													3
	5	tr10						3												3

* Time of seeding of sparse cultures.
† Proportion of clones formed over all cells plated.
‡ Numbers in parentheses indicate number of weeks of observation.
§ Twenty-day-old hamsters were inoculated with 5×10^6 to 10^7 cells of the focal lines indicated in column 2.
** The numbers in parentheses indicate the total number of clones counted.

TABLE 2

TRANSPLANTABILITY OF CLONAL DERIVATIVES OF FOCAL LINE 79

Type of clone	Clone	Transfer	Tumor of Walnut Size Within Weeks 4	5	6	7	8	9	10	11	12	13	No tumor	Total number of animals
Thin	5	4											2(12)	2
	8	6			3	1	1							5
	11	2						3		1				4
	14	4, 7				1	2					1		4
	15*	3, 7			1	1	1	2						5
	15-A2	3			1	1	3							5
	15-C1	2		1		3		1						5
	15-C2	2								1	4			5
Total				1	5	7	7	6		2	4	1	2	35
Dense	13	2	1	3										4
	15-A7	3	5											5
	15-A10	3	5											5
	15-A12	3	3	2										5
	15-C3	2	3											3
Total			17	5										22

* Clone derived from a single-cell isolation.

dependent events and were accidentally mixed in the focus. Two lines of experimental evidence point to the first possibility.

The first type of evidence derives from the study of the properties of cells of nonfocal lines. If cells with the capacity to form dense clones had been scattered all over the sparse cultures but inhibited by the surrounding cells from forming a focus, cell platings from the nonfocal lines should have given rise to dense clones. This was never observed.

The second line of evidence comes from the study of a clonal line derived from a single cell of a focal culture. The single-cell isolation, which was done by C. Basilico, was performed under microscopic observation and by using X-rayed mouse embryo cells as feeder-layer. The cell was isolated when the focal line was at its eighth transfer, i.e., 56 days after the original infection. Many attempts to isolate single cells from the first or second transfer of focal lines had been unsuccessful for unforseeable difficulties (see later). At the early transfers, the clonal line gave rise to clones of the thin type only. After six weeks of culturing, however, dense clones of the nodular, strand, and uniform type appeared in a low proportion (0.01 per cent). Cultures from these dense clones gave rise to tumors of walnut size within four weeks (Table 2). Cells forming clones of the dense type had a strong selective advantage *in vitro* and tended to outgrow the other type. This explains why in previous experiments cultures of hamster embryo cells infected with polyoma virus and maintained as mass cultures by regular transfers became ultimately converted into pure cultures of cells of the dense clone type.[7]

The cells of the focal lines were examined for two other properties: the presence of infectious polyoma virus and the presence of chromatid breaks.

The absence of demonstrable virus in the mass cultures of transformed hamster embryo cells at later stages has already been reported, as well as the impossibility of inducing virus release from these cells.[2] Similar negative results were obtained with the focal cultures at early transfers. At the second transfers, 10 to 20 plaque-forming units of polyoma virus were usually found per culture; at the third and later transfers, the cultures contained no infectious virus. Induction experiments

were carried out at the third to sixth transfer of the focal lines. No production of infectious virus or of infectious viral DNA could be obtained after thymidine starvation induced by aminopterin as previously described. X-rays and over-crowding were equally ineffective as inducing agents.

The search for chromatid breaks was prompted by the presence of an often unusually high number of dead cells in the cultures of the focal lines at a time when no polyoma virus could be detected. A measure for chromatid breakage was obtained by scoring mitotic figures at late anaphase and early telophase for the presence of chromatid bridges. Coverslip cultures were prepared at various transfers

TABLE 3

FREQUENCY OF CHROMATID BRIDGES IN FOCAL, NONFOCAL, AND CONTROL LINES

Type of cell line	Line	Transfer	Number of bridges per anaphase							Percentage of anaphases with bridges
			0	1	2	3	4	>4	n	
Focal	592-B1	tr2 (27)‡	23	11	16	18	17	15	100	77.0
		tr3 (31)	16	16	8	4	4	2	50	68.0
	592-B2	tr3 (31)	19	9	3	4	6	9	50	62.0
		tr6 (43)	14	13	10	2	5	6	50	72.0
	612-F41	tr3 (37)	47	25	11	4	7	6	100	53.0
	614-E30	nt* (35)	8	12	7	12	6	5	50	84.0
	614-E98	nt (35)	39	24	17	10	4	6	100	61.0
	620-L48	tr1 (17)	40	15	14	15	4	12	100	60.0
		nt (26)	40	16	15	9	9	11	100	60.0
	622-M26	nt (21)	15	6	6	8	3	2	40	62.5
Non-focal	592-NoF4	tr2 (31)	185	8	3	1	2	1	200	7.5
	612-NoF2	tr1 (23)	88	5	6	1			100	12 0
	612-NoF5	tr1 (23)	97	2			1		100	3.0
	612-NoF9	tr1 (23)	80	12	6	1		1	100	20.0
	612-NoF22	tr1 (24)	91	4	3	1		1	100	9.0
	614-NoF22	tr2 (21)	95	3	1			1	100	5.0
		tr3 (25)	91	2	3	1	1	2	100	9.0
		tr4 (29)	90	6	3	1			100	10.0
Control	592-CoB5	tr2 (24)	91	6		2		1	100	9.0
		tr4 (31)	166	8	7	6	4	9	200	17.0
	598-CoD1	tr2 (25)	91	2	2	1	2	2	100	9.0
	598-CoD2	tr2 (25)	93	3	1	2		1	100	7.0
	598-CoD3	tr2 (25)	90	5	3		2		100	10.0
	588-CoC1-1†	tr4 (28)	34	7	6		1		48	29.0

* nt = no trypsin was used for the growth of these lines.
† This line was derived from an area of unusually high activity.
‡ Numbers in brackets = days after original infection.

of the focal lines; the coverslips were stained with acetic-orcein after fixation with acetic acid-alcohol (3:2).

The results of this investigation are given in Tables 3 and 4. They showed that the proportion of dead cells, as estimated semi-quantitatively, correlated well with the proportion of mitoses which contained chromatid bridges. This proportion was without exception strikingly high (53–84 per cent) at the early transfers; at later transfers, it decreased and progressively tended to that of the controls. The decrease occurred at a variable rate in different focal lines. In general, an abnormal occurrence of bridges could be observed for at least six transfers.

To evaluate the relationship of the presence of chromatid breaks with the transformation of the cells by polyoma virus, the frequency of chromatid bridges in

nonfocal lines and in noninfected control lines is also entered in Table 3. As can be seen from the table, both types of control lines showed a significantly smaller proportion of mitoses with bridges than the focal lines. In these controls, the highest frequency of bridges (29 per cent) was found in a clone of normal cells already mentioned, which showed an unusually high growth ability. Whether these two properties are correlated is unknown.

Since trypsinization is known to induce chromatid breakage,[8] some of the focal lines were grown without trypsinization. The results showed no difference between trypsinized and nontrypsinized cultures.

These observations leave therefore no doubt that the production of chromatid breaks leading to bridge formation is characteristic of the transformation induced by polyoma virus in this *in vitro* system.

TABLE 4

FREQUENCY OF CHROMATID BRIDGES AFTER LONGER PERIODS OF CULTIVATION

Focal line	Transfer	Number of bridges per anaphase							Percentage of anaphases with bridges
		0	1	2	3	4	>4	*n*	
592-B1	tr2 (27)†	23	11	16	18	17	15	100	77.0
	tr3 (31)	16	16	8	4	4	2	50	68.0
	tr6 (43)	23	7	6	7	2	5	50	54.0
	tr10 (56)	71	17	3	4	3	2	100	29.0
592-B1-F1*	tr9 (62)	64	27	4	4	1		100	36.0
592-B1-F2*	tr9 (62)	63	19	12	4	2		100	37.0
592-B1-F3*	tr9 (62)	80	10	5	5			100	20.0
568-26	tr6 (60)	34	12	9	2	3	4	64	47.0
568-43	tr9 (68)	48	17	9	3	7	9	93	48.0
568-61	tr7 (63)	98	43	11	8	2	9	171	43.0
570-80	tr6 (61)	33	6	4	3	1	1	48	31.0
	tr8 (73)	55	4					59	7.0
572-28-6	tr6 (75)	27	17	9	4	1	8	66	59.0
572-29	tr9 (60)	82	12		3		3	100	18.0
	tr12 (74)	79	13	2	2		4	100	21.0
572-78	tr5 (61)	95	4	1				100	5.0
574-30	tr8 (69)	65	20	6	1	1	7	100	35.0
576-18	tr6 (62)	71	21	3	3	1	1	100	29.0
	tr9 (75)	87	9	1	1	1	1	100	13.0
	tr11 (78)	81	17	1			1	100	19.0
580-4	tr9 (84)	88	10				2	100	12.0

* Subcultures from dense clones.
† Numbers in brackets = days after original infection.

Discussion.—The focal lines derived from the infected cultures contain various cell types of which none is present in noninfected cultures. The cell types can be grouped into two main classes: cells forming thin clones and cells forming dense clones. The results described above lead to the conclusion that cells forming thin clones are produced by the primary action of the virus, whereas cells forming dense clones arise from the former type by variation. Only cells forming dense clones have a high degree of transplantability. The neoplastic transformation of normal hamster embryo cells caused by polyoma virus occurs therefore in at least two steps and the action of the virus is twofold: on one hand, it causes the primary transformation of the cells; on the other hand, it provides the mechanism for the additional variation of the transformed cells.

By using a tissue-culture-adapted, rapidly growing line of hamster cells, MacPher-

son and Stoker[10] have obtained transformation to the malignant state in a single step. This finding need not be at variance with the results of the present investigation. In fact, the cells of the line used by these investigators have already spontaneously undergone profound changes which allow their unlimited and rapid multiplication *in vitro*. Thus, a single additional step, caused by the virus, may be sufficient to transform these cells to a malignant state.

The evolution of the focal cultures described in this article is probably one aspect of the phenomenon of *progression*[9] which has been recognized as a constant property of cancers in animals. In the present experiments, the progression appears to be, at least to a certain extent, a necessary consequence of the primary transformation and not a superimposed accidental complication.

Chromatid breaks were observed in a large proportion of the cells of most focal cultures, with the highest frequency during the early transfers. This finding raises the question whether the progression observed in this system is due to gross chromosomal alterations caused by the breaks; such a view would be supported by the preliminary findings of aneuploidy in cells which form dense clones. On the other hand, the chromatid breaks may not be directly involved in the progression; they could rather be a symptom of irregularities in the process of DNA replication in the transformed cells, able to cause several different consequences, including the progression. The inability to find chromatid breaks in one focal line (572–78) may be attributed to a precocious healing of the process causing the breaks, which tends to heal in all lines at later transfers.

The present observations are relevant to the problem of the fate of the viral DNA in the transformed cells. The results previously obtained, that the cells of the dense clones do not contain the viral nucleic acid in a state detectable by infectivity, has now been extended; it has in fact been shown that this is true also for the cells of the thin clones. The results still leave the question open whether the virus-cell interaction which leads to transformation is nonproductive from the start or becomes so after a small number of cell generations.

As pointed out in the past,[2] these results show that autonomously replicating polyoma virus DNA is not present in the transformed cells; they do not, however, exclude the presence of an integrated viral DNA. A new point in favor of the latter possibility is the production of chromatid breaks in the focal lines. These breaks, which are characteristic of the transformed hamster embryo cells, continue to be produced after infectious virus has disappearaed. A continued production of chromosomal alterations and of chromatid breaks has also been observed in human cells transformed by the simian SV40 virus,[11, 12] which is related to polyoma virus, and in cell lines of the Chinese hamster which survived an infection with the DNA-containing herpes virus.[13, 14] The continued production of chromosomal alterations suggests that a specific agent—possibly the viral DNA—is continuously present in these cells after the infection.

Functionally, the primary action of the virus in the transformation of the hamster embryo cells appears to be a release of the regulation of cell multiplication; this is revealed by the ability of the cells of the thin-clone type to form foci. In cells in which this original change has taken place, some of the chromosomal aberrations subsequently produced acquire, at least *in vitro*, a selective value. A stepwise process in this system leads thus finally to the malignant cell.

We gratefully acknowledge the skillful assistance of Mrs. B. Keeley and Mrs. A. Drew.

* This work was aided by grants from the American Cancer Society, Inc., the National Foundation, and the U.S. Public Health Service, Grant No. E5131.

[1] Vogt, M., and R. Dulbecco, these PROCEEDINGS, **46,** 365–370 (1960).
[2] Vogt, M., and R. Dulbecco, *Virology*, **16,** 41–51 (1962).
[3] Dulbecco, R., and G. Freeman, *Virology*, **8,** 396–397 (1959).
[4] Fourfold concentration of amino acids and vitamins + 0.4 mM glycine, 0.4 mM serine, and 0.04 mM inositol.
[5] Puck, T. T., S. J. Cieciura, and A. Robinson, *J. Exp. Med.*, **108,** 945–955 (1958).
[6] Puck, T. T., P. I. Marcus, and S. J. Cieciura, *J. Exp. Med.*, **103,** 273–284 (1956).
[7] Dulbecco, R., and M. Vogt, these PROCEEDINGS, **46,** 1617–1623 (1960).
[8] Levan, A., and J. J. Biesele, *Ann. N.Y. Acad. Sci.*, **71,** 1022–1053 (1958).
[9] Foulds, L., *Canc. Res.*, **14,** 327–339 (1954).
[10] Macpherson, I., and M. Stoker, *Virology*, **16,** 147–151 (1962).
[11] Shein, H. M., and J. F. Enders, these PROCEEDINGS, **48,** 1164–1172 (1962).
[12] Koprowski, H., J. A. Ponten, F. Jensen, R. G. Ravdin, P. Moorhead, and E. Saksela, *J. Cell and Comp. Physiol.*, **59,** 281–292 (1962).
[13] Hampar, B., and S. A. Ellison, *Nature*, **192,** 145–147 (1961).
[14] Hampar, B., and S. A. Ellison, *Abstr. 40th Mtg. IADR*, p. 19 (1962).

---

*SPIN 1/2 WAVE EQUATION IN DE-SITTER SPACE**

BY F. GÜRSEY AND T. D. LEE†

MIDDLE EAST TECHNICAL UNIVERSITY, ANKARA, TURKEY, AND COLUMBIA UNIVERSITY, NEW YORK

Communicated by Robert Serber, November 16, 1962

1. *Introduction.*—The de-Sitter space can be represented by a 4-dimensional pseudo-sphere embedded in a 5-dimensional space. Let $\xi_\mu (\mu = 1, 2, \ldots, 5)$ be the five real coordinates of the 5-dimensional space. The de-Sitter space is described by the surface

$$\xi^\mu \xi_\mu = R^2, \tag{1}$$

where

$$\xi^\mu = \eta^{\mu\nu} \xi_\nu. \tag{2}$$

$\eta^{\mu\nu}$ is the (μ, ν)th matrix element of the diagonal matrix

$$\eta = \begin{pmatrix} 1 & & & & \\ & 1 & & & \\ & & 1 & & \\ & & & -1 & \\ & & & & 1 \end{pmatrix}, \tag{3}$$

and the real constant R is the radius of the pseudo-sphere. The totality of all homogeneous linear transformations among ξ^μ that leave the surface (1) invariant forms a ten-parameter group. In the limit $R \to \infty$, the de-Sitter space becomes simply the usual flat 4-dimensional space, and this ten-parameter group reduces to that of the inhomogeneous Lorentz transformation.

Much of our present knowledge of particle physics are simple consequences of invariance requirements under certain group transformations such as Lorentz transformations, isotopic rotations, etc. It seems, therefore, useful to examine the physical consequences by demanding that the field equations of elementary particles be invariant under the ten-parameter transformations in de-Sitter space.

This problem has been studied by Dirac.[1] His equation for a spin $^1/_2$ particle in the de-Sitter space is given by[2]

$$(^1/_2)\gamma^\mu\gamma^\nu L_{\mu\nu}\chi = \mathrm{R}\lambda\chi, \tag{4}$$

where χ is the wave function,

$$L_{\mu\nu} = -i\left(\xi_\mu \frac{\partial}{\partial\xi^\nu} - \xi_\nu \frac{\partial}{\partial\xi_\mu}\right) \tag{5}$$

and γ^1, γ^2, γ^3, $i\gamma^4$, γ^5 are five *constant* (4×4) Hermitian matrices that satisfy

$$\gamma^\mu\gamma^\nu + \gamma^\nu\gamma^\mu = 2\eta^{\mu\nu}. \tag{6}$$

In the limit $\mathrm{R} \to \infty$, equation (4) becomes the usual Dirac equation in a flat space and λ the mass of this spin $^1/_2$ particle. However, Dirac found that for a finite R the eigenvalue λ must be a complex number with a small imaginary part:

$$\mathrm{Im}(\lambda) = -(2/\mathrm{R}). \tag{7}$$

The physical meaning of this nonzero imaginary part does not appear to be completely clear. The fact that $|\lambda| \geqq (2/\mathrm{R})$ makes, e.g., the equation of a neutrino in the de-Sitter space seem (at least at first sight) somewhat ambiguous, since any equation with $\lambda = 0(\mathrm{R}^{-1})$ would, in the limit of infinite R, approach that of a particle with zero mass.

In this paper, the same problem is investigated from a different approach, by starting from an invariant Lagrangian. The resulting equation differs in form from that obtained by Dirac. With this new form, certain aspects of the physical consequences of invariance in the de-Sitter space become more apparent. For example, the generalization of a two-component theory of the neutrino seems to appear in a natural way. The relation between this new form and equation (4) is discussed.

2. *The Lagrangian.*—We start from the Lagrangian

$$\mathfrak{L} = i\int_D \left[\frac{1}{2}\left(\bar\psi\gamma^\mu \frac{\partial\psi}{\partial\xi^\mu} - \frac{\partial\bar\psi}{\partial\xi^\mu}\gamma^\mu\psi\right) + m\bar\psi\psi\right]\prod_1^5 d\xi^\nu, \tag{8}$$

where ψ is a (4×1) column matrix describing the spin $^1/_2$ particle, $\bar\psi$ is related to its hermitian conjugate $\psi\dagger$ by

$$\bar\psi = \psi\dagger\gamma^4, \tag{9}$$

and the mass of the particle is given by the real number m. In (8), the integration extends over the region D which is bounded by $\rho = \mathrm{R}$

and
$$\rho = \mathrm{R} + \epsilon, \tag{10}$$

where
$$\rho^2 = \xi^\mu\xi_\mu \tag{11}$$

and ϵ is a positive infinitesimal quantity. As $\epsilon \to 0$, D becomes simply the de-Sitter space.

From the definition (8), it is clear that the Hermitian operator $\mathfrak{L}$ is invariant under the ten-parameter transformations in the de-Sitter space. The equation for a spin $^1/_2$ particle is now given by

$$\delta\mathfrak{L} = 0 \tag{12}$$

for arbitrary small variation $\delta\psi$ of the wave function provided that

$$\psi \text{ is independent of } \rho. \tag{13}$$

3. *The Wave Equation.*—Without loss of generality, we introduce the curvilinear coordinates x^μ, which are related to the ξ^μ by

$$\xi^\mu = (x^5/\mathrm{R})f^\mu(x^1, x^2, x^3, x^4), \tag{14}$$

where the five f^μ satisfy the condition[2]

$$f^\mu f_\mu = \mathrm{R}^2 \tag{15}$$

but are otherwise completely arbitrary functions of the four variables x^1, x^2, x^3, and x^4. From (15), it follows that

$$x^5 = \rho. \tag{16}$$

The line element in the five-dimensional space is given by[2]

$$(ds)^2 = d\xi^\mu d\xi_\mu = g_{ij}dx^i dx^j + (d\rho)^2, \tag{17}$$

where

$$g_{ij} = \left(\frac{\partial\xi^\mu}{\partial x^i}\right)\left(\frac{\partial\xi_\mu}{\partial x^j}\right) \tag{18}$$

and the part $g_{ij}dx^i dx^j$ determines its component in the de-Sitter space. It is useful to introduce the five matrices

$$\beta^\mu \equiv \left(\frac{\partial x^\mu}{\partial\xi^\nu}\right)\gamma^\nu. \tag{19}$$

By using (6), (14), and (16), we find

$$\beta^5 = (\xi_\mu\gamma^\mu)/\rho, \tag{20}$$

$$\beta^5\beta^i + \beta^i\beta^5 = 0 \tag{21}$$

and

$$\beta^i\beta^j + \beta^j\beta^i = g^{ij}, \tag{22}$$

where

$$g^{ij} = (\partial x^i/\partial\xi^\mu)(\partial x^j/\partial\xi_\mu). \tag{23}$$

In terms of x^i and β^i, the Lagrangian (8) becomes

$$\mathfrak{L} = i\epsilon\int\left[\frac{1}{2}\left(\bar\psi\beta^i\frac{\partial\psi}{\partial x^i} - \frac{\partial\bar\psi}{\partial x^i}\beta^i\psi\right) + m\bar\psi\psi\right](-g)^{1/2}\prod_1^4 dx^i, \tag{24}$$

where

$$g = [\text{determinant } |g_{ij}|] \times \left(\frac{\mathrm{R}}{\rho}\right)^8 \tag{25}$$

and ψ is a spinor function depending only on x^i. The variational derivative $(\delta\mathfrak{L}/\delta\psi)$ can now be easily carried out. By using the identity (proved in Appendix 1)

$$\frac{\partial}{\partial x^i}\left[(-g)^{1/2}\frac{\partial x^i}{\partial \xi^\mu}\right] = -\frac{4}{\rho^2}\,\xi_\mu\,(-g)^{1/2}, \tag{26}$$

we find the wave equation for a spin $^1/_2$ particle in the de-Sitter space to be

$$\left(\beta^i\frac{\partial}{\partial x^i} - \frac{2}{\rho}\beta^5\right)\psi + m\psi = 0 \tag{27}$$

evaluated at $\rho = \mathrm{R}$.

The conjugate equation of (27) is given by

$$\left(\frac{\partial\bar{\psi}}{\partial x^i}\beta^i - \frac{2}{\rho}\bar{\psi}\beta^5\right) - m\bar{\psi} = 0. \tag{28}$$

4. *Discussion.*—(1) The invariance property of (27) under the ten-parameter transformations in the de-Sitter space can be easily inferred from the structure of $\mathfrak{L}$. It can also be verified by establishing the following commutation relations:

$$\left[J_{\mu\nu},\ \beta^i\frac{\partial}{\partial x^i}\right] = 0 \tag{29}$$

and

$$[J_{\mu\nu},\ \beta^5] = 0, \tag{30}$$

where the ten operators,

$$J_{\mu\nu} \equiv L_{\mu\nu} - \frac{1}{2}i\gamma_\mu\gamma_\nu \tag{31}$$

are the generators of the group of transformations in the de-Sitter space.

(2) By using (26), (27), and (28), it can be readily seen that the current conservation law is given by

$$\frac{\partial}{\partial x^i}\left[(-g)^{1/2}\bar{\psi}\beta^i\psi\right] = 0. \tag{32}$$

(3) For particles of zero mass, we have $m = 0$ and

$$\left(\beta^i\frac{\partial}{\partial x^i} - \frac{2}{\mathrm{R}}\beta^5\right)\psi = 0. \tag{33}$$

Utilizing the anti-commutation relation

$$\beta^5\left(\beta^i\frac{\partial}{\partial x^i} - \frac{2}{\rho}\beta^5\right) + \left(\beta^i\frac{\partial}{\partial x^i} - \frac{2}{\rho}\beta^5\right)\beta^5 = 0, \tag{34}$$

the four-component field ψ can be decomposed into two uncoupled two-component fields $(1 + \beta^5)\psi$ and $(1 - \beta^5)\psi$, each of which can be used as the equation for a two-component neutrino in the de-Sitter space.

(4) To discuss the connection between the de-Sitter space and the usual flat 4-space, it is necessary only to study the behavior of the wave equation within a

small region in the de-Sitter space. Since all points are equivalent, we may choose this region to be the neighborhood of

$$(\xi^1, \xi^2, \ldots, \xi^5) = (0, 0, 0, 0, \mathrm{R}). \tag{35}$$

By setting in (14),

$$\rho = \mathrm{R},$$

$$\xi^i = x^i \tag{36}$$

and neglecting $0(x^i/\mathrm{R})$, we find

$$\beta^\mu = \gamma^\mu. \tag{37}$$

Therefore, all the above equations reduce to the usual ones in the flat space.

It will be shown in the subsequent section that the effects of de-Sitter space actually show up only if terms of the order of R^{-2} [not $0(\mathrm{R}^{-1})$] are kept.

5. *Local Coordinate System (Vierbein).*—To understand more fully the behavior of the wave equation (27), it is convenient to introduce the local coordinate system. Without specifying the particular choice of our curvilinear coordinates x^i, we can choose at every point in the de-Sitter space a local system which is determined by four base vectors $e_a{}^i$ ($a = 1, 2, 3, 4$), where[2]

$$e_a{}^i e_b{}^j g_{ij} = \eta_{ab} \tag{38}$$

and η_{ab} is the (a, b)th matrix element of the matrix η given by (3). The metric of the local system is, therefore, simply given by η_{ab}.

It is useful to define

$$\alpha^i \equiv e_a{}^i \gamma^a. \tag{39}$$

By using (6), (22), and (23), we find that the matrices α^i satisfy the same anti-commutation relations as that between the β^i; i. e.

$$\alpha^i \alpha^j + \alpha^j \alpha^i = 2g^{ij}. \tag{40}$$

Therefore, there exists a transformation matrix S which relates the α^i with the β^i:

$$\alpha^i = S\beta^i S^{-1}. \tag{41}$$

It is shown in Appendix 2 that under the S transformation the wave equation (27) becomes

$$\alpha^i \left(\frac{\partial}{\partial x^i} + \Gamma_i \right) \phi + m\phi = 0, \tag{42}$$

where

$$\phi = S\psi, \tag{43}$$

$$\alpha^i \Gamma_j - \Gamma_j \alpha^i = \left(\frac{\partial \alpha^i}{\partial x^j} \right) + \Gamma^i{}_{jk} \alpha^k, \tag{44}$$

and $\Gamma^i{}_{jk}$ is the usual Christoffel symbol given by

$$\Gamma^i{}_{jk} = \frac{1}{2} g^{ia} \left(\frac{\partial g_{ja}}{\partial x^k} + \frac{\partial g_{ak}}{\partial x^j} - \frac{\partial g_{jk}}{\partial x^a} \right). \tag{45}$$

The above equation (42) is exactly the same as that given by the method[3, 4] of covariant derivative. It must be emphasized that by using covariant derivatives,

the spin $^1/_2$ equation in a space of arbitrary metric can be easily written down. However, in such a derivation there is no requirement that the resulting equation should satisfy any invariance condition. Under a transformation of the coordinate system, the method of covariant derivative merely gives a compact way to transform the equation to the new system. Thus, as a by-product, we also establish the interesting result that, by applying the usual method of covariant derivative to the de-Sitter space, the resulting equation *automatically* satisfies the invariance requirement under the ten-parameter group of transformations.

It is interesting to notice that the matrix β^5 is related to the constant matrix γ^5 by

$$S\beta^5 S^{-1} = \gamma^5. \tag{46}$$

If the mass $m = 0$, then both $(1 + \gamma^5)\phi$ and $(1 - \gamma^5)\phi$ are solutions of (42). In the local coordinate system, the reduction from four to two components proceeds exactly in the same way as that in the flat space.

A particularly convenient and symmetrical coordinate system is given by

$$\xi^i = (x^5/\mathrm{R})(1 + s)^{-1}x^i$$

and

$$\xi^5 = x^5(1 + s)^{-1}(1 - s), \tag{47}$$

where

$$s = (4\mathrm{R}^2)^{-1}x^i x^j \eta_{ij}. \tag{48}$$

In the de-Sitter space,

$$x^5 = \mathrm{R}.$$

Therefore, we have

$$g_{ij} = (1 + s)^{-2}\eta_{ij} \tag{49}$$

and

$$\Gamma^i{}_{jk} = [2(1 + s)\mathrm{R}^2]^{-1}[x^i\eta_{jk} - \delta_j{}^i x_k - \delta_k{}^i x_j], \tag{50}$$

where $\delta_j{}^i = 1$ if $j = i$ and 0 otherwise. In this coordinate system, the wave equation (42) can be written in a particularly simple form in terms of the constant matrices γ^i:

$$(1 + s)\gamma^i \frac{\partial\phi}{\partial x^i} - \frac{3}{4}\mathrm{R}^{-2}(x^i\gamma^j\eta_{ij})\phi + m\phi = 0. \tag{51}$$

It is clear that neglecting terms proportional to R^{-2}, (51) is identical with the usual Dirac equation in the flat space.

6. *Dirac's Form.*—The remaining task is to establish the relation between our basic equation (27) and the equation obtained by Dirac. By using (13) and the identities

$$\beta^5(\gamma^\mu\gamma^\nu L_{\mu\nu}) = 2\rho\gamma^\mu \frac{\partial}{\partial\xi^\mu} - 2\beta^5\rho\frac{\partial}{\partial\rho} \tag{52}$$

and

$$(\gamma^\mu\gamma^\nu L_{\mu\nu})\beta^5 + \beta^5(\gamma^\mu\gamma^\nu L_{\mu\nu}) = 8\beta^5, \tag{53}$$

it can be readily shown that the solution ψ of (27) is related to the solution χ of

$$\frac{1}{2}(\gamma^\mu\gamma^\nu L_{\mu\nu})\chi = \mathrm{R}\lambda\chi \tag{54}$$

by
$$\chi = (1 \pm i\beta^5)\psi \tag{55}$$

and
$$\lambda = \pm m - i(2/\mathrm{R}). \tag{56}$$

Therefore, the mass of the particle is determined only by the real part of λ. The imaginary part of λ has no direct physical meaning; it is merely a result of the fact that $\gamma^\mu\gamma^\nu L_{\mu\nu}$ does not satisfy the hermiticity condition.

Appendix 1.—To prove (26), we first establish the following equations:

(1) By differentiating
$$(\partial\xi/^\nu\partial x^\alpha)(\partial x^i/\partial\xi^\nu) = \delta_\alpha{}^i \tag{A.1}$$

with respect to x^i and by using
$$\left(\frac{\partial x^5}{\partial\xi^\mu}\right)\left(\frac{\partial x^i}{\partial\xi^\nu}\right)\left[\frac{\partial}{\partial x^i}\left(\frac{\partial\xi^\nu}{\partial x^5}\right)\right] = \frac{4\xi_\mu}{\rho^2}, \tag{A.2}$$

we find
$$\frac{\partial}{\partial x^i}\left(\frac{\partial x^i}{\partial\xi^\mu}\right) = -\left(\frac{\partial x^j}{\partial\xi^\mu}\right)\left(\frac{\partial x^i}{\partial\xi^\nu}\right)\left[\frac{\partial}{\partial x^i}\left(\frac{\partial\xi^\nu}{\partial x^j}\right)\right] - \left(\frac{4\xi_\mu}{\rho^2}\right). \tag{A.3}$$

(2) From
$$-\frac{\partial g}{\partial x^i} = -gg^{jk}\left(\frac{\partial g_{jk}}{\partial x^i}\right), \tag{A.4}$$

$$\left(\frac{\partial x^i}{\partial\xi^\mu}\right)\left(\frac{\partial\xi^\nu}{\partial x^i}\right) = \delta_\mu{}^\nu - \left(\frac{\xi_\mu\xi^\nu}{\rho^2}\right), \tag{A.5}$$

and
$$\xi^\mu\left(\frac{\partial x^i}{\partial\xi^\mu}\right) = 0, \tag{A.6}$$

it follows that
$$\frac{\partial}{\partial x^i}(-g)^{1/2} = (-g)^{1/2}\frac{\partial x^j}{\partial\xi^\nu}\frac{\partial}{\partial x^i}\left(\frac{\partial\xi^\nu}{\partial x^j}\right). \tag{A.7}$$

Equation (26) can be readily obtained by using (A.3) and (A.7).

Appendix 2.—We notice that
$$\alpha^i\gamma^5 + \gamma^5\alpha^i = 0.$$

Therefore, under the S-transformation,
$$S\beta^5S^{-1} = \gamma^5, \tag{A.8}$$

and equation (27) becomes
$$\alpha^i\frac{\partial}{\partial x^i}\phi + \alpha^i\Lambda_i\phi - \frac{2\gamma^5}{\mathrm{R}}\phi + m\phi = 0, \tag{A.9}$$

where
$$\Lambda_i = -\left(\frac{\partial S}{\partial x^i}\right)S^{-1} = S\left(\frac{\partial S^{-1}}{\partial x^i}\right). \tag{A.10}$$

It is useful to introduce the reciprocal base vectors $\epsilon_i{}^a$ such that
$$e_a{}^i\epsilon_j{}^a = \delta_j{}^i$$

and $$e_a{}^i\epsilon_i{}^b = \delta_a{}^b. \tag{A.11}$$

Thus, we have $$S^{-1}\gamma^a S = \epsilon_i{}^a\beta^i \tag{A.12}$$

and $$S\gamma^\mu S^{-1} = \frac{\partial\xi^\mu}{\partial x^j}\alpha^j + \left(\frac{\xi^\mu}{R}\right)\gamma^5. \tag{A.13}$$

Upon differentiating (A.12), we find

$$\alpha^j\Lambda_i - \Lambda_i\alpha^j = \frac{\partial\alpha^j}{\partial x^i} - \alpha^k\left(\frac{\partial\xi^\mu}{\partial x^k}\right)\left[\frac{\partial}{\partial x^i}\left(\frac{\partial x^j}{\partial\xi^\mu}\right)\right] - \left(\frac{\xi^\mu}{R}\right)\left[\frac{\partial}{\partial x^i}\left(\frac{\partial x^j}{\partial\xi^\mu}\right)\right]\gamma^5. \tag{A.14}$$

Let us define

$$\Delta_i \equiv \frac{1}{2}\epsilon_j{}^a\eta_{ab}\left(\frac{\xi^\mu}{R}\right)\left[\frac{\partial}{\partial x^i}\left(\frac{\partial x^j}{\partial\xi^\mu}\right)\right]\gamma^5\gamma^b \tag{A.15}$$

and $$\Gamma_i \equiv \Lambda_i - \Delta_i.$$

The commutation between Γ_i and α^j is given by

$$\alpha^j\Gamma_i - \Gamma_i\alpha^j = \left(\frac{\partial\alpha^j}{\partial x^i}\right) - \alpha^k\left(\frac{\partial\xi^\mu}{\partial x^k}\right)\left[\frac{\partial}{\partial x^i}\left(\frac{\partial x^j}{\partial\xi^\mu}\right)\right]. \tag{A.16}$$

Equation (42) now follows by showing that

$$\alpha^i\Delta_i = (2\gamma^5/R) \tag{A.17}$$

and $$\Gamma^i{}_{jk} = -\left(\frac{\partial\xi^\mu}{\partial x^k}\right)\left[\frac{\partial}{\partial x^i}\left(\frac{\partial x^j}{\partial\xi^\mu}\right)\right]. \tag{A.18}$$

* This work was supported in part by the U. S. Atomic Energy Commission.

† On leave of absence from the Institute for Advanced Study, Princeton, New Jersey.

[1] Dirac, P. A. M., *Ann. Math.*, **36**, 657 (1935).

[2] Throughout this paper the natural units $\hbar = c = 1$ are used. All Greek indices such as $\mu, \nu, \ldots$ vary from 1 to 5, all Roman indices such as a, b, i, j, k, . . . vary from 1 to 4, and all repeated indices are to be summed over. In the 5-dimensional space, a covariant five-vector, say f_μ, is related to the contravariant five-vector f^μ, by $f^\mu = \eta^{\mu\nu} f_\nu$.

[3] See, e.g., Bade, W. L., and H. Jehle, *Rev. Mod. Phys.*, **25**, 714 (1953) for a review of the literature on covariant derivatives.

[4] Brill, D. R., and J. A. Wheeler, *Rev. Mod. Phys.*, **29**, 465 (1957), have discussed the motion of a neutrino in an arbitrary gravitational field by using the method of covariant derivative.

*THE RELATIONSHIP OF BODY SIZE, NERVE CELL SIZE, AXON LENGTH, AND GLIAL DENSITY IN THE CEREBELLUM**

By Rejnhard L. Friede†

MENTAL HEALTH RESEARCH INSTITUTE, UNIVERSITY OF MICHIGAN

Communicated by R. W. Gerard, December 14, 1962

It is generally recognized that the nerve cells of large animals are somewhat larger than the nerve cells of small animals. A quantitative comparison of cell size to body size is difficult to establish because of the variations of shape and size of nerve cells, even within one nucleus. Also, measurements of perikarya only are not an adequate determination of total cell volume because of variations in the extent of dendrite ramification.

A comparative study of cell size is facilitated in the cerebellar cortex which, in its anatomical architecture and physiological function, persists remarkably constant throughout phylogenetic development. The diameter of Purkinje cells can be measured with ease. Since all the dendrites extend toward the surface of the molecular layer, the thickness of this layer can be regarded as a parameter of maximal dendrite length. The width of the area covered by dendrite branchings can be estimated by the distance between Purkinje cells if the sections are cut in the plane of dendrite branching, that is, perpendicular to the axis of the gyri. Such measurements of nerve cells, in addition, can be compared with relative changes of glial density. The following provides a short investigation in eighteen species with the aim of indicating trends among species rather than to establish norms for each individual species.

Material and Methods.—The vermis of the cerebellum was investigated in each of the following species: horse, cow, elk, man, deer, lion, sheep, pig, dog, rhesus monkey, cat, rabbit, rat, gerbil, canary, parakeet, mouse, and frog. The tissues were fixed in 10 per cent neutral formalin. Frozen sections, 15 μ and 30 μ thick, were cut exactly perpendicular to the axis of the gyri and were stained with chromalum gallocyanin. The sections were mounted in glycerin-gel, thus eliminating shrinkage from dehydration. Measurement in many brains of rat and man[8] had shown that the individual variations of such measurements were quite small; this was in agreement with Ellis'[3] observation.

The following methods were used for measurements:

A. *The thickness of the molecular layer* was measured between its surface and an imaginary line through the center of the majority of Purkinje cells; from 27–90 measurements were made for each species; the fewer measurements were made if there was little scatter of the data.

B. *The area ratio of molecular to granular layer* was determined by planimetric measurements of drawings of sections projected on cardboard. In these drawings, large pieces of cortex, including several convolutions, were separated from the rest of the cortex by lines which cut each layer at 90°. The area of granular and molecular layer then was measured planimetrically.[7, 8]

C. *The maximal diameter of Purkinje cells* was measured in a plane parallel to the cortical surface; about 50 measurements were made per species. Hyperchromic shrunken cells were disregarded. The volume of the cells was calculated, assuming

spherical shape. This represented only an approximation, and the true volume was assumed to be somewhat larger. This difference, however, evidently did not affect the comparison of species.

D. *The distance between Purkinje cells* in a 15 μ section was determined by projecting and drawing the cerebellar cortex on cardboard. The actual length of a given portion of Purkinje cell layer between two easily recognizable landmarks was calculated from comparison with a millimeter scale projected on the same drawing. Then the tissue section was studied microscopically and Purkinje cells distinguishable between the above-mentioned landmarks were counted.

There is an error inherent in counting particles of different sizes in tissue sections of equal thickness; thus, the counts were corrected by using Abercrombie's formula[1] to eliminate a distortion of the data due to the species difference of Purkinje cell size. From these data, the number of "nuclear points" of Purkinje cells per mm of Purkinje layer in a 15 μ section was calculated. Since the distance between Purkinje cells is different in the gyri than in the sulci,[7, 2] equal portions of both were included.

E. *The glial density (Bergmann cells) in the Purkinje layer* was also determined. An arbitrary definition of the thickness of the Purkinje layer had to be used because of the gradual transition between the Purkinje layer and the molecular layer. This was done using two parallel lines of an object micrometer as delineation of the Purkinje layer; in the tissue, these lines represented a distance of 31.9 μ. The deeper line touched tangentially the deep circumference of the majority of Purkinje cells. All glial cells between the two lines were counted through several continuous millimeters of cortical length. Approximately 800 cells were counted per species. Care was taken not to count granular cell nuclei displaced into the Purkinje layer. These were distinguished from Bergmann glial cells by their spherical shape, smaller size, and darker staining. The data from *D* and *E* permitted one to calculate the number of glial cells per one Purkinje cell. The data in Table 1 represent counts corrected for both size of Purkinje cells and size of glial cells. As stated in paragraph *D* above, Abercrombie's formula[1] was used for the corrections.

F. *The glial density per volume of molecular layer* was counted with an ocular net micrometer. No attempt was made to distinguish between types of glial cells, but endothelial nuclei were counted separately. The latter were identified by their attachment to the basal membrane of vessels which were easily distinguishable in glycerin-gel mounted sections with the condenser in a lowered position. The counts in Table 1 represent the total number of all nuclei minus the number of nuclei unquestionably identified as endothelial or vascular cells. The data in Table 1 represent an average of 50 counts each.

G. Determination of the true *average axonal length of Purkinje cells* is practically impossible. The majority of these axons terminate in the cerebellar nuclei; others bypass them and terminate in the vestibular nuclei.[11] The radius of the vermis should provide a rough estimate for the probable differences of axonal length among species. Since the diameter of the vermis varies greatly in different directions, the following method was developed: the area of a median-sagittal section of the vermis was measured planimetrically. This area was considered a circle. The radius of this circle represented a factor which characterized differences, among species, in average axon lengths of the Purkinje cells of the vermis. It is logical that the axons in a

TABLE 1*

	Cow	Man	Horse	Sheep	Elk	Pig	Dog	Deer	Lion
Average radius of vermis in mm (factor indicating "axon length").	37	36	27	27	23	23	22	18	17
Glial cells per one Purkinje cell.	53	44	50	43	46	21	25	33	43
Body weight in grams.	500,000	160,000	650,000	50,000	386,000	250,000	13,000	65,000	125,000
Diameter of Purkinje cells in μ; (vol. of Purkinje cells 1000μ^3 in parentheses).	32 ± 2 (17)	27 ± 1 (10)	31 ± 2 (16)	31 ± 2 (16)	27 ± 1 (10)	29 ± 2 (13)	30 ± 1 (14)	29 ± 2 (13)	29 ± 2 (13)
Thickness of molecular layer in μ (factor indicating "dendrite length").	409 ± 48	398 ± 18	416 ± 56	383 ± 25	380 ± 19	375 ± 27	378 ± 19	364 ± 23	318 ± 12
Spacing of Purkinje cells ("dendrite spread").	43	61	42	43	50	37	37	49	43
Glial cells per volume in the molecular layer.	22 ± 4	29 ± 4	28 ± 4	23 ± 3	21 ± 3	12 ± 2	22 ± 3	18 ± 3	24 ± 4
Basal metabolic rate calories/kilogram/day.	16	24	?	26	?	14	36	?	?
Ratio of molecular layer to granular layer.	1.52	1.58	1.64	1.50	1.52	1.50	1.69	1.58	1.41

	Monkey	Cat	Rabbit	Gerbil	Rat	Parakeet	Canary	Mouse	Frog
Average radius of vermis in mm (factor indicating "axon length").	17	11.5	9.5	5.5	5	5	5	3	0.1
Glial cells per one Purkinje cell.	17	18	15	9	9	9	6	5	1
Body weight in grams.	3,200	3,000	3,500	100	200	30	16	20	50
Diameter of Purkinje cells in μ; (vol. of Purkinje cells 1000μ^3 in parentheses).	26 ± 1 (9)	30 ± 1 (14)	22 ± 1 (6)	18 ± 1 (3)	16 ± 1 (2)	20 ± 1 (4)	18 ± 1 (3)	19 ± 1 (4)	7 ± 2 (1.5)
Thickness of molecular layer in μ (factor indicating "dendrite length").	328 ± 16	402 ± 14	292 ± 10	216 ± 27	199 ± 16	234 ± 23	207 ± 21	156 ± 12	240
Spacing of Purkinje cells ("dendrite spread").	27	31	34	14	22	9	9	10	8
Glial cells per volume in the molecular layer.	35 ± 5	22 ± 4	17 ± 3	58 ± 11	50 ± 8	49 ± 6	60 ± 8	50 ± 4	24 ± 8
Basal metabolic rate calories/kilogram/day.	48	50	47	?	130	225	310	170	?
Ratio of molecular layer to granular layer.	1.64	1.63	1.50	1.31	1.61	1.37	1.40	1.22	0.73?

* Since all measurements were done in the vermis, the species were listed in order of the average radium of the vermis (factor indicating "axon length"); this arrangement was considered more proper than either body weight (which can be quite misleading; e.g., in the pig) or brain weight (which depends largely on the development of the hemispheres). The order used in Table 1 places deer and lion, for some unknown reason, lower than one would place them according to their body size.

4-mm cerebellum are about 1/10 of those in a 4-cm cerebellum, even if the true length of any given axon is not known. The lengths of projections to the vestibular nuclei will vary proportionally and will, therefore, not affect the usefulness of this factor.

Results.—The results of the measurements are collected in Table 1. This table is self-explanatory, but a few comments may be in order to interpret the observations.

1. *The ratio of molecular layer-granular layer* was surprisingly constant among the species, except for a slight decrease in the smaller species. This observation agreed with previous investigations,[7, 2] which indicated that the ratio of molecular layer to granular layer in various mammals represents a constant and biologically important parameter. Large shifts of this ratio in human brain are pathological and represent a sensitive indicator of edema.[8]

2. *The size of the Purkinje cells* increased with body size, but the extent of increase did not nearly keep pace with that of body size. The diameter of the Purkinje cells of the cow, for example, was only about twice that of the mouse. A comparison of cell volume and body weight evidenced a crude logarithmic relationship of nerve cell size and body size (Fig. 1). There was considerable scatter of the measurements, but one cannot anticipate that a more precise prediction of the size of a nerve cell could be made from body weight.

Since all the dendrites of the Purkinje cells extend toward the surface of the molecular layer, its thickness provided an estimate for average dendrite length.

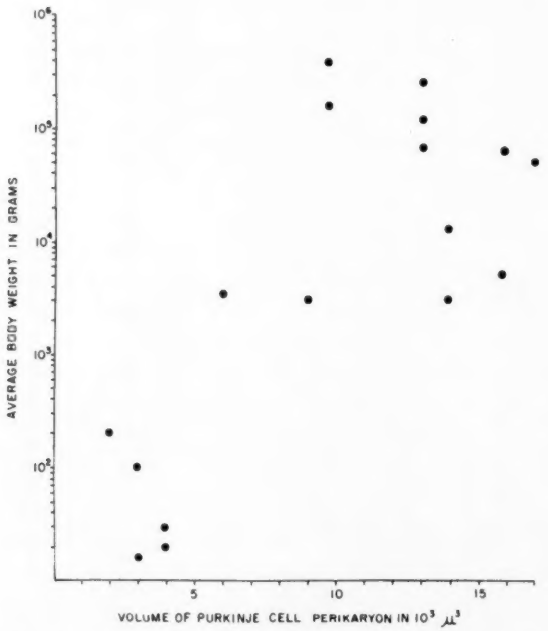

FIG. 1.—Data from Table 1: Scatter graph showing the logarithmic relationship of body weight and volume of the perikarya of Purkinje cells.

The thickness of the molecular layer increased proportionally with the increase of the diameter of Purkinje cells. Therefore, the ratio of cell size to dendritic ramification could be assumed to be approximately constant for Purkinje cells. In the developing rat brain, Ellis[3] observed an increase of the thickness of the molecular layer with body weight.

Since the dendrites of Purkinje cells branch within a two-dimensional plane, the distance between Purkinje cells can provide a parameter of the lateral extent of dendrite spread. The distance between Purkinje cells increased somewhat more than did either the diameter of the Purkinje cells or thickness of the molecular layer. If one assumes that there was also a change of spacing in depth, the disproportion between thickness of the molecular layer and the spacing of Purkinje cells is understandable. It would seem, therefore, that the increases of the size of perikarya, of the dendrite length, and of the dendrite spread were in proportion with each other.

Tentative measurements of the nuclei of granular cells were made. The diameter of these nuclei likewise increased with body size: the diameter increased from 4 μ in the canary to 7 μ in the horse, the rest of the species being graded accordingly.

3. *The ratio of glia cells to Purkinje cells* (glia index) in the Purkinje layer increased with body size and cell size, but showed the best correlation with average axon length (Fig. 2). A simple calculation showed that not only the glia-Purkinje cells ratio, but also the absolute glial density in the Purkinje layer, increased with brain size. Measurements of the diameter of Bergmann-glia nuclei showed a scatter between 6 and 8 μ, without a consistent trend of change.

4. One would expect that the *glial cell density of the molecular layer* would be fairly constant, that is, the same number of glial cells available for a given volume of molecular layer or length of dendrites. It was surprising, therefore, to observe striking differences of the glial density of the molecular layer among species. These data did not show evident correlation with any other measurement. Since it is known that brain respiration[4, 12, 13] and respiratory enzyme activity,[5, 15] as well as basal metabolic rate, vary inversely with body size, we added, in Table 1, some data on the basal metabolic rate from Spector's handbook.[14] This section was incomplete, as no such comparison had been intended at the beginning of the investigation.

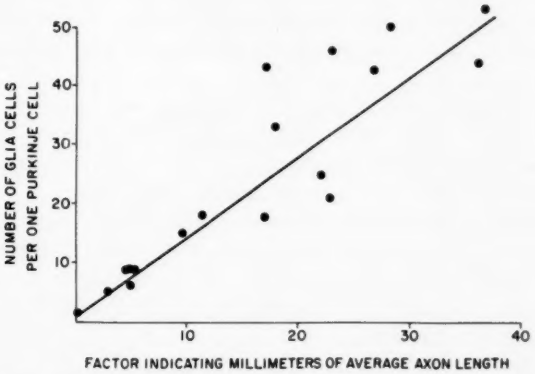

FIG. 2.—Data from Table 1: Scatter graph showing the linear relationship between average axon cells per one Purkinje cell.

It was suggested, however, that high glial density in the molecular layer might have some relationship with high basal metabolic rate.

Discussion.—The increase of the size of Purkinje cells shows a *logarithmic* relationship to the increase of body size. Axon length, on the other hand, must inherently increase in a *linear* relationship with brain size. That implies that nerve cells in large brains have to maintain a relatively much larger volume of axoplasm than nerve cells in small brains. This difference is even more evident if one considers that all of the increase of the perikarya of nerve cells could be accounted for by the increased length and ramification of their dendrites; thus, there would be virtually no increase of the perikaryon to account for the longer axon. Our data suggest that the difference in proportion between the perikarya and their processes, particularly the axon length, is compensated by a numerical increase of attached glia cells. The glial cells themselves are not markedly larger in larger species. The number of glial cells per Purkinje cell was in a surprisingly good linear relation with the average axon length. This observation is in agreement with previous findings in Clarke's column,[9] where the number of perineuronal glial cells showed a linear relation to axon length. (Clarke's column facilitated the investigation of this relationship because the approximate lengths of the axons of large cells depended on the segment in which the cell bodies were residing.) Likewise, nuclei with short intra-nuclear connections have very few glial cells per nerve cell, while nuclei with long projections showed more glial cells per nerve cell.[9] The number of glial cells per nerve cell generally increased with brain size.[6] Hawkins and Olszewski[10] showed very high glia-indices in the whale cortex.

All these observations support the theory that glial cells serve as "auxiliary metabolic units"[9] which are attached to the nerve cells when there is an increased metabolic demand on the nerve cells. The addition of glial cells could be homologous to the hypertrophy of cells in other organs.

An increased demand may be conditioned *anatomically* by the proportion of perikaryon to axon. Increased demand, on the other hand, may be conditioned *physiologically* by the metabolic rate of the nerve cell; no anatomical factor, for example, could be invoked to explain the marked variations of glial cell density per volume of molecular layer. Physiological factors, such as the metabolic rate, might be considered. The actual glial density of the nucleus, therefore, probably represents the result of a complex interaction of several anatomical and physiological factors.

Summary.—Measurements of the thickness of layers, cell size, and glial density were made in the cerebellar cortex of 15 species. The ratio of molecular layer per granular layer was remarkably constant. The size of the perikarya of the Purkinje cells increased in a roughly logarithmic relation with body size. Dendrite length and dendrite spread increased in proportion with the perikarya. The number of glial cells per Purkinje cell showed a linear relationship to average axon length. The glial density per volume of molecular layer, in contrast, was not related to any anatomical factor; tentative comparison suggested a crude correlation with the basal metabolic rate of the species.

The author wishes to thank Dr. William Field, D. V. M., Lansing, for his help and cooperation in providing specimens of elk, deer, and lion.

* This investigation was supported by U. S. Public Health Grant B-3250.

† The author wishes to acknowledge the technical assistance of Albert Vossler.

[1] Abercrombie, M., *Anat. Record*, **94**, 239 (1946). Abercrombie's formula: $P = A \times M/(L + M)$ (P = average number of nuclear points per section; A = crude count; M = thickness of section; L = particle size. Explanation: "Ideal points" would be found in only one tissue section each. Particles of finite size will be cut once or more depending on both their dimensions and the thickness of the sections. This represents a source of error in counting particles in tissue sections, which can be corrected with the above formula.

[2] Braitenberg, V., and R. P. Atwood, *J. Comp. Neuro.*, **109**, 1 (1958).

[3] Ellis, R. S., *J. Comp. Neuro.*, **32**, 1 (1920).

[4] Elliott, K. A. G., *J. Neurophys.*, **11**, 437 (1948).

[5] Fried, G. H., and S. R. Tipton, *Proc. Soc. Exp. Bio. Med.*, **82**, 531 (1953).

[6] Friede, R. L., *Acta Anat.*, **20**, 290 (1954).

[7] Friede, R. L., *Acta Anat.*, **25**, 65 (1955).

[8] Friede, R. L., *A. M. A. Arch. Neuro.*, **8**, 67(1963).

[9] Friede, R. L., and W. H. van Houten, these PROCEEDINGS, **48**, 817 (1962).

[10] Hawkins, A., and J. Olszewski, *Science*, **126**, 76 (1957).

[11] Jansen. J., and A. Brodal, in *Aspects of Cerebellar Anatomy* (Oslo: Tanum, 1954).

[12] Krebs, H. A., *Biochem. Biophys. Acta*, **4**, 249 (1950).

[13] Locker, A., and R. M. Kaps, *Z. ges. exp. Med.*, **134**, 29 (1960).

[14] Spector, W. S., ed., *Handbook of Biological Data* (Philadelphia: Saunders, 1956).

[15] Vernberg, F. J., *Biol. Bull.*, **106**, 360 (1954).

---

*FINE STRUCTURAL CHANGES IN HEART MUSCLE IN RELATION TO THE LENGTH-TENSION CURVE**

BY E. H. SONNENBLICK, D. SPIRO, AND T. S. COTTRELL

DEPARTMENTS OF MEDICINE AND PATHOLOGY, COLLEGE OF PHYSICIANS AND SURGEONS, COLUMBIA UNIVERSITY

Communicated by Dickinson W. Richards, December 12, 1962

It is the purpose of this communication to relate the ultrastructure of heart muscle to its physiological performance as precisely defined by increasing muscle length along the length-tension curve. The ascending limb of the active length-tension curve has been explored with special interest since it is the only physiologically functional portion of the curve. These studies provide support for the view that cardiac muscle shortening occurs by a change of configuration of thin (presumably actin) filaments relative to fixed thicker filaments (presumably myosin). This is consistent with a "folding" model for contraction[1] but cannot be reconciled with a "sliding" model as proposed for skeletal muscle.[2]

Methods.—Papillary muscles were obtained from the right ventricles of cats (1.0–1.5 kg) anaesthetized with intraperitoneal sodium pentobarbital (25 mg/kg). Details of this preparation have been described elsewhere.[3] Papillary muscles measured 5 to 11 mm unstretched with a cross-sectional area (calculated on the basis of weight, assuming the muscle to be a cylinder) of 0.9 to 1.3 mm.[2] The muscle was placed in Krebs solution bubbled with a mixture of 95% O_2 and 5% CO_2. The base of the muscle was firmly fixed while its upper free end was tied by wire to a tension transducer (Statham G1–1000). The tension transducer could be moved with a micrometer stage allowing the length of the muscle to be changed at will. The muscle was stimulated with a Grass Pulse Generator (Model S4). Resting (or passive) and active isometric tension were continuously recorded on a Sanborn multichannel oscillograph.

The initial length (L_0) of the papillary muscle was ascertained at zero resting tension. Muscle

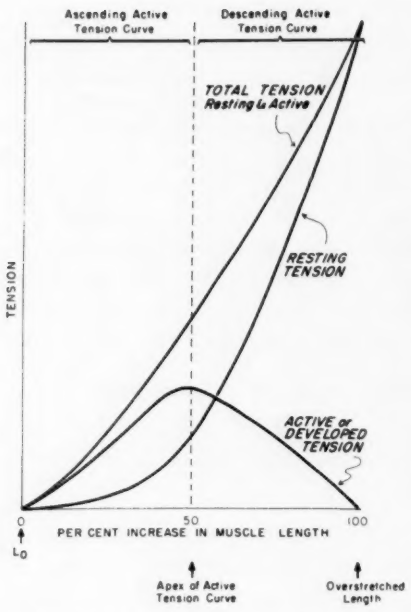

FIG. 1.—Length Tension (LT) relation of cat papillary muscle, from a typical experiment. Total tension = resting (or passive) plus active (or developed) tension.

length could then be increased at known increments above L_0. Recorded tension without stimulation was called *resting tension*. With stimulation, an active contraction was superimposed on the resting tension. This developed tension was termed *active tension*, while the sum of resting and active tension denoted *total* tension. The relation between muscle length and tension comprised the length tension (*LT*) curve as shown in Figure 1.

After a period of equilibration (generally 1 hr), the *LT* curve of the stimulated muscle was explored. Once this was defined, a muscle length was selected at a known place on the length-tension curve and stimulation stopped. The muscle was then fixed for electron microscope study.

Muscles were fixed in the myograph for 30 min with a solution of 6.25% glutaraldehyde in phosphate buffer at pH 7.4.[4] Tension was continuously recorded during the fixation process. Glutaraldehyde was specifically chosen for initial fixation since it produced less change in muscle tension during the fixation process than conventional osmium tetroxide. Muscles were further fixed in the glutaraldehyde solution for an additional 3 hr and then washed in phosphate buffer for 12 hr. Thin strips of muscle tissue were post-fixed in osmium tetroxide and embedded in araldite according to a previously described procedure.[5] Thin sections were cut with attention to orient the myofibrils parallel to the cutting edge in order to avoid compression artifacts.[6] Sections were examined in a well-calibrated RCA EMU 3F electron microscope with care being taken to normalize all lenses to insure reproducibility in electron optical magnification. Preservation of cytological structure was noted to be excellent.

Results.—The length-tension curves of 16 cat papillary muscles have been explored. Resting (or passive) tension is zero when active (or developed) tension approaches zero. This muscle length is called L_0. As muscle length is increased both resting and active tension rise. Active tension reaches a maximum with an average increment in muscle length of 45 per cent (range 41–52%) over L_0, marking the *apex* of the active tension curve. With continued muscle extension, resting tension rises precipitously while active tension declines. At this point, considerable stress relaxation is first observed. The portion of the curve approaching the apex of the active tension curve is called the *ascending* limb of the active tension curve while the curve beyond this point is termed the *descending* limb of the active length-tension curve (see Fig. 1). Zero active tension is approached on the descending limb of the curve with approximately a 100 per cent increase in muscle length above L_0.

Papillary muscles fixed for electron microscope study at different places along the length-tension curve have been studied. Sarcomere lengths (*Z* to *Z* line measurement) as well as *A* and *I* bands and *H* zone widths were carefully analyzed (see Fig. 8).

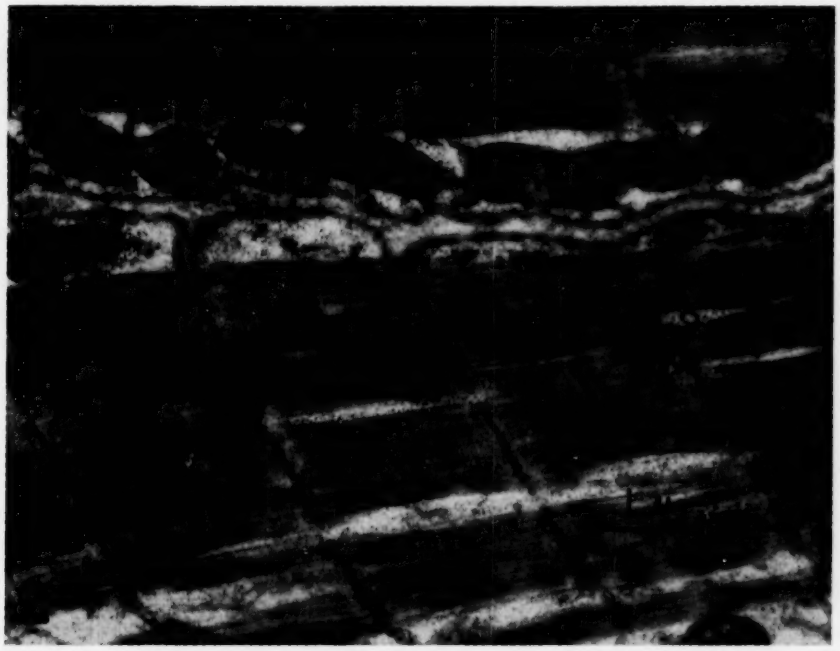

FIG. 2.—No *I* bands are present in this electron micrograph of papillary muscle fixed at L_0 (7 mm) as noted in Fig. 1. × 20,000.

In Figure 2 an electron micrograph (*EM*) of a papillary muscle fixed at L_0 is shown. Sarcomere lengths at L_0 are quite uniform (1.5 μ). In all specimens at L_0 sarcomere lengths range from 1.4 to 1.6 μ. No *I* band is present although a small *H* zone is consistently seen.

As muscle length is extended along the ascending limb of the active tension curve, sarcomere length increases with the appearance of an *I* band. This is shown in Figure 4. In all instances, increases in sarcomere length are accounted for by lengthening of the *I* band only. Slight variation in *I* band width is occasionally noted, but *A* and *H* band widths remain constant relative to L_0.

At the apex of the active length-tension curve (Figs. 5 and 6), the over-all sarcomere length is 2.2 μ. In all specimens at this length, sarcomere length ranged from 2.1 to 2.4 μ. No change in the *H* zone is noted despite a prominent increase in the *I* band which accounts for the increase in sarcomere length. No change in the *A* band is found.

With continued increments in muscle length (Figs. 7 and 8), active tension declines and sarcomere length increases somewhat further (2.5–2.8 μ) due to lengthening of the *I* band. However, *I* band lengthening does not totally account for increments in over-all muscle length. Again, no significant changes in the width of the *A* band or *H* zone are observed.

The relation of band widths (*A*, *I*, and *H*) to sarcomere lengths are shown in Figure 9. As noted *I* band width is a linear function of sarcomere length, while *A*

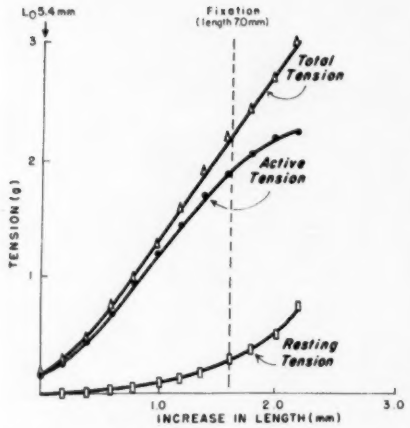

FIG. 3.—LT curve of cat papillary muscle fixed on ascending limb of the active tension curve. L_0 5.4 mm. Prefixation tension 0.7 *g*, postfixation 0.9 *g*.

band (1.5 μ) and *H* zone (0.125 μ) are constant. This results in the inverse *A*/*I* ratio to sarcomere length.

Discussion.—Previous studies of skeletal[7] and cardiac muscle[5] have demonstrated that the sarcomere, which is the fundamental structural and functional unit of contraction, consists of two sets of partially interdigitating filaments. Thicker filaments, probably composed of myosin,[8, 9] are limited to the *A* band including the central *H* zone. Thinner filaments, presumably containing actin[8, 9] course from the *Z* lines through the *I* and *A* bands and terminate at the edges of the *H* zones. Thus, there is an overlapping array of both the thick and thin filaments only within the *A* band. On the basis of these and other observations, a "sliding" filament model has been proposed for skeletal muscle contraction.[10, 11] This hypothesis maintains that with contraction thin actin filaments slide by thick myosin filaments without major changes in filament lengths or

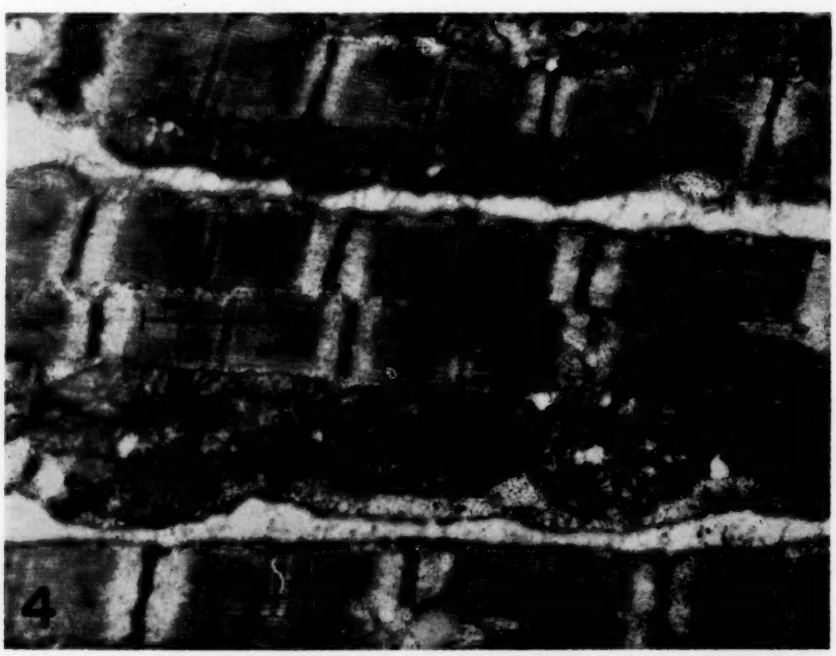

FIG. 4.—Papillary muscle as fixed in Fig. 3 on the ascending portion of the LT curve. Small I bands are seen but lengths of *A* bands and *H* zones are similar to those in Fig. 2. × 20,000.

configuration. The morphological support for this theory rests in large part on an increase in the width of the *H* zone and *I* bands with passive stretch, indicating a decrease in thick and thin filament overlap within the *A* band which itself remains constant in length.[10-12]

In heart muscle, the *H* zone, consisting of a narrow light area bisected by a dark central *M* line, measures a constant 0.125 μ at all sarcomere lengths. Passive stretch produces an increase in sarcomere length by an increase in the *I* band width without a change in length of *A* band or *H* zone. This suggests that thin myofilaments are fixed centrally and are stretched with increasing muscle length. These findings would indicate that when muscle shortening occurs as a result of narrowing of the *I* band a folding of thin filaments must take place within the *A* band—unless one were to suggest that filaments pass through the center of the sarcomere or "pile up" at the *H* zone. Neither of these latter views is supported by the present findings. Even in supercontracted heart muscle, we have observed that an *H* zone is present despite the appearance of contracture bands at the *Z* lines. Thus, these results provide support for the view that cardiac muscle shortening derives from a change in thin (actin) filament configuration relative to thick (myosin) filaments which is the essential postulate of a thermodynamically analyzed "folding" model.[1] Furthermore, these findings are not consonant with a purely "sliding" model.[2, 10, 11] The present study also shows that in heart muscle the increases in sarcomere length, and thus the increases in the length of the thin actin filaments prior to the onset of contraction, form the structural basis of the ascending active length-tension curve. This then represents the ultrastructural counterpart of the classical Frank-Starling relation.[13, 14]

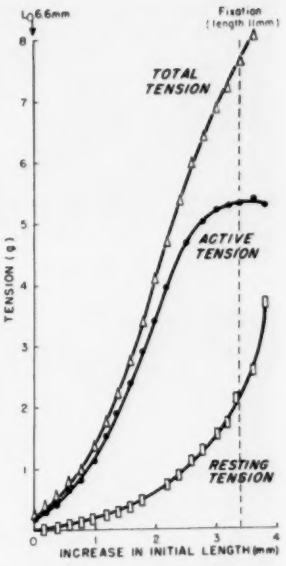

FIG. 5.—LT curve of cat papillary muscle fixed at the apex of the active tension curve. L_0 6.6 mm. Cross section 1.2 mm.[2] Prefixation resting tension 2.1 *g*, postfixation 2.3 *g*.

In overstretched heart muscle (L_0 + 100%), the over-all length increment cannot be explained entirely by changes in sarcomere band widths and thus by further lengthening of their filaments. The possibility of slippage of individual heart muscle cells relative to one another may be suggested here.

It should be noted that observations of sarcomere band widths, on which a sliding model for skeletal muscle depends, have been made primarily on the descending limb of the active length-tension curve[12] and do not furnish an explanation for the ascending physiologically important portion of the curve. Furthermore, the light optical observations made along the ascending portion of the curve do not provide sufficient resolution for accurate definition of band widths.[10, 11] We have re-explored this problem with respect to frog sartorius skeletal muscle using techniques identical to those employed in the present study. On the ascending portion of the active length-tension curve, results analagous to those observed for heart muscle have been found, namely, a change in *I* band proportional to changes in sarcomere

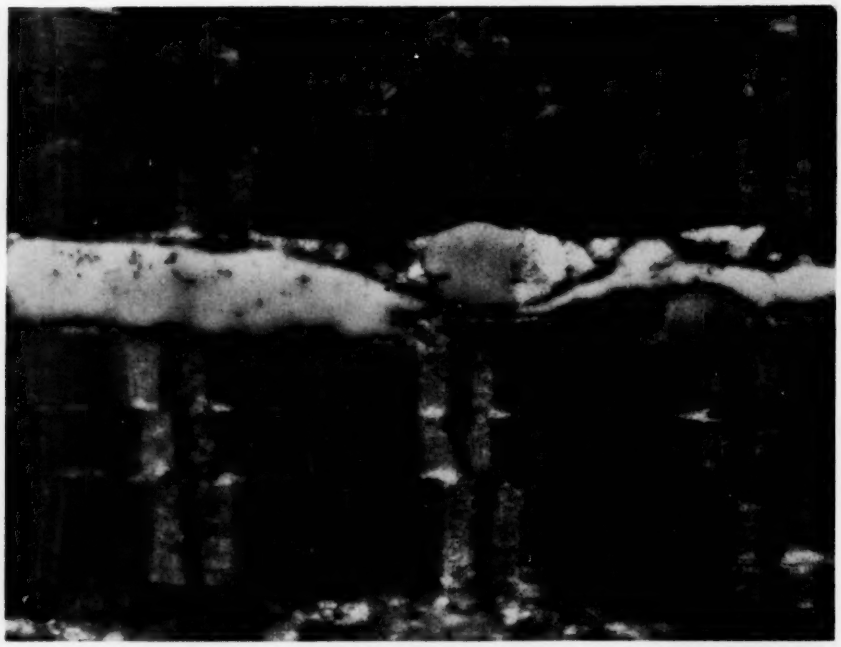

FIG. 6.—Papillary muscle as fixed in Fig. 5 at the apex of the LT curve. *I* bands are increased in length relative to Fig. 4, but *A* bands and *H* zones show no changes in length.

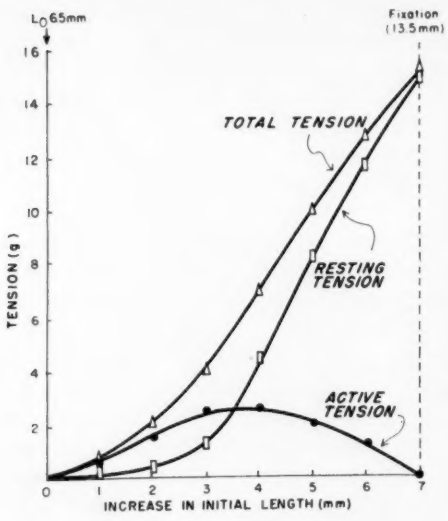

FIG. 7.—LT curve of papillary muscle fixed when active tension approached zero on the descending limb of the active tension curve. L_0 6.5 mm. Prefixation tension 15.2 *g*, postfixation 12.8 *g*.

length with but relatively little change in the *H* zone.[15] However, when the skeletal muscle is taken to the apex of the active length-tension curve and beyond, the *H* zone enlarges as previously shown,[7] a situation clearly different from that existing in heart muscle.

Summary.—The ultrastructure of cat papillary muscle has been studied in relation to the resting and active length-tension curve. Sarcomere structure has been analyzed at known increments in muscle length. It is observed that: (1) Increasing muscle length increases sarcomere length from 1.5 μ at L_0, where resting and active tension approach zero, to 2.2 μ at the apex of the active length-tension curve. The apex of the active length-tension is attained with a 45 per cent increase

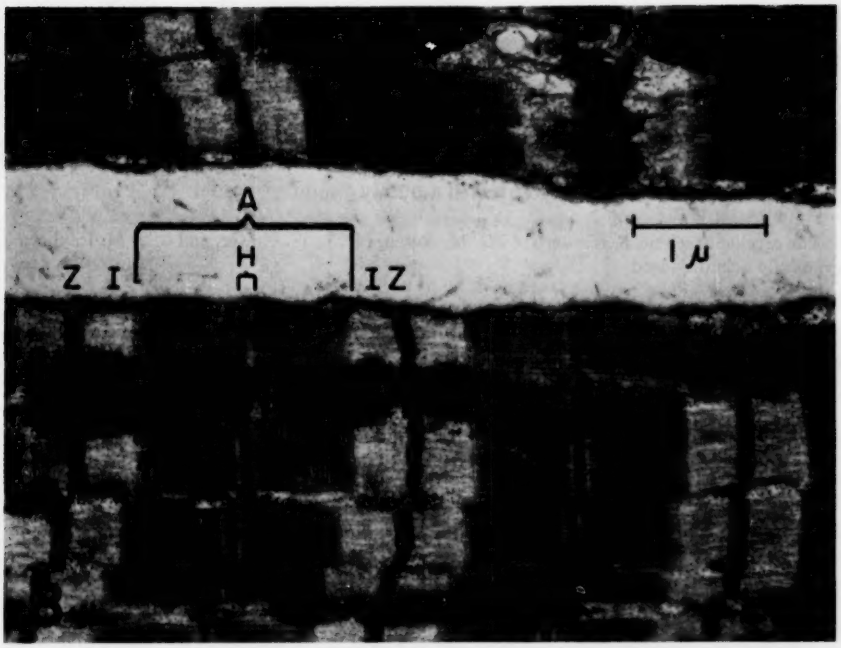

FIG. 8.—Papillary muscle as fixed in Fig. 7 at over-stretched length. *I* bands are further increased in length but *A* and *H* are again unchanged. × 20,000.

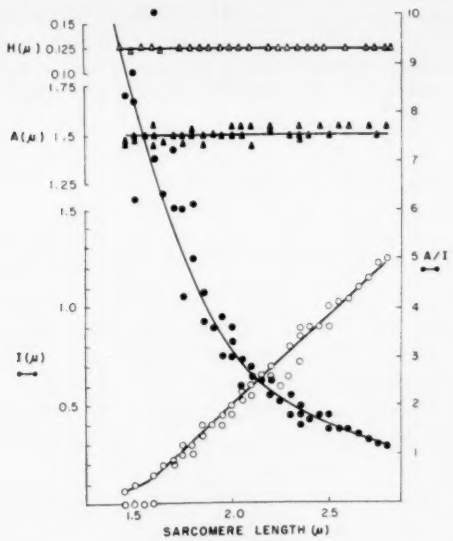

FIG. 9.—Relation of sarcomere length to the width of *A*, *I*, and *H* bands. Sarcomeres have been measured randomly from papillary muscles encompassing the entire LT curve.

in muscle length above L_0. With further increments in muscle length, active tension declines, approaching zero again with an extension of 100 per cent over L_0. (2) The I band is absent at L_0 and increases as a function of sarcomere length. (3) No change in the H band occurs over the entire length-tension curve. Similarily, the A band is constant.

These observations support a "folding" myofilament model for myocardial contraction and are not consistent with a purely "sliding" model.

The excellent technical assistance of Mr. M. Rosen, Mr. L. W. Koster, and Miss M. Rayborn is gratefully acknowledged.

* This work was supported by grants H7247 and H5906 from the National Heart Institute, U. S. Public Health Service, and by the Health Research Council of the City of New York under contract U-1075, and USPHS training grant 2G-865.

[1] Podolsky, R. J., *Ann. N. Y. Acad. Sci.*, **72,** 522 (1959).

[2] Huxley, A. F., in *Progress in Biophysics* (London: Pergamon Press, 1957), vol. 7, pp. 255–318.

[3] Sonnenblick, E. H., *Am. J. Physiol.*, **202,** 931 (1962).

[4] Sabatini, D. D., K. G. Bench, and R. J. Barrnett, *Fifth International Congress of Electron Microscopy* (Academic Press, New York, 1962), vol. 2, L 3.

[5] Stenger, R. J., and D. Spiro, *J. Biophys. and Biochem. Cytol.*, **9,** 325 (1961).

[6] Spiro, D., *J. Biophys. and Biochem. Cytol., Suppl.*, **2,** 157 (1956).

[7] Huxley, H. E., and J. Hanson, *Structure and Function of Muscle* (New York: Academic Press, 1960), vol. 1, p. 183.

[8] Hasselbach, W., *Z. ges. Naturwiss.*, **86:b,** 449 (1953).

[9] Hanson, J., and H. E. Huxley, *Nature*, **172,** 530 (1953).

[10] Huxley, H. E., and E. J. Hanson, *Nature*, **173,** 973 (1954).

[11] Huxley, A. F., and R. Niedergerke, *Nature*, **173,** 971 (1954).

[12] Carlsen, F., G. G. Knappeis, and F. Buchthal, *J. Biophys. and Biochem. Cytol.*, **11,** 95 (1961).

[13] Starling, E. H., *Linacre Lecture* on "The Law of the Heart" (New York: Longmans, Green, 1918).

[14] Frank, O., *Z. Biol.*, **32,** 370 (1895).

[15] Spiro, D., T. S. Cottrell, and E. H. Sonnenblick, *Fed. Proc.*, **21** (in press, 1962).

LYAPUNOV FUNCTIONS FOR THE PROBLEM OF LUR'E IN AUTOMATIC CONTROL*

By R. E. Kalman

RESEARCH INSTITUTE FOR ADVANCED STUDY (RIAS), BALTIMORE, MD.

Communicated by S. Lefschetz, December 18, 1962

1. About 1950, Lur'e[1] initiated the study of a class of (closed-loop) control systems whose governing equations are

$$dx/dt = Fx - g\varphi(\sigma), \qquad d\xi/dt = -\varphi(\sigma), \qquad \sigma = h'x + \rho\xi. \tag{L}$$

In (L), σ, ξ, ρ are real scalars, x, g, h are real n-vectors, and F is a real $n \times n$ matrix. The prime denotes the transpose. F is stable (all its eigenvalues have negative real parts). $\varphi(\sigma)$ is a real-valued, continuous function which belongs to the class A_κ: $\varphi(0) = 0, 0 < \sigma\varphi(\sigma) < \sigma^2\kappa$.

We ask: Is the equilibrium state $x = 0$ of (L) g.a.s. (globally asymptotically stable) for any $\varphi \in A_\kappa$?

2. This problem is related to the well-known 1946 conjecture of Aizerman: *If* (L) *is g.a.s. for every linear* $\varphi \in A_\kappa$, *then it is also g.a.s. for any* $\varphi \in A_\kappa^1$. In this crude form, however, Aizerman's conjecture was found to be false, and Lur'e was led to consider a more special situation:[1, 2]

Problem of Lur'e. *Find conditions on* ρ, g, h, *and* F *which are necessary and sufficient for the existence of a Lyapunov function* V *of a special type (namely* V = *a quadratic form in* (x, σ) *plus the integral of* $\varphi(\sigma)$*) which assures g.a.s. of* (L) *for any* $\varphi \in A_\infty$.

This is essentially an algebraic problem.

3. Even if $\varphi(\sigma) = \epsilon\sigma$, with $\epsilon > 0$ and arbitrarily small, (L) can be g.a.s. only if $\rho > 0$. This follows easily by examining the characteristic equation of (L) when $\varphi(\sigma) = \epsilon\sigma$. Henceforth, it will be always assumed that $\rho > 0$.

4. The best information available to date concerning the Problem of Lur'e is the highly important 1961

Theorem of Popov.[3] *Assume that* F *is stable and that* $\rho > 0$. *Then* (L) *is g.a.s. if the condition*

$$\mathrm{Re}(2\alpha\rho + i\omega\beta)[h'(i\omega I - F)^{-1}g + \rho/i\omega] \geqq 0 \quad \textit{for all real } \omega \tag{P}$$

holds for $2\alpha\rho = 1$ *and some* $\beta \geqq 0$.

Popov has also studied, but did not resolve, the question of existence of a Lyapunov function which assures g.a.s. whenever (P) holds. We shall settle this question completely and at the same time solve the Problem of Lur'e.

5. In the same paper, Popov proved also: *Consider the most general function* $V(x, \sigma)$ *which is a quadratic form in* (x, σ) *plus a multiple of the integral of* $\varphi(\sigma)$:

$$V(x, \sigma) = x'Px + \alpha(\sigma - h'x)^2 + \beta\int_0^\sigma \varphi(\sigma)d\sigma + \sigma w'x \quad (\alpha, \beta \text{ real}). \tag{1}$$

If for any $\varphi \in A_\epsilon$ $(\epsilon > 0)$ *the function* $V \geqq 0$ *and* $\dot{V}$ *(its derivative along solutions of* (L)*) is* $\leqq 0$, *then* $w = 0$.

Assuming $w = 0$, V will be nonnegative for any $\varphi \in A_\infty$ if and only if $\alpha \geqq 0$,

$\beta \geqq 0$, and $P = P' \geqq 0$ (nonnegative definite). From (L) and (1) (with $w = 0$), we get

$$\dot{V}(x, \sigma) = x'(PF + F'P)x - 2\varphi(\sigma)x'(Pg - \alpha\rho h - (1/2)\beta F'h) - \beta(\rho + h'g)\varphi^2(\sigma) - 2\alpha\rho\sigma\varphi(\sigma). \quad (2)$$

$\dot{V} \leqq 0$ for any $\varphi \in A_\infty$ implies $\gamma = \beta(\rho + h'g) \geqq 0$. If

$$\text{(a) } Q = -PF - F'P, \qquad \text{(b) } \sqrt{\gamma}q = r = Pg - \alpha\rho h - (1/2)\beta F'h, \quad (3)$$

defines Q, q, and r, we can write $\dot{V}$ as

$$\dot{V}(x, \sigma) = -[x'(Q - qq')x + (\sqrt{\gamma}\varphi(\sigma) + q'x)^2 + 2\alpha\rho\sigma\varphi(\sigma)]. \quad (4)$$

If $\gamma > 0$, $\dot{V} \leqq 0$ for any $\varphi \in A_\infty$ if and only if $Q - qq' \geqq 0$. If $\gamma = 0$, $\dot{V} \leqq 0$ for any $\varphi \in A_\infty$ if and only if $r = 0$ and $Q \geqq 0$. (In this case, q is not defined by (3b) but may be picked always so that $Q \geqq qq'$.)

6. Our solution of the Lur'e Problem will utilize and extend results of Popov,[3] Yakubovich,[4] and LaSalle.[5] In addition, the following observation is of crucial technical importance.

By the writer's canonical structure theorem,[6] F, g, h defining a linear subsystem of (L) may be replaced by F_{BB}, g_B, and h_B (notations of ref. 6), without loss of generality as far as the g.a.s. of (L) is concerned. In fact, $h'(i\omega I - F)^{-1}g$ in (P) is equal to $h_B'(i\omega I - F_{BB})^{-1}g_B$.

Hence it may and *it will be assumed without loss of generality that the pair* (F, g) *is completely controllable and* (F, h') *is completely observable.*

All that is needed from controllability theory[7] in the subsequent discussion is the lemma:

The following statements are equivalent: (i) (F, g) *is completely controllable;* (ii) $\det [g, Fg, \ldots, F^{n-1}g] \neq 0$; (iii) $x'[\exp Ft]g \equiv 0$ *for all* t *implies* $x = 0$; (iv) g *does not belong to any proper* F*-invariant subspace of* R^n.

By definition, (F, h') *is completely observable if and only if* (F', h) *is completely controllable.*

7. THEOREM (Solution of the Problem of Lur'e). *Consider* (L), *where* $\rho > 0$, F *is stable,* (F, g) *is completely controllable, and* (F, h') *is completely observable. We seek a suitable Lyapunov function* V *from the class defined by* (1).

(A) $V > 0$ *and* $\dot{V} \leqq 0$ *for any* $\varphi \in A_\infty$ *(hence* V *is a Lyapunov function which assures Lyapunov stability of* $x = 0$ *of* (L) *for any* $\varphi \in A_\infty$*) if and only if* $w = 0$ *and there exist real constants* α, β *such that* $\alpha \geqq 0$, $\beta \geqq 0$, $\alpha + \beta > 0$, *and* (P) *holds.*

(B) *Suppose* V *satisfies the preceding conditions. Then* V *is a Lyapunov function which assures g.a.s. of* (L) *if and only if either* (i) $\alpha \neq 0$ *or* (ii) $\alpha = 0$ *and the equality sign in* (P) *occurs only at those values of* ω *where* $\mathrm{Re}\{h'(i\omega I - F)^{-1}g\} \geqq 0$.

(C) *There is an "effective" procedure for computing* V.

The constants α, β whose existence is required are precisely those used in (1) to define V.

8. The principal tool in the proof of the theorem is the following result, itself of great interest in linear system theory:

MAIN LEMMA. *Given a real number* γ, *two real* n*-vectors* g, k, *and a real* $n \times n$ *matrix* F. *Let* $\gamma \geqq 0$, F *stable, and* (F, g) *completely controllable. Then* (i) *a real* n*-vector* q *satisfying*

$$\text{(a)}\quad F'P + PF = -qq', \qquad \text{(b)}\quad Pg - k = \sqrt{\gamma}q \tag{5}$$

exists if and only if

$$(1/2)\gamma + \operatorname{Re}\{k'(i\omega I - F)^{-1}g\} \geqq 0 \quad \textit{for all real } \omega. \tag{6}$$

Moreover, (ii) $X_1 = \{x : x'Px = 0\}$ *is the linear space of unobservable states*[6] *relative to* (F, k'); (iii) q *can be "effectively" computed;* (iv) (5) *implies* (6) *even if* qq' *is replaced by* $qq' + R$, *where* $R = R' \geqq 0$.

Observe that (5a) and the stability of F imply that P is symmetric, nonnegative definite.

9. *Proof of the Main Lemma:* Necessity: Add and subtract $i\omega I$ from (5a). Multiply (5a) by $(i\omega I - F)^{-1}$ on the right and by $(-i\omega I - F')^{-1}$ on the left. Using (5b) yields

$$2\operatorname{Re}\{k'(i\omega I - F)^{-1}g\} = |q'(i\omega I - F)^{-1}g|^2 - 2\sqrt{\gamma}\operatorname{Re}\{q'(i\omega I - F)^{-1}g\}, \tag{7}$$

which implies (6). Adding $R = R' \geqq 0$ to qq' in (5a) does not diminish the right-hand side of (7). Hence (iii).

Sufficiency, We exhibit a constructive procedure for finding q, hence V. Let a_k be the coefficient of s^k in the polynomial $\det(sI - F) = \psi(s)$. Let $e_n = g$, $e_{n-1} = Fg + a_{n-1}g, \ldots, e_1 = F^{n-1}g + a_{n-1}F^{n-2}g + \ldots + a_0 g$. Because (F, g) is completely controllable, these vectors are linearly independent, hence form a basis for R^n. Relative to this basis, F, g, and h have the form

$$F = \begin{pmatrix} 0 & 1 & & \\ & \ddots & \ddots & \\ & & & 1 \\ -a_0 & \cdots & -a_{n-2} & -a_{n-1} \end{pmatrix}, \quad g = \begin{pmatrix} 0 \\ \vdots \\ 0 \\ 1 \end{pmatrix}, \quad h = \begin{pmatrix} b_0 \\ \vdots \\ b_{n-2} \\ b_{n-1} \end{pmatrix}.$$

Using the theory of the Laplace transformation, etc.,[8] it follows that

$$h'(sI - F)^{-1}g = (b_0 + \ldots + b_{n-1}s^{n-1})/\psi(s). \tag{8}$$

This formula identifies the components of any vector q (relative to the basis $e_1, \ldots, e_n$) with the numerator coefficients of the rational function $q'(sI - F)^{-1}g$.

Setting $s = i\omega$ and assuming (6), we can write

$$\gamma + 2\operatorname{Re}\{k'(i\omega I - F)^{-1}g\} = |\theta(i\omega)|^2/|\psi(i\omega)|^2 \geqq 0, \tag{9}$$

where θ is a polynomial in $i\omega$ of degree n with real coefficients.

θ is determined as follows. The numerator of the left-hand side of (9) is the polynomial $\Gamma(-\omega^2) = [\gamma - 2k'F(\omega^2 I + F^2)^{-1}g] \cdot [\det(\omega^2 I + F^2)]$. Since Γ has real coefficients and is nonnegative, its zeros λ_k are complex conjugate and of even multiplicity if real, negative. The zeros of $\Lambda(i\omega) = \Gamma(-\omega^2)$ are $\pm\sqrt{\lambda_k}$ and occur in complex conjugate pairs. The reflection of a pair of complex conjugate zeros of Λ about the imaginary axis is also a pair of zeros of Λ. Therefore $\theta(i\omega)$ exists and may be taken, e.g., as the product of all factors of Λ with left-half-plane zeros. θ so defined has complex conjugate zeros and therefore it is a polynomial with real coefficients. The above choice of θ is not unique, but convenient.

Since the leading coefficient of θ is $\sqrt{\gamma}$, $\nu = -\theta + \sqrt{\gamma}\psi$ is a polynomial of (formal) degree $n - 1$. If the coefficients of ν, arranged in the order of ascending powers, are identified with the vector q, then $\nu(i\omega)/\psi(i\omega) = q'(i\omega I - F)^{-1}g$ by (8). By retracing the steps of the necessity proof, it is easily verified that q so defined satisfies (5).

Let $X_1 = \{x : q'[\exp Ft]x \equiv 0\}$. By (5a), $x_1 \in X_1$ if and only if $x_1'Px_1 = 0$. Then (5b) implies $k'[\exp Ft]x_1 \equiv 0$. Hence, $X_1 \subset X_2 = \{x : k'[\exp Ft]x \equiv 0\}$. But it can be shown[8] that dim $X_1 = \{$degree of the largest common divisor of ν, $\psi\}$ $= \{$degree of largest common divisor of the numerator and denominator of $k'(i\omega I - F)^{-1}g\}$ = dim X_2. Hence, $X_1 = X_2$, which implies (ii) and completes the proof of the main lemma.

A weaker version of this lemma was proved by Yakubovich.[4]

10. *Proof of Part A of the Theorem:* Define $k = \alpha\rho h + (1/2)\beta F'h$.

Sufficiency. (a) *If* $\alpha \geqq 0, \beta \geqq 0$, *then condition* (P) *implies the following:* $\gamma \geqq 0$ *and there is a* q *satisfying* (3b). Indeed, if $\beta = 0$, then obviously $\gamma = 0$. If $\beta > 0$, then the left-hand side of (P) tends asymptotically to $\rho + h'g$ as $|\omega| \geqq \infty$ so that $\rho + h'g$ and hence γ must be nonnegative. By the definition of k, (P) is equivalent to (6). Since $\gamma \geqq 0$, the main lemma shows that q exists and satisfies (5*b*), which is the same as (3b).

(b) If $Q = qq'$ then P, Q satisfy (3a) because P, qq' satisfy (5a). Thus we have constructed a V of the form (1), and $V \geqq 0$ and $\dot{V} \leqq 0$ for any $\varphi \in A_\infty$.

(c) *If* $\alpha \geqq 0$, *and* (P) *holds, then* V *is positive definite if* $\alpha + \beta > 0$. Indeed, if either $\alpha = 0$ or $\beta = 0$, the pair (F, k') is completely observable because so is (F, h'). By (ii) of the main lemma $P > 0$. If both $\alpha, \beta > 0$, then again by (ii) of the main lemma $x'Px = 0$ only if $k'[\exp Ft]x \equiv 0$. But there is no $x \neq 0$ for which this condition can hold jointly with $h'x = 0$, because that would contradict complete observability of (F, h'). Hence, $P + \alpha hh' > 0$. Thus V is positive definite.

Necessity. Suppose $V > 0$ and $\dot{V} \leqq 0$. Then $\alpha \geqq 0, \beta \geqq 0$, and $\alpha + \beta > 0$ are certainly necessary; moreover, there must exist P, Q, and q satisfying (3) and we must have also $\gamma \geqq 0$, $Q = qq' + R$ ($R = R' \geqq 0$.) Since (3) corresponds to (5), it follows by (i) of the main lemma that (6) is satisfied. (6) is equivalent to (P), so that (P) is necessary.

11. *Proof of Part B of the Theorem.* Let V be the Lyapunov function constructed in §10. We recall Theorem VIII of ref. 9 (p. 66): *If* $V > 0$ *and* $\dot{V} \leqq 0$, *then every solution bounded for* $t > 0$ *tends to some invariant set contained in* $\dot{V} = 0$. Thus to establish g.a.s. of (L) we have to show that (a) every solution of (L) is bounded, and (b) the only invariant set of (L) in $\dot{V} = 0$ is $\{0\}$.

(a) This can be proved by exactly the same technique as was used by LaSalle[5] in similar context.

(b) We seek a solution $(x(t), \sigma(t))$ of (L), not identically zero, whose values lie in its own positive limit set as well as in $\dot{V} = 0$. Since V may be multiplied by a positive constant, there are two cases to be considered:

(i) Let $2\alpha\rho = 1$. By (4) $\dot{V} = 0$ only if $\sigma(t) \equiv 0$. so that $h'x(t) = -\rho\xi_0 =$ const. Moreover, $x(t) = [\exp Ft]x_0$ since $\varphi \equiv 0$. But $x_0 \neq 0$ would contradict complete observability of (F, h').

(ii) Now let $\alpha = 0$. By (4) $\dot{V} = 0$ implies

$$\sqrt{\gamma}\varphi(\sigma(t)) \equiv -q'x(t). \tag{10}$$

If $q'x(t) \equiv 0$, we have again the previous case. Otherwise $\gamma > 0$. Then $x(t)$ is the solution of the linear differential equation $dx/dt = (F + \gamma^{-1/2}gq')x$. By (a) above $x(t)$ is bounded. Hence $x(t)$ can lie in its own positive limit set only if it is almost periodic. Therefore at least one pair of eigenvalues of $F + \gamma^{-1/2}gq'$ must be $\pm i\omega_k \neq 0$, which implies that (6) holds with the equality sign at $\omega = \omega_k$. But then (10) and the requirement $\mathrm{Re}\{h'(i\omega_k I - F)^{-1}g\} \geqq 0$, $k = 1, 2, \ldots$ are incompatible. Hence $\{0\}$ is the only invariant set in $\dot{V} = 0$.

On the other hand, the modified condition (P) in (*B-ii*) of the theorem is necessary for g.a.s. since it is the Nyquist stability criterion for linear functions in A_-.

12. Even if we drop the assumption of complete controllability and observability of the subsystem (F, g, h), the theorem remains valid with respect to the completely controllable and completely observable state variables (x_B, σ). Since F is stable, $F_{AA}, \ldots, F_{DD}$ (see ref. 6) must be also stable. Thus, our theorem actually implies g.a.s. of the entire system (L), i.e., of the variables (x, σ). In particular, it implies Popov's theorem.

The question then arises whether the Lyapunov function (1), constructed on (x_B, σ), can be extended to (x, σ). If (P) holds as a strict inequality (so that $\dot{V} < 0$), this is quite easy to show and was explicitly pointed out by Morozan[10] using Yakubovich's version of our main lemma. But if $\dot{V} \leqq 0$, it seems unlikely that an explicit Lyapunov function can be constructed in general which specializes to (1) on (x_B, σ).

I am greatly indebted to Professor S. Lefschetz for his constant interest and encouragement during the course of this research.

* This research was supported in part by the U.S. Air Force under Contracts AF 49(638)-382 and AF 33(657)-8559 as well as by the National Aeronautical and Space Administration under Contract NASr-103.

[1] Lur'e, A. I., *Nekotorye Nelineinye Zadachi Teorii Avtomaticheskogo Regulirovaniya* (Moscow: Gostekhizdat, 1951).

[2] Letov, A. M., *Stability in Nonlinear Control Systems*, translation of USSR edition of 1955 (Princeton University Press, 1961).

[3] Popov, V. M., "Absolute stability of nonlinear systems of automatic control," *Avt. i Telemekh.*, **22**, 961–979 (1961).

[4] Yakubovich, V. A., "The solution of certain matrix inequalities in automatic control theory," *Dokl. Akad. Nauk USSR*, **143**, 1304–07 (1962).

[5] LaSalle, J. P., "Complete stability of a nonlinear control system," these PROCEEDINGS, **48**, 600–603 (1962).

[6] Kalman, R. E., "Canonical structure of linear dynamical systems," these PROCEEDINGS, **48**, 596–600 (1962).

[7] Kalman, R. E., Y. C. Ho, and K. S. Narendra, "Controllability of Linear Dynamical Systems," in *Contributions to Differential Equations* (New York: Interscience-Wiley, to appear, 1963), vol. 1.

[8] Kalman, R. E., "Mathematical description of dynamical systems," *SIAM J. of Control*, 1963 (to appear).

[9] LaSalle, J. P. and S. Lefschetz, *Stability by Lyapunov's Direct Method* (New York: Academic Press, 1961).

[10] Morozan, T., "Remarques sur une Note de V. Yakoubovitsch," *C. R. Acad. Sci. (Paris)*, **254**, 4127–4129 (1962).

*REGULARITY AT THE BOUNDARY OF THE $\bar{\partial}$-NEUMANN PROBLEM**

By J. J. Kohn

DEPARTMENT OF MATHEMATICS, BRANDEIS UNIVERSITY

Communicated by D. C. Spencer, December 17, 1962

1. *Introduction.*—In this note, we formulate the regularity theorem 5.13 and outline the method of proof. We also show (in section 6) how the regularity theorem implies the existence of the operator N which solves the $\bar{\partial}$-Neumann problem. The detailed account of the work discussed here will appear in the second part of a paper by the author.[1] The $\bar{\partial}$-Neumann problem has various applications, including a representation of the $\bar{\partial}$-cohomology by harmonic forms and several existence theorems for holomorphic functions on complex and almost-complex manifolds.[1-3]

A variant of the $\bar{\partial}$-Neumann problem was first formulated by Garabedian and Spencer.[4] The $\bar{\partial}$-Neumann problem in its present form was investigated by Spencer and the author[5] by means of singular integral equations. The main result of this note is based on the basic *a priori* estimates I and II which are described in section 3. Morrey[3] proved I in the case of (0,1)-forms on sufficiently small tubular neighborhoods of real analytic manifolds (obtained by complexification). Morrey's discovery of this estimate was the author's starting point for the solution of the problem.[6] M. E. Ash[7] established I by means of calculations with respect to moving frames; this method enabled him to prove I in greater generality. The introduction of moving frames also simplifies the statement and derivation of II.

The method of proving regularity by studying the families of norms depending on the parameters δ and τ was suggested to the author by L. Hörmander; essential use is made of some results (stated in section 4) which are developed in his book.[8]

2. *Notation.*—Let M' be a Hermitian complex analytic manifold of complex dimension n and let M be an open submanifold of M', such that $\bar{M}$ (the closure of M) is compact and bM (the boundary of M) is a C^∞ submanifold of real dimension $2n-1$. We denote by $\mathfrak{A}^{p,q}$ the space of C^∞ complex-valued forms on M of type (p,q); in terms of local holomorphic coordinates $z^1, \ldots, z^n$, a form $\phi \in \mathfrak{A}^{p,q}$ is given by: $\phi = \phi_{I\bar{J}} dz^I d\bar{z}^J$, where I and J run through all the ordered p-tuples and q-tuples of integers between 1 and n; and $dz^I = dz^{i_1} \wedge \cdots \wedge dz^{i_p} d\bar{z}^{j_1} \wedge \cdots \wedge d\bar{z}^{j_q}$.

The complex gradient $\bar{\partial}$: $\mathfrak{A}^{p,q} \to \mathfrak{A}^{p,q+1}$ is defined by

$$\bar{\partial}\phi = \phi_{I\bar{J},\bar{k}}\, d\bar{z}^k \wedge dz^I d\bar{z}^J \tag{2.1}$$

where

$$\phi_{I,\bar{J}\bar{k}} = \frac{1}{2}\left(\frac{\partial \phi_{I\bar{J}}}{\partial x^k} + \sqrt{-1}\,\frac{\partial \phi_{I\bar{J}}}{\partial y^k}\right)$$

and $x^k = Re(z^k)$, $y^k = Im(z^k)$.

Let $\mathfrak{A}^{p,q}$ be the subspace of $\mathfrak{A}^{p,q}$ consisting of those forms which can be extended to C^∞ forms on M' (i.e., forms which are C^∞ up to and including the boundary). If $\phi, \psi \in \mathfrak{A}^{p,q}$ we define

$$(\phi, \psi) = \int_M \langle \phi, \psi \rangle dV \qquad \text{and} \qquad \|\phi\|^2 = (\phi, \phi), \tag{2.2}$$

where $\langle \phi, \psi \rangle$ is the inner product at each point which is induced by the Hermitian

metric. Let $\mathfrak{L}^{p,q}$ denote the Hilbert space obtained by completion under this inner product. Let $\mathfrak{d}$: $\mathfrak{A}^{p,q} \to \mathfrak{A}^{p,q-1}$ be the formal adjoint of $\bar{\partial}$, that is, $\mathfrak{d}\phi$ is defined by requiring that

$$\int_M \langle \mathfrak{d}\phi, \psi \rangle dV = \int_M \langle \phi, \bar{\partial}\psi \rangle dV$$

for all compactly supported $\psi \in \mathfrak{A}^{p,q-1}$.

Now let T be the closure of $\bar{\partial}$ and let $\mathfrak{D}_T{}^{p,q}$ denote the domain of T, so that T: $\mathfrak{D}_T{}^{p,q} \to \mathfrak{L}^{p,q+1}$. Let T^* be the Hilbert space adjoint of T then T^*: $\mathfrak{D}_T{}^{p,q} \to \mathfrak{L}^{p,q-1}$. Further, let $\mathfrak{D}^{p,q} = \mathfrak{D}_T{}^{p,q} \cap \mathfrak{D}_T{}^{*p,q}$. Then $\mathfrak{D}^{p,q}$ is a Hilbert space under the inner product $\mathbf{D}(\phi, \psi)$ defined by

$$\mathbf{D}(\phi, \psi) = (T\phi, T\psi) + (T^*\phi, T^*\psi) + (\phi, \psi). \tag{2.3}$$

Let $L = TT^* + T^*T$, L: $\mathfrak{D}_L{}^{p,q} \to \mathfrak{L}^{p,q}$. It can be shown[1] that L is self-adjoint and that $L + I$ is the Friedrich's representative of $\mathbf{D}$, i.e., if $\phi \in \mathfrak{D}_L{}^{p,q}$ then

$$\mathbf{D}(\phi, \psi) = ((L + I)\phi, \psi) \tag{2.4}$$

for all $\psi \in \mathfrak{D}^{p,q}$.

For each $P \in M'$, we denote by $R(P)$ the geodesic distance of P to bM. Let r: $M' \to \mathbf{R}$ be a C^∞ function such that in some neighborhood of bM we have

$$r(P) = \begin{cases} \sqrt{2}\, R(P) & \text{if } P \notin M \\ -\sqrt{2}\, R(P) & \text{if } P \in M. \end{cases} \tag{2.5}$$

Finally, for each non-negative real number τ we define

$$(\phi, \psi)_\tau = \int_M \langle \phi, \psi \rangle w_\tau dV \quad \text{and} \quad \|\phi\|_\tau{}^2 = (\phi, \phi)_\tau, \tag{2.6}$$

where

$$w_\tau(P) = \exp \tau |r(P)|.$$

Observe that the norms $\| \ \|_\tau$ are all equivalent. On the space $\mathfrak{D}^{p,q}$, we define the corresponding family of inner products:

$$\mathbf{D}_\tau(\phi, \psi) = (T\phi, T\psi)_\tau + (T^*\phi, T^*\psi)_\tau + (\phi, \psi)_\tau. \tag{2.7}$$

3. *The a priori estimates.*—Let $\dot{\mathfrak{D}}^{p,q} = \mathfrak{D}^{p,q} \cap \dot{\mathfrak{A}}^{p,q}$, then we have:

3.1. THEOREM. *If M is strongly pseudo-convex then there exists $C > 0$, such that*

$$E(\phi)^2 \leq C\mathbf{D}(\phi, \phi) \tag{I}$$

for all $\phi \in \mathfrak{D}^{p,q}$ with $q > 0$, and $E(\phi)$ is defined by

$$E(\phi)^2 = \|\phi\|_{\frac{1}{2}}{}^2 + \int_{bM} |\phi|^2 dS + \|\phi\|^2, \tag{3.2}$$

where

$$\|\phi\|_{\frac{1}{2}}{}^2 = \sum_{\alpha,I,J,k} \int_{U_\alpha \cap M} |\phi_{I,\bar{J},\bar{z}k}|^2 dV, \tag{3.3}$$

$\{U_\alpha\}$ is a finite covering of M by holomorphic coordinate systems, and dS is the volume element in bM.

If $P_0 \in bM$, let U be a coordinate neighborhood with origin at P_0 such that (2.4) holds in U. Now let $\zeta^1, \ldots, \zeta^n$ be a set of (1,0)-forms which at each point is a basis of the (1,0)-forms and such that $\zeta^n = \partial r$. If u is a differentiable function on U then we define u_{ζ^i} and $u_{\bar{\zeta}^i}$ by

$$u_{\zeta^i} = \langle du, \zeta^i \rangle \quad \text{and} \quad u_{\bar{\zeta}^i} = \langle du, \bar{\zeta}^i \rangle, \tag{3.4}$$

where the $\bar{\zeta}^i$ are conjugates of the ζ^i. In $U \cap M$, in terms of the ζ's $\phi \in \mathfrak{A}^{p,q}$ is given by

$$\phi = \phi_{I\bar{J}} \zeta^{IJ}, \tag{3.5}$$

where $$\zeta^{I\bar{J}} = \zeta^{i_1} \wedge \cdots \wedge \zeta^{i_p} \wedge \bar{\zeta}^{j_1} \wedge \cdots \wedge \bar{\zeta}^{j_q}.$$

The following lemma is obtained by integration by parts.

3.6 LEMMA. *If $\phi \in \dot{\mathfrak{A}}^{p,q}$, then a necessary and sufficient condition for $\phi \in \dot{\mathfrak{D}}^{p,q}$ is $\phi_{I\bar{J}} = 0$ on bM whenever $n \in J$, where $\phi_{I\bar{J}}$ are the components of ϕ described by (3.5).*

If u is a differentiable function on U then we have

$$u_{\zeta^i \bar{\zeta}^j} - u_{\bar{\zeta}^j \zeta^i} = \Sigma\, (c_{ij}^k u_{\zeta^k} - c_{ji}^k u_{\bar{\zeta}^k}). \tag{3.7}$$

The strong pseudo-convexity is equivalent to the positive definiteness of the $(n-1)$ by $(n-1)$ matrix $(c_{ij}^n)_{i,j<n}$ evaluated on bM.

The inequality (I) can then be derived using this description of pseudoconvexity.[7, 1] The same method gives the following estimate.[1]

Let U be a neighborhood as described above and suppose that it is small enough so that the above matrix is positive definite at all points of U. Then we have

3.8. THEOREM. *If M is strongly pseudo-convex, then there exists $C > 0$ such that for all $\phi \in \dot{\mathfrak{D}}^{p,q}$, $q > 0$, and support of ϕ is contained in $U \cap \bar{M}$ we have*

$$\tau \|\phi\|_\tau^2 \leq C(\mathbf{D}_\tau(\phi, \phi) + \tau^2 \sum_{n \in J} \|\phi_{I\bar{J}}\|_\tau^2), \tag{II}$$

where the $\phi_{I\bar{J}}$ are components as in (3.5).

4. *The spaces $\mathfrak{L}_s^{p,q}$.*—Let $t^1, t^2, \ldots, t^{2n-1}, r$ be a real C^∞ coordinate system on U such that r is defined by (2.4) and $\langle dt^k, dr \rangle = 0$ at each point of U. Now if u is a C^∞ function on $\bar{M}$ whose support lies in $U \cap \bar{M}$, we also denote by u the function on $\mathbf{R}^{2n} = \{(t^1, \ldots, t^{2n-1}, r) \in \mathbf{R}^{2n} \mid r \leq 0\}$ defined by identifying $U \cap \bar{M}$ with the corresponding set in $\mathbf{R}^{2n}$ and setting u equal to zero outside this set. We define the partial Fourier transform $\tilde{u}$ by

$$\tilde{u}(\xi, r) = \int_{\mathbf{R}^{2n-2}} \exp(-it \cdot \xi)\, u(t, r)\, dt, \tag{4.1}$$

where $t = (t^1, \ldots, t^{2n-1})$, $\xi = (\xi^1, \ldots, \xi^{2n-1})$, $t \cdot \xi = \Sigma_1^{2n-1} t^k \xi^k$,

and $dt = dt^1 \ldots dt^{2n-1}$. For any real number s, we define the norm $\|u\|_s$ by

$$\|u\|_s^2 = \int_{\mathbf{R}^{2n-2}} \int_{-\infty}^0 (1 + |\xi|^2)^s |\tilde{u}(\xi, r)|^2\, dt\, dr. \tag{4.2}$$

If $\phi \in \dot{\mathfrak{A}}^{p,q}$ and if the support of ϕ lies in $U \cap \bar{M}$, we define $\|\phi\|_s$ by

$$\|\phi\|_s^2 = \Sigma_{I,J} \|\phi_{I\bar{J}}\|_s^2, \tag{4.3}$$

where the $\phi_{I\bar{J}}$ are the components given in (3.5). For any $\phi \in \dot{\mathfrak{A}}^{p,q}$, we define $\|\phi\|_s$ by $\|\phi\|_s^2 = \Sigma \|f_j \phi\|_s^2$, where $\{f_j\}$ is an appropriate partition of unity. We denote by $\mathfrak{L}_s^{p,q}$ the space obtained by completion under $\| \quad \|_s$.

For $k = 1, \ldots, 2n-1$ let $D_k = \partial/\partial t^k$ and let $D_{2n} = \partial/\partial r$. Using 3.1, we have the following estimate.[1]

4.4. LEMMA. *There exists $C > 0$ such that for all $\phi \in \dot{\mathfrak{D}}^{p,q}$, $q > 0$, with support in $U \cap \bar{M}$ we have $\|D_k \phi_{I\bar{J}}\|_{-1/2}^2 \leq C\, \mathbf{D}(\phi, \phi)$ for $1 \leq k \leq 2n$.*

We define the following families of norms:

$$\|u\|^2_{s,\delta} = \int_{\mathbf{R}^{2n-2}} \int_{-\infty}^{0} |\tilde{u}(\xi, r)|^2 (1 + |\xi|^2)^{s+1}(1 + |\delta\xi|^2)^{-1} d\xi\, dr \tag{4.5}$$

and

$$\|u\|^2_{s,(\delta)} = \int_{\mathbf{R}^{2n-2}} \int_{-\infty}^{0} |\tilde{u}(\xi, r)|^2 (1 + |\xi|^2)^{s+1/2}(1 + |\delta\xi|^2)^{-1/2} d\xi\, dr. \tag{4.6}$$

It is clear that for all $\delta > 0$ the norms $\| \ \|_{s,\delta}$, $\| \ \|_{s,(\delta)}$, and $\| \ \|_s$ are equivalent on $\mathfrak{L}^{p,q}_s$ and that

$$\|\phi\|_{s,\delta} \nearrow \|\phi\|_{s+1} \text{ when } \delta \searrow 0 \tag{4.7}$$

and

$$\|\phi\|_{s,(\delta)} \nearrow \|\phi\|_{s+1/2} \text{ when } \delta \searrow 0. \tag{4.8}$$

Let χ be a compactly supported function on R^{2n-1} and assume that

$$\hat{\chi}(\xi) = 0(|\xi|^k), \qquad \xi \to 0 \tag{4.9}$$

but that if $\hat{\chi}(\lambda\xi) = 0$ for all real λ then $\xi = 0$. If u is a function as above, we define the functions $S_\epsilon u$ and $S_\epsilon' u$, where $0 < \epsilon \leq 1$, by

$$S_\epsilon u(t,r) = \epsilon^{-2n+1} \int_{\mathbf{R}^{2n-1}} u(t',r)\, \chi\left(\frac{t - t'}{\epsilon}\right) dt' \tag{4.10}$$

and

$$S_\epsilon' u(t,r) = \epsilon^{-2n+1} \int_{\mathbf{R}^{2n-1}} u(t',r)\, \chi\left(\frac{t' - t}{\epsilon}\right) dt'.$$

If $\phi \epsilon \mathfrak{A}^{p,q}$ and if the support of ϕ lies in $U \cap \bar{M}$, then we set $S_\epsilon(\phi) = S_\epsilon(\phi_{IJ})\zeta^{IJ}$ and $S_\epsilon'(\phi) = S_\epsilon'(\phi_{IJ})\zeta^{IJ}$. The following is an immediate consequence of 3.6.

4.11. LEMMA. *If $\phi \in \dot{\mathfrak{D}}^{p,q}$ and if the support of ϕ lies in $U \cap \bar{M}$, then $S_\epsilon(\phi) \in \dot{\mathfrak{D}}^{p,q}$ and $S_\epsilon'(\phi) \in \dot{\mathfrak{D}}^{p,q}$.*

The inequalities listed below are very similar to those given by Hörmander[5] and they can be proved by slight modifications of his proofs.

For $0 < \delta \leq 1$, there exist positive constants C_1 and C_2 independent of δ and u but depending on s and χ such that

$$C_1\|u\|^2_{s,\delta} \leq \int_0^1 \|S_\epsilon u\|^2 \epsilon^{-2s-2}(1 + \delta^2/\epsilon^2)^{-1} d\epsilon/\epsilon + \|u\|_{s^2} \leq C_2\|u\|^2_{s,\delta} \tag{4.12}$$

and

$$C_1\|u\|^2_{s,(\delta)} \leq \int_0^1 \|S_\epsilon u\|^2 \epsilon^{-2s-1}(1 + \delta^2/\epsilon^2)^{-1/2} d\epsilon/\epsilon + \|u\|_{s^2} \leq C_2\|u\|^2_{s,(\delta)}. \tag{4.13}$$

If a is a differentiable function whose support lies in $U \cap \bar{M}$ and if $s < k$ (k given by (4.9)), then there exists $C > 0$ such that when $0 < \delta \leq 1$ we have

$$\int_0^1 \|aS_\epsilon u - S_\epsilon(au)\|^2 \epsilon^{-2s-2}(1 + \delta^2/\epsilon^2)^{-1} d\epsilon/\epsilon \leq C\|u\|^2_{s-1,\delta} \tag{4.14}$$

and

$$\int_0^1 \|aS_\epsilon u - S_\epsilon(au)\|^2 \epsilon^{-2s-1}(1 + \delta^2/\epsilon^2)^{-1/2} d\epsilon/\epsilon \leq C\|u\|^2_{s-1,(\delta)}. \tag{4.15}$$

5. *The Regularity Theorem.*—Let $\mathfrak{D}_1^{p,q}$ denote the closure, under the norm induced by the inner product $\mathbf{D}$, of $\dot{\mathfrak{D}}^{p,q}$. If $\phi \in \dot{\mathfrak{A}}^{p,q}$ has support in $U \cap \bar{M}$ we define $D_k\phi \in \mathfrak{A}^{p,q}$, for $1 \leq k \leq 2n$, by $D_k\phi = (D_k\phi_{I\bar{J}})\zeta^{I\bar{J}}$.

5.1. PROPOSITION. *If M is strongly pseudo-convex and if $q > 0$, then there exists $\tau > 0$ such that if $\alpha \in \dot{\mathcal{A}}^{p,q}$, if $\phi \in \mathfrak{D}_1^{p,q}$, and if $\mathbf{D}_\tau(\phi, \psi) = (\alpha, \psi)_\tau$ for all $\psi \in \mathfrak{D}_1^{p,q}$ then for any integers $k_1, \ldots, k_m$ with $1 \leq k_j \leq 2n - 1$ and for any C^∞ function f with support in $U \cap \bar{M}$ we have $D_{k_1} D_{k_2} \ldots D_{k_m}(f\phi) \in \mathfrak{D}_1^{p,q}$.*

The proof of this proposition uses the following lemma.

5.2. LEMMA. *If $\phi \in \mathfrak{D}_1^{p,q}$, $q > 0$ and if for some $\alpha \in \dot{\mathcal{A}}^{p,q}$ and some $\tau \geq 0$ we have $\mathbf{D}_\tau(\phi, \psi) = (\alpha, \psi)_\tau$ for all $\psi \in \mathfrak{D}_1^{p,q}$ then $\bar{\delta}\phi \in \mathfrak{L}_{1/2}^{p,q+1}$ and $\mathfrak{d}\phi \in \mathfrak{L}_{1/2}^{p,q-1}$.*

Proof: Let $\{U_j\}$, $\{V_j\}$, and $\{W_j\}$ be finite collections of sets in M' each of which covers bM and such that the W_j are holomorphic coordinate domains which also admit the coordinates (t,r); assume further that $\bar{U}_j \subset V_j \subset \bar{V}_j \subset W_j$. Choose the support of χ so small that if u has support in $U_j \cap \bar{M}$ then $S_\epsilon u$ has support in $V_j \cap \bar{M}$ for $0 < \epsilon \leq 1$. Let $\{f_j\}$ be real-valued C^∞ functions such that the support of f_j is contained in U_j and $\Sigma f_j = 1$ in a neighborhood of bM. Let $\{g_j\}$ be real-valued C^∞ functions such that $g_j(P) = 1$ if $P \in V_j$ and such that the support of g_j is contained in W_j and also $\Sigma g_j \geq 1$ in a neighborhood of bM. Now let $\{\phi_k\}$ be a sequence, $\phi_k \in \dot{\mathfrak{D}}^{p,q}$ such that ϕ is the limit of the ϕ_k under the $\mathbf{D}$-norm. Then we have

$$
\begin{aligned}
(5.3)\quad \|S_\epsilon f_j \bar{\delta}\phi\|_\tau^2 &= (S_\epsilon f_j \bar{\delta}\phi,\ S_\epsilon f_j(\bar{\delta}\phi - \bar{\delta}\phi_k))_\tau \\
&\quad - (S_\epsilon f_j \bar{\delta}\phi,\ S_\epsilon(\operatorname{der} f_j)\phi_k)_\tau \\
&\quad + (S_\epsilon f_j \bar{\delta}\phi,\ [S_\epsilon,\ \text{coeff}]\ \text{tan der}\ (f_j\phi_k))_\tau \\
&\quad - (S_\epsilon g_j \bar{\delta}\phi,\ (\operatorname{der} f_j)\ S_\epsilon(f_j\phi_k))_\tau \\
&\quad + ([S_\epsilon, f_j] g_j \bar{\delta}\phi,\ \bar{\delta}(S_\epsilon f_j \phi_k))_\tau \\
&\quad + ([S_\epsilon,\ \text{coeff}]\ g_j \bar{\delta}\phi,\ \text{tan der}\ (f_j S_\epsilon f_j \phi_k))_\tau \\
&\quad + (\bar{\delta}\phi,\ \bar{\delta}(S_\epsilon f_j S_\epsilon f_j \phi_k))_\tau,
\end{aligned}
$$

where "der" stands for a combination of first derivatives, "tan der" for a combination of first derivatives with respect to the t^i and "coeff" for coefficients of the D_k in the expression for $\bar{\delta}\phi$ in terms of the ζ's. The coefficients of D_{2n} in this expression are constants, and that is the reason that only tangential derivatives appear in conjunction with the commutator $[S_\epsilon, \text{coeff}]$. A formula similar to (5.3) holds for $\|S_\epsilon f_j \mathfrak{d}\phi\|_\tau^2$. We add these, use the fact that $\mathbf{D}_t[(\phi, S_\epsilon' f_j S_\epsilon f_j \phi_k) = (\alpha, S_\epsilon' f_j S_\epsilon f_j \phi_k)_\tau$, multiply by $\epsilon^{-1}(1 + \delta^2/\epsilon^2)^{-1/2}$, and use the Schwarz inequality and the inequality $ab \leq \lambda a^2 + \lambda^{-1} b^2$; finally, we multiply by $d\epsilon/\epsilon$, integrate, sum over j, and, using (4.13) and (4.15), obtain

$$
\begin{aligned}
(5.4)\quad \|\bar{\delta}\phi\|_{0,(\delta)}^2 + \|\mathfrak{d}\phi\|_{0,(\delta)}^2 &\leq C\{\|\bar{\delta}(\phi - \phi_k)\|_{0,(\delta)}^2 + \|\mathfrak{d}(\phi - \phi_k)\|_{0,(\delta)}^2 \\
&\quad + \|\phi_k\|_{0,(\delta)}^2 + \|\bar{\delta}\phi\|_{-1/2,(\delta)}^2 + \|\mathfrak{d}\phi\|_{-1/2,(\delta)}^2 + \|\alpha\|_{0,(\delta)}^2 + \|\phi\|_{0,(\delta)}^2\},
\end{aligned}
$$

where C is independent of δ.

Taking the limit as $k \to \infty$, we obtain

$$
\begin{aligned}
(5.5)\quad \|\bar{\delta}\phi\|_{0,(\delta)}^2 + \|\mathfrak{d}\phi\|_{0,(\delta)}^2 &\leq C(2\|\phi\|_{0(\delta),}^2 + \|\bar{\delta}\phi\|_{-1/2,(\delta)}^2 + \|\mathfrak{d}\phi\|_{-1/2,(\delta)}^2 + \|\alpha\|_{0,(\delta)}^2) \\
&\leq C'(\|\phi\|_{1/2}^2 + \|\bar{\delta}\phi\|^2 + \|\mathfrak{d}\phi\|^2 + \|\alpha\|_{1/2}^2) \\
&\leq C''\|\alpha\|_{1/2}^2,
\end{aligned}
$$

so that $\|\partial\phi\|_{0,(\delta)}$ and $\|\mathfrak{d}\phi\|_{0,(\delta)}$ are bounded independently of δ; hence the desired result follows from (4.8).

Proof of proposition 5.1: Using the same notation as in the above proof, we first compare $\mathbf{D}_\tau(\phi, S_\epsilon' f_j S_\epsilon f_j \phi_k)$ with $\mathbf{D}_\tau(S_\epsilon f_j \phi_k, S_\epsilon f_j \phi_k)$. Using formulas similar to

(5.3), applying the estimate (II) of 3.8 to $S_\epsilon f_J \phi_k$, and reasoning along the same lines as above, we obtain

$$(5.6)\quad \tau\|\phi w_\tau\|^2_{0,\delta} \leq C\{\|\phi w_\tau\|^2_{0,\delta} + \|(\bar\partial\phi)w_\tau\|^2_{-1/2,\delta} + \|(\mathfrak{d}\phi)w_\tau\|^2_{-1/2,\delta} + \|\alpha w_\tau\|^2_{0,\delta} + \tau^2 \sum_j \sum_{n\in J} \|f_j\phi_{IJ}w_\tau\|^2_{0,\delta}\},$$

where C is independent of τ and δ. Hence, if τ is sufficiently large, we have

$$(5.7)\quad \begin{aligned}\|\phi\|^2_{0,\delta} &\leq C_1\{\|\bar\partial\phi\|^2_{-1/2,\delta} + \|\mathfrak{d}\phi\|^2_{-1/2,\delta} + \|\alpha\|^2_{0,\delta} + \sum_j \sum_{n\in J} \|f_j\phi_{IJ}\|^2_{0,\delta}\}\\ &\leq C_2\{\|\bar\partial\phi\|^2_{1/2} + \|\mathfrak{d}\phi\|^2_{1/2} + \|\alpha\|^2_1 + \sum_j \sum_{n\in J} \|f_j\phi_{IJ}\|^2_1\}\\ &\leq C_3\|\alpha\|^2_1,\end{aligned}$$

where C_1, C_2 and C_3 are independent of δ. Therefore $\phi \in \mathfrak{L}_1^{p,q}$ so that $D_j(f\phi) \in \mathfrak{L}^{p,q}$ for $1 \leq j \leq 2n-1$. Using the same argument as in 5.2, we conclude that $\bar\partial\phi \in \mathfrak{L}_1^{p,q+1}$ and $\mathfrak{d}\phi \in \mathfrak{L}_1^{p,q-1}$. To show that $D_j(f\phi) \in \mathfrak{D}_1^{p,q}$, we construct a sequence $\{\psi_k\}$, $\psi_k \in \dot{\mathfrak{D}}^{p,q}$, which converges to $D_j(f\phi)$ in the D-norm. First, we choose a sequence $\{\phi_k\}$ so that $\|\phi - \phi_k\|_{0,1/k}$, $\|\bar\partial(\phi - \phi_k)\|_{0,1/k}$ and $\|\mathfrak{d}(\phi - \phi_k)\|_{0,1/k}$ tend to zero as $k \to \infty$. Then, we define ψ_k by

$$(5.8)\quad (\widetilde{\psi}_k)_{IJ} = (\widetilde{f\phi}_k)_{IJ}\xi_j(1 + 1/k^2|\xi|^2)^{-1/2}\rho_k(\xi),$$

where ρ_k is a compactly supported C^∞ function on $\mathbf{R}^{2n-1}$, which equals one on a suitably large set. It can then be shown that the ψ_k converge to $D_j(f\phi)$ as required. Thus, the proposition is proved for $m = 1$. To prove the proposition for $m = 2$, we use $S_\epsilon f_i\psi_k$ instead of $S_\epsilon f_j\phi_k$ in the above argument and we compare $\mathbf{D}_\tau(S_\epsilon f_i\psi_k, S_\epsilon f_i\psi_k)$ with $-\mathbf{D}_\tau(\phi, D_j(S_\epsilon' f_i S_\epsilon f_i\psi_k)) = (D_j\alpha, S_\epsilon' f_i S_\epsilon f_i\psi_k)_\tau$. We apply the same procedure repeatedly to obtain the theorem for any m.

5.9. PROPOSITION. *There exists $\tau > 0$ such that if ϕ satisfies the same hypotheses as in 5.1, then $\phi \in \dot{\mathfrak{A}}^{p,q}$.*

Proof: By Sobolev's lemma, all we need to prove is that all the derivatives of $f\phi$ are in $\mathfrak{L}^{p,q}$. Since every derivative is a combination of the $\bar z$-derivatives and the t-derivatives, then, by the above proposition, we conclude that all the first derivatives of $D_{k_1} \cdots D_{k_m}(f\phi)$, $1 \leq k_j \leq 2n-1$, are in $\mathfrak{L}^{p,q}$. The ϕ_{IJ} satisfy a second-order system of partial differential equations, from which we obtain

$$(5.10)\quad \frac{\partial^2}{\partial t^2}\phi_{IJ} = -\alpha_{IJ} + \ldots,$$

where the remaining terms contain only first derivatives with respect to t. Hence, we conclude that $(\partial^2/\partial t^2)\phi_{IJ}$ is square-integrable, and by differentiating (5.10), we conclude that every derivative of ϕ_{IJ} is square-integrable.

5.11. THEOREM. *If M is strongly pseudo-convex then $\mathfrak{D}_1^{p,q} = \mathfrak{D}^{p,q}$, i.e., $\dot{\mathfrak{D}}^{p,q}$ is dense in $\mathfrak{D}^{p,q}$ under the $\mathbf{D}$-norm.*

Proof: Choose τ so that 5.9 holds. Let $\gamma \in \mathfrak{D}^{p,q}$ be orthogonal to $\mathfrak{D}_1^{p,q}$ in the $\mathbf{D}_\tau$ inner product; that is,

$$\mathbf{D}_\tau(\gamma, \psi) = 0$$

for all $\psi \in \dot{\mathfrak{D}}^{p,q}$. Let $\alpha_k \in \dot{\mathfrak{A}}^{p,q}$ be a sequence such that $\gamma = \lim \alpha_k$ in the $\|\ \|$-norm. Let $\phi_k \in \mathfrak{D}_1^{p,q}$ be such that

$$\mathbf{D}_\tau(\phi_k, \beta) = (\alpha_k, \beta)_\tau \tag{5.12}$$

for all $\beta \in \mathfrak{D}_1^{p,q}$. Then $\phi_k \in \dot{\mathfrak{D}}^{p,q}$ and hence it follows[1] that (5.12) holds for all $\beta \in \mathfrak{D}^{p,q}$; so that in particular $\mathbf{D}_\tau(\phi_k, \gamma) = (\alpha_k, \gamma)_\tau = 0$, and since $\|\gamma\|_\tau^2 = \lim (\alpha_k, \gamma) = 0$, we conclude that $\gamma = 0$ and hence $\mathfrak{D}_1^{p,q} = \mathfrak{D}^{p,q}$.

5.13 THEOREM. *If M is strongly pseudo-convex, if $\phi \in \mathfrak{D}^{p,q}$, $q > 0$ and if $\mathbf{D}(\phi, \psi) = (\alpha, \psi)$ for some $\alpha \in \dot{\mathfrak{A}}^{p,q}$ and for all $\psi \in \mathfrak{D}^{p,q}$ then $\phi \in \dot{\mathfrak{A}}^{p,q}$.*

Proof: First we observe that there exists $C > 0$, independent of τ so that for all $\psi \in \dot{\mathfrak{D}}^{p,q}$, with support in $U \cap \bar{M}$, we have

$$\mathbf{D}_\tau(\psi, \psi) \leq C\Big\{\big|\mathbf{D}(\psi, \psi w_\tau)\big| + \tau^2\Big(\sum_{n \in J} \|\psi_{I\bar{J}}\|_\tau^2 + \sum_{n \in L} \|(\bar{\delta}\psi)_{K\bar{L}}\|_\tau^2\Big)\Big\}. \tag{5.14}$$

Since $\bar{\delta}\phi \in \mathfrak{D}_1^{p,q+1}$ (by theorem 5.11) we have

$$\sum_{n \in L} \|(\bar{\delta}(f\phi))_{K\bar{L}}\|_1^2 \leq C\, \mathbf{D}(\bar{\delta}(f\phi), \bar{\delta}(f\phi)) \leq C'\|\alpha\|^2.$$

Then letting $\psi = S_\epsilon f_j \phi_k$, we can proceed exactly as in the proof of 5.9 but using (5.14) instead of (II).

6. *Conclusion.*—Let $\mathfrak{H}^{p,q}$ be the null space of L, then we have the orthogonal decomposition $\mathfrak{L}^{p,q} = \overline{L\mathfrak{D}_L{}^{p,q}} \oplus \mathfrak{H}^{p,q}$. An easy Hilbert-space argument[1] shows that $L\mathfrak{D}_L{}^{p,q}$ is closed if $\mathbf{D}$ is completely continuous on $\mathfrak{D}^{p,q}$ and $L\mathfrak{D}_L{}^{p,0}$ is closed if $\mathbf{D}$ is completely continuous on $\mathfrak{D}^{p,1}$. Thus, applying Theorem 5.11 and the result that $\mathbf{D}$ is completely continuous on $\mathfrak{D}_1^{p,q}$, $q > 0$, we conclude that $L\mathfrak{D}_L{}^{p,q}$ is closed for all p and q and that $\mathfrak{H}^{p,q}$ is finite-dimensional for $q > 0$. Let H: $\mathfrak{L}^{p,q} \to \mathfrak{H}^{p,q}$ be the orthogonal projection on $\mathfrak{H}^{p,q}$. Now if $\phi \in \mathfrak{L}^{p,q}$ we have $\phi = L\beta + H\phi$ and we define N: $\mathfrak{L}^{p,q} \to \mathfrak{L}^{p,q}$ by $N\phi = \beta - H\beta$. Then, by the same method as the proof of 5.13, we prove that N: $\dot{\mathfrak{A}}^{p,q} \to \dot{\mathfrak{A}}^{p,q}$ for $q > 0$; furthermore, it then follows that H: $\dot{\mathfrak{A}}^{p,q} \to \dot{\mathfrak{A}}^{p,q}$ even if $q = 0$, since if $\alpha \in \dot{\mathfrak{A}}^{p,0}$ then $H\alpha = \alpha - \mathfrak{d}N\bar{\delta}\alpha$. Now observe that $H(\dot{\mathfrak{A}}^{p,q})$ is dense in $\mathfrak{H}^{p,q}$, and since for $q > 0$, $\mathfrak{H}^{p,q}$ is finite-dimensional, we have $\mathfrak{H}^{p,q} \subset \dot{\mathfrak{A}}^{p,q}$ if $q > 0$. These results are summarized in the following theorem.

6.1. THEOREM. *If M is a strongly pseudo-convex manifold then there exists a map N: $\mathfrak{L}^{p,q} \to \mathfrak{L}^{p,q}$ which has the following properties:*

(a) $\mathfrak{L}^{p,q} = TT^*N\mathfrak{L}^{p,q} \oplus T^*TN\mathfrak{L}^{p,q} \oplus \mathfrak{H}^{p,q}$.

(b) $TN = NT$ *and* $T^*N = NT^*$.

(c) N *is bounded,* $N(\mathfrak{A}^{p,q} \cap \mathfrak{L}^{p,q}) \subset \mathfrak{A}^{p,q})$, *and* $N(\dot{\mathfrak{A}}^{p,q}) \subset \dot{\mathfrak{A}}^{p,q}$.

(d) *If $q > 0$ then N is completely continuous.*

(e) $H(\dot{\mathfrak{A}}^{p,q}) \subset \dot{\mathfrak{A}}^{p,q}$ *for all p and q, and if $q > 0$ then* $\mathfrak{H}^{p,q} \subset \dot{\mathfrak{A}}^{p,q}$.

* This work was partly supported by the National Science Foundation through research projects at Brandeis University and at the Institute for Advanced Study.

[1] Kohn, J. J., "Harmonic integrals on strongly pseudo-convex manifolds, I and II," *Ann. Math.* (to appear).

[2] Spencer, D. C., "Potential theory and almost-complex manifolds," in *Lectures on Functions of a Complex Variable* (Ann Arbor: University of Michigan Press, 1955), pp. 15–43.

[3] Morrey, C. B., "The analytic embedding of abstract real analytic manifolds," *Ann. Math.*, **68,** 159–201 (1958).

[4] Garabedian, P. R., and D. C. Spencer, "Complex boundary-value problems," *Trans. Amer. Math. Soc.*, **73,** 223–242 (1952).

[5] Kohn, J. J., and D. C. Spencer, "Complex Neumann problems," *Ann. Math.*, **66,** 89–140 (1957).

[6] Kohn, J. J., "Solution of the $\bar{\partial}$-Neumann problem on strongly pseudo-convex manifolds," these Proceedings, **47**, 1198–1202 (1961).

[7] Ash, M. E., "The basic estimate of the $\bar{\partial}$-Neumann problem in the non-kählerian case," (to appear).

[8] Hörmander, L., "Lectures on partial differential operators," mimeographed notes, Stanford University, 1960.

ON THEORIES CATEGORICAL IN UNCOUNTABLE POWERS

BY MICHAEL MORLEY

DEPARTMENT OF MATHEMATICS, UNIVERSITY OF CALIFORNIA, BERKELEY

Communicated by Saunders Mac Lane, December 31, 1962

Suppose Σ is a theory formalized in some countable, first-order (with equality) language, L. One says Σ is *categorical in power* K if Σ has a model of power K and all models of Σ of power K are isomorphic.[1] For example, the theory of dense linearly ordered sets without end points is categorical in power $\aleph_0$ but is not categorical in any higher power. On the other hand, the theory of algebraically closed fields of characteristic O is not categorical in power $\aleph_0$ but is categorical in every higher power. In 1954 Łoś raised the following question: *Is a theory categorical in one uncountable power necessarily categorical in every uncountable power?* We give an affirmative answer to this question.

Several recent papers[2] have pointed out the close connections between the properties of models of a theory and certain Boolean algebras of formulas. The isolated points in the dual spaces of these Boolean algebras play a particularly important role. We consider a certain class of such spaces and a certain category of continuous onto maps between them. The crux of our proof is an analog for such categories of the Cantor-Bendixson theorem. We also use methods related to those of Ehrenfeucht and Mostowski[3] and the previously cited paper[2] of Vaught.

1. There will be no loss of generality in assuming Σ to be a complete theory in L. Suppose A is a model of Σ and $X \subseteq |A|$. (The set $|A|$ is the *universe* of A, i.e., A consists of the set $|A|$ and a set of relations on $|A|$.) We define an enlarged language, $L(A, X)$ by adding to L a new individual constant $\bar{x}_A$ for each $x \in X$. $(A,x)_{x \in X}$ is the model formed from A by taking each $x \in X$ as a distinguished element.) Denote by $\Sigma(A, X)$ the set of sentences of $L(A, X)$ which are valid in $(A, x)_{x \in X}$. Then $\Sigma(A, X)$ is obviously a complete theory in $L(A, X)$. We identify formulas of $L(A, X)$ which are equivalent in the theory $\Sigma(A, X)$ and denote by $F(A, X)$ the set of formulas having no free variable except some fixed one, say v_0. We may consider $F(A, X)$ as a Boolean algebra with the Boolean operations of $\cap$, $\cup$, and $'$ corresponding to the logical connectives $\wedge$, $\vee$, and $\sim$, respectively.

By the celebrated result of Stone[4] the set of maximal dual ideals of $F(A, X)$ form a totally disconnected compact space which we denote by $S(A, X)$. The space $S(A, X)$ has a basis of power $\leq \bar{\bar{X}} + \aleph_0$. The points of $S(A, X)$ may be thought of as the kind of elements which may appear in models of $\Sigma(A, X)$. In particular, for each $a \in A$ there is a $p_a \in S(A, X)$ such that p_a consists of precisely those formulas of $F(A, X)$ satisfied by a in $(A, x)_{x \in X}$. We say a *realizes* p_a in A.

If A is a model of Σ, we say A is *saturated* if for every $X \subseteq |A|$ with $\overline{\overline{X}} < \overline{A}$ every $p \in S(A, X)$ is realized in A. It can be shown[5] that:

THEOREM 1. *If A and B are saturated models of Σ having the same power then A is isomorphic to B.*

The proof involves extending isomorphisms between subsystems one element at a time.

Vaught recognized that this theorem could be used in considering the problem of categoricity in power, and he showed[5] (assuming the generalized continuum hypothesis) that if a theory is categorical in an increasing sequence of powers then it is categorical in the limit power.

Suppose A and B are models of Σ, $X \subseteq |A|$ and $Y \subseteq |B|$, and f maps X into Y. We say f is an *elementary monomorphism* of (A, X) into (B, Y) if whenever $n \in \omega$, ψ is a formula of L with free variables among $v_0, \ldots, v_{n-1}$ and $x_0, \ldots, x_{n-1} \in X$, then $\vdash_A \psi(x_0, \ldots, x_{n-1})$ if and only if $\vdash_B \psi(f(x_0), \ldots, f(x_{n-1}))$. In particular, if $A \subseteq B$ and the identity map of A into B is an elementary monomorphism we say B is an *elementary extension* of $A (A < B)$. One advantage of dealing only with elementary monomorphisms is that they have the *amalgamation property;* that is, if A and B_i $(i \in I)$ are models of Σ, $X \subseteq |A|$, $Y_i \subseteq |B_i|$ $(i \in I)$ and $f_i : (A, X) \to (B_i, Y_i) (i \in I)$ are elementary monomorphisms, then there is a model C of Σ, and a set $Z \subseteq |C|$ and elementary monomorphisms $g_i : (B_i, Y_i) \to (C, Z) (i \in I)$ such that for all $i, j \in I$, $g_i f_i = g_j f_j$.

It is easy to see that an elementary monomorphism $f : (A, X) \to (B, Y)$ induces a Boolean monomorphism of $F(A, X)$ into $F(B, Y)$ (by mapping $\bar{x}_A$ to $f(x)_B$), which, by Stone's results induces a continuous onto map $f^* : S(B, Y) \to S(A, X)$. Thus with each complete theory Σ we may associate: (1) a class (denoted by $\mathfrak{S}(\Sigma)$) of topological spaces—namely, the class of all spaces $S(A, X)$ where A is a model of Σ and $X \subseteq |A|$; and (2) the category, $\mathfrak{C}(\Sigma)$, of those continuous onto maps between members of $\mathfrak{S}(\Sigma)$ which are induced by elementary monomorphisms. It is to this class of spaces and category of maps that we wish to apply an analysis similar to that of a single space in terms of its derived sequence of spaces. (That a single Boolean algebra could be analyzed in terms of the derived sequence of its dual space was explicitly recognized by Mostowski and Tarski[6]). To do this we define a notion stronger than that of an isolated point: a point $p \in S \in \mathfrak{S}(\Sigma)$ is *algebraic* if for every $f \in \mathfrak{C}(\Sigma)$ with range S, $f^{-1}(p)$ is a set of isolated points. (The term "algebraic" is suggested by the case where Σ is the theory of algebraically closed fields of characteristic O. It is also consistent with a generalized notion of algebraic extension considered by Jónsson.)

We define $S' = S - \{\text{algebraic points of } S\}$. It turns out (essentially because all the spaces are compact and $\mathfrak{C}(\Sigma)$ satisfies the dual of the amalgamation property) that if $(f : S_1 \to S_2) \in \mathfrak{C}(\Sigma)$ then $f(S_1') = S_2'$. Therefore, we may define $\mathfrak{S}'(\Sigma) = \{S';\ S \in \mathfrak{S}(\Sigma)\}$ and $\mathfrak{C}'(\Sigma) = \{(f | S_1' : S_1' \to S_2');\ (f : S_1 \to S_2) \in \mathfrak{C}(\Sigma)\}$. We may now repeat this process and find the algebraic points of S' (considered now as a member of $\mathfrak{S}'(\Sigma)$). If p is algebraic in S' we say it is *transcendental in rank* 1 in $S(p \in Tr^1(S))$. We define S^2 as $S' - Tr^1(S)$ and $\mathfrak{S}^2(\Sigma) = \{S^2;\ S \in \mathfrak{S}(\Sigma)\}$. We proceed inductively to define:

$$S^\alpha = S - \bigcup_{\beta<\alpha} Tr^\beta(S)$$

$$Tr^{\alpha}(S) = \{\text{algebraic points of } S^{\alpha} \text{ (considered as a member of } \mathfrak{S}^{\alpha})\}$$

$$\mathfrak{S}^{\alpha}(\Sigma) = \{S^{\alpha};\ S \in \mathfrak{S}(\Sigma)\}.$$

It may happen that for some ordinal α_0 and some $S \in \mathfrak{S}(\Sigma)$, S^{α_0} is empty. It will then follow that for every $S \in \mathfrak{S}(\Sigma)$, S^{α_0} is empty. (Again, this is essentially a consequence of the amalgamation property.) In this case we say that Σ is *totally transcendental* (because every $p \in S \in \mathfrak{S}(\Sigma)$ is transcendental in some rank).

THEOREM 2. *If Σ is totally transcendental and $S(A, X) \in \mathfrak{S}(\Sigma)$, then $\overline{S(A, X)} \leq \overline{\overline{X}} + \aleph_0$.*

Proof: The space $S(A, X)$ has a basis corresponding to the elements of $F(A, X)$ and hence of power $\leq \overline{\overline{X}} + \aleph_0$. Since the points of $Tr^{\alpha}(S)$ are isolated points in S^{α}, S must have a vanishing perfect kernel. Any compact Hausdorf space with a vanishing perfect kernel has power $\leq$ the power of any basis of it.

The more difficult result is the converse:

THEOREM 3. *The theory Σ is totally transcendental if and only if whenever $S(A, X) \in \mathfrak{S}(\Sigma)$ and X is countable then $S(A, X)$ is countable.*

Theorem 3 is the analogue of the Cantor-Bendixson theorem and its proof is similar to proofs of that theorem.

2. The next step is to establish that every theory categorical in an uncountable power satisfies the countability condition of theorem 3 and is therefore totally transcendental. Vaught[5] has already established this for theories categorical in power $\mathrm{K}^{\aleph_0}$. To establish it in general we use the following variant of a result of Ehrenfeucht and Mostowski.

THEOREM 4. *If Σ is a theory having an infinite model and X an arbitrary linearly ordered set, then there is a model A of Σ, and a set $X \subseteq |A|$ such that if $Y_1, Y_2 \subseteq X$ and $f: Y_1 \to Y_2$ is an order isomorphism then f is an elementary monomorphism of (A, Y_1) to (A, Y_2).*

By the well known method of replacing existential quantifiers with function symbols we may replace Σ by a new theory Σ', which has essentially the same models as Σ and such that if A is a model of Σ' and $X \subseteq |A|$ we may define the submodel, $M(X, A)$, generated by X: indeed, $M(X, A)$ is just the closure of X in A by all the functions.

THEOREM 5. *If Σ is a theory with an infinite model and $\mathrm{K} \geq \aleph_0$, then there is a model of Σ, B, such that $\overline{B} = \mathrm{K}$ and if $X \subseteq |B|$ and X is countable then only a countable number of points of $S(B, X)$ are realized in B.*

We sketch the proof. Replace Σ by the theory Σ' described above. Let Y be a linearly ordered set having the order type of K (i.e., of the ordinals having power $<$ K). Let A be a model of Σ' containing Y and satisfying theorem 4 (with Y in place of X). Then $B = M(A, Y)$ is the required model. (It is necessary to arrange things so that $B < A$, but this can always be done.)

THEOREM 6. *If Σ is categorical in some uncountable power then Σ is totally transcendental.*

Proof: If Σ were not totally transcendental then there would be a model A of Σ, and a countable set $X \subseteq |A|$ such that $S(A, X)$ was not countable. By applying the completeness theorem one easily shows that for each uncountable power, K, there is a model B of Σ, such that $\overline{B} = \mathrm{K}$, $X \subseteq |B|$, and B realizes an uncountable

number of points of $S(B, X)$. Then B is certaintly not isomorphic to any model satisfying theorem 5 and hence Σ could not be categorical in power K.

3. We define a somewhat weaker notion than saturated. A model A is *countably saturated* if for every countable $X \subseteq |A|$ every point of $S(A, X)$ is realized in A.

THEOREM 7. *If Σ is totally transcendental (and has an infinite model) then for every $K > \aleph_0$ there is a countably saturated model of Σ of power K.*

Proof. Let A_0 be any model of Σ of power K. By Theorem 2, $S(A_0, |A_0|)$ has power K. From the completeness theorem it follows that there is a model, A_1, such that $A_1 \supseteq A_0$, $\overline{A_1} = K$, and A_1 realizes every point of $S(A_1, |A_0|)$. We iterate this process ω_1 times (taking unions at limit ordinals). Then A_{ω_1} satisfies the theorem. For if $X \subseteq |A_{\omega_1}|$ and X is countable, then there is an $\alpha < \omega_1$ such that $X \subseteq |A_\alpha|$ and hence each point of $S(A\omega_1, X)$ is realized already in $A_{\alpha+1}$.

THEOREM 8. *If Σ is totally transcendental and has an uncountable model which is not saturated, then for every $K \geq \aleph_1$ there is a model of Σ of power K which is not countably saturated.*

Our proof of this theorem is complicated and we shall not give it here. We remark, however, that it involves several transfinite inductions, in which at each step we pick a point of a particular transcendental rank (or often, the point of minimal transcendental rank which satisfies some condition). Thus, we here explicitly use the fact that each $p \in S \in S(\Sigma)$ has a definite transcendental rank. By contrast, in proving theorem 7 we used only the cardinality result of theorem 2.

From Theorems 7 and 8 now follows immediately:

THEOREM 9. *If Σ is categorical in some power $K > \aleph_0$ then every uncountable model of Σ is saturated.*

Theorem 9 and Theorem 1 provide an affirmative answer to the question of Łoś.

[1] Łoś, J., "On the categoricity in power of elementary deduction systems," *Coll. Math.*, **3,** 58–62 (1954); Vaught, R., "Applications of the Löwenheim-Skolem-Tarski theorem to problems of completeness and decidability," *Indag. Math.*, **16,** 467–472 (1954).

[2] Rull-Nardzewski, C., "On theories categorical in power $\leq \aleph_0$," *Bull. Acad. Polon. Sc.*, Cl. III, **7,** 545–548 (1959); Vaught, R., "Denumerable models of complete theories," *Proceeding of the Symposium on the Foundations of Mathematics: Infinitistic Methods*, 303–321, Warsaw, 1959.

[3] Ehrenfeucht, A., and A. Mostowski, "Models of axiomatic theories admitting automorphisms," *Fund. Math.*, **43,** 50–68 (1956); Ehrenfeucht, A., "On theories categorical in power," *Fund. Math.*, **44,** 241–248 (1957).

[4] Stone, M. H., "Applications of the theory of Boolean rings to general topology," *Trans. Amer. Math. Soc.*, **41,** 321–364 (1937).

[5] Morley, M., and R. Vaught, "Homogenous universal models," *Math. Scand.*, to appear.

[6] Mostowski, A., and A. Tarski, "Boolesche Ringe mit geordneter Basis," *Fund. Math.*, **32,** 69–86 (1939).

BOUNDS OF ANALYTIC FUNCTIONS OF TWO COMPLEX VARIABLES IN DOMAINS WITH THE BERGMAN-ŠILOV BOUNDARY

By J. Śladkowska

DEPARTMENT OF MATHEMATICS, STANFORD UNIVERSITY

Communicated by D. C. Spencer, June 12, 1962

Let $\mathfrak{B}$ be a bounded domain in the space $\mathfrak{E}$ of two complex variables z_1,z_2, $z_\kappa = x_\kappa + iy_\kappa$, $\kappa = 1,2$. (κ assumes everywhere the values 1 and 2.) Its boundary $\mathfrak{b}^3$ consists of finitely many segments $\mathfrak{e}_k^3$, $k = 1, \ldots, n$, of analytic surfaces. Each $\mathfrak{e}_k^3$ is given by the parametric representation

$$z_\kappa = h_{\kappa k}(Z_k,\lambda_k), \tag{1}$$

where $h_{\kappa k}$ are continuously differentiable functions of Z_k, λ_k in the set $\{Z_k,\lambda_k \,|\, |Z_k| \leq 1, \lambda_k \in \langle 0,2\pi\rangle\}$, (1$a$)(1$a$ = hypothesis (1a)) and

$$(h_{1k}(Z_k',\lambda_k'),\ h_{2k}(Z_k',\lambda_k')) \neq (h_{1k}(Z_k'',\lambda_k''),\ h_{2k}(Z_k'',\lambda_k'')) \tag{2}$$

for $(Z_k',\lambda_k') \neq (Z_k'',\lambda_k'')$, $|Z_k'|, |Z_k''| < 1$ (1b). For every point (z_1^0,z_2^0), $z_\kappa^0 = h_{\kappa k}(Z_k^0,\lambda_k^0)$, $|Z_k^0| < 1$, and for every sufficiently small neighborhood $\mathfrak{U}$ of this point, there exists $\sigma > 0$ such that the set of points of $\mathfrak{b}^3$ which belong to $\mathfrak{U}$ consists only of points (1) for which $|Z_k - Z_k^0| < \sigma$ and $|\lambda_k - \lambda_k^0| < \sigma$ hold, (1c). For a fixed k and λ_k, the corresponding set of points (1) is called a lamina of $\mathfrak{e}_k^3$ and is designated by $\mathfrak{Z}_k^2(\lambda_k)$. The set $\mathfrak{F}^2$ of points (1) corresponding to the values $|Z_k| = 1$, $k = 1, \ldots, n$, constitutes the so-called Bergman-Šilov boundary surface of $\mathfrak{B}$ on which the maximum principle is valid for functions $f(z_1,z_2)$ holomorphic in $\mathfrak{B}$ and continuous in $\overline{\mathfrak{B}}$ (see ref. 1).

Let $\mathfrak{G}_0^2$ designate an analytic surface of the form $z_\kappa = g_\kappa(\zeta)$, $\zeta \in \overline{\mathfrak{D}}$, where $\mathfrak{D}$ is a domain in the ζ-plane and g_κ are functions regular in $\mathfrak{D}$ and continuous in $\overline{\mathfrak{D}}$. We assume that $\mathfrak{G}_0^2$ has common points with $\mathfrak{B}$ and its whole boundary lies in $\mathfrak{E} \setminus \overline{\mathfrak{B}}$. Concerning the intersection of $\mathfrak{G}_0^2$ with $\mathfrak{B}$, we list the following properties to be assumed as indicated in the various Theorems 1–4). The intersection $\mathfrak{G}^2 = \mathfrak{G}_0^2 \cap \mathfrak{B}$ has the following representation $\mathfrak{G}^2 = \{z_\kappa \,|\, z_\kappa^2 = g_\kappa(\zeta),\ |\zeta| < 1\}$, (2$a$). The boundary curve $\mathfrak{g}^1$ of $\mathfrak{G}^2$ is simultaneously the intersection $\overline{\mathfrak{G}}_0^2$ with $\mathfrak{b}^3$, (2b). $\mathfrak{g}^1 = \{z_\kappa \,|\, z_\kappa = g_\kappa(e^{i\varphi}),\ \varphi \in \langle 0,2\pi\rangle\}$ can be divided into J parts: $\mathfrak{g}_j^1 = \{z_\kappa \,|\, z_\kappa = g_\kappa(e^{i\varphi}),\ \varphi \in \langle \varphi_j, \varphi_{j+1}\rangle\}$, $j = 1, \ldots, J$, $\varphi_1 < \varphi_2 < \ldots < \varphi_{J+1} = \varphi_1 + 2\pi$, so that $\mathfrak{g}_j^1 \subset \mathfrak{e}_{k_j}^3$, $1 \leq k_j \leq n$, $k_{j_1} \neq k_{j_2}$ if $j_1 \neq j_2$, and only the points $(g_1(e^{i\varphi_j}), g_2(e^{i\varphi_j}))$ belong to $\mathfrak{F}^2$, (2c). Every point of $\mathfrak{g}_j^1$ lies in a certain lamina, say $\mathfrak{Z}_{k_j}^2(\lambda_{k_j})$. Hence, by (2) functions $\lambda_{k_j} = \lambda_{k_j}^*(\varphi)$, $Z_{k_j} = Z_{k_j}^*(\varphi)$, $\varphi \in \langle \varphi_j, \varphi_{j+1}\rangle$, exist such that $\mathfrak{g}_j^1 = \{z_\kappa \,|\, z_\kappa = h_{\kappa k_j}(Z_{k_j}^*(\varphi), \lambda_{k_j}^*(\varphi)),\ \varphi \in \langle \varphi_j,\varphi_{j+1}\rangle\}$. We assume that $\lambda_{k_j}^*(\varphi)$ and $Z_{k_j}^*(\varphi)$ are continuous in $\langle \varphi_j,\varphi_{j+1}\rangle$, (2$d$). $\lambda_{k_j}^*(\varphi)$ are monotone in $\langle \varphi_j,\varphi_{j+1}\rangle$ and $|\lambda_{k_j}'(\varphi)| \geq 1/Q$, $Q > 0$, $\varphi \in \langle \varphi_j,\varphi_{j+1}\rangle$, $j = 1, \ldots, J$, (2e). The expressions $1 - |Z_{k_j}^*(\varphi)|$ go to zero not faster than some positive power of $\varphi - \varphi_j$ or $\varphi - \varphi_{j+1}$ if $\varphi \to \varphi_j +$ or $\varphi \to \varphi_{j+1} -$, respectively, (2$f$). The expressions $1 - |Z_{k_j}^*(\varphi)|$ go to zero not faster than $(\varphi - \varphi_j)^{a_j}$ or $(\varphi - \varphi_{j+1})^{b_j}$, where $0 < a_j, b_j < 1/2P$, $P > 0$, when $\varphi \to \varphi_j +$ or $\varphi \to \varphi_{j+1} -$, respectively, (2$f_1$).[2]

Concerning the function $f(z_1,z_2)$ of two complex variables z_1,z_2, we list the following hypotheses to be assumed in the various theorems (see below). $f(z_1,z_2)$ is regular in

the set $\mathfrak{B}_1 = \overline{\mathfrak{B}} \setminus \tilde{\mathfrak{F}}^2$ and continuous in $\mathfrak{B}_2 = \mathfrak{B}_1 \cup \mathfrak{g}^1 \cap \tilde{\mathfrak{F}}^2$, (3*a*). $f(z_1,z_2) \neq 0$ in $\mathfrak{B}_2$, (3*b*). Let $n_k(Re^{i\theta}, \lambda_k)$ denote the number of $Re^{i\theta}$-points of $f(z_1,z_2)$ in the lamina $\mathfrak{Z}_k^2(\lambda_k)$. Let $p_j(\lambda_{kj}) \overset{\text{def}}{=} \sup_{0<R<\infty} \frac{1}{R^2} \int_0^R \frac{1}{2\pi} \int_0^{2\pi} n_{kj}(\rho e^{i\theta}, \lambda_{kj}) d\theta d(\rho^2)$. We assume that $\frac{1}{J} \sum_{j=1}^{J} \left(\frac{1}{2\pi} \int_{\alpha_j}^{\beta_j} p_j^2(\lambda_{kj}) d\lambda_{kj} \right)^{1/2} \leq P$, $P > 0$, where $\langle \alpha_j, \beta_j \rangle = \lambda_{kj}(\langle \varphi_j, \varphi_{j+1} \rangle)$, $j = 1, \ldots, J$, (3*c*).[3] $p_j(\lambda_{kj}) \leq P$, $\lambda_{kj} \in \langle \alpha_j, \beta_j \rangle$, (3*c*$_1$). Let $\mathfrak{l}_j^1 = \{ z_\kappa | z_\kappa = h_{\kappa kj}(0,\lambda_{kj}), \lambda_{kj} \in \langle \alpha_j, \beta_j \rangle \}$ and $\mathfrak{l}^1 = \bigcup_{j=1}^{J} \mathfrak{l}_j^1$. We set $l = \min_{\mathfrak{l}^1} |f(z_1,z_2)|$, $L = \max_{\mathfrak{l}^1} |f(z_1,z_2)|$, $l = \min(1,l)$, $L = \max(1,L)$. We assume in the following that $\mathfrak{B}$ satisfies the conditions 1*a*-1*c*.

THEOREM 1. *Let $\mathfrak{G}_0^2$ satisfy conditions 2a–2f. For every $\epsilon > 0$, there exists r_0, $0 < r_0 < 1$, such that at every point of $\mathfrak{G}^2$, say at $z_\kappa^0 = g_\kappa(\zeta_0)$, and for every function $f(z_1,z_2)$ which has the properties 3a–3c, the inequality*

$$\left(e^{-2\pi PQ - 1/2 - \epsilon} l \left(\frac{1 - r_0}{1 + r_0} \right)^{2JQP} \right)^{\frac{1+|\zeta_0|}{1-|\zeta_0|}} \leq |f(z_1^0, z_2^0)| \leq \left(e^{2\pi PQ + 1/2 + \epsilon} L \left(\frac{1 + r_0}{1 - r_0} \right)^{2JQP} \right)^{\frac{1+|\zeta_0|}{1-|\zeta_0|}} \quad (3)$$

holds.

THEOREM 2. *Let $\mathfrak{G}_0^2$ satisfy 2a–2d, 2f. For every $\epsilon > 0$, there exists r_0, $0 < r_0 < 1$, such that at every point of $\mathfrak{G}^2$, say at $z_\kappa^0 = g_\kappa(\zeta_0)$, and for every function $f(z_1,z_2)$ which has the properties 3a,3b,3c$_1$, the inequality*

$$\left(e^{-2\pi P - 1/2 - \epsilon} l \left(\frac{1 - r_0}{1 + r_0} \right)^{2P} \right)^{\frac{1+|\zeta_0|}{1-|\zeta_0|}} \leq |f(z_1^0, z_2^0)| \leq \left(e^{2\pi P + 1/2 + \epsilon} L \left(\frac{1 + r_0}{1 - r_0} \right)^{2P} \right)^{\frac{1+|\zeta_0|}{1-|\zeta_0|}} \quad (4)$$

holds.

THEOREM 3. *Let $\mathfrak{G}_0^2$ satisfy 2a–2d, 2f$_1$. For every $\epsilon > 0$, there exists r_0, $0 < r_0 < 1$, such that at every point of $\mathfrak{G}^2$, say at $z_\kappa^0 = g_\kappa(\zeta_0)$ and for every function $f(z_1,z_2)$ which has the properties 3a,3b,3c$_1$, the inequality*

$$\frac{1 - |\zeta_0|}{1 + |\zeta_0|} \left(l \left(\frac{1 - r_0}{1 + r_0} \right)^{2P} - \epsilon \right) \leq |f(z_1^0, z_2^0)| \leq \frac{1 + |\zeta_0|}{1 - |\zeta_0|} \left(\tilde{L} \left(\frac{1 + r_0}{1 - r_0} \right)^{2P} + \epsilon \right) \quad (5)$$

holds. We set $\mathfrak{e}_{kr_0}^3 = \{ z_\kappa | z_\kappa = h_{\kappa k}(Z_k, \lambda_k), |Z_k| \leq r_0, \lambda_\kappa \in \langle 0, 2\pi \rangle \}$.

THEOREM 4. *Let $\mathfrak{E}_0^2$ satisfy the conditions 2a and 2b and moreover let $\mathfrak{g}^1 \subset \mathfrak{e}_{kr_0}^3$. For every $(z_1^0, z_2^0) \in \mathfrak{G}^2$ and for every function $f(z_1,z_2)$ which has properties 3a,3b and 3c$_1$, the inequality*

$$l \left(\frac{1 - r_0}{1 + r_0} \right)^{2P} \leq |f(z_1^0, z_2^0)| \leq L \left(\frac{1 + r_0}{1 - r_0} \right)^{2P} \quad (6)$$

holds.

Note that in (3)–(6) bounds for $|f|$ are expressed in terms of the minimum and maximum of $|f|$ on a *one-dimensional* boundary manifold Γ^1. This manifold is independent of (z_1^0, z_2^0) and of f.

In the proof of Theorems 1 and 2, we express the value of $f(z_1,z_2)$ at (z_1^0,z_2^0) by using the Poisson formula applied to the harmonic function $\log |f(g_1(\zeta), g_2(\zeta))|$. For the proof of Theorem 3, we apply the Cauchy integral formula to the holomorphic function $f(g_1(\zeta), g_2(\zeta))$, and for Theorem 4 the maximum principle.

Similar results are obtained by Bergman[1, 6, 7] and Charzyński.[8] Bergman considered functions which omit in every lamina two values and functions which are univalent on every lamina. Charzyński assumes that the functions

$$f(h_{1k}(Z_1,\lambda_k), h_{2k}(Z_k,\lambda_k))$$

as functions of Z_k belong to a normal family (but he considers only the case in which $\mathfrak{g}^1 \subset \mathfrak{e}^3_{kr_0}$). The first step in the proof of the Theorems 1–3 is similar to the approach used in references 2 and 3. However only the use of completely new additional procedures will yield our result.

[1] Bergman, S., *Math. Z.*, **63,** 173–194 (1955).

[2] The hypotheses 2*a*–2*d* are the same as hypotheses 1–3 in ref. 1, p. 188. Instead of hypothesis G, we have the weaker hypothesis 2*f* ($2f_1$).

[3] From 3*c*, it follows that the functions $f(h_{1k_j}(Z_{k_j}, k_j), h_{2k_j}(Z_{k_j}, \lambda_{k_j}))$ in $|Z_{k_j}| < 1$ are mean valent functions of order $p(\lambda_{k_j})$ in the sense of Spencer (see refs. 4 and 5).

[4] Spencer, D. C., *Trans. Am. Math. Soc.*, **48,** 418–435 (1940).

[5] Spencer, D. C., *Proc. London Math. Soc.*, (2), **47,** 201–211 (1941).

[6] Bergman, S., *Trav. Inst. Math. Tbilissi*, **1,** 187–204 (1937).

[7] Bergman, S., *Compositio Mathematica*, **14,** 107–123 (1938).

[8] Charzyński, Z., *Math. Z.*, **75,** 29–35 (1961).

---

*THE EFFECT OF EXOGENOUS RNA AND DNA ON AMINO ACID INCORPORATION BY SUBCELLULAR FRACTIONS PREPARED FROM ERYTHROID TISSUES**

BY SIEGMUND FISCHER,† GAIL P. BRUNS, BERTRAM A. LOWY,‡ AND IRVING M. LONDON

DEPARTMENTS OF MEDICINE AND BIOCHEMISTRY, ALBERT EINSTEIN COLLEGE OF MEDICINE, YESHIVA UNIVERSITY, NEW YORK CITY

Communicated by David Rittenberg, December 12, 1962

This paper describes the components of cell-free systems, obtained from the bone marrow of normal rabbits and from the bone marrow and reticulocytes of acetylphenylhydrazine (APH) treated rabbits, capable of incorporating amino acids into trichloracetic acid-insoluble products. The effects of exogenous RNA and DNA in these systems are described.

Materials and Methods.—Bone marrow subcellular fractions: Bone marrow, obtained from either normal New Zealand rabbits or rabbits of the same strain made anemic by treatment with APH, was collected directly into either a sucrose-medium A buffer[1] or into a Tris buffer medium containing β-mercaptoethanol.[2] The bone marrow was homogenized at 2°C for one min with a motor-driven Teflon pestle and centrifuged at 15,000 × *g* for 20 min at 2°C. The supernatant solution

was centrifuged at 105,000 × *g* for 2 hr and the resultant microsomal pellet was resuspended by gentle homogenization in the same medium. Both the microsomal suspension and the supernatant solution were recentrifuged at 105,000 × *g* for 2 hr. The soluble supernatant solution (S-100) was removed, and in some experiments pH 5 fractions and pH 5 soluble supernatant solutions were prepared.[3] The microsomal pellet was resuspended again in a small volume of the same medium. The fractions were used immediately or were either dialyzed against 100 volumes of the Tris buffer for 18 hr at 3°C and stored at −20°C, or stored at 0° without dialysis.

Reticulocyte subcellular fractions: Blood was obtained from APH treated rabbits and the cells were washed with a solution containing 0.13 *M* NaCl, 0.0052 *M* KCl, and 0.0075 *M* $MgCl_2$. Subcellular fractions (ribosomes, pH 5 fraction, pH 5 soluble supernatant solution) were prepared as described by Lamfrom,[3] except for the substitution of Tris buffer[2] for Medium A.[1] The fractions were either dialyzed or stored directly as described above.

The protein content of subcellular fractions was determined.[4]

DNA and RNA preparations: DNA was prepared from the 15,000 × *g* residue obtained from the bone marrow homogenates.[5] Microsomal, ribosomal, and soluble RNA were prepared by a modified phenol procedure.[6, 7] RNA samples were hydrolyzed by formic acid in sealed bomb tubes,[8] and the hydrolysates were chromatographed on Whatman #4 paper.[9]

Incubation conditions: The incubation conditions are described in the footnote to each table or figure. The composition of the amino acid mixture was as follows, expressed as mg per cent of L-amino acid: alanine 180, arginine hydrochloride 100, aspartic acid 380, cysteine 50, glycine 400, histidine 500, hydroxyproline 150, isoleucine 40, leucine 130, lysine 330, methionine 50, phenylalanine 260, proline 160, serine 175, threonine 200, tryptophan 60, tyrosine 150, valine 370. The amino acids were dissolved in isotonic saline and the solution was adjusted to pH 7.75 prior to the addition of glutamine 117. (We are indebted to Dr. Henry Borsook for describing the composition of the amino acid mixture.)

At the end of the incubation period samples were either centrifuged to separate microsomes or ribosomes from the soluble supernatant solution or else the entire incubation mixture was treated with 10% trichloracetic acid (TCA). The precipitate was washed twice with 3.5% TCA, and was then dissolved in 0.25 *N* NaOH. The protein was reprecipitated with 10% TCA, and was washed twice with 3.5% TCA.[10]

In the radiocarbon experiments, the final precipitate was dissolved in 0.2 *M* NH_4OH and assayed for radioactivity. Self-absorption corrections were applied.

In the experiments with tritiated valine, the final TCA precipitate was dissolved in one ml of hyamine, the solution was heated at 65°C for 2 hr and one ml of methanol was added. Radioactivity was assayed by standard techniques.

Results and Discussion.—The incorporation of L-valine-U-C^{14} into an acid-insoluble product by subcellular fractions obtained from normal rabbit bone marrow is described in Table 1. With increased concentrations of microsomes the incorporation of valine-U-C^{14} was augmented, while marked reduction in amino acid incorporation was noted in the absence of either S-100 or microsomes or in the absence of added ATP and an ATP-generating system. Amino acid incorporation was stimulated by the presence of a mixture of 17 amino acids, in agreement with the findings of Allen and Schweet in a rabbit reticulocyte system.[11]

Similar results were obtained with subcellular fractions prepared from APH rabbit bone marrow, as shown in Table 2. Reduction in amino acid incorporation was observed when either GTP, ATP, or ATP and the ATP-generating system was omitted from the incubation mixture. Only a slight decrease in amino acid incorporation was observed when CTP and UTP or the mixture of 17 amino acids was omitted. The latter observation is in agreement with the findings of Korner[12] with rat liver preparations. The optimal ratio of concentrations of magnesium to ATP was found to be 5:1, also in accord with the data of Korner[12] for rat liver. A fourfold increase in the concentration of ATP eliminated the requirement for an ATP-generating system.

TABLE 1

VALINE-U-C^{14} INCORPORATION BY SUBCELLULAR FRACTIONS FROM NORMAL RABBIT BONE MARROW

	Millimicromoles valine incorporated
Complete system: microsomes 0.125 mg of protein	0.050
" " " 0.250 " " "	0.080
" " " 0.500 " " "	0.120
" " " 0.500 mg, minus S-100	0.075
" " " " " , minus AA	0.055
" " " " " , minus CrP, CrPK, ATP	0.080
" " minus microsomes	0.030

Incubation conditions: In a total volume of 2.0 ml, micromoles per incubation flask: Tris buffer 200 (pH 7.8), magnesium acetate 20, KCl 100, β-Mercaptoethanol 12, ATP 2, creatine phosphate (CrP) 20, creatine phosphate kinase (CrPK) 300 micrograms, GTP 0.54, UTP 0.12, CTP 0.12. Amino Acid mixture (AA) minus valine 0.3 ml, L-valine-U-C^{14} 301,500 cpm/850 millimicromoles. 0.850 mg S-100 protein was added to all tubes except where stated. Incubated for 30 min at 37°C.

TABLE 2

VALINE-U-C^{14} INCORPORATION BY SUBCELLULAR FRACTIONS PREPARED FROM APH RABBIT BONE MARROW

	Millimicromoles valine incorporated
Complete system	0.0225
" " minus AA	0.0220
" " " CTP and UTP	0.0210
" " " GTP	0.0190
" " " ATP	0.0170
" " " ATP, CrP, and CrPK	0.0080

Incubation Conditions: In a total volume of 0.625 ml, micromoles per incubation flask: Tris buffer 25 (pH 7.8), magnesium acetate 2.5, KCl 12.5, β-Mercaptoethanol 1.2, ATP 0.5, CrP 5, CrPK 75 micrograms, GTP 0.14, UTP 0.03, CTP 0.03. AA minus valine (diluted 1:4) 0.25 ml, L-valine-U-C^{14} 454,000 cpm/50 millimicromoles. 0.9 mg microsomal protein, 0.6 mg of pH 5 fraction protein, and 1.0 mg of pH 5 soluble supernatant solution protein were added to all tubes. Incubated for 30 min at 37°C.

The incorporation of tritiated valine into an acid-insoluble product by a subcellular system derived from rabbit reticulocytes is described in Table 3. In agreement with the data obtained with APH bone marrow, a striking reduction in amino acid incorporation occurred when ATP, GTP, or the ATP-generating system was omitted, although the requirement for the ATP-generating system could not be eliminated by increasing the concentration of ATP fourfold. As in the bone marrow system, a magnesium to ATP ratio of 5:1 was found to be optimal. The omission of CTP and UTP did not affect the incorporation of amino acids, while the addition of RNase resulted in almost complete inactivation of the system. Amino acid incorporation was not enhanced by addition of the amino acid mixture, even when dialyzed subcellular fractions were used. The basis for the difference in the effect of amino acid addition in the several subcellular systems is not apparent.

The subcellular components required for amino acid incorporation have been described by a number of investigators, and the data obtained from the bone marrow and reticulocyte systems conform with those findings. In the systems under discussion, the omission of microsomal or ribosomal fractions results in a marked diminution in amino acid incorporating ability. However, the consistent observation of amino acid incorporation in the absence of added microsomal or ribosomal fractions may reflect their presence in the high speed supernatant solutions (S-100, pH 5 fraction, pH 5 soluble supernatant solution) and conforms with the observations of Palade and Siekevitz[13] on guinea pig pancreas. When the S-100 fraction of bone marrow or the pH 5 fraction of the reticulocyte was recentrifuged at 105,000

TABLE 3

DL-VALINE-2,3-H^3 INCORPORATION BY SUBCELLULAR FRACTIONS PREPARED FROM RABBIT RETICULOCYTES

	Millimicromoles valine incorporated
Complete system	0.490
" " minus pH 5 fraction	0.255
" " " ribosomes	0.225
" " " GTP	0.365
" " " ATP	0.210
" " " CrP and CrPK	0.300
" " " ATP, GTP, CTP, UTP, CrP, CrPK	0.220

Incubation conditions: In a total volume of 0.675 ml, micromoles per incubation flask: Tris buffer 25 (pH 7.8), magnesium acetate 2.5, KCl 12.5, β-Mercaptoethanol 1.2, ATP 0.5, GTP 0.14, UTP 0.03, CTP 0.03, CrP 5.0, CrPK 75 micrograms. AA minus valine, (diluted 1:4) 0.025 ml, DL-valine-2,3-H^3, 478,000 cpm/100 millimicromoles. 1.4 mg ribosomal protein, 0.80 mg pH 5 fraction protein, and 1.6 mg of pH 5 soluble supernatant solution protein were added to all tubes except where stated. Incubation time: 30 min at 37°C.

$\times g$ for 12 to 16 hr, a small pellet was obtained which substituted for microsomes or ribosomes in the subcellular systems. Within the concentration range studied, amino acid incorporation is proportional to the concentration of microsomes or ribosomes present.

Although the omission of the S-100 fraction from both the normal and APH bone marrow systems results in considerable decrease in amino acid incorporation, the omission of the pH 5 soluble supernatant solution from the reticulocyte system had no effect, suggesting that transfer and activating enzymes in the pH 5 fraction are adequate for the extent of incorporation observed in the reticulocyte subcellular system. Amino acid incorporation was reduced by 50 per cent when the pH 5 fraction was omitted.

The subcellular fractions obtained from bone marrow and from reticulocytes exhibit considerable variation in amino acid incorporating ability from preparation to preparation. The observed differences in amino acid incorporation between bone marrow and reticulocyte preparations may be related, in part, to their nuclease activities, since greater ribonuclease activity has been found in the microsomal and supernatant fractions obtained from bone marrow than that found in reticulocyte preparations.[14]

The effect of the addition of various types of microsomal and ribosomal RNA preparations on an APH bone marrow subcellular system is shown in Table 4. A 35–55% increase in amino acid incorporation into one or more components of the isolated supernatant fraction was observed upon the addition of microsomal or ribosomal RNA obtained from reticulocytes, bone marrow, and spleen of APH treated rabbits. Slight stimulation of amino acid incorporation occurred with microsomal RNA obtained from normal rat liver. A similar pattern of stimulation of amino acid incorporation was also observed in the reisolated microsomal pellets in this experiment.

In the rabbit reticulocyte system, enhancement of amino acid incorporation into a trichloracetic acid precipitable product by exogenous RNA has been observed. The data, presented in Figure 1, reveal a linear enhancement of leucine incorporation by the addition of rabbit reticulocyte ribosomal RNA to an incubation mixture. The specificity of the RNA enhancement observed was investigated by the addition of samples of RNA from diverse sources (Table 5). In agreement with the observations in the bone marrow system, a number of microsomal and ribosomal

TABLE 4

EFFECT OF VARIOUS TYPES OF RNA ON THE INCORPORATION OF DL-VALINE-2,3-H^3 INTO THE ISOLATED SUPERNATANT FRACTION BY SUBCELLULAR FRACTIONS PREPARED FROM APH RABBIT BONE MARROW

	Millimicromoles valine incorporated into isolated supernatant fraction
Complete system	0.075
" " plus reticulocyte ribosomal RNA 4.87 mg	0.100
" " plus APH bone marrow microsomal RNA 3.25 mg	0.115
" " plus APH spleen microsomal RNA 3.25 mg	0.110
" " plus normal rat liver microsomal RNA 2.65 mg	0.090

Incubation Conditions: In a total volume of 3.0 ml, micromoles per incubation flask: 4 times the amount of all constituents as in Table 2 except DL-valine-2,3-H^3 1.92×10^7 cpm/150 millimicromoles. 5.9 mg of microsomal protein, 2.1 mg of pH 5 fraction protein, and 5.9 mg of pH 5 soluble supernatant solution protein were added to all tubes. Incubated for 60 min at 37°C. At the end of the incubation, the supernatant fraction, obtained by centrifugation of the incubation mixture at $105,000 \times g$ for 2 hr, was isolated.

RNA samples enhanced amino acid incorporation. It is of interest to note that rabbit spleen microsomal RNA was most effective in the rabbit reticulocyte subcellular system, while only *E. coli* sRNA was not stimulatory, even at high concentrations. The ribosomal and microsomal RNA samples used in these experiments had a 260/280 optical density ratio of 1.9–2.1 and contained approximately 62 per cent guanine + cytosine. The protein content of all samples was less than one per cent.

An extension of the studies to include the effect of addition of DNA to bone marrow and reticulocyte subcellular preparations revealed an enhancement of amino acid incorporation resulting from the addition of DNA from normal rabbit bone marrow. The data of Table 6 show a 58 per cent stimulation of valine incorpora-

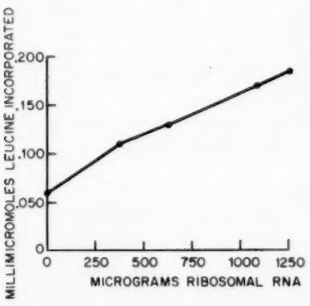

FIG. 1.—Effect of various concentrations of rabbit reticulocyte ribosomal RNA on the incorporation of L-leucine-U-C^{14} by subcellular fractions prepared from rabbit reticulocytes. *Incubation conditions:* In a total volume of 0.675 ml. micromoles as in Table 3 except L-leucine-U-C^{14} 133,500 cpm/50 millimicromoles. 0.70 mg ribosomal protein, 0.90 mg pH 5 fraction protein and 1.20 mg of pH 5 soluble supernatant solution protein were added to all tubes. Incubation time: 30 min at 37°C.

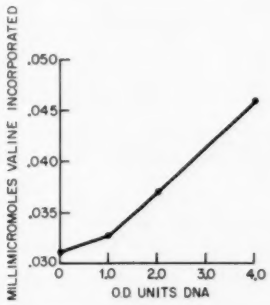

FIG. 2.—Effect of various concentrations of normal rabbit bone marrow DNA on the incorporation of L-valine-U-C^{14} by subcellular fractions prepared from rabbit reticulocytes. *Incubation conditions:* In a total volume of 0.675 ml, micromoles as in Table 3 except valine-U-C^{14} 666,500 cpm/100 millimicromoles. DNA was dissolved in 0.2 M Tris buffer (pH 7.8) and is expressed as O.D. units at 260 mμ. 1.0 mg ribosomal protein and 3.2 mg S-100 protein were added to all tubes. Incubation time: 30 min at 37°C.

TABLE 5

EFFECT OF VARIOUS TYPES OF RNA ON THE INCORPORATION OF L-LEUCINE-U-C^{14} BY SUBCELLULAR FRACTIONS PREPARED FROM RABBIT RETICULOCYTES

	Millimicromoles leucine incorporated
Complete system	0.140
" " plus normal rat liver microsomal RNA 1.85 mg	0.195
" " plus *E. coli* ribosomal RNA 1.6 mg	0.170
" " plus APH rabbit spleen microsomal RNA 1.8 mg	0.230
" " plus duck reticulocyte ribosomal RNA 1.5 mg	0.190
" " plus *E. coli* sRNA 1.0 mg	0.145

Incubation conditions: In a total volume of 0.675 ml, micromoles added as in Table 3 except L-leucine-U-C^{14} 133,500 cpm/50 millimicromoles. 0.70 mg ribosomal protein, 0.90 mg pH 5 fraction protein, and 1.20 mg pH 5 soluble supernatant solution protein were added to all tubes. RNA content was calculated based upon 1.0 O.D. unit at 260 mμ. equivalent to 46.4 micrograms of RNA/ml. Incubation time: 30 min at 37°C.

tion when 1.0 optical density unit of DNA was included in the APH rabbit bone marrow subcellular incubation mixture, although increased amounts of DNA did not lead to further stimulation. The addition of DNase in the presence of DNA markedly decreased the stimulatory effect. The addition of DNA to a reticulocyte subcellular system is shown in Figure 2. In contrast to the DNA effect in the bone marrow system, enhancement of amino acid incorporation by exogenous DNA in the reticulocyte system is linear over the range of 1.0 to 4.0 O.D. units. The explanation for this difference is not apparent.

TABLE 6

EFFECT OF NORMAL RABBIT BONE MARROW DNA ON THE INCORPORATION OF L-VALINE-U-C^{14} BY SUBCELLULAR FRACTIONS PREPARED FROM APH RABBIT BONE MARROW

	Millimicromoles valine incorporated
Complete system	0.0180
" " plus DNA 1.0 O.D. unit	0.0275
" " " " 2.0 O.D. units	0.0270
" " " " 4.0 O.D. units	0.0285
" " " " 2.0 O.D. units plus DNase (5.0 micrograms)	0.0210
" " " DNase (5.0 micrograms)	0.0200

Incubation conditions: As in Table 2 except L-valine-U-C^{14} 666,500 cpm/100 millimicromoles. DNase (pancreatic) 200 micrograms/ml in 0.2 M Tris Buffer (pH 7.8). 1.35 mg of microsomal protein, 1.58 mg of S-100 protein were added to all tubes. DNA concentration expressed as optical density units (optical density units = O.D. 260 mμ × vol).

Several explanations may be advanced for the observed effects of nucleic acid supplementation. The RNA samples may function as polyanions which protect microsomal structures or they may serve as substrates for endogenous ribonucleases and thus spare microsomal RNA. It is also possible that the added RNA preparations may contain functional messenger RNA. Since Nirenberg and Matthaei[7] and Arnstein *et al.*[15] have suggested that preincubation of ribosomal preparations may be necessary in order to demonstrate the effect of exogenous synthetic polynucleotides, the effect of preincubation was studied with reticulocyte subcellular fractions. When rabbit reticulocyte ribosomal RNA was added to preincubated and nonpreincubated fractions, no augmented enhancement was observed in the preincubated fractions.

Although the mechanism of stimulation by DNA in these experiments is not known, the effect may be a reflection of the presence of RNA polymerase in the erythroid subcellular fractions studied and the exogenous DNA may possibly be serving as a primer for the synthesis of an RNA responsible for augmenting amino acid

incorporation. However, the addition of purified *E. coli* RNA polymerase[16] plus normal rabbit bone marrow DNA to the reticulocyte subcellular system did not enhance amino acid incorporation, although normal rabbit bone marrow DNA serves efficiently as a primer for *E. coli* RNA polymerase.[17] The species and organ specificity and the mechanism of stimulation of incorporation by exogenous DNA are under investigation. Preliminary experiments suggest that the protein, whose formation is stimulated by the addition of reticulocyte ribosomal RNA or normal bone marrow DNA to the reticulocyte subcellular system, is hemoglobin.

Summary.—Evidence has been presented that subcellular fractions prepared from erythroid tissues of normal and APH-treated rabbits incorporate amino acids into TCA-insoluble material. The addition, to subcellular incubation mixtures, of microsomal or ribosomal RNA from several sources, or of rabbit bone marrow DNA, stimulates amino acid incorporation.

It is a pleasure to thank Dr. J. Hurwitz for a gift of RNA polymerase and for his advice in the preparation of the enzyme. The very able technical assistance of Mrs. Gloria Siegman is acknowledged.

* Supported by the U.S. Public Health Service (A-2803, H-2655).

† Permanent address: Department of Virology, School of Medicine, University of Chile, Santiago, Chile.

‡ Recipient of Career Development Award, U.S. Public Health Service (GM-K3-3059).

[1] Zamecnik, P. C., and E. B. Keller, *J. Biol. Chem.*, **209**, 337 (1954).
[2] Matthaei, J. H., and M. W. Nirenberg, these PROCEEDINGS, **47**, 1580 (1961).
[3] Lamfrom, H., *J. Mol. Biol.*, **3**, 241 (1961).
[4] Lowry, O. H., N. F. Rosebrough, and A. L. Farr, *J. Biol. Chem.*, **193**, 265 (1951).
[5] Kirby, K. S., *Biochim. et Biophys. Acta*, **47**, 18 (1961).
[6] Kirby, K. S., *Biochem. J.*, **64**, 405 (1956).
[7] Nirenberg, M. W., and J. H. Matthaei, these PROCEEDINGS, **47**, 1588 (1961).
[8] Wyatt, S. R., *Biochem. J.*, **48**, 584 (1951).
[9] Kirby, K. S., *Biochim. et Biophys. Acta*, **18**, 575 (1955).
[10] Schweet, R., H. Lamfrom, and E. Allen, these PROCEEDINGS, **44**, 1029 (1958).
[11] Allen, E. H., and R. S. Schweet, *J. Biol. Chem.*, **237**, 760 (1962).
[12] Korner, A., *Biochem. J.*, **81**, 168 (1961).
[13] Palade, G. E., and P. Siekevitz, *J. Biophys. Biochem. Cytol.*, **2**, 671 (1956).
[14] Fischer, S., and G. P. Bruns, unpublished observations.
[15] Arnstein, H. R. V., R. A. Cox, and J. A. Hunt, *Nature*, **194**, 1042 (1962).
[16] Furth, J. J., J. Hurwitz, and M. Anders, *J. Biol. Chem.*, **237**, 2611 (1962).
[17] Hurwitz, J., personal communication.

BASIS OF ACTINOMYCIN ACTION, II. EFFECT OF ACTINOMYCIN ON THE NUCLEOSIDE TRIPHOSPHATE-INORGANIC PYROPHOSPHATE EXCHANGE

By I. H. Goldberg, M. Rabinowitz, and E. Reich

DEPARTMENTS OF MEDICINE AND BIOCHEMISTRY, UNIVERSITY OF CHICAGO; ARGONNE CANCER RESEARCH HOSPITAL;* LABORATORY OF BIOCHEMICAL GENETICS, THE ROCKEFELLER INSTITUTE

Communicated by E. L. Tatum, September 4, 1962

In a preceding paper,[1] we have described the effect of actinomycin on the different synthetic reactions catalyzed by RNA†-polymerase, and the relationship between actinomycin action and the structure and base composition of DNA. This paper presents the results of experiments concerned with the effect of actinomycin on the nucleoside triphosphate-inorganic pyrophosphate exchange reaction.

Materials and Methods.—The isolation of RNA-polymerase from *Escherichia coli* B and the assay conditions used during its purification were as described by Chamberlin and Berg.[2] All reactions contained 4.1 μg enzyme protein/0.25 ml.

Incorporation of radioactive pyrophosphate (PP^{32}) into the terminal pyrophosphate position of nucleoside triphosphates ("exchange reaction") was determined as follows: PP^{32}, prepared according to Jones *et al.*,[3] was incubated with the components of the standard assay mixture, in the absence of Mn^{++}, at a concentration of 1.6 μmoles/ml; $MgCl_2$ was present at 8 μmoles/ml. The reaction was stopped by chilling, adding a large excess of nonradioactive phosphate and pyrophosphate buffers, carrier bovine serum albumin and yeast RNA (2 mg each per reaction vessel) and trichloracetic acid (final concentration 5%). After centrifugation, the supernatant solution was treated with charcoal; the latter was washed four times with acetate buffer (0.1 *M* pH 4.5) containing phosphate and pyrophosphate (0.03 *M*), transferred to a planchet, dried, and the adsorbed radioactivity measured in a thin-window gas-flow counter. Nucleic acid concentrations were based on the phosphorus content determined according to Fiske and Subba-Row.[4] Protein was measured according to Lowry *et al.*[5] Actinomycin concentrations were based on the absorption of a standard solution of 25 μg/ml, giving an O.D. (440 mμ) of 0.358 in 0.01 *M* Tris pH 7.4 with 1 cm light path. The absorption of pure actinomycin is appreciably greater than this value which was established several years ago for a preparation containing inert material.

DNA preparations: All DNA solutions were made in 0.01 *M* Tris (pH 7.4)−0.01 *M* NaCl, except for crab dAT, which was dissolved in 0.75 *M* NaCl−0.05 *M* phosphate (pH 6.7). Highly polymerized calf thymus DNA was purchased from Sigma Chemical Co., St. Louis, Mo.; DNA from *Micrococcus lysodeikticus* and *Tetrahymena pyriformis* was prepared by the method of Marmur,[6] according to a modification suggested by N. Sueoka. Synthetic deoxyadenylic-deoxythymidylic (dAT) and deoxyguanylic-deoxycytidylic polymers (dGC), and crab dAT, were generously provided by A. Kornberg and N. Sueoka, respectively. Nonradioactive NTP was obtained from Pabst Laboratories and Sigma Chemical Co.

Results.—Effect of actinomycin of NTP-PP^{32} exchange reaction: RNA-polymerase catalyzes a DNA-dependent exchange reaction between a single NTP and inorganic PP. This reaction is less sensitive to actinomycin than the synthetic reaction with the same DNA preparations[1, 7] (Fig. 1). Nevertheless, the difference in actino-

mycin-sensitivity between synthetic reactions primed by calf thymus, *T. pyriformis*, and *M. lysodeikticus* DNAs[1] has its counterpart in the exchange reactions directed by the same DNAs. This difference is most striking at higher concentrations of actinomycin. With calf thymus DNA, a substantial residual exchange activity persists at actinomycin concentrations (50 μg/ml and 100 μg/ml) which totally suppress the same reactions with *M. lysodeikticus* DNA. This residual activity might be due to the presence of relatively long guanine-free sequences in calf thymus DNA which would not bind actinomycin and would thereby remain capable of priming the exchange reaction. In order to test this possibility, the four NTPs were separated by paper electrophoresis after an incubation in the presence of calf thymus DNA, actinomycin (50 μg/ml) and PP^{32}. All four NTPs were radioactive. Therefore, if guanine-free sequences are responsible for the exchange remaining at higher concentrations of actinomycin, the priming of this residual exchange reaction violates the base-pairing principles which seem to govern the synthetic reaction. An alternative possibility is that some guanine-containing sequences may bind actinomycin very poorly or not at all. Such sequences may be present in higher frequency in calf thymus DNA compared with *M. lysodeikticus* DNA and prime the exchange reaction of all four NTPs even at very high concentrations of actinomycin.

All combinations of NTPs—singly, as well as all possible mixtures of equal concentrations of two, three, and four NTPs—have been found to be inhibited by actinomycin in the exchange reaction. At 100 μg actinomycin/ml, the exchange with each NTP singly was inhibited more than 90 per cent. However, the significance of the varying degrees of inhibition of exchange with the different individual nucleotides is difficult to assess since the rate of the reaction is markedly affected, for each nucleotide, by variations in its concentration and in the total NTP concentrations.

Exchange reaction directed by dAT and dGC: The data in Figure 2 show that the rates of exchange of individual NTPs with pyrophosphate need not reflect base composition of the priming DNA. As shown in Figure 1, the exchange reaction directed by dAT is totally resistant to actinomycin, as was the synthetic reaction. The rate of the exchange reaction in the presence of both UTP and ATP when polynucleotide synthesis is proceeding is substantially lower than with the equivalent concentrations of UTP alone, but these conditions permit an exchange of pyrophosphate with ATP which is much greater than that (Fig. 2) with ATP alone. The effect of actinomycin on exchange reactions primed by dGC is shown in Figure 3. The exchange reaction with GTP alone is less sensitive to actinomycin than with CTP alone, resembling the corresponding homopolymer formation.[1] Exchange reactions, with one exception, appear considerably more resistant to actinomycin than the homologous synthetic reactions. The single exception is the exchange with CTP alone primed by *M. lysodeikticus* DNA, whose actinomycin sensitivity closely parallels that of poly C formation[1] primed by the same DNA.

Discussion.—Studies on actinomycin binding to DNA and actinomycin inhibition of RNA-polymerase synthetic reactions have shown that both are dependent on the presence of guanine in the polydeoxyribonucleotide.[1] However, not all sequences containing guanine showed equal affinity in binding actinomycin or equal susceptibility to its inhibitory action on the priming of RNA synthesis. The bind-

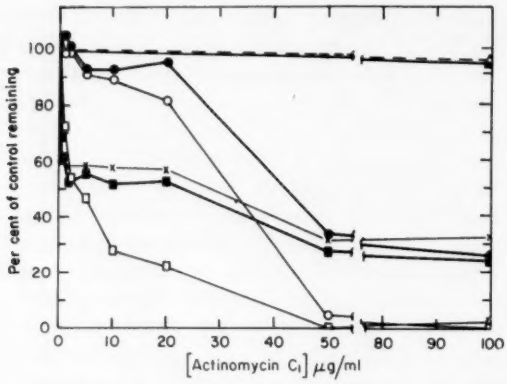

FIG. 1.—Actinomycin inhibition of NTP–PP exchange reaction. With crab dAT, 400 mμmoles each of ATP and UTP were present, otherwise each NTP was at 100 mμmoles per 0.25 ml under standard conditions with 49 mμmoles DNA-P as primer. With four NTP 100 per cent incorporation was 1.39, 1.25, and 0.72 mμmoles with calf thymus (■—■), *T. pyriformis* (×—×), and *M. lysodeikticus* (□—□) DNA respectively. With ATP, GTP, and CTP, 100 per cent equals 1.35 mμmoles with calf thymus (●—●), and 0.61 mμmoles with *M. lysodeikticus* DNA (○—○). With crab dAT (▲—▲), present at 0.025 O.D. units (260 mμ) and synthetic dAT (△—△), present at 0.085 O.D. units (260 mμ), 100 per cent incorporation with ATP and UTP were 1.21 and 0.99 mμmoles respectively.

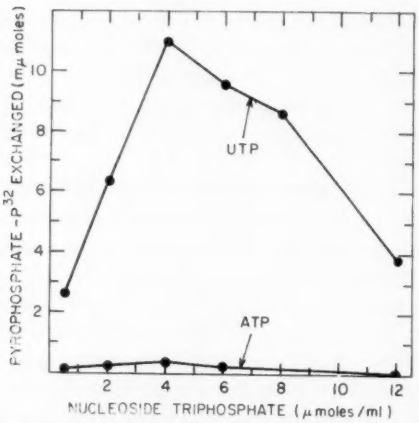

FIG. 2.—Effect of NTP concentration on NTP–PP^{32} exchange with either UTP or ATP alone, crab dAT (0.025 O.D. units 260 mμ/0.25 ml) as primer. The exchange is expressed as mμmoles per ml reaction volume. Standard reaction conditions.

ing effectiveness for actinomycin of a given DNA preparation could be directly correlated with its actinomycin-susceptibility in priming RNA synthesis.[1] It is also correlated with actinomycin-susceptibility in directing the NTP-PP^{32} exchange. Previous conclusions[1] concerning the basis of actinomycin action are thus strengthened by the present results. Since the exchange reaction can proceed with single NTP independently of concurrent polynucleotide synthesis, it is likely that many short segments of DNA containing the requisite complementary bases can serve as primers of exchange. The relative actinomycin-resistance of the exchange reaction compared with that of the synthetic reaction is therefore not unexpected, since a scattering of bound actinomycin molecules which would prevent the formation of acid-insoluble polynucleotides could still leave significant areas of the DNA free to direct the pyrophosphate exchange.

An unexpected finding is the failure of dAT to prime an exchange reaction with ATP in the absence of UTP. This fact may have physiological significance. The sequence of nucleotides in dAT is known to be a perfectly alternating one of de-

oxyadenylic and thymidylic acids.[8] It is apparent that in this sequence pattern ATP cannot interact with enzyme and primer to exchange its terminal pyrophosphate unit. However, such interaction is possible with either calf thymus or *M. lysodeikticus* DNA where the priming thymidylate residues presumably exist in all possible sequence patterns and the same interaction can take place with dAT provided UTP is present and polyribonucleotide chain growth is proceeding. It is possible that with dAT only UTP can serve to initiate polyribonucleotide chain growth. Thus the failure of ATP to exchange with PP^{32} in dAT-primed reactions may represent a model for visualizing DNA sequences which establish the starting point of RNA template synthesis under normal conditions. The ability of a given NTP to initiate polyribonucleotide chain growth may be determined not merely by the presence of its complementary base in the primer, but by the *sequence* of which such a base forms only one part.

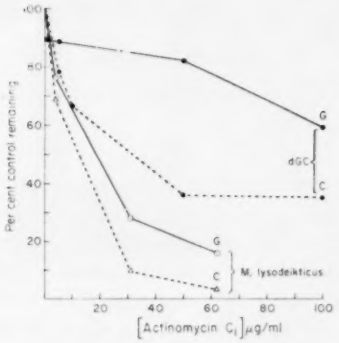

FIG. 3.—Effect of actinomycin on NTP-PP^{32} exchange with either CTP or GTP, in the presence of either dGC or *M. lysodeikticus* DNA. The standard reaction conditions were modified by increasing the period of incubation to 30 min and by increasing the concentration of the individual NTP to 4 μmoles/ml. The primer concentrations were 1.11 mμmoles dGC in 0.1 ml, and 49 mμmoles *M. lysodeikticus* DNA in 0.25 ml reaction volume. 100 per cent incorporation was 0.171 and 0.128 mμmoles with GTP and CTP respectively (dGC primer) and 0.175 and 0.429 mμmoles with GTP and CTP respectively (*M. lysodeikticus* DNA primer). *M. lysodeikticus* DNA priming of the exchange reaction is much less efficient and more actinomycin-sensitive than dGC.

We thank E. L. Tatum for his interest and encouragement, the American Cancer Society (I. H. G.), the Helen Hay Whitney Foundation (E. R.), the National Science Foundation, and the National Institutes of Health for support.

* Operated by the University of Chicago for the U. S. Atomic Energy Commission.

† Abbreviations: NTP-ribonucleoside triphosphate; ATP, CTP, GTP, UTP; AMP, CMP, GMP, UMP; 5′-triphosphate, 3′(2′) monophosphate, respectively of adenosine, cytidine, guanosine, uridine. DNA-deoxyribonucleic acid; RNA-ribonucleic acid.

[1] Goldberg, I. H., M. Rabinowitz, and E. Reich, these PROCEEDINGS, **48,** 2094 (1962).

[2] Chamberlin, M., and P. Berg, these PROCEEDINGS, **48,** 81 (1962).

[3] Jones, M. E., F. Lipmann, H. Hilz, and F. Lynen, *J. Am. Chem. Soc.*, **75,** 3285 (1953).

[4] Fiske, C. H., and Y. Subba-Row, *J. Biol. Chem.*, **66,** 375 (1925).

[5] Lowry, O. H., N. J. Rosebrough, A. L. Farr, and R. J. Randall, *J. Biol. Chem.*, **193,** 265 (1951).

[6] Marmur, J., *J. Mol. Biol.*, **3,** 208 (1961).

[7] Hurwitz, J., J. J. Furth, M. Malamy, and M. Alexander, these PROCEEDINGS, **48,** 1222 (1962).

[8] Swartz, M. N., T. Trautner, and A. Kornberg, *J. Biol. Chem.*, **237,** 1961 (1962)

*ON THE CHEMISTRY OF THE THYMUS GLAND**

By Andrew Hegyeli, Jane A. McLaughlin, and Albert Szent-Györgyi

THE INSTITUTE FOR MUSCLE RESEARCH, MARINE BIOLOGICAL LABORATORY, WOODS HOLE, MASSACHUSETTS

Communicated December 12, 1962

We reported earlier[1] that certain extracts of the thymus gland of calves inhibited malignant growth, while others promoted the same. The substance responsible for the first action was called "retine," while the latter was termed "promine." We found that extracts having a promotor action also sterilized mice, both male and female. We supposed that both actions, growth promotion and sterilizing, were due to promine. We show, in the present paper, that the two actions can be separated by paper chromatography and are thus due to two different substances. We propose to call the sterilizing factor "infertine" and will call a unit its smallest quantity which, when injected in 8-week-old mice (28–30 gm) daily, renders females reversibly sterile in two days.

Figure 1 shows the result of an experiment. The purified extract was placed on paper (Whatman 17, 46 × 57 cm), airdried, and ascending chromatography was made with the butanol phase of a mixture containing butanol, acetic acid, and water in the proportion 4:1:5. Before chromatography the paper was exposed for 10 min to the vapors of the water phase of the mixture. After completion (about 17 hr), the paper was dried, cut into segments which then were extracted with a 9:1 mixture of methanol and 0.1 *N* HCl. The extracts were evaporated and the residue redissolved in a small quantity of propylene glycole. Then, gradually, water was added. The final concentration of the glycole did not exceed 5 per cent.

The abscissa in Figure 1 gives the Rf; the ordinate, the activity of the extract in units. The width of the squares corresponds to the width of the paper strips in relation to Rf. The double hatching corresponds to growth promoting, the single hatching to sterilizing activity. As will be seen from Figure 1, the two activities are found in different segments of the paper without overlap, the separation thus being complete. The sterilizing extracts contained, also, the growth-inhibiting factor as impurity. This method of chromatography is thus unsuited for the separation of the sterilizing and inhibitory action but can be used for the separation of promine and infertine.

The purified solutions still contain some choline and betaine. Table 1 shows the Rf value of the various substances in question. Similar results could be obtained in column chromatography using dry Schleicher and Schülls' No. 289 filter paper pulp, or Whatman cellulose powder, standard grade, both having been washed before the experiment with 0.1 *N* HCl and methanol and then dried at 105°C.

Figure 2 shows analogous results obtained on predried paper (Whatman 17, 46 × 57 cm). In this case, butanol was used as moving phase, saturated with *N* HCl. In this figure, the doubly hatched areas correspond to promine, mixed with sterilizing factor. The singly hatched areas correspond to retine. Table 2 sums up the Rf values.

As Figure 2 and Table 2 show, the sterilizing factor was immobile and was not separated from promine. Promine and retine were separated but the separation was not complete, there being an overlapping zone between the two.

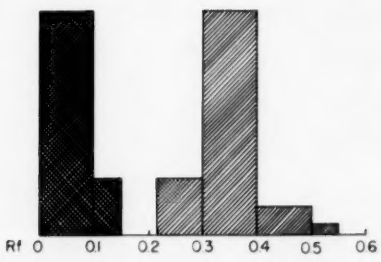

FIG. 1

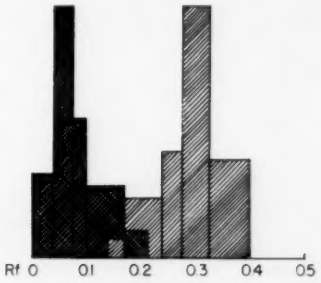

FIG. 2

The sterilizing activity seems to be limited to extracts of the thymus gland. Analogous extracts from spleen, liver, lungs, heart, and body muscle did not show a similar activity. The presence of a sterilizing factor seems to be in line with what is known of the physiology of the thymus gland which has its highest development in prepuberty when animals do not produce progeny. In prepuberty, the body may need the sexual steroids in order to be able to develop the sexual organs, but may also need a factor depressing fertility.

The extracts were tested for sterilizing activity in the following way: Groups of 3 of 8-week-old female Swiss albino mice received subcutaneous injections of the material in 0.25 ml on two consecutive days. On the third day a male was added to the group and the injections continued for a fortnight. Fourteen days contain at least two sexual periods of 5 days. Then the treatment was discontinued, the male eliminated, and the females observed for gravidity.

If sexually mature animals were used for the test the animals could become pregnant later. The sterilizing action was thus reversible. However, we found that if sexually immature animals were treated with infertine they remained sterile permanently. This observation demands corroboration and extension.

In the following lines we give a brief outline of the steps of the chemical manipulations which preceded the chromatography. In Table 3 we give a schematic outline. DW stands for the dry weight in grams, U for units of infertine.

Material.—As material, the thymus glands of calves were used which were carefully cleaned of connective tissue and frozen soon after death. The glands were transported frozen and reduced to a snow in this condition. The snow was dropped

TABLE 1

	Rf
Promine	0.05
Retine	0.30
Infertine	0.35
Choline	0.28
Betaine	0.35

TABLE 2

	Rf
Promine	0.05
Retine	0.30
Infertine	0.0
Choline	0.12
Betaine	0.17

TABLE 3

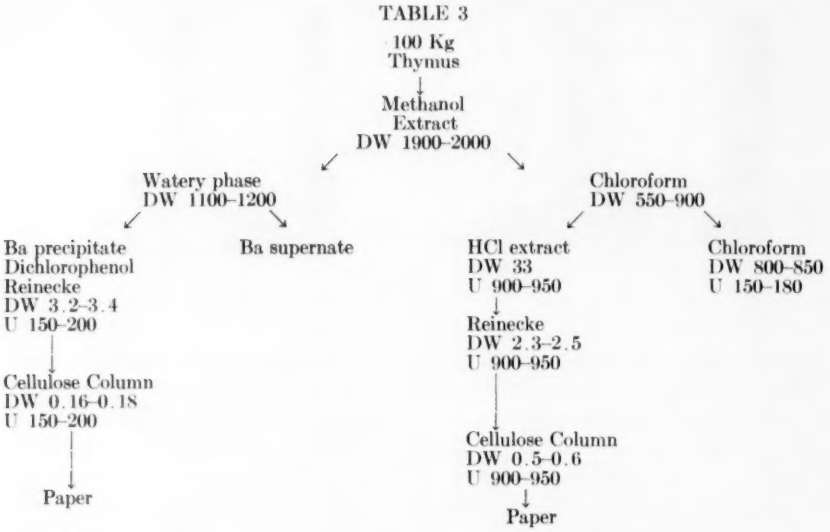

straight into methanol which was then heated to boiling. The methanol was evaporated at low temperature and the aqueous residue was shaken out with chloroform at pH 5. At this point the extract was thus divided into a chloroform extract and the extracted aqueous residue.

The *chloroform extract* was shaken out with 0.01 and 0.1 *N* HCl. This extracted the infertine which was then precipitated with Reinecke salt. The precipitate was separated, and the Reinecke salt eliminated. The material was purified further in cellulose column chromatography and finally on paper. This latter step caused a further strong drop in dry weight without a considerable loss of activity.

The *aqueous phase* was precipitated with $Ba(OH)_2$ at pH 8. The precipitate was separated and the inactive supernate rejected. The precipitate was suspended in methanol and the barium was precipitated by sulphuric acid. The pH was then adjusted to 4 and the fluid evaporated, redissolved in a small amount of water which then was shaken out twice with 10 per cent 2,4-dichlorophenol, which extracts the active substance. The infertine then was extracted from the dichlorophenol by shaking out the latter with *N* HCl. The infertine was precipitated as Reinecke salt. Finally, the extract was purified by cellulose column chromatography on paper.

As Table 3 shows, about $^4/_5$ of the activity is extracted by chloroform, can be extracted from the chloroform with acid water, can be precipitated with Reinecke salt and chromatographed without major loss. The behavior towards Reinecke salt suggests a substance containing nitrogen with a pK of about 2–3. The chloroform, methanol, and water solubility suggests a substance which is not a protein and has a lower molecular weight.

* This research was supported by a grant from the National Institutes of Health (No. GM-10383), and the National Science Foundation (No. G-5836).

[1] Szent-Györgyi, A., A. Hegyeli, and Jane A. McLaughlin, these PROCEEDINGS, **48,** 1439 (1962).

*GENESIS OF MITOCHONDRIA IN NEUROSPORA CRASSA**

By David J. L. Luck

THE ROCKEFELLER INSTITUTE, NEW YORK

Communicated by George E. Palade, December 31, 1962

Observations with the light and electron microscopes have suggested three possible mechanisms for the formation of new mitochondria:[1, 2] (1) growth and subdivision of existing mitochondria, (2) *denovo* synthesis, and (3) derivation from other nonmitochondrial membranous structures. In an attempt to distinguish between these basic possibilities, we have carried out the following experiment: Cells fully labeled with a radioactive constituent of mitochondria were transferred to nonradioactive medium. During the subsequent logarithmic growth period purified mitochondrial fractions were isolated, and the distribution of label among their individual mitochondria was determined using a quantitative radioautographic technique.[3, 4a]

In this type of experiment, the distribution of autographic grains among mitochondria could be expected to fit one of three patterns: (1) A dispersive pattern in which label would be distributed among all mitochondria, the average grain count per mitochondrion decreasing as a function of cell growth. This pattern is consistent with mitochondrial multiplication by division. (2) A conservative distribution in which the proportion of labeled mitochondria would decrease during growth in unlabeled medium as a logarithmic function of time, the average grain count per mitochondrion in the labeled population remaining the same. Such a pattern is consistent with *de-novo* synthesis. (3) An intermediate pattern, in which the label would not be randomly distributed, and the proportion of labeled individuals would decrease less rapidly than in the truly conservative case, the total grain count of the labeled population decreasing, remaining the same, or increasing slightly. This would be consistent with formation of mitochondria from labeled (possibly structural) precursors.

In these studies radioactive choline was used as a label, because lecithin into which it is incorporated is a major constituent of mitochondrial phospholipids.[5, 6] Efficient and chemically specific labeling was obtained by working with a choline-requiring strain of *Neurospora crassa* (*chol-1*, #34486).[7] This cholineless strain appears to be blocked at the earliest step in the synthesis of choline from ethanolamine; it can make neither mono- nor dimethyl-ethanolamine, though it can use these compounds for the synthesis of choline.[8, 9]

The experiment which has been outlined can yield the information needed, provided several prerequisites are fulfiled: (*a*) The cells under study must constitute a homogeneous population with a reproducible and prolonged logarithmic growth phase. (*b*) The mitochondrial fractions used for analysis must be free of contamination by other cellular structures. (*c*) The radioactive choline which is incorporated must behave as a stable mitochondrial label. Much of the experimental evidence is directed toward demonstrating that these prerequisities are satisfied.

Materials and Methods.—Materials: Cytochrome *c*, Type III (horse heart) was purchased from Sigma Chemical Company; C^{14}- and H^3-methyl-labeled choline chloride were purchased

from the New England Nuclear Corporation. The specific activity of the tritium-labeled compound was 100 mC/mmole.

Large scale production of conidia: 125 ml Erlenmeyer flasks containing 15 ml of minimal medium[10] supplemented with 25 μg choline chloride per ml and 2 per cent agar (a thin coating of the medium covered the walls of the flasks) were inoculated with small amounts of conidia from stock cultures. Flasks were maintained at 30°C for three days, and then, following the suggestion of Zalokar,[11] were moved to a 25°C room and illuminated with a 60 watt incandescent lamp at a distance of 14 in. After two days, conidia were harvested with a loop into a small volume of minimal media; they were freed of their mycelial attachments by shaking with glass beads, and separated therefrom by filtration through a thin layer of glass wool. Aliquots of the filtered conidial suspension were counted in a Spencer "bright-line" counting chamber.

General culture conditions: Stock cultures were maintained on slants of complete medium[12, 13] at 25°C. Experimental cultures were grown in liquid medium according to methods described in the text.

Analytic procedures: Lipid soluble radioactivity was determined on aliquots of fractions precipitated with 10 per cent TCA, washed once with 5 per cent TCA, and finally extracted for 30 min at room temperature with 2:1 chloroform-methanol.

Cytochrome oxidase was assayed according to the method of Nielsen and Lehninger.[14]

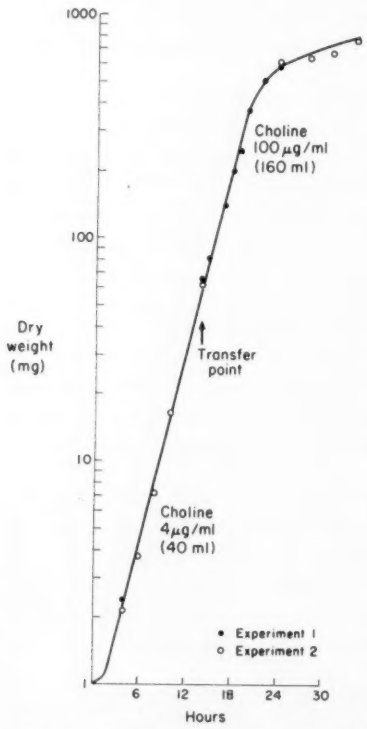

FIG. 1.—Dry mass increase in shaken cultures of *Neurospora crassa*. 300 ml Florence flasks containing 40 ml of minimal medium[10] supplemented by 4 μg/ml choline chloride were inoculated with 7×10^6 conidia per ml. At 14 hr, contents of the flasks were transferred to 1000 ml Florence flasks containing 120 ml of minimal medium with 100 μg/ml choline chloride. The flasks were maintained at 27.5°C and agitated in a reciprocating shaker at ~160 excursions per minute.

Results.—Growth conditions: Growth of *Neurospora* in shaken liquid cultures provided a reproducible and prolonged logarithmic growth phase. Preliminary experiments indicated that the growth rate of the *chol-1* strain did not change when the concentration of choline chloride in the medium was varied from 1 to 100 μg/ml. Thus it was possible to use a two concentration growth system like that shown in Figure 1. The initial growth period at 4 μg/ml choline was used for labeling, and the final period at 100 μg/ml, for a 100-fold dilution of specific radioactivity of the external choline. Figure 1 shows that there is no alteration in the dry mass growth rate in such a two-step system, and that during the logarithmic growth period the dry mass doubling time is 2 hr.

Zalokar[11] studied *Neurospora* grown under similar conditions and pointed out that during the logarithmic growth period, the hyphae grow mainly in length, showing no cytological indications of differentiation along the growing filament, and no autoradiographic evidence[15] of localized protein or RNA synthesis. These studies suggest that though *Neurospora* is a coenocytic fungus, certain processes occur at a uniform rate

throughout the length of logarithmically growing hyphae.

Preparation of a mitochondrial fraction: A highly purified mitochondrial fraction was prepared by isopycnic centrifugation in a sucrose density gradient. When the results of such a fractionation were monitored by drop-wise collection of fractions from the centrifuge tube (Fig. 2), they revealed two separate peaks of C^{14}-choline radioactivity. One coincided with a distinct visible band at a density range 1.16 to 1.20 (fractions 3 and 4) and another (fractions 7, 8, and 9) at a density of 1.08 to 1.14. The high density peak corresponded to the only peak of cytochrome oxidase activity. The heavy fraction was examined with electron microscopy and found to contain, almost exclusively, mitochondria resembling those found *in situ;* except that the isolate showed over-all swelling and distension of the outer mitochondrial membrane. The light fraction consisted of small irregularly shaped vesicles, with very rare recognizable mitochondria or mitochondrial fragments.

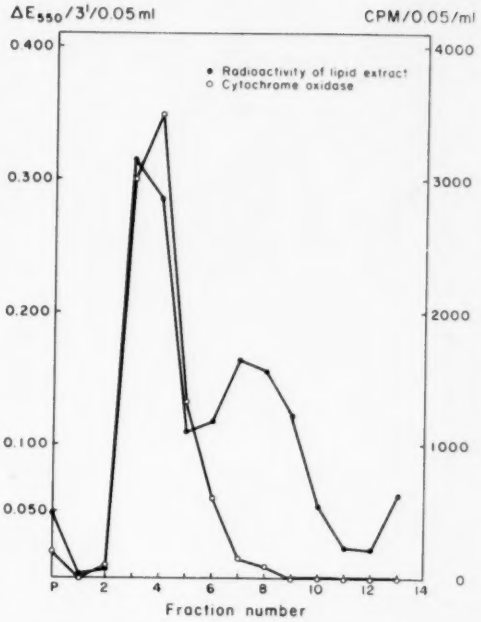

FIG. 2.—Distribution of cytochrome oxidase and lipid extractable radioactivity in cell fractions prepared by centrifugation in a sucrose density gradient. The original homogenate was derived from cells grown (from conidia) for 14 hr in C^{14}-labeled choline according to the procedure of Figure 1. Cells were ground with sand in 0.44 *M* sucrose (0.001 *M* EDTA), and nuclei and debris were removed by centrifugation at 500 × *g* for 10 min. One ml of the homogenate was layered over a 4 ml continuous sucrose gradient[19] ranging from 1.9 to 0.58 *M* sucrose. The entire gradient was 0.001 *M* in EDTA. After centrifugation for 5 hr at 40,000 rpm in the SW 39 rotor of the Spinco model L ultracentrifuge, the bottom of each tube was perforated and its contents collected into 13 fractions. The small pellet (P) was resuspended for analysis. Neither the position nor the general shape of the radioactive and enzymatic peaks shown here was changed when centrifugation was prolonged to 15 hr.

In subsequent experiments mitochondrial fractions were collected from each centrifuge tube as an 0.8 ml aliquot, using the visible band as a guide for collection. On the basis of cytochrome oxidase recovery, such a fraction represents 60 per cent of the total mitochondrial population. All the radioactivity of this mitochondrial fraction is extractable by lipid solvents.

Stability of the mitochondrial label: The data given in Figure 3 suggest that radioactive choline incorporated into mitochondria is preserved through three mass doubling cycles in unlabeled choline. Cultures started with labeled conidia were grown in radioactive choline for 14 hr, and then transferred to the dilution medium. Mitochondria were isolated at the time of transfer (shown in Fig. 3 as zero time) and at various time points during the subsequent 6-hr logarithmic growth period. For each time point the ratio—lipid extractable radioactivity to cytochrome

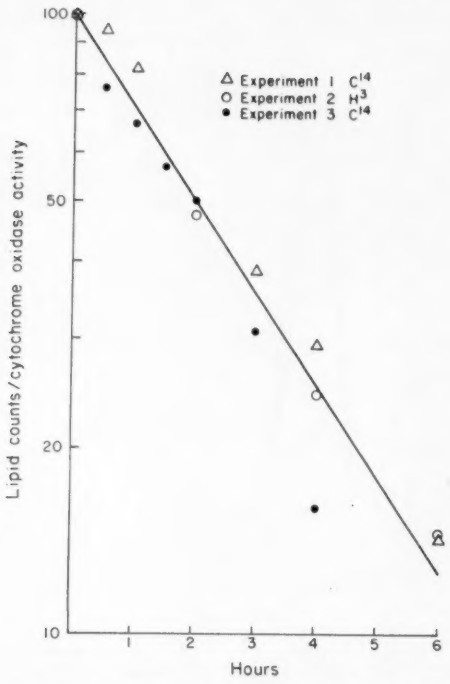

FIG. 3.—Decrease in "specific radioactivity" of mitochondrial fractions isolated during logarithmic growth of fully labeled mycelia after transfer to unlabeled medium. Labeled conidia were grown in media containing radioactive choline (of the same specific activity as that used for preparation of conidia) and after 14 hr transferred to unlabeled media according to the procedures of Figure 1. At the time of transfer (shown as zero time) and during the subsequent 6 hr in the dilution medium, mycelia were harvested from culture flasks and mitochondrial fractions were isolated. Results are plotted as lipid soluble radioactivity per cytochrome oxidase, versus time of growth in unlabeled medium. Data from three separate experiments were plotted on the same scale by taking the value at zero time in each experiment as 100 and expressing subsequent values as fractions thereof. The line is the theoretical line expected for a mitochondrial population (as measured by cytochrome oxidase) which preserves the label and increases at the same rate as the dry mass.

oxidase—was determined. In order to combine three separate experiments the value of this ratio at zero time was taken as 100, and the remaining values were plotted as fractions of that value. These values fit the line expected for the decrease in this ratio in a mitochondrial population whose doubling time is the same as that of the dry mass, 120 min, in a system in which there is no pool and no turnover of label.

Radioautographic studies: With a reliable growth system, a satisfactory mitochondrial preparation, and evidence that choline could serve as a stable mitochondrial label, it was possible to carry out radioautographic experiments with H^3-labeled choline, using the techniques of Caro and van Tubergen.[16] Labeled conidia were grown in labeled medium for fourteen hr according to the procedure given in Figure 1. At 2, 4, and 6 hr after transfer to the dilution medium, mycelia were harvested from individual flasks. Then mitochondria were isolated, fixed with osmium tetroxide in suspension, dialyzed against water, spread on slides, and finally covered with photographic emulsion for radioautography. The fixation and dialysis procedure preserved 90–100 per cent of the counts originally present in the fraction. After exposure and development, preparations were systematically scanned, and 300 mitochondria were grouped into classes bearing 0, 1, 2, 3, etc., autographic grains per mitochondrion.

Table 1 gives the average grain counts found in this experiment when radioautographs were exposed for varying time periods. As expected from the results of Figure 3, the average grain count for each doubling point is one half that for the preceding time point, and doubling of the exposure time can compensate for the decreased radioactivity of the later time points. The data of Table 1 suggest that latent image fading[17] becomes a problem only after 24 days of exposure.

TABLE 1

AVERAGE GRAIN COUNTS PER MITOCHONDRION DURING THREE MASS DOUBLING CYCLES OF A LABELED CULTURE GROWING IN UNLABELED MEDIUM

Data are taken from a representative experiment.

Doublings	Exposure Time for Radioautograph			
	3 days	6 days	12 days	24 days
Zero time	2.0			
1	1.1	1.9		
2	0.5	1.1	1.8	
3	...	0.5	0.9	1.2

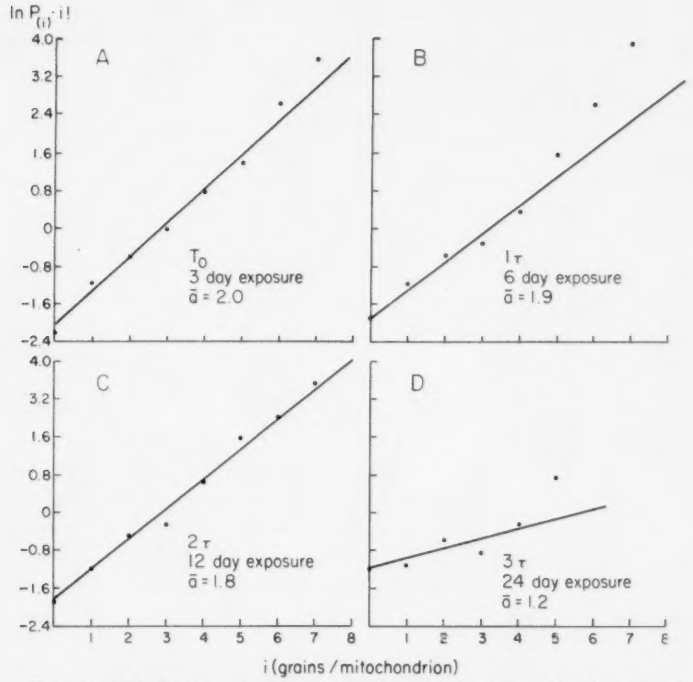

FIG. 4.—Distribution of radioautographic grains among mitochondria at zero time and at three successive mass doubling times during growth in unlabeled media. Labeled conidia were grown in H^3-choline for 14 hr and transferred to dilution medium as in the experiment of Figure 3. Mitochondria were prepared at the time of transfer and at 2, 4, and 6 hr. The distribution of radioautographic grains for each time point is plotted as ln $(P_{(i)} \cdot i!)$ versus i. where $P_{(i)}$ is the probability of finding i grains per mitochondrion. The method of plotting was suggested by van Tubergen and Setlow[4] and comes from the following transformations of the Poisson equation:

$$P_{(i)} = \frac{\bar{a}^i e^{-\bar{a}}}{i!} \text{ where } \bar{a} \text{ is the average grain count per mitochondrion.}$$

$$i! \cdot (P_{(i)} = \bar{a}^i e^{-\bar{a}}$$

$$\ln (P_{(i)} \cdot i!) = i \ln \bar{a} - \bar{a}$$

Therefore in this plot the Poisson relationship is rendered by a straight line whose slope is ln ā and whose intercept at $i = 0$ is $-\bar{a}$. In each case the line represents the Poisson distribution expected for the average grain count found experimentally, and the points show the values of $P_{(i)}$ actually found. The data are taken from a representative experiment.

If the mitochondria are uniform in the amount of label they contain, the distribution of grains among individual mitochondria can be expected to follow a

Poisson relationship.[4a] In Figure 4 the distribution of grains is given in a logarithmic plot which renders the Poisson relationship as a straight line. In order to obtain enough categories of grain counts (i's) to give a reliable test of fit, we have chosen to work with a grain count average near 2, and have adjusted exposure times for the different growth stages to obtain nearly uniform averages.[4b] At the average grain counts used, there are few mitochondria which fall into the 6 and 7 grain classes, so that P values for these points are statistically unreliable. Within the limits of the method, the data of Figure 4 indicate that through three mass doubling cycles in dilution medium, there is uniform or nearly uniform distribution of label among all mitochondria. This dispersive distribution of label suggests that existing mitochondrial material is directly and randomly transmitted to progeny in the formation of new mitochondria. Before this conclusion was drawn, other possible mechanisms of randomization of the label were considered.

Control experiments to exclude randomization of label introduced by the isolation procedure: To rule out the possibility that homogenization and cell fractionation introduced randomization of mitochondrial label, the mixing experiment shown in Figure 5 was carried out. When paired labeled and unlabeled cultures were mixed and processed together, the resulting distribution of radioautographic grains did not fit the Poisson distribution expected for the average grain count experimentally determined. The data did fit the distribution expected for a population of 50 per cent unlabeled mitochondria and 50 per cent labeled mitochondria with average grain count of 2.0. The results indicate that the preparative procedures have introduced no redistribution of label.

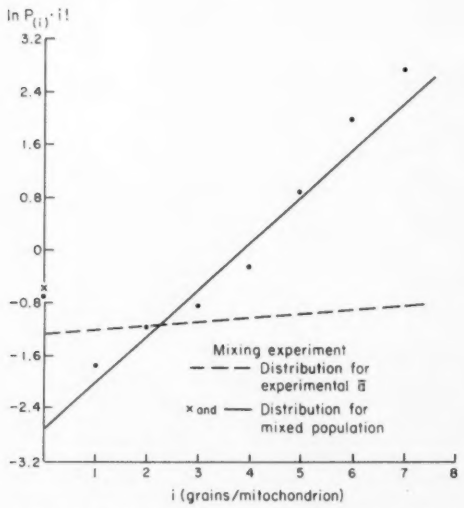

FIG. 5.—Distribution of radioautographic grains in a mixing experiment. Identical conidial inocula were placed in flasks containing in one case H^3-choline and in the other unlabeled choline. After 14 hr of growth the contents of both flasks were mixed and processed together for mitochondrial isolation and radioautography. The results shown here were obtained after 3 days exposure of radioautographs. The distribution of grains does not fit the Poisson distribution (broken line) expected from the experimentally determined average grain count (1.09). It does fit the Poisson distribution which would be expected for a 50% unlabeled population and a 50% labeled population with average grain count 2.0 (unbroken line and X). Data are taken from a representative experiment.

Control experiments to rule out the randomization of label by mitochondrial fusion and fission: To explore the possibility that the randomization of label found in our experiments is achieved *in vivo* by the process of mitochondrial fusion and fission recorded by Frederic and Chevremont,[18] we carried out a pulse labeling experiment. As shown in Figure 6, when mitochondria were isolated from mycelia exposed to H^3-choline for only 10 min, the distribution of radioautographic grains fit a Poisson distribution. If this random distribution of

label were the result of mitochondrial fusions and fissions, one can estimate that these events would have to occur more frequently than once per 1.5 min per mitochondrion. Such an estimate assumes instantaneous equilibration of label between a fusing pair, an event hardly expected in structures as complex as mitochondria. As such, it represents a low figure for the frequency of fusion-fission. In any case, microscopic observations of living *Neurospora*, under conditions where filaments were growing at a rate of 8 microns per min, revealed that fusions and fissions were rare events, far less frequent than the number required. In view of these findings we would exclude the possibility that label is redistributed *in vivo* by fusion-fission of mitochondria.

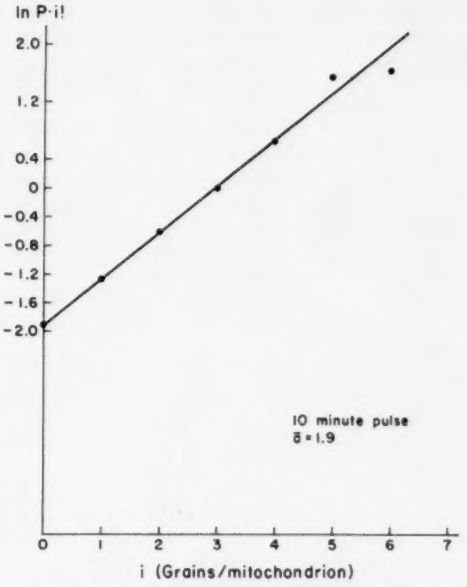

FIG. 6.—Distribution of radioautographic grains among mitochondria after 10-min pulse labeling. Conidia were grown in the 40 ml growth system outlined in Figure 1, with a choline chloride concentration of 10 μg/ml. At 14 hr mycelia were collected on a Milipore filter (pore size 1.2μ) and transferred to 40 ml medium containing H^3-choline at 10 μg/ml. After ten min culture flasks were quickly chilled, and the cells were processed for isolation of mitochondria and radioautography. Exposure time 21 days.

Discussion and Summary.—In logarithmically growing cultures of *Neurospora crassa*, mitochondrial lipids can be labeled with H^3- or C^{14}-choline. Under the conditions of a washout experiment, radioactive choline is preserved in the mitochondrial population and serves as a satisfactory label through three mass doubling cycles. Radioautographic analyses show that the label is randomly distributed in mitochondrial populations, isolated as mitochondrial fractions from fully labeled cells, as well as from cells undergoing three subsequent doubling cycles in unlabeled choline. This random distribution does not appear to be the result of the cell fractionation procedures, nor would it seem to be effected *in vivo* through repeated mitochondrial fusions and fissions.

These data, which fit a dispersive distribution of label, exclude the possibility of *de-novo* formation, and do not favor the hypothesis of structural mitochondrial precursors. The most likely interpretation of the findings is that in growing *Neurospora*, the mitochondrial mass increases by a continuous process of addition of new choline-containing lipid units to the existing mitochondrial structure. The number of individuals in the population is increased by division of mitochondria and the division process distributes the label at random so that pre-existing membrane material is transmitted uniformly or nearly uniformly to all progeny.

I am grateful to Dr. George E. Palade for guidance in these studies, and to Dr. Lucien Caro for instruction in radioautographic technique.

* Supported in part by a grant from the National Science Foundation.

[1] Rouiller, Ch., in *International Review of Cytology*, ed. G. H. Bourne and J. F. Danielli (New York: Academic Press, 1960), vol. 9, p. 227.

[2] Novikoff, A. B., in *The Cell*, ed. J. Brachet and A. E. Mirsky (New York: Academic Press, 1961), vol. 2, p. 299.

[3] Forro, Jr., F., and S. A. Wertheimer, *Biochim. Biophys. Acta*, **40**, 9 (1960).

[4a] van Tubergen, R. P., and R. D. Setlow, *Biophys. J.*, **1**, 589 (1961).

[4b] There was limitation in the choice of average grain counts used for radioautographic analysis, because at higher averages, some mitochondria were obscured by their associated grains. At the average grain counts used in our analyses, small populations of highly labeled or of unlabeled mitochondria could be detected, but mixtures of labeled populations with small differences in their average grain counts would not be resolved.

[5] Biran, L. A., and W. Bartley, *Biochem. J.*, **79**, 159 (1961).

[6] Getz, G. S., W. Bartley, W. F. Stirpe, B. M. Notton, and A. Renshaw, *Biochem. J.*, **83**, 181 (1962).

[7] Horowitz, N. H., and G. W. Beadle, *J. Biol. Chem.*, **150**, 325 (1943).

[8] Horowitz, N. H., D. Bonner, and M. B. Houlahan, *J. Biol. Chem.*, **159**, 145 (1945).

[9] Horowitz, N. H., *J. Biol. Chem.*, **162**, 413 (1946).

[10] Vogel, H. J., and D. M. Bonner, *Microbial Genetics Bull.*, No. 13, 43 (1956).

[11] Zalokar, M., *Am. J. Bot.*, **46**, 555 (1959).

[12] Tatum, E. L., R. W. Barratt, N. Fries, and D. Bonner, *Am. J. Botany*, **37**, 38 (1950).

[13] Lester, H. E., and S. R. Gross, *Science*, **129**, 572 (1959).

[14] Nielsen, S. O., and A. Lehninger, *J. Biol. Chem.*, **215**, 555 (1955).

[15] Zalokar, M., *Am. J. Bot.*, **46**, 602 (1959).

[16] Caro, L. G., and van Tubergen, R. P., *J. Cell Biol.*, **15**, 173 (1962).

[17] Demers, P., *Ionographie les Emulsions Nucléaires Principes et Applications* (Ottawa: Les Presses Universitaires de Montréal, 1958).

[18] Frederic, *J., Arch. Biol.* (Liége) **69**, 167 (1958).

[19] Britten, R. J., and R. B. Roberts, *Science*, **131**, 32 (1960).

---

*DEMONSTRATION OF AN UNSTABLE RNA AND OF A PRECURSOR TO RIBOSOMAL RNA IN HELA CELLS**

BY KLAUS SCHERRER, HARRIET LATHAM, AND JAMES E. DARNELL

DEPARTMENT OF BIOLOGY, MASSACHUSETTS INSTITUTE OF TECHNOLOGY, CAMBRIDGE

Communicated by S. E. Luria, December 13, 1962

Strong evidence has accumulated in favor of the following scheme of protein synthesis in bacteria: The structural site of protein synthesis is the ribonucleoprotein particle, the ribosome.[1, 2] Amino acids in an activated form are brought by specific carrier RNA molecules (s-RNA) to the ribosomes, where organization into polypeptide chains is directed by informational or messenger RNA (m-RNA).[3–6] The bacterial DNA directs the formation of m-RNA by attracting ribonucleotides appropriate for hydrogen bonding to the bases of DNA according to the Watson-Crick model.[7] This is then followed by the enzymatic polymerization of these ribonucleotides into complementary strands of RNA.[8, 9] An important feature of the m-RNA of bacterial cells is that it is impermanent, being used in protein synthesis only 10–20 times on the average.[10] This instability of the m-RNA allows the bacterium to change quickly and efficiently its complement of enzymes by changing the type of messenger RNA that is synthesized.

Some of the elements of this scheme of protein synthesis, e.g., s-RNA and ribonucleoprotein particles are known to exist and function in animal cells. Indeed some of the earliest observations leading to the development of systems that can synthesize protein *in vitro* were made with extracts from animal tissues.[11] The nature of the informational RNA in animal cells is unclear, however. In an attempt to answer this and other questions concerning RNA from animal cells we have undertaken a study of the RNA of a strain of human cells growing in culture.

Materials and Methods.—Cells and fractional procedures: Suspension cultures of HeLa cells[12] growing with a generation time of 18–24 hr were used throughout. RNA was isolated by a hot phenol extraction technique;[13] DNA was prepared according to Marmur.[14] The acid soluble nucleotide pool was prepared as previously described.[15]

RNA was labeled with either uridine-2-C^{14} (New England Nuclear) or $P^{32}O_4^{---}$ and was uncontaminated by DNA. DNA was labeled with thymidine-2-C^{14} (New England Nuclear).

Isotope determinations: Radioactivity in macromolecules was determined by precipitation with 5–10 per cent cold trichloracetic acid and collection of the precipitate on membrane filters for counting. One mgm or less of solids gave little or no self-absorption of either P^{32} or C^{14} counts.

Ultracentrifugal studies: Sedimentation analysis of RNA was done by sucrose gradient sedimentation;[15] density separation was done in CsCl equilibrium density gradients.[17]

Base analysis of nucleic acids: Electrophoresis of ribonucleotides was performed on alkaline hydrolysates of RNA[18] in 0.05 *M* formate buffer, pH 3.5. After hydrolysis of the DNA in formic or perchloric acid[19, 20] the bases were separated by paper chromatography using isopropanol–HCl as the solvent.[21]

Results.—Sedimentation analysis of RNA labeled for varying periods of time: Earlier experiments had shown that when RNA from cells exposed for various times to uridine-2-C^{14} was separated by sucrose gradient centrifugation two species of RNA distinct from the bulk of the cellular RNA could be detected.[13] The most rapidly sedimenting fraction (S value ~45) became labeled first; within 30–60 min after the addition of label, radioactivity appeared in the second (35S) species (see Fig. 1, control, and Fig. 2, upper left). After longer exposure times (4–24 hr), the accumulation of radioactivity in those species of RNA which comprise the

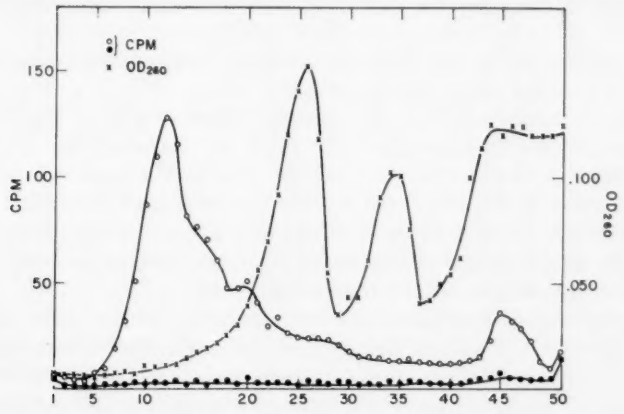

FIG. 1.—Effect of actinomycin on uridine-2-C^{14} incorporation into RNA by HeLa cells. Exponentially growing HeLa cells were exposed to actinomycin D (5 μg/ml) and 10 min later uridine-2-C^{14} (0.01 mM and 5 μc/μm) was added for an additional 10 min (●). Control cells not exposed to actinomycin were also labeled for 10 min (-○). RNA was extracted and examined in a sucrose gradient as previously described.[13]

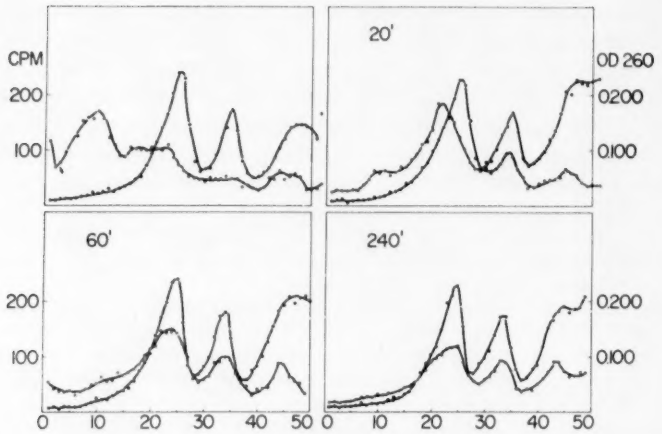

FIG. 2.—Fate of 45S RNA after actinomycin treatment. Uridine-2-C^{14} (0.01 mM and 1 μc/micromole) was added to 600 ml of HeLa cells in suspension culture. After 30 min 150 ml of the culture was removed and actinomycin D (5 μg/ml) was added to the remainder. Samples of 150 ml were removed 20, 60, and 240 min after the addition of actinomycin. RNA from each sample was extracted and analyzed by sucrose gradient sedimentation (○ = CPM, ● = OD_{260}). See Table 3 for specific activity of the total RNA in this experiment.

TABLE 1

RECOVERY OF RNA, PROTEIN, AND DNA IN AQUEOUS PHASE AFTER HOT PHENOL EXTRACTION

C^{14} Precursor	Total CPM incorporated	Recovered after phenol extraction Total	%
Uridine	27,800	20,800	75
Thymidine	133,000	135	0.1
Valine	235,000	940	0.4

Growing HeLa cells were labeled for 30 min with uridine-2-C^{14} (0.5 μc/micromole), 18 hr with thymidine-C^{14} (0.1 μc/micromole) or for 18 hr with valine-C^{14} (0.1 μc/micromole) and extracted with hot phenol.[13] The efficiency of recovery of each label was compared by determining the acid precipitable radioactivity before and after extraction. Sucrose gradient analysis (see Fig. 1) was performed on each of the above extracts and no valine or thymidine radioactivity was present in the 35 or 45S regions where more than 70% of the uridine counts could be recovered.

bulk of the cellular RNA (28S, 16S, and 4S) obscured the relatively smaller amounts of radioactivity in the 35S and 45S material.

The extraction and sucrose gradient analysis (Table 1) of RNA from cells labeled with valine C^{14} or with thymidine-2-C^{14} ruled out the possibility that the large (35S and 45S) RNA was sedimenting rapidly because of attachment to or aggregation with protein or DNA. The recovery of incorporated uridine-2-C^{14} in RNA was high, and the specific activity of the small amount of RNA left in the phenol phase was found not to exceed that in the aqueous phase, as has been reported to occur when different extraction procedures are used.[22]

Sedimentation analysis of the 35 and 45S materials in acetate buffer, pH 5.1, containing versene 10^{-3} M and no Mg^{++}, or in tris buffer, pH 7.4, containing 10^{-4} M Mg^{++}, when compared to analysis in the usual acetate buffer, pH 5.1 with 10^{-4} M Mg^{++}, failed to reveal any major difference in either size or relative proportion of these materials.

Nuclear localization of rapidly labeled RNA: During the first hour of exposure of cells to uridine-2-C^{14} at least 70–75 per cent of the incorporated activity was in the 35S or 45S fractions. Recent experiments with HeLa cells from this laboratory[23]

have indicated that almost all of the early incorporation of RNA precursors occurs in the nucleus. Hence, we conclude that the 35 and 45S RNA exists in the nucleus. This is in accord with observations on a number of different animal cell systems that the earliest incorporation of precursors into RNA is nuclear.[24, 25, 36]

Base ratios of various RNA species: The base ratios of the various classes of RNA (45S, 35S, 28S, 16S, and 4S) were determined by preparing from a sucrose gradient samples of each kind of RNA labeled with P^{32}, hydrolyzing with alkali, and analyzing the distribution of radioactivity in the resulting 2′, 3′ ribonucleotides. The validity of this method for determining base ratios has been discussed at length.[9]

The results of the base ratio analyses are given in Table 2. The outstanding

TABLE 2

BASE COMPOSITION OF HELA CELL RNA AND DNA

Material analyzed	Sedimentation constant	% of Nucleic Acid as A	U(T)	G	C
RNA	45 S	19.8	20.1	29.3	29.8
	35 S	19.9	20.7	28.8	30.4
	28 S	20.5	19.3	28.3	31.9
	16 S	23.2	23.2	25.2	28.0
	4 S	22.4	24.5	24.8	28.3
DNA, total	...	29.1	27.5	22.0	21.4

Various fractions of P^{32}-labeled HeLa cell RNA were separated by sucrose gradient sedimentation, collected, precipitated with PCA, washed with ethanol, and hydrolyzed with 0.3N KOH 16–18 hr at 37°. The resulting 2′, 3′ mononucleotides were then separated by ionophoresis at pH 3.5 in 0.05 *M* formate buffer. The radioactivity of each mononucleotide was determined as described in *Methods*. Figures given in the table represent averages of at least six determinations in each case. (A = adenylic or adenine; C = cytidylic or cytosine; G = guanylic or guanine; U = uridylic or uracil; T = thymine).

characteristic of all classes of RNA is the high (55–60 per cent) content of guanylic acid (=G) plus cytidylic acid (=C) compared to the DNA, which has only 43.5 per cent G + C. This was true of the rapidly labeled 45S and 35S material whether the time of labeling was 15, 30, or 60 min. The 28S, 16S, and 4S RNA analyzed in these experiments came from cells that had been labeled for 24 hr. Results similar to these have been reported by others for the ribosomal RNA of HeLa cells,[26] and the high G + C content has been observed consistently[27] in animal-cell RNA.

Fate of 45 and 35S RNA: The antibiotic actinomycin D has been shown to inhibit RNA synthesis in bacterial and mammalian cells[28] presumably by virtue of its action on DNA-dependent RNA synthesis.[29] This substance makes it possible, therefore, to investigate the fate of the early labeled RNA in HeLa cells in the absence of further RNA synthesis. Cells were labeled with uridine-2-C^{14} for 30 min and then actinomycin was added to the culture at 5 μg/ml. This concentration of antibiotic effectively stops the synthesis of any further large molecular weight RNA in a few min (Fig. 1). As can be seen from Figure 2, the radioactivity from the 45S peak in the treated cultures is largely conserved and is transferred sequentially to the 35S, then to 28S and 16S fractions, which represent ribosomal RNA. The majority of the 45S and 35S RNA, therefore, appears to be precursor material to ribosomal RNA, which is itself stable.

Unstable RNA: The study of radioactively labeled RNA subsequent to actinomycin treatment offers the opportunity of determining the proportion of metabolically unstable RNA as well as the fate of the stable fraction. HeLa cells which have been exposed to uridine-2-C^{14} for 30 min quickly lose about one-third of the acid

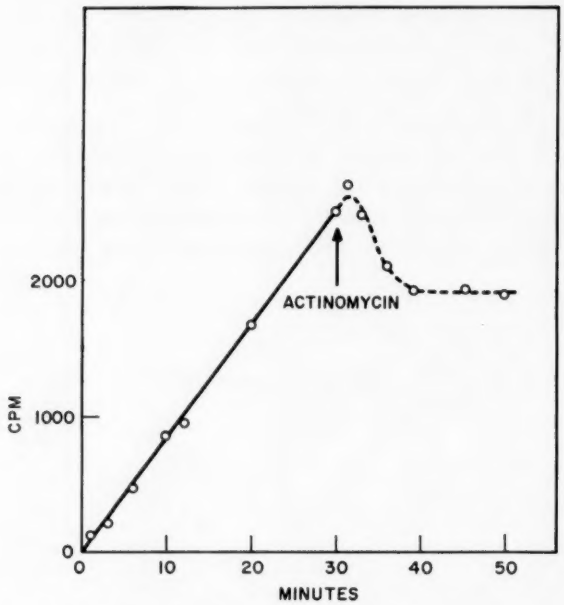

FIG. 3.—Uptake of uridine-2-C^{14} into RNA of HeLa cells and the demonstration of an unstable RNA fraction.

Uridine-2-C^{14} (12 μC/micromole) was added to a growing culture of HeLa cells and 1 ml samples were taken at indicated times (O), and chilled immediately to 0°. Cells were separated from the medium by centrifugation, treated with 1 ml of cold 5% trichloracetic acid, and the precipitate was collected on membrane filters for radioactivity determinations. Actinomycin D (5 μg/ml) was added to a portion of the culture at 30 min and samples were taken at intervals thereafter (- - - - - - -).

precipitable radioactivity following treatment with actinomycin (Fig. 3). The amount of this unstable fraction relative to the total RNA content of the cell can be estimated by assuming a 1.5 per cent increase of the RNA content of the cell in 30 min (generation time = 24 hr). The unstable fraction would then represent 0.5 per cent of the total RNA of the cell. Evidence has been presented by Levinthal *et al.*[10] that the messenger RNA fraction in *B. subtilis* has similar characteristics of instability.

Corroborative evidence that the loss of acid-precipitable radioactivity following actinomycin treatment of HeLa cells actually represents the loss of a fraction of RNA comes from examination of phenol extracts of labeled cells (Table 3). The total RNA from a culture that has been labeled for 30 min has a greater specific

TABLE 3

EFFECT OF ACTINOMYCIN D ON SPECIFIC ACTIVITY OF RNA EXTRACTABLE FROM HELA CELLS

Conditions of labeling	RNA extracted: Total CPM	RNA extracted: OD_{260} units	Specific activity CPM/OD unit
Uridine-2-C^{14} for 30′	7,840	33.5	234
" " " Actinomycin for 20′	5,780	39.5	147
" " " " " 60′	5,020	33.6	150
" " " " " 210′	4,660	33.0	141

Total RNA samples from the experiment described in Figure 3 were examined prior to sucrose gradient analysis or acid precipitable radioactivity and UV absorbancy and specific activities were calculated.

activity than the RNA from a culture which has been labeled, then treated with actinomycin. No loss of radioactivity from RNA of cells that had been labeled for 18 hr prior to treatment with actinomycin could be detected, a further indication that the unstable fraction was small relative to the total RNA of the cell.

Pertinent to the question of the sedimentation characteristics of the unstable fraction is the observation that, after a 30 min exposure to uridine-2-C^{14}, about 70 per cent of the total radioactivity in RNA is in 35S and 45S material (Fig. 2). Subsequent to actinomycin treatment, radioactivity accumulates in fractions of smaller size (28S, 16S, 4S). These observations suggest that most of the unstable fraction of RNA is contained in the 35 and 45S peaks.

Stimulation of in vitro protein synthesis by HeLa cell RNA: *In vitro* protein synthesis by *E. coli* extracts can be made dependent on the addition of RNA to the system.[30] The fraction of the bacterial RNA that has the greatest stimulatory capacity is also the RNA that is most rapidly labeled. Since this system from *E. coli* responds to many other types of RNA, it affords a means of testing the capacity of any species of RNA to serve as messenger. Various classes of HeLa-cell RNA were prepared and added to the *E. coli* system described by Nirenberg and Matthaei.[30] Table 4 shows that the 45S RNA has the greatest stimulatory capacity for the incorporation of C^{14} valine into protein.

TABLE 4

STIMULATION BY HELA CELL RNA OF *in vitro* PROTEIN SYNTHESIS BY EXTRACTS OF *E. coli*

Size of RNA	Amount (μg)	CPM incorporated above background	CPM/μg
45 S	36	48	1.33
35	97	57	0.59
28	136	55	0.40
16	125	54	0.44
10	78	25	0.32
4	163	13	0.08

Various classes of RNA from HeLa cells were prepared by sucrose gradient sedimentation, as described in Figure 1, and precipitated with 0.5 mg of *E. coli* S-RNA by the addition of ethanol. The precipitates were taken almost to dryness to remove the ethanol and redissolved in 0.25 ml of the *in vitro* protein synthesizing mixture described by Nirenberg and Matthaei.[30] The incorporation of C^{14}-valine after 30 min at 37° was determined after three extractions with 5% TCA at 95°. The background (16) represents incorporation by the extract in absence of added RNA except the s-RNA. Radioactivity determinations were made on a gas-flow counter with a background of 2 cpm and all determinations represent 1000 counts or more.

Hybridization of HeLa RNA with DNA: Spiegelman and co-workers[31, 32] have recently shown that both informational RNA and ribosomal RNA can attach specifically to homologous DNA by hydrogen bonding. Furthermore, it is clear from their work that in a mixture of the total bacterial DNA with the total RNA (informational RNA as well as ribosomal RNA) there is a much greater chance for hybridization of the informational RNA. This implies that in the bacterial cell the portion of DNA which functions in the formation of informational RNA is much larger than that concerned with the production of ribosomal RNA.

If in HeLa cells the number of loci which produce ribosomal RNA is small relative to the total number of gene loci, and if the DNA that is functioning in these cells (other than that responsible for ribosomal RNA) has the average composition of the total DNA, then hybridization of pulse-labeled RNA from these cells should reveal any DNA-like RNA.

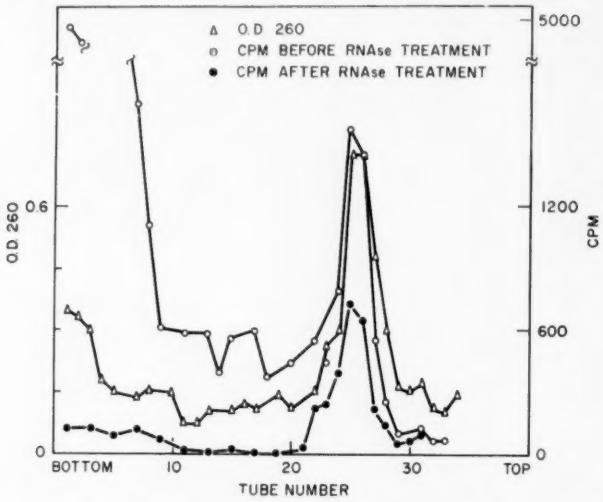

FIG. 4.—Hybridization of HeLa cell RNA with DNA. RNA labeled with P^{32} from the 35S region of a sucrose gradient was collected by alcohol precipitation and dissolved in saline citrate buffer (0.3 *M* NaCl and 0.03 *M* Na citrate, pH 7.8). This was mixed with 0.8 mg of HeLa cell DNA which had been heated to 100°C for 15 min and cooled to 0° in 30 sec. The DNA-RNA mixture was brought to 60° and slowly cooled over 36 hr to 28°. After dilution with saline-citrate buffer, solid CsCl was added to give a density of 1.765 in a final volume of 4.5 ml. The material was then analyzed by density gradient sedimentation in a model L Spinco ultracentrifuge (SW 39 rotor, 35,000 rpm for 60 hr). The ribonuclease treatment was performed by diluting samples from the gradient 30-fold in buffer containing $5 \times 10^{-3}M$ tris, $10^{-4}M$ Mg Cl_2, and digesting with 5 μg ribonuclease for 30 min at 37°.

TABLE 5

COMPOSITION OF HYBRIDIZED FRACTION OF RNA

	G + C Content	
	Total before hybridization	*Hybridized fraction*
35 and 45S RNA	59.2	50.5
Total RNA	59.5	46.0
DNA	43.6	...

RNA from the experiments described in Figure 4 analyzed for base composition as in Table 2. Only total G + C content is presented in order to facilitate comparisons.

The results of experiments of this type are given in Figure 4 and Table 5. It is clear that RNA labeled for 60 min with P^{32} can hybridize with HeLa cell DNA forming a complex that resists digestion by ribonuclease, the criterion of a true hybrid according to Hall and Spiegelman.[31] The base ratio of the hybridized RNA is significantly lower in G + C than the total RNA or the 35 and 45S RNA, an indication that there is in the 35 and 45S material an RNA fraction resembling DNA in base composition mixed with the ribosomal type RNA. Further work will be necessary to determine whether only molecules of RNA with low G + C content (DNA-like) are hybridized or whether the hybridized material is still a mixture of high G + C (ribosomelike) and low G + C RNA.

Discussion.—The following conclusions can be drawn from the experiments reported in this paper: (1) Ribosomal RNA in the HeLa cell is formed as part of very large RNA molecules which are then converted into smaller pieces. (2) There

is in these cells a fraction of RNA that is rapidly synthesized and degraded, but the majority of the RNA is metabolically stable. (3) Of the total RNA a small fraction, which preferentially hybridizes with DNA, has a base ratio nearer to that of DNA than the majority of the RNA. This fraction possibly corresponds to the DNA-like RNA described by others in animal cells.[33, 34]

The first question raised by these experiments is the molecular nature and significance of the very large RNA molecules which are chiefly, if not entirely, precursors of ribosomal RNA. Several lines of evidence indicate that these molecules are not artifacts. Their size is extremely reproducible; the 45S is always formed first, followed by the 35S, then 16S and 28S; the absence of divalent cations seems not to affect their size; these fractions are uncontaminated with protein or DNA; the procedure used to isolate the RNA—heating with phenol to 60° three times for 3 minutes and cooling to −5° in 30 seconds—should not allow the type of complementary pairing of RNA which has been reported by Geiduschek *et al.*[35] Moreover, RNA of similar size has now been found in animal cells of several different types.[36]

What is the meaning of 45S RNA? One possibility is that several ribosomal RNA cistrons lie together and the 45S material is a complex of several ribosomal RNA molecules. This arrangement of ribosomal cistrons in bacteria has been suggested by Yankofsky and Spiegelman[32] to explain some properties of the bacteria DNA-ribosomal RNA hybrids. Implicit in this scheme is a mechanism for accurately dividing the large molecule into smaller ones of specific sizes.

The second problem to which this work is pertinent is the question of whether there is in animal cells any protein synthesis governed by a species of RNA analogous to messenger RNA in bacteria. The observations that the RNA from HeLa cells can stimulate *in vitro* protein synthesis by *E. coli* extracts, that an unstable fraction of RNA exists, and that a small fraction of the total RNA has DNA-like base ratios suggest that messenger RNA does indeed exist in animal cells. Further work aimed at isolating the unstable fraction in order to determine its composition, intracellular localization, and function will be necessary before a definite conclusion can be drawn concerning not only the existence but also the quantitative role of an unstable messenger RNA in protein synthesis by animal cells.

* This work was supported by a grant (C-5789) from the National Cancer Institute.

[1] McQuillen, K., R. B. Roberts, and R. J. Britten, these PROCEEDINGS, **45,** 1437 (1959).

[2] Tissières, A., D. Schlessinger, and F. Gros, these PROCEEDINGS, **46,** 1450 (1960).

[3] Berg, P., F. H. Bergmann, E. J. Ofengand, and M. B. Dieckmann. *J. Biol. Chem.*, **236,** 1726 (1961).

[4] Stephenson, M. L., and P. C. Zamecnik, these PROCEEDINGS. **47,** 1627 (1961).

[5] Jacob, F., and J. Monod, *J. Mol. Biol.* **3,** 318 (1961).

[6] Gros, F., W. Gilbert, H. H. Hiatt, G. Attardi, P. F. Spahr, and J. D. Watson, *Cold Spring Harbor Symposia on Quantitative Biology*, **26,** 111 (1961).

[7] Watson, J. D., and F. H. C. Crick, *Cold Spring Harbor Symposia on Quantitative Biology*, **18,** 123 (1953).

[8] Hurwitz, J., J. J. Furth, M. Anders, P. J. Ortiz, and J. T. August, *Cold Spring Harbor Symposia on Quantitative Biology*, **26,** 91 (1961).

[9] Spiegelman, S., *Cold Spring Harbor Symposia on Quantitative Biology*, **26,** 75 (1961).

[10] Levinthal, C., A. Keynan, and A. Higa, these PROCEEDINGS, **48,** 1631 (1962).

[11] Hoagland, M. B., P. C. Zamecnik, and M. L. Stephenson, in *A Symposium on Molecular Biology* (Chicago University Press, 1959), Chap. 9, p. 105.

[12] Eagle, H., *Science*, **130,** 432 (1959).

[13] Scherrer, K., and J. E. Darnell, *Biochem. Biophys. Res. Comm.*, **7**, 486 (1962).
[14] Marmur, J., *J. Mol. Biol.*, **3**, 208 (1961).
[15] Darnell, J. E., L. Levintow, M. M. Thoren, and J. L. Hooper, *Virology*, **13**, 271 (1961).
[16] Britten, R. J., and R. B. Roberts, *Science*, **131**, 32 (1960).
[17] Messelson, M., F. W. Stahl, and J. Vinograd, these PROCEEDINGS, **43**, 581 (1957).
[18] Davidson, J. N., and R. M. S. Smellie, *Biochem. J.*, **52**, 594 (1952).
[19] Marshak, A., and H. J. Vogel, *J. Biol. Chem.*, **189**, 597 (1951).
[20] Vischer, E., and E. Chargaff, *J. Biol. Chem.*, **176**, 715 (1948).
[21] Wyatt, G. R., *Biochem. J.*, **48**, 454 (1951).
[22] Sibatani, A., K. Kimura, K. Yamana, and T. Takahashi, *Nature*, **186**, 215 (1960).
[23] Zimmerman, E. F., M. Corcoran, and J. E. Darnell, *Virology*, in press.
[24] Goldstein, L., and J. Micou, *J. Biophys. Biochem. Cytol.*, **6**, 1 (1959).
[25] Amano, M., and C. P. Leblond, *Exptl. Cell Res.*, **20**, 250 (1960).
[26] Holland, J., *Biochem. and Biophys. Res. Comm.*, **6**, 196 (1961).
[27] Hoagland, M. B., in *The Nucleic Acids*, ed. E. Chargaff, and J. N. Davidson (New York: Academic Press, 1960), vol. 3.
[28] Reich, E., R. M. Franklin, A. J. Shatkin, and E. L. Tatum, *Science*, **134**, 556 (1961).
[29] Hurwitz, J., J. J. Furth, M. Malamy, and M. Alexander, these PROCEEDINGS, **48**, 1222 (1962).
[30] Nirenberg, M., and J. H. Matthaei, these PROCEEDINGS, **47**, 1588 (1961).
[31] Hall, B. D., and S. Spiegelman, these PROCEEDINGS, **47**, 137 (1961).
[32] Yankofsky, S. A., and S. Spiegelman, these PROCEEDINGS, **48**, 1069, and 1466 (1962).
[33] Sibatani, A., S. R. de Kloet, V. G. Allfrey, and A. E. Mirsky, these PROCEEDINGS, **48**, 471 (1962)
[34] Georgiev, G. P., and V. L. Mantieva, *Biochem. Biophys. Acta*, **61**, 153 (1962).
[35] Geiduschek, E. P., J. W. Moohr, and S. B. Weiss, these PROCEEDINGS, **48**, 1078 (1962).
[36] Hiatt, H. H., *J. Mol. Biol.*, **5**, 217 (1962); Lerner, A. M., and J. E. Darnell, unpublished observations.

---

*TRANSFER OF CHLOROPHYLL EXCITATION ENERGY IN GREEN PHOTOSYNTHETIC BACTERIA**

BY CHRISTIAAN SYBESMA† AND JOHN M. OLSON

BIOLOGY DEPARTMENT, BROOKHAVEN NATIONAL LABORATORY, UPTON, NEW YORK

Communicated by Britton Chance, December 27, 1962

Beginning with Katz and Wassink,[1] several investigators[2–4] have obtained from suspensions and extracts of green photosynthetic bacteria, absorption spectra which suggest the presence of a minor chlorophyll component in addition to the major characteristic pigment, chlorobium chlorophyll (bacteriviridin). The fluorescence emission spectra of whole cells recently observed by Krasnovskii *et al.*[5] are even more suggestive in this respect than the absorption spectra. Isolation of the partially purified minor chlorophyll was accomplished by Olson and Romano.[6] This pigment, which has a striking spectroscopic resemblance to bacteriochlorophyll, was named "chlorophyll-770" because of the position of its red absorption peak in ether. *In vivo* the absorption band at about 810 mμ due to chlorophyll-770 is only 5 to 10 per cent of the main red band due to chlorobium chlorophyll. To test the suggestion[6] that the predominant chlorobium chlorophyll acts as an accessory pigment which transfers excitation energy to the minor component, chlorophyll-770, we have investigated the fluorescence of the protein-chlorophyll-770 complex *in*

vitro and the complete pigment system *in vivo*. Transfer of excitation energy *in vivo* to chlorophyll-770 is shown to occur with a quantum efficiency of at least 30 per cent under physiological conditions, and the fluorescence yield of chlorophyll-770 *in vivo* is observed to decrease as the intensity of excitation is decreased.

Materials and Methods.—*Chloropseudomonas ethylicum*, strain 2K, and *Chlorobium thiosulfatophilum*, strain L, were grown on 0.1 per cent ethanol and 0.1 per cent $Na_2S_2O_3 \cdot 5H_2O$ respectively, as described previously.[4, 7] A purified protein-chlorophyll-770 preparation was obtained from *Cps. ethylicum* in the following manner: Fraction 2 of Olson and Romano,[6] an $(NH_4)_2SO_4$ precipitate containing the desired protein pigment, was dissolved in 0.02 *M* phosphate buffer pH 7.8, dialyzed, and adsorbed on diethylaminoethyl cellulose.[8] Elution with 0.25 *M* NaCl yielded an initial blue fraction completely free of chlorobium chlorophyll (see Fig. 1). Absorp-

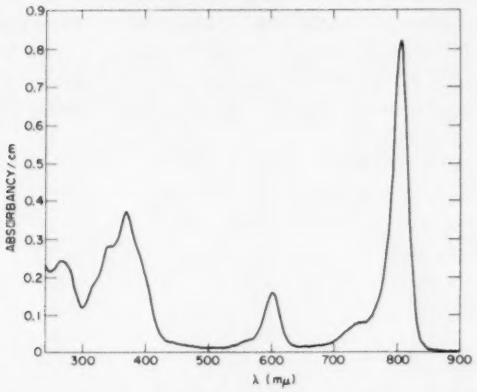

FIG. 1.—Absorption spectrum of the protein-chlorophyll-770 complex from *Cps. ethylicum* dissolved in 0.25 *M* NaCl and 0.02 *M* phosphate buffer pH 7.8 after elution from diethylaminoethyl cellulose.

tion spectra were measured on a Cary 14R recording spectrophotometer with monochromatic illumination of the sample at all wavelengths. Fluorescence emission spectra were obtained with a fluorometer[9] based on the design of Duysens and Amesz.[10] The spectral sensitivity was determined by placing a tungsten ribbon filament lamp, calibrated for a color temperature of 2870°K by the National Bureau of Standards, in the sample position. Assuming that the true temperature of the filament was 2800°K, the spectral sensitivity of the fluorometer was calibrated from the emission spectrum of tungsten.[11] Exciting light (366 or 436 mμ) was isolated from a mercury lamp (GE H-85A3-UV) by an interference filter-color filter combination. A red cut-off filter prevented excitation light scattered by the sample from entering the fluorescence analyzer.

The Pyrex sample cell ($2 \times 8 \times 10$ mm³ ID) was mounted on the end of a long glass tube which was inserted into a quartz Dewar with unsilvered walls around the sample position at the bottom. For low temperature measurements, the Dewar was filled with liquid nitrogen.

The quantum intensity of the exciting light was determined from the fluorescence of totally absorbing standard samples: for the 366 mμ line a packed powder sample

of the N.B.S. standard phosphor No. 1030 ($(MgO)_x(As_2O_5)_y-Mn$)[12] and a 10^{-2} M solution of Rhodamine B in ethanol[13] and for both the 366 mμ and the 436 mμ lines a 10^{-2} M solution of 9-aminoacridine in ethanol.[13] From the spectral sensitivity of the fluorometer and the quantum yields of the fluorescing standards the quantum intensity of the exciting light was calculated. The values for the intensity of the 366 mμ exciting light, obtained as described, agreed to within ±5 per cent of the mean value.

Fluorescence emission spectra ($dQ/d\bar{\nu}$) are given in quanta per cm^2 per second per unit wave number (μ^{-1}) per unit solid angle. Total quantum emission, given by the area under the spectral distribution curves for each sample, was determined by the weighing method.

Results and Discussion.—Figure 1 shows the absorption spectrum of the protein-chlorophyll-770 complex in aqueous solution. The absorbancy ratio D_{808}/D_{270} is assumed to be a measure of the chlorophyll to protein ratio, estimated to be approximately 3×10^{-5} M chlorophyll per gram protein in this preparation on the basis of $D_{808}/D_{270} = 3.4$, $\epsilon_{808} \simeq 10^5\ M^{-1}\ cm^{-1}$, and $\epsilon_{270} \simeq 1\ (g/l)^{-1}\ cm^{-1}$.

Figure 2 shows, in addition to the far red absorption band (808 mμ), the fluores-

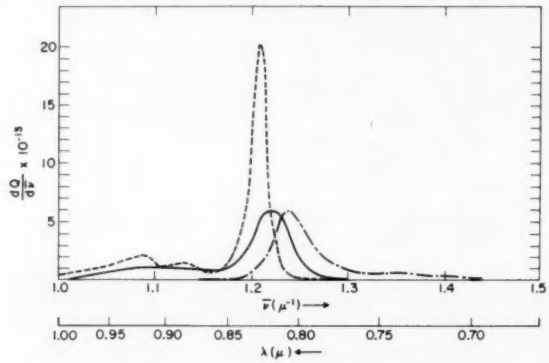

FIG. 2.—Fluorescence emission spectra ($dQ/d\bar{\nu}$) at 294° (———) and 77°K (— — —) of the protein-chlorophyll-770 complex from *Cps. ethylicum*, caused by excitation at 366 mμ, and the far red absorption band (— — — — —) of the same preparation, normalized to the main fluorescence peak at 294°K.

cence emission of the protein-chlorophyll-770 complex in aqueous solution. Cooling of the solution to 77°K causes a red shift of the fluorescence maximum from 818 mμ to 827 mμ and resolves the broad shoulder on the high wavelength side into two minor peaks at about 880 mμ and 917 mμ respectively. The main fluorescence peak is enhanced and sharpened at low temperature with a 50 per cent increase in quantum yield. By comparison with the N.B.S. phosphor 1030 ($\phi_f = 0.75$),[12] Rhodamine B ($\phi_f = 0.97$)[13] and 9-aminoacridine ($\phi = 0.99$)[13] the fluorescence yield of the protein-chlorophyll-770 complex is estimated to be 0.19 at room temperature and 0.29 at 77°K within limits of error of about ±7 per cent.

Figure 3 shows the fluorescence emission of a young culture of *Cps. ethylicum*. At the excitation wavelength (436 mμ) less than one per cent of the exciting light is absorbed by the chlorophyll-770 in the cells, as may be concluded from a comparison of the spectrum given in Figure 1 and an absorption spectrum of whole cells.[2]

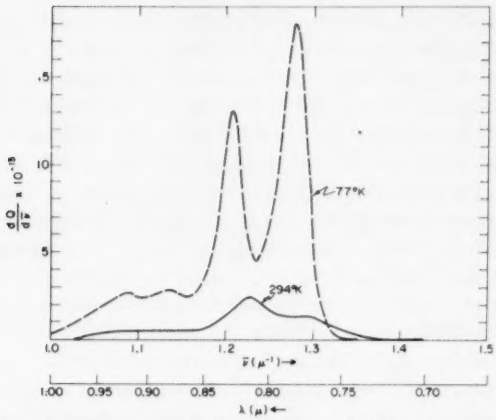

FIG. 3.—Fluorescence emission spectra ($dQ/d\bar{\nu}$) from whole cells at 77°K and 294°K caused by excitation at 436 mμ. The cell suspension was taken from a one-day-old culture of *Cps. ethylicum*.

Essentially all of the light is absorbed by the chlorobium chlorophyll-660 and the main carotenoid, γ-carotene.[7] (Carotenoids are estimated to absorb about 25 per cent of the exciting light.) At room temperature the fluorescence spectrum has two maxima at 769 mμ and at 814 mμ respectively; at 77°K these maxima sharpen up to peaks at 781 mμ and 827 mμ. Corresponding maxima at both temperatures were also shown by *C. thiosulfatophilum*, strain L. The peaks also correspond to two of the three found by Krasnovskii, Erokhin, and Yui-Tsun[5] in another *Chlorobium* strain. They found an additional maximum at 675 mμ, which they attributed to a nonaggregated form of chlorobium chlorophyll-660. We have observed this peak also, but only in older cultures (15 to 20 days) of green bacteria. The fluorescence maximum at about 769 mμ (294°K) in both young and old cells comes from the "aggregated" chlorobium chlorophyll-660 which has maximum absorption between 740 and 750 mμ *in vivo*. The higher wavelength fluorescence maximum (814 mμ at 294°K and 827 mμ at 77°K) clearly corresponds to monomeric chlorophyll-770 (cf. Fig. 2) rather than to another aggregated form of chlorophyll-660 as suggested by Krasnovskii *et al.*[5] Since essentially all of the exciting light is absorbed by chlorophyll-660 and carotenoid, some excitation energy must be transferred to chlorophyll-770. The enhancement and sharpening of the chlorophyll-770 fluorescence peak *in vivo* upon cooling to 77°K increases the quantum emission to about 3.5 times the room temperature value. If it is assumed that the amount of nonradiative decay of the excited states *in vivo* is the same as *in vitro*, this indicates an increase in the efficiency of energy transfer upon cooling. The relative increase in fluorescence emission for chlorophyll-770 is, however, substantially less than for the "aggregated" chlorophyll-660. This may be explained by the observations[5, 14] that aggregated forms of pigments show more fluorescence enhancement upon cooling than do the monomeric forms, due to the higher probability of nonradiative decay of the excited state at room temperature in aggregated forms.

For an estimate of the efficiency of energy transfer to chlorophyll-770 from the data of Figure 2, the quantum intensity of the excitation at 436 mμ is required.

The quantum intensity ratio for the 436 mμ and 366 mμ excitation beams was obtained by measuring the fluorescence of 9-aminoacridine at both wavelengths. The absolute quantum intensity at 436 mμ was then calculated from this ratio and the quantum intensity at 366 mμ determined by the fluorescence of the standard samples mentioned previously. The intensity of the exciting beam at 436 mμ (about 10^{18} quanta sec^{-1} cm^{-2}) was roughly 200 times the intensity required for saturating the light-induced cytochrome oxidation reaction with red light. Estimates of the efficiency of energy transfer to chlorophyll-770 and of the fluorescence yield of chlorophyll-660 *in vivo* were made on the basis of the following assumptions: (1) The fraction of the absorbed light utilized for the chemical processes of photosynthesis is negligible. (2) The excitation light absorbed by chlorophyll-770 is negligible. (3) The fluorescence yield of chlorophyll-770 *in vivo* is the same as that for the protein-chlorophyll-770 complex in aqueous solution.

The estimated efficiency of energy transfer at room temperature may be too low since nonradiative decay of the excited states of chlorophyll-770 at room temperature may be more probable *in vivo* than is assumed. The estimates along with a diagram of the excitation energy pathways at 294°K and at 77°K are given in Figure 4. The limit of error in each estimate is about ± 10 per cent.

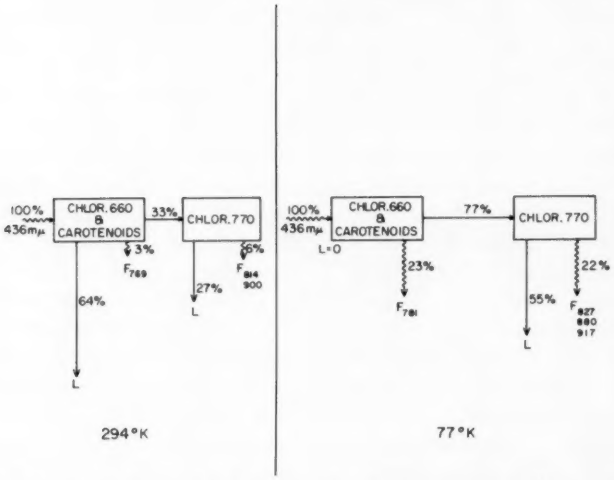

FIG. 4.—Pathways for dissipation of excitation energy at 294°K and 77°K in *Cps. ethylicum*. The symbols *L* and *F* represent nonradiative losses and fluorescence respectively. The percentages shown are estimates of the quantum yields in a one-day-old culture.

When the intensity of the exciting light is diminished to levels at which the energy utilization for photochemical processes can become competitive with fluorescence emission, *Cps. ethylicum* (294°K) shows a significant change in the ratio of the peak heights at 769 and 819 mμ. As the intensity of the 436 mμ exciting light is decreased from 10^{18} to 10^{16} quanta sec^{-1} cm^{-2}, the fluorescence yield of chlorophyll-770 drops as much as 20 per cent, while the yield of the "aggregated" chlorophyll-660 remains constant.

The substantial energy transfer from carotenoid and chlorophyll-660 to chlorophyll-770 shown in the present study demonstrates that chlorophyll-770 can serve as a *terminal* excitation energy acceptor. The fact that light absorbed mainly by chlorophyll-770 *in vivo* induces cytochrome oxidation[6] indicates that chlorophyll-770 is an energy acceptor which sensitizes a primary photosynthetic oxidation-reduction reaction. A confirmation of this and an indication that chlorophyll-770 might be the *unique* energy acceptor which couples the absorbed light energy to photosynthesis is given by the drop in fluorescence yield of chlorophyll-770 *in vivo* when the intensity of the exciting light is decreased sufficiently.

The authors wish to thank Dr. Simon Freed for sharing methods and materials for low temperature fluorescence measurements and Dr. Geoffrey Zubay for demonstrating how to purify the protein-chlorophyll-770 complex.

* Research carried out at Brookhaven National Laboratory under the auspices of the U.S. Atomic Energy Commission.

† On leave from the Department of Endocrinology and Metabolic Diseases, University Hospital, Leiden, The Netherlands.

[1] Katz, E., and E. C. Wassink, *Enzymologia*, **7**, 97 (1939).

[2] Larsen, H., in *Radiation Biology*, ed. A. Hollaender (New York: McGraw-Hill, 1956), vol. 3, p. 372.

[3] Lascelles, J., data in Fig. 1 of R. Y. Stanier and J. H. C. Smith, *Biochim. Biophys. Acta*, **41**, 478 (1960).

[4] Bergeron, J. A., and R. C. Fuller, in *Biological Structure and Function*, ed. T. W. Goodwin and O. Lindberg (London-New York: Academic Press, 1961), vol. 2, p. 307.

[5] Krasnovskii, A. A., Yu. E. Erokhin, and Kh. Yui-Tsun, *Doklady Akad. Nauk. S. S. S. R.*, **143**, 456 (1962).

[6] Olson, J. M., and C. A. Romano, *Biochim. Biophys. Acta*, **59**, 726 (1962).

[7] Kondrat'eva, E. N., and L. V. Moshentseva, *Doklady Akad. Nauk. S. S. S. R.* **135**, 460 (1960).

[8] Zubay, G., *J. Mol. Biol.*, **4**, 347 (1962).

[9] Avi-Dor, Y., J. M. Olson, M. D. Doherty, and N. O. Kaplan, *J. Biol. Chem.*, **237**, 2377 (1962).

[10] Duysens, L. N. M., and J. Amesz, *Biochim. Biophys. Acta*, **24**, 19 (1957).

[11] de Vos, J. C., *Physica*, **20**, 690 (1954).

[12] Bril, A., and W. Hoekstra, *Philips Res. Rept.*, **16**, 356 (1961).

[13] Weber, G., and F. W. J. Teale, *Trans. Faraday Soc.*, **53**, 646 (1957).

[14] Brody, S. S., *Science*, **128**, 838 (1958).

AN IMIDAZOLE PUMP MODEL OF ELECTRON TRANSPORT

BY DAN W. URRY* AND HENRY EYRING

DEPARTMENT OF CHEMISTRY, UNIVERSITY OF UTAH, SALT LAKE CITY

Communicated December 28, 1962

When the rates of mitochondrial electron transport[1] are compared to those of nonbiological systems[2, 3] the biological rates are found to be remarkably rapid. This is due, of course, to the nature of the electron carriers and the integrity of the mitochondrial membrane. The steric arrangement of the biological carriers and the extensive conjugated system of the porphyrins serve to allow for proper juxtaposition or overlapping of orbitals and to allow for low energy transitions, thereby permitting a rapid flow of electrons. There are several important criteria when

dealing with transition metals which favor rapid redox rates. In order to obtain ease of electron transfer a symmetrical activated state is preferred, the bond lengths should be allowed to vary, the so-called *trans effect* is often influential, and, in general, ligand-field effects are of primary importance.

The first two criteria arise from considerations of the Franck-Condon principle which, simply stated, is that the time required for electron transfer is instantaneous relative to nuclear motion. If at the time of transfer the bond distances of the acceptor are displaced from what will be the zero point vibrational range, then the new species is formed in a vibrationally excited state, having necessitated an electronic activation energy.[4, 5] If, on the other hand, by suitable vibration there is a symmetrization and equalization of the bond distances, then transfer of electrons can take place with a minimum of electronic excitation. The vibrational energy expended in symmetrization is less than the increased electronic activation energy required for transfer when the system is asymmetrical. The concept of a *trans effect* was introduced by Chernyaev[6] relative to displacement reactions involving Pt^{+2} complexes, e.g., dichlorodiammineplatinum. The observed effect is that a negative ligand, in particular, tends to labilize the ligand trans to it; that is, exchange or transfer occurs more readily along the line of centers of the transition metal and the coordinating atoms of the negative ligand. This effect has been explained by Syrkin[7] on the basis of resonance and hybridization. Another concept which clarifies the *trans effect* as well as other problems of valency is the principle of minimum bending of orbitals.[8, 9] This suggests that electron transfer would be facilitated by a linear path.

When one considers the symmetry requirements, bond length changes, and the *trans effect*, one is provisionally constrained to look for electron transfer at the fifth and sixth coordination positions of the iron porphyrin system. This immediately implicates the imidazole group of histidine as it is known to be one of the ligands in cytochrome *c* and in myoglobin and hemoglobin. Though the latter two do not function in the electron transport chain, they do have different oxidative states. Also, two histidine residues have been suggested as necessary for the enzymatic activity of catalase.[10] Furthermore, the unique properties of imidazole would allow it to function nicely in an electron transport capacity. Imidazole has been found to have marked semiconduction properties;[11a] it has been implicated in the active sites and active centers of numerous enzymes, and it forms a symmetrical species which is considered a principal factor in its catalytic ability. At a pH below six it is found as the symmetrical ImH^+ species where one hydrogen is attached to each of the two nitrogens.

The Imidazole Pump Model.—An electron transport model can be constructed utilizing porphyrins and imidazoles in a stacked manner as indicated by the set of reactions in Figure 1. Looking at the iron-porphyrin system on edge at a cross section through the iron, we see that initially the imidazoles are attached at the left. By the series of electron shifts[11b] indicated, the imidazoles become attached to the iron on the right. If we now allow a donor to interact covalently with the iron at the left, then a second series of shifts is possible which returns the imidazoles to their original positions leaving two electrons for O_2 which with $2H^+$ can form hydrogen peroxide. The net effect of a complete cycle—of the imidazoles going from attachment at the left to attachment at the right and then returning to the left—is

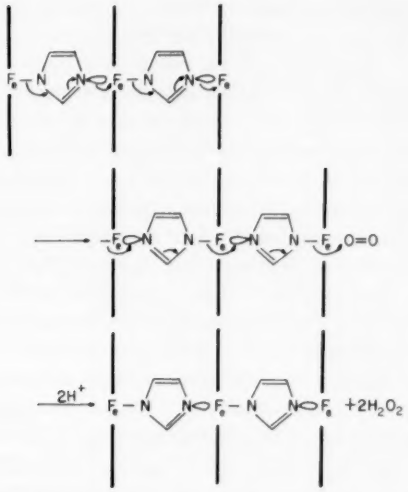

FIG. 1.—An imidazole pump model of electron transport. See text for discussion.

the removal of two electrons from a nucleophilic electron donor and the delivery of two electrons to an electrophilic acceptor. With each complete cycle the imidazole pump delivers two electrons to a suitable acceptor on the extreme right. This mechanism has symmetry and a certain simplicity, and it is in accord with the criteria listed for ease of electron transfer. In order to see this more clearly we may examine the two steps, as given in Figure 2, in some detail.

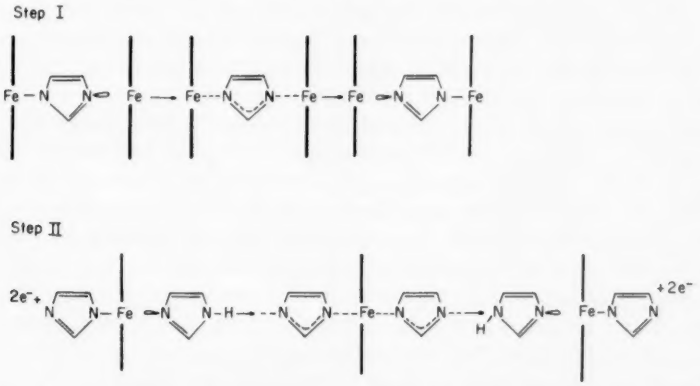

FIG. 2.—Step I and Step II of the imidazole pump model of electron transport showing the symmetry of the activated complex.

Step I begins with the imidazole attached at the left. By vibration of sufficient amplitude, the ligand may pass through a position of symmetry between the two iron atoms. At the instant at which there is a plane of symmetry exactly between the two iron porphyrin systems, the electron shifts can occur with a minimum of electronic activation energy. Such a transfer would be in adherence to the Franck-

Condon principle. The central figure in Step I represents the activated complex or transition state. After electron transfer the system readjusts its vibrational state such that the equilibrium position of the imidazole is nearer the iron on the right. Thus we have a bridged (inner sphere) activated complex[12, 5] involving the coordination shells of both cations, and conduction is through an unsaturated ligand of known semiconduction properties.[11a] One might think of the electron shifts[11b] as the following: the pair of electrons in the nonbonding orbital of the tertiary nitrogen enters into a covalent interaction with the iron on the right; the pair of π electrons then shifts into the nonbonding orbital of the newly formed pyrrole-type nitrogen; and the pair of electrons that was bonding the nitrogen to the iron on the left shifts into the π system. These electron shifts are indicated in the first step in Figure 1. This first step represents an interesting case where the direction of electron flow is the same as the direction of group transfer.

Further, to clarify Step I, it is useful to discuss the oxidative states of the transition metal. In determining the valency of a cation, one assigns a likely charge to the ligand and the remainder of the charge is relegated to the metal ion.[13] Since an imidazole anion is highly unlikely except at very high pH in a medium of large dielectric, one would be encouraged to take the imidazolyl group as neutral and assign the negative charge to the iron. Thus initially, the valence of the iron on the left would be +2 and that on the right would be +3. After electron transfer the iron-porphyrin system on the right is reduced and that on the left is oxidized. We therefore have a model in which there are univalent changes in the oxidative states, yet there is no need to postulate a high energy, free radical mechanism. Quantum mechanical considerations suggest that only one electron is transferred at a time. However, in a mechanism of this type the transfers may occur in rapid succession without the formation of a long-lived free radical.

Another point which makes this mechanism appealing is that the Franck-Condon barrier is also expected to be small when transfer is between t_{2g} orbitals;[5] t_{2g} orbitals are formed when the transition metal is in an octahedral environment.[13] And if, as is possible, we are dealing with a strong ligand-field, then the transfer of an electron from a d^6 to a d^5 system of iron involves transfer between t_{2g} orbitals. For a particular system of interest the strength of the ligand-field may be checked by the magnetic moment, by the presence or absence of charge transfer bands, or by the presence of an absorption band around 500 mμ.[14] The Pullman group, using the molecular orbital method, has calculated that the covalent ferroporphyrin system has a high lying, highest filled molecular orbital giving it unusually strong donor properties, whereas the covalent ferriporphyrin has pronounced acceptor properties. Of course, net electron transport would be further facilitated if the porphyrins on the right had increasingly more negative oxidation potentials. This could possibly be brought about by different substituents on the porphyrin unit.

Step II also has interesting symmetry as seen in Figure 2. Again we have an inner sphere activated complex in which the plane of symmetry is coincident with the plane of the porphyrin. This mechanism is of the S_N2 type.[16] In the initial state the iron is in an asymmetrical octahedral field as it is in the final state, while in the transition state the iron is in a symmetrical octahedral field. Furthermore, we have a *trans effect* and the electron transfer is linear through the iron. As in Step

I this step is facilitated by a proper donor and a suitable acceptor. However, here the direction of electron flow is in the opposite direction to group transfer as is commonly found in chloroammine-platinum complexes[17] and many other systems.[12] It is also worth noting that Step II does not involve a change in the valence of iron.

On the Coupling of Oxidation and Phosphorylation.—The imidazole pump model of electron transport provides a simple electron transfer pattern which is very flexible in its ability to be varied to concur with experimental data. We wish at this point only to point out a possibility or two as to how one may alter this model to include high energy bond formation. How can electron flow be maintained in the process of high energy bond formation? We could, for example, introduce quinones as well as additional imidazoles into the sequence. This could be done in such a way as to include both H_2O^{18}-Pi and ATP-Pi^{32} exchanges. For the case where the redox potentials are favorable, a situation such as Figure 3 may be considered. The electron shifts indicated would deliver a negative charge to the distant oxygen of the quinone. If, simultaneous with the electron shifts, the negative oxygen were directed into the phosphorus of a phosphate, then a high energy bond could be formed with liberation of a hydroxyl. The process would be facilitated if Mg^{+2} were to neutralize the two negative oxygen atoms and thereby increase the positive character of the phosphorus.[18] The result would be a reduced quinone (a quinol), a ferriporphyrin, and a high energy quinol phosphate. The phosphate could then be transferred to an appropriate acceptor and the quinol could subsequently be oxidized, thus maintaining the flow of electrons.

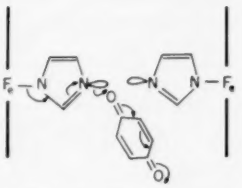

FIG. 3.—Possible coupling mechanisms involving quinone. See text for discussion.

The work of Cramer *et al.*[19] on phosphoryl-imidazoles raises the possibility of this species being formed at one of the coupling sites. (We have heard from Prof. D. M. Greenberg that Prof. P. D. Boyer has actually isolated a phosphoryl-histidine residue from an actively phosphorylating mitochondrial preparation.) In such a case two possibilities are immediately suggested: one is that phosphoryl could become directly attached to imidazole without the necessity of a quinol being interspersed. The other possibility is that a phosphoryl could possibly displace a quinol which became attached to the imidazole. In order to maintain electron flow the quinol would need to become attached to an imidazole at the left of an iron porphyrin (considering electron flow to the right). With reference to Figure 3, let us suppose that the quinone has been reduced by the shifts indicated and is now attached to the imidazole. If we further suppose that the quinol be transferred with its electrons to the nitrogen of the second imidazole as a functioning member of Step II (see Figs. 1 and 2), we now have the quinol attached to the second imidazole with the first imidazole being reattached to its iron. If we introduce ortho-phosphate and the phosphoryl moiety should enter into covalent linkage with the nitrogen displacing quinol as quinone and liberating an hydroxyl ion, we then have a high energy phosphoryl which may be transferred to an acceptor. In this process the second imidazole would become reattached to its iron. The net effect would be the transfer of two electrons and the formation of a high energy bond.

Summary.—We have presented a model of electron transport which has favorable

electronic and geometric properties and which can be varied to include the formation of high energy bonds in a manner concurring with experimental data.[20] Nor need it be confined to this application as cytochromes and quinones have been implicated in photophosphorylation.[21] Both steps in the model have the feature that the activated complex is entirely symmetrical and would require only a small vibrational activation energy and a minimum of reorganizational free energy.[2] The problem of electron transfer and the coupling of chemical reactions will be presented in more detail elsewhere using reaction rate theory.[22]

Note added in proof (January 30, 1963): It has just come to our attention that A. Ehrenberg and H. Theorell (*Acta Chem. Scand.*, **9**, 1193, 1955), on the basis of their proposed structure of cytochrome *c*, suggested that "electron transfer could then be imagined to take place through the resonating bonds of the imidazole ring," which is in accord with our model based on other considerations.

The authors would like to thank Mr. Dan Boone for calling attention to the criteria of bond length changes and for useful references. They also wish to thank Professors J. M. Sugihara and R. E. Hamm for helpful comments on the model. One of us (D. W. U.) would like to thank Corning Glass Works for support during the preparation of this manuscript. We wish to thank Barbara Staker for drawing the figures.

* Corning Glass Works Foundation Fellow for the year 1962–1963.

[1] Chance, B., and G. R. Williams, *Adv. Enzymol.*, **17**, 65 (1956).

[2] Zwolinsky, B. J., R. J. Marcus, and H. Eyring, *Chem. Revs.*, **55**, 157 (1955).

[3] Stranks, D. R., in *Modern Coordination Chemistry*, ed. by J. Lewis and R. G. Willkins (New York: Interscience Publishers Inc., 1960), p. 78.

[4] Libby, W. F., *J. Phys. Chem.*, **56**, 863 (1952).

[5] Halpern, J., and L. E. Orgel, *Faraday Soc. Disc.*, **29**, 7 (1960).

[6] Chernyaev, I. I., *Ann. inst. platine U.S.S.R.*, **4**, 261 (1926).

[7] Syrkin, Y. K., *Bull. acad. sci. U.R.S.S. classe sci. chim.*, 69 (1948).

[8] Eyring, H., G. H. Stewart, and R. P. Smith, these PROCEEDINGS, **44**, 259 (1958).

[9] Stewart, G. H., and H. Eyring, *J. Chem. Ed.*, **35**, 550 (1958).

[10] Nakatani, M., *J. Biochem.*, **49**, 98 (1961).

[11a] Aftergut, S., and G. P. Brown, *Nature*, **191**, 379 (1961).

[11b] A good description of the properties of imidazole[23] is obtained by the molecular orbital theory[24] in which case six electrons are considered to be hybridized over the ring, one electron from each of the carbons, one from the tertiary nitrogen, and two electrons (the nonbonding pair) from the secondary nitrogen. However, the electron shifts as indicated serve well for illustration.

[12] Taube, H., in *Advances in Inorganic Chemistry and Radiochemistry*, ed. by H. J. Emeleus and A.G. Sharpe (New York: Academic Press, 1959) vol. 1, p. 1.

[13] Orgel, L. E., *An Introduction to Transition-Metal Chemistry: Ligand-Field Theory* (New York: John Wiley and Sons, Inc., 1960).

[14] Brill, A. S., and R. J. P. Williams, *Biochem. J.*, **78**, 246 (1961).

[15] Pullman, B., C. Spanjaard, and G. Berthier, these PROCEEDINGS, **46**, 1011 (1960).

[16] Basolo, F., and R. G. Pearson, *Mechanisms of Inorganic Reactions* (New York: John Wiley and Sons, Inc., 1958).

[17] Basolo, F., M. L. Morris, and R. G. Pearson, *Faraday Soc. Disc.*, **29**, 80 (1960).

[18] Cohn, M., *J. Cellular Comp. Physiol.*, **54**, Suppl. 1, 17 (1959).

[19] Cramer, F., H. Schaller, H. A. Staab, *Chem. Ber.*, **94**, 1612 (1961).

[20] Lehninger, A. L., and C. L. Wadkins, *Ann. Rev. Biochem.*, **31**, 47 (1962).

[21] Bishop, N. I., *Ciba Symposium on Quinones in Electron Transport* (1960), p. 385.

[22] Eyring, H., and D. W. Urry, in preparation.

[23] Bernard, E. A., and W. D. Stein, *Adv. Enzymol.*, **20**, 51 (1958).

[24] Bassett, I. M., R. D. Brown, and A. Penfold, *Chem. and Ind.*, London, 892 (1956).

*INTERMEDIATE REACTIONS IN THE PHOSPHORYLATION COUPLED TO THE OXIDATION OF REDUCED CYTOCHROME C**

By George Webster,† Archie L. Smith, and Marc Hansen‡

INSTITUTE FOR ENZYME RESEARCH, UNIVERSITY OF WISCONSIN, MADISON

Communicated by David E. Green, December 3, 1962

The mechanism of mitochondrial oxidative phosphorylation is a major unsolved problem of present-day biochemistry. The elucidation of the structure of the mitochondrial electron transfer chain and of the arrangement of the oxidation-reduction components[1] opened the way to a direct attack on the coupling problem. The oxidative phosphorylation system of beef heart mitochondria has been resolved into a submitochondrial particle (modified ETP_H[5]) and three soluble protein coupling factors.[2, 3] Each coupling factor is specific for one of the three phosphorylation sites on the electron transfer chain.

It has now been possible to split the cytochrome oxidase complex from the electron transfer chain under conditions which permit the partially purified cytochrome oxidase to catalyze the single phosphorylation associated with the oxidation of reduced cytochrome *c*. The reduced cytochrome *c* coupling factor[2] is an absolute requirement for this phosphorylation step. With this system, it has been found that the phosphorylation process associated with the oxidation of reduced cytochrome *c* can be separated into two reactions. The first reaction results in the formation of a high-energy nonphosphorylated compound which appears to be of the type described by Pinchot[4] in his studies on oxidative phosphorylation by bacterial extracts. The second reaction results in ATP formation from ADP and orthophosphate concomitant with the degradation of the intermediate compound. The present communication deals with some characteristics of the two reactions.

Methods.—Modified ETP_H was prepared as described by Linnane and Titchener.[5] The cytochrome oxidase was purified from modified ETP_H by an adaptation of the original procedure of Green *et al.*[6] for cleaving the respiratory chain. A suspension of modified ETP_H (approximately 40 mg protein per ml) in 0.25 *M* sucrose-0.01 *M* Tris (pH 7.5) was diluted with $^2/_5$ volume of 0.9 per cent KCl. The resulting suspension was mixed with $^1/_8$ volume of tertiary amyl alcohol containing 2 per cent redistilled isooctane. The mixture was homogenized for 30 sec with a power-driven Potter-Elvehjem glass homogenizer and allowed to stand at 38°C for 3–5 min (or until the suspension exhibited a pale brownish-green color). The pale green particles were sedimented at 75,000 × *g* for 15 min and were separated from the red supernatant material. The sediment was suspended in a solution containing 5 mg/ml sonicated phospholipid in a solution 0.25 *M* in sucrose, 0.01 *M* in Tris (pH 7.5), and 0.0005 *M* in EDTA, and the mixture was allowed to stand in this solution for 10 min at 1°C. The sonicated phospholipid was prepared from Asolectin (Associated Concentrates, Woodside, N. Y.) as described by Lester and Smith.[7] The particles were then washed at least six times with the phospholipid solution. It is essential that the washing be continued until the odor of tertiary amyl alcohol can no longer be detected, as preparations containing detectable amounts of the alcohol have always failed to phosphorylate. The preparation was then washed three times with a solution 0.25 *M* in sucrose and 0.01 *M* in Tris (pH

7.5). The cytochrome oxidase particles contained 2.5–3.5 mμmoles of heme *a* per mg protein (determined as described by Griffiths and Wharton[8]) and 0–0.1 mμmoles flavin (determined according to Basford *et al.*[9]). These values are similar to those previously reported by Green[10] for comparable preparations. The reduced cytochrome *c* coupling factor employed in these experiments was at the same stage of purity as that described previously.[2] The assay system for phosphorylation coupled to the oxidation of reduced cytochrome *c* was that already described,[2] except that 0.2 mg of cytochrome *c* (Sigma) was present in each assay containing a cytochrome oxidase preparation.

The reaction system for the production of the high-energy intermediate consisted of: 750 μmoles sucrose, 150 μmoles Tris (pH 7.5), 60 μmoles $MgCl_2$, 0.31 μmoles reduced cytochrome *c*, 3.0 mg reduced cytochrome *c* coupling factor, and 3.0 mg cytochrome oxidase complex in a total volume of 3 ml. After incubation for 15 min at 38°C, the cytochrome oxidase complex was removed by centrifugation at 105,000 × *g* for 15 min. The intermediate was purified from the supernatant solution by chromatography on carboxymethyl-cellulose. ATP formation from the intermediate was measured by incubation of the intermediate for 5 min at 38°C with: 40 μmoles Tris (pH 7.5), 25 μmoles KCN, 10 μmoles $MgCl_2$, 10 μmoles ADP, 10 μmoles $K_2HP^{32}O_4$ (20,000,000 cpm), 40 μmoles glucose, and 10,000 units of yeast hexokinase in a total volume of 4 ml. The incorporation of radioactive phosphate into glucose-6-phosphate was used routinely as a measure of ATP formation.

Results.—Phosphorylation by the cytochrome oxidase preparation: As is shown in Table 1, the partially purified cytochrome oxidase preparations obtained by treatment of modified ETP_H with tertiary amyl alcohol readily oxidize reduced cytochrome *c* but have no detectable ability to oxidize either DPNH or succinate in the presence of added cytochrome *c*. It should be noted that the rates of oxidation of reduced cytochrome *c* are considerably less than maximal because the reaction system that is optimal for phosphorylation is not optimal for oxidation. The preparation is able to catalyze phosphorylation coupled to the oxidation of reduced cyto-

TABLE 1

OXIDATIVE PHOSPHORYLATION BY THE CYTOCHROME OXIDASE PARTICLES

Reaction system*	Oxygen consumed†	P/O
Complete	0.11	0.8
Minus coupling factor	0.12	0
Minus magnesium ions	0.16	0
Minus cytochrome *c*	0.01	0
Plus 0.001 *M* KCN	0	0
Plus 0.001 *M* dinitrophenol	0.14	0
Plus 0.02 mg antimycin	0.10	0.8
Ascorbate replaced by 0.001 *M* DPNH	0	0
Ascorbate replaced by 0.001 *M* succinate	0	0
Cytochrome *c* coupling factor replaced by DPNH coupling factor	0.12	0
Cytochrome *c* coupling factor replaced by QH_2 coupling factor	0.10	0

* The reaction system consisted of: 0.25 *M* sucrose, 0.002 *M* ATP, 0.002 *M* ADP, 0.006 *M* $MgCl_2$, 0.024 *M* glucose, 0.01 *M* Tris, 0.005 *M* potassium phosphate-P^{32} (2,000,000 cpm), 10,000 units of hexokinase, 0.2 mg cytochrome *c* (Sigma), 0.03 *M* potassium ascorbate (pH 7.5) 10 μg reduced cytochrome *c* coupling factor, the additions listed in the table, and 2 mg of particles in a total volume of 2 ml. Oxygen consumption was measured with a GME recording oxygraph, and phosphorylation was measured by determination of P_i^{32} incorporated into glucose-6-phosphate.

† μatoms oxygen/min/mg protein.

chrome *c*. Under optimal conditions, a P/O ratio as high as 0.9 is attained, although the P/O ratio is usually about 0.8. Phosphorylation is apparently dependent upon the removal of residual tertiary amyl alcohol from the particles, because particles which have not been equilibrated repeatedly with phospholipid fail to phosphorylate. Addition of tertiary amyl alcohol to actively phosphorylating modified ETP_H or cytochrome oxidase particles likewise inhibits phosphorylation. Phosphorylation is also completely inhibited by 0.001 *M* DNP or by omission of reduced cytochrome *c*, magnesium ions, or the reduced cytochrome *c* coupling factor from the reaction system. Replacement of the reduced cytochrome *c* coupling factor by the DPNH coupling factor[3] or the $CoQH_2$ coupling factor[3] also eliminates phosphorylation. The complete dependence of phosphorylation on the presence of the specific coupling factor provides additional evidence in support of our previous conclusion[2, 3] that the coupling factors are essential components of the phosphorylation mechanism of mitochondria.

Exchange and ATPase activities of the cytochrome oxidase preparation: The transition from modified ETP_H to the derivative particles of the cytochrome oxidase preparation is accompanied by striking changes in ATPase and ATP-P_i exchange activities. As is evident from Table 2, the cytochrome oxidase particles have a markedly lower ATPase activity than that of modified ETP_H. This applies not only to the basal ATPase activity but also to the ATPase activity promoted by

TABLE 2

ATPASE AND ATP-P_i EXCHANGE ACTIVITIES OF MODIFIED ETP_H AND OF THE CYTOCHROME OXIDASE PARTICLES

Activity	Addition to system	Modified ETP_H	Cytochrome oxidase preparation
ATPase	—	0.37	0
ATPase	Mg^{++}	0.65	0.03
ATPase	DNP	0.42	0.01
ATPase	Mg^{++} + DNP	0.75	0.08
ATP-P_i Exchange	—	0.01	0

Reaction system for ATPase assay: 0.05 *M* Tris (pH 7.5), 0.01 *M* ATP, 1 mg of particle protein, and, where indicated, 0.01 *M* $MgCl_2$ and 0.001 *M* DNP in a total volume of 1 ml. Activity is expressed as μmoles P_i formed in one min by one mg of protein at 37°C.

Reaction system for ATP-P_i exchange: 0.05 *M* Tris (pH 7.5), 0.005 *M* potassium phosphate-P^{32} (20,000,000 cpm), 0.005 *M* ATP, 0.005 *M* $MgCl_2$, 0.15 *M* sucrose, 10 μg reduced cytochrome *c* coupling factor, and 2 mg particle protein in a total volume of 1 ml. Activity is expressed as μmoles P_i incorporated into ATP in one min by one mg of protein at 37°C.

magnesium ions or DNP. That the reduction in ATPase activity is not entirely due to an inactivation of ATPase during the preparation of the cytochrome oxidase particles is indicated by the fact that at least 80 per cent of the total ATPase activity of modified ETP_H can be found in the red supernatant solution which is discarded during the preparation of the cytochrome oxidase particles from modified ETP_H.

Along with the reduction in ATPase activity that accompanies the transition from modified ETP_H to the derivative cytochrome oxidase preparation, there is complete elimination of ATP-P_i exchange activity, even in the presence of the coupling factor. Again, most of the total exchange activity of the modified ETP_H can be found in the discarded red supernatant solution. It was previously shown that with purification of the reduced cytochrome *c* coupling factor, both ATPase and ATP-P_i exchange activities are eliminated.[2] Therefore, the phosphorylation step accompanying the oxidation of reduced cytochrome *c* by the cytochrome oxidase particles can

proceed with a P/O ratio as high as 0.9, but without any accompanying ATP-P_i exchange.

Formation of a high-energy intermediate of oxidative phosphorylation: The availability of the phosphorylating cytochrome oxidase preparation permits an examination of the mechanism of this phosphorylation step which is unencumbered by the reactions involved in the other two phosphorylation steps coupled to electron transfer. The surprising removal of ATPase and ATP-P_i exchange activities during the preparation of the cytochrome oxidase particles (below the level of significance) has virtually ruled out the pertinence of these two activities to the coupled oxidation of reduced cytochrome *c*. Instead, it has been found that the cytochrome oxidase preparation catalyzes the formation of a soluble, high-energy substance during the oxidation of reduced cytochrome *c* in the presence of the coupling factor and magnesium ions. This substance will then react with ADP and P_i to form ATP.

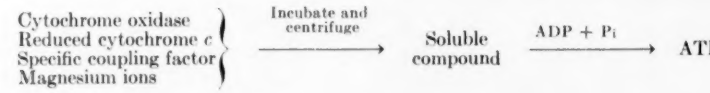

The conditions for formation, and the character, of this high-energy substance appear to be similar to those reported by Pinchot[4] earlier in a study of a bacterial system oxidizing DPNH and to those observed by Smith, Hansen, and Webster[11] in a study of the coupled oxidation of DPNH by ETP_H. The formation of ATP by the cytochrome oxidase system has been confirmed by the isolation of glucose-6-phosphate-P^{32} by chromatography (along with authentic glucose-6-phosphate) on Dowex-1 by the procedure of Khym and Cohn[12] and by paper chromatography in the alkaline solvent of Bandurski and Axelrod.[13] In Table 3, the formation of

TABLE 3

ASSAY OF ATP FORMATION

System	P^{32} incorporation into total organic phosphate (mμmole)	Paper chromatographic separation of glucose-6-P^{32} (mμmole)	Isolation of glucose-6-P^{32} on Dowex-1 (mμmole)
Complete	40	33	45
minus cytochrome *c*	0	0	0
minus hexokinase	0	0	0

The reaction system and experimental procedures were those described in the *Methods* and *Results* sections.

ATP as measured by these two methods is compared with the formation of total organic phosphates as measured by the Martin and Doty[14] procedure.

As can be seen from Table 4, the formation of the activated substance requires the presence of the cytochrome oxidase preparation, reduced cytochrome *c*, the reduced cytochrome *c* coupling factor, and magnesium ions. Formation of the substance is eliminated if oxidation does not occur, due either to the presence of HCN or to the substitution of oxidized for reduced cytochrome *c*. The presence of DNP also inhibits formation of the activated material. That the formation of this substance is not an artifact arising from the preparation of the cytochrome oxidase particles is demonstrated by the ability of modified ETP_H to form the intermediate.

TABLE 4

REQUIREMENTS FOR THE FORMATION OF THE SOLUBLE INTERMEDIATE

System		mμmoles glucose-6-P^{32} formed
Complete		40
Complete	minus cytochrome oxidase	0
Complete	minus reduced cytochrome *c*	0
Complete	minus coupling factor	0
Complete	minus $MgCl_2$	0
Complete	plus 0.001 *M* dinitrophenol	0
Complete	plus 0.001 *M* KCN	0
Complete	reduced cytochrome *c* replaced by oxidized cytochrome *c*	0
Complete	cytochrome oxidase replaced by modified ETP_H	28

The reaction system and experimental procedures were those described in the *Methods* section.

The function of the particle in the formation of the intermediate substance appears to be catalytic. If the cytochrome oxidase preparation is removed from an incubation mixture in which the intermediate has been formed and is placed in a fresh mixture of reactants, it again forms an amount of intermediate that is approximately equivalent to that found during the first incubation.

That the intermediate is used up during ATP formation is indicated by the fact that incubation of the intermediate for five min with ADP and nonradioactive P_i, followed by addition of P_i^{32}, does not lead to formation of ATP^{32}. Furthermore, as is evident from Table 5, the total yield of ATP is directly proportional to the

TABLE 5

DEPENDENCE OF ATP FORMATION ON THE AMOUNT OF ACTIVATED SUBSTANCE

Activated substance added (ml)	ATP formed (mμmoles)
0	0
1.0	15
2.0	28
3.0	41

The activated material was formed in the first incubation described in the *Methods* section. After removal of the particles by centrifugation, the indicated amounts of the supernatant solution were incubated for 5 min at 38° with 40 μmoles Tris (pH 7.5), 25 μmoles KCN, 10 μmoles $MgCl_2$, 10 μmoles ADP, 10 μmoles $K_2HP^{32}O_4$ (20,000,000 cpm), 40 μmoles glucose, 10,000 units of hexokinase, and water to make a total of 4 ml.

amount of activated substance incubated with the ADP and P_i^{32}. These two findings indicate that we are dealing with a substance that has been formed and not with an ATP-P_i exchange catalyzed by an enzyme released from the particles during the initial incubation. The lack of a detectable ATP-P_i exchange and the need for all of the components of the reaction system for the formation of the intermediate also argue against a simple exchange being responsible for the incorporation of P_i^{32} into ATP.

Although the formation of the activated substance is inhibited by DNP, ATP formation from ADP, P_i, and the activated material is unaffected by 0.001 *M* DNP. After exposure of the activated substance to 100°C for 3 min at pH 7.5 or to pH 11 for 30 min at 0°C, no formation of ATP takes place when the substance is subsequently incubated with ADP and P_i. Only moderate diminution of ATP synthesis (15–25 per cent) is observed when the substance is exposed to pH 3 for 30 min at 0°C. The formation of ATP from the activated substance, ADP, and P_i

is extremely rapid, and the reaction is completed in less than one min at 38°C. In contrast, the rate of formation of the activated material is much slower and parallels the rate of oxidation of the system.

Evidence that the activated substance is a distinct compound is presented by the data in Figures 1 and 2. In Figure 1 is given the elution pattern from a carboxymethyl-cellulose column of the components of the reaction system employed in these experiments. The activated substance is eluted from the column as a distinct peak just ahead of cytochrome *c*. Likewise, as is seen in Figure 2, the activated substance migrates as a discrete band during electrophoresis in starch gel. When reduced cytochrome *c* is omitted from the reaction system, or when 0.001 *M* DNP is added to the system, the intermediate band fails to appear.

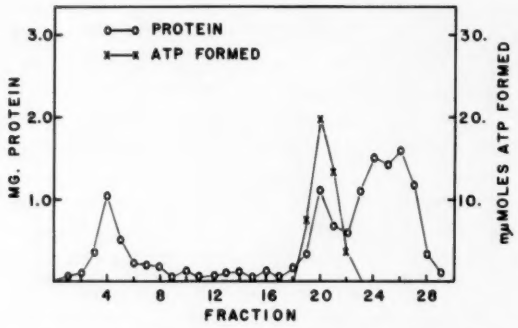

FIG. 1.—Separation of the activated substance on a carboxymethylcellulose column. The substance was formed as described in the *Methods* section. Each fraction was assayed for ATP formation with the reaction system described with Table 5. The eluting agent was Tris buffer of pH 7.5 of increasing concentration from 0.05 *M* to 0.5 *M*.

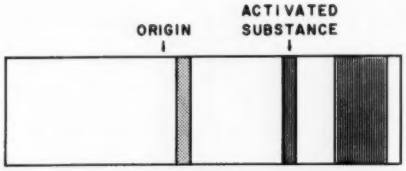

FIG. 2.—Separation of the activated substance by electrophoresis on starch gel. The activated substance was formed and assayed for ATP formation as described in the *Methods* section. Electrophoresis was for 6 hr at 300 volts in a 15 per cent starch gel containing 0.1 *M* Tris of pH 7.5.

Discussion.—This investigation has led to two findings which would seem to be of importance for future investigations on mitochondrial oxidative phosphorylation. First, the preparation of a particle which catalyzes only the phosphorylation coupled to the oxidation of reduced cytochrome *c* provides a system for the investigation of a single phosphorylation step without the interference of the enzymes associated with the other two phosphorylation sites on the electron transfer chain. One of the major difficulties in the study of the mechanism of oxidative phosphorylation at the level of the intact mitochondrion has been the enzymic complexity of the intact mitochondrion. The preparation of phosphorylating submitochondrial particles of decreasing complexity[15–20] has aided the study of the phosphorylation mechanism. However, the isolation of soluble coupling factors which are specific for each phosphorylation site makes it essential that each phosphorylation step be studied separately, because the mechanism at each site may differ somewhat.

The second finding of interest is the formation, during the oxidation of cytochrome *c*, of an intermediate which can react with ADP and P_i to form ATP. Further experiments are necessary to determine unequivocally whether this substance is a true intermediate in oxidative phosphorylation by mitochondria. However,

the high reactivity of the substance with ADP and P_i and the absolute dependence of its formation on the oxidation of cytochrome *c* and on the presence of the specific coupling factor argue in favor of its intermediate nature.

The formation of this activated substance seems to be in remarkable accord with the prior observations of Pinchot[4] of the formation of a nonphosphorylated, DPN-containing intermediate during DPNH oxidation by bacterial electron transfer particles. The reaction of this substance with ADP and P_i results in both the formation of ATP and the stoichiometric release of free DPN.[21] Current studies in this laboratory[11] have shown the formation of a similar substance during DPNH oxidation by the submitochondrial particle, ETP_H. Thus, the formation of a nonphosphorylated substance which reacts with ADP and P_i to form ATP has been demonstrated in both bacterial and mitochondrial preparations and at two different sites on the mitochondrial electron transfer chain. Although further study is required to establish the chemical nature of this substance, it would seem that the formation of a high-energy, nonphosphorylated substance during the oxidation of DPNH, coenzyme QH_2, or reduced cytochrome *c* may well be an initial stage in oxidative phosphorylation.

Summary.—A cytochrome oxidase-containing particle which catalyzes only the phosphorylation step coupled to the oxidation of reduced cytochrome *c* has been prepared from beef heart mitochondria. Oxidative phosphorylation by this particle exhibits an absolute requirement for the reduced cytochrome *c* coupling factor. During the oxidation of cytochrome *c* by this particle in the presence of the specific coupling factor and magnesium ions, a soluble, nonphosphorylated substance is formed which readily reacts with ADP and P_i to form ATP. The substance is formed only if cytochrome *c* is oxidized in the presence of the coupling factor, and the formation is prevented by dinitrophenol. The activated substance can be purified by chromatography or by starch gel electrophoresis.

The authors wish to thank D. E. Green for his advice and encouragement during this investigation. The expert technical assistance of Richard Wood, Ann DeLill, and Jean Glasgow is gratefully acknowledged.

* This work was supported in part by research grant HE-00458 from the National Heart Institute (USPHS). Meat by-products were generously supplied by Oscar Mayer and Company, Madison. The electrophoretic separations were kindly performed by Sandra L. Whitman, University of Wisconsin, Department of Biochemistry.

† Special Research Fellow, Division of General Medical Sciences (USPHS).

‡ Postdoctoral Trainee, National Institute of Arthritis and Metabolic Diseases (USPHS).

§ Abbreviations used: ADP, adenosine diphosphate; ATP, adenosine triphosphate; DNP, dinitrophenol; DPNH, reduced diphosphopyridine nucleotide; EDTA, ethylenediamine tetraacetate; ETP_H, electron transfer particle prepared from heavy beef heart mitochondria in the presence of divalent cations; modified ETP_H, electron transfer particle prepared from heavy beef heart mitochondria in the presence of EDTA; P_i, orthophosphate; Tris, tris (hydroxymethyl) aminomethane.

[1] Green, D. E., Plenary Lecture, *Proceedings of the Fifth International Congress of Biochemists*, (London: Pergamon Press, in press).

[2] Webster, G., *Biochem. Biophys. Research Comm.*, **7**, 245 (1962).

[3] Smith, A. L., and M. Hansen, *Biochem. Biophys. Research Comm.*, **8**, 136 (1962).

[4] Pinchot, G., these PROCEEDINGS, **46**, 929 (1960).

[5] Linnane, A. W., and E. B. Titchener, *Biochim. et Biophys. Acta*, **39**, 469 (1960).

[6] Green, D. E., S. Mii, and P. M. Kohout, *J. Biol. Chem.*, **217**, 551 (1955).

[7] Lester, R. L., and A. L. Smith, *Biochim. et Biophys. Acta*, **47**, 475 (1961).
[8] Griffiths, D. E., and D. C. Wharton, *J. Biol. Chem.*, **236**, 1850 (1961).
[9] Basford, R. E., H. D. Tisdale, J. L. Glenn, and D. E. Green, *Biochim. et Biophys. Acta*, **24**, 108 (1957).
[10] Green, D. E., in *Enzymes: Units of Biological Structure and Function* (New York: Academic Press, 1956).
[11] Smith, A. L., M. Hansen, and G. Webster, unpublished observations.
[12] Khym, J. X., and W. E. Cohn, *J. Am. Chem. Soc.*, **75**, 1153 (1953).
[13] Bandurski, R. S., and B. Axelrod, *J. Biol. Chem.*, **193**, 405 (1951).
[14] Martin, J. B., and D. M. Doty, *Anal. Chem.*, **21**, 965 (1947).
[15] Cooper, C., T. M. Devlin, and A. L. Lehninger, *Biochim. et Biophys. Acta*, **18**, 159 (1955).
[16] Ziegler, D. M., R. L. Lester, and D. E. Green, *Biochim. et Biophys. Acta*, **21**, 80 (1956).
[17] Kielley, W. W., and J. R. Bronk, *Biochim. et Biophys. Acta*, **23**, 448 (1957).
[18] McMurray, W., G. F. Maley, and H. Lardy, *J. Biol. Chem.*, **230**, 219 (1958).
[19] Linnane, A. W., and D. M. Ziegler, *Biochim. et Biophys. Acta*, **29**, 630 (1958).
[20] Linnane, A. W., *Biochim. et Biophys. Acta*, **30**, 221 (1958).
[21] Pinchot, G., and M. Hormanski, *Fed. Proc.*, **21**, 54 (1962).

SEPARATION OF THE LIGHT AND DARK REACTIONS IN ELECTRON TRANSFER DURING PHOTOSYNTHESIS

BY F. R. WHATLEY, K. TAGAWA, AND DANIEL I. ARNON*

DEPARTMENT OF CELL PHYSIOLOGY, UNIVERSITY OF CALIFORNIA, BERKELEY

Communicated December 26, 1962

Ever since the discovery of oxygen production by green plants, almost two hundred years ago,[1] a continuing objective of research in photosynthesis has been the chemical isolation of the first stable molecular species that is formed by trapping and converting radiant energy into chemical energy. Based on chemical isolation alone, the first physiological, stable products formed at the expense of radiant energy were identified as starch about a hundred years ago,[2] as phosphoglyceric acid twelve years ago,[3] as $TPNH_2$† eleven years ago,[4–6] and as ATP eight years ago.[7] In 1957 ATP formation was found to be coupled to TPN reduction[8] and these two compounds, ATP and $TPNH_2$, jointly called assimilatory power, were put forward as the first stable chemical products of photosynthesis that are subsequently used to drive the dark reactions of CO_2 assimilation.[9] By fractionating isolated chloroplasts, the photochemical formation of ATP and $TPNH_2$ was separated, in time and space, from the subsequent dark reactions of carbon assimilation in chloroplasts.[9]

This article describes further progress in the separation of the light and dark reactions of photosynthesis. The earliest, chemically isolated, reductant formed at the expense of radiant energy trapped during photosynthesis has now been identified as reduced ferredoxin. These findings stem from the recent subdivision[10] of the TPN reducing system in chloroplasts into two components: (*a*) a flavoprotein enzyme (the TPN reductase proper, now prepared in crystalline form[11]); and (*b*) a nonheme iron-protein electron carrier, one of a family of ferredoxins, members of which have been shown in the last year to be widely distributed in hydrogenase-containing nonphotosynthetic bacteria[12, 13] and also in green plants

and photosynthetic bacteria.[10] (Ferredoxin of chloroplasts is the same substance as the photosynthetic pyridine nucleotide reductase (PPNR) of San Pietro, the haem-reducing factor of Davenport, Hill, and Whatley and the TPN-reducing factor of Arnon, Whatley, and Allen. This change in nomenclature, discussed in more detail elsewhere,[10] is based on the recently discovered chemical and functional similarities of ferredoxins from bacteria and chloroplasts.[10])

The flavoprotein TPN reductase of chloroplasts was shown to catalyze, with the aid of ferredoxin, the reduction of TPN by one of two electron donor systems: by chloroplast fragments (grana) in the light (the physiological system), or by hydrogen gas plus hydrogenase in the dark (an experimental system). Spinach ferredoxin was found[10] to have a redox potential, $E_0' = -432$ mV (pH 7.55), close to that of hydrogen electrode, and is thus capable of transferring to appropriate enzyme systems the most reducing electrons in cellular metabolism: those that come from hydrogen gas or from chlorophyll "activated" by light.

The photoreduction of TPN by illuminated chloroplasts, which is reported here, has been physically separated into two steps: (*a*) a light-induced reduction of ferredoxin by the chloroplast pigment system, followed by (*b*) the *dark* reduction of TPN by reduced ferredoxin—a step that is catalyzed by the TPN reductase present in the chloroplasts.

Methods.—The reactions were carried out in Thunberg-type cuvettes which contained in the optical compartment the chloroplast preparation plus the ferredoxin, and had TPN in the sidearm. The progressive photoreduction of ferredoxin by illuminated chloroplasts was followed by measuring spectral changes with a Cary recording spectrophotometer. After the ferredoxin was reduced by the illuminated chloroplasts, TPN was tipped from the sidearm in the dark and the resultant reoxidation of ferredoxin was measured by the reappearance of its oxidized spectrum. Ferredoxin was prepared as previously described.[10]

Results.—Figure 1 shows a progressive photoreduction of "substrate" amounts of ferredoxin by the illuminated chloroplast preparation, in the absence of TPN. The ferredoxin reduced by light was stable and, under the strictly anaerobic conditions of the experiments, was not spontaneously reoxidized in a subsequent dark period. However, the reduced ferredoxin became quickly and fully reoxidized in the dark when an excess of TPN was added (Fig. 2).

The spectral changes in ferredoxin at 340, 420, and 463 mμ resulting from photoreduction and dark reoxidation by TPN are summarized in Table 1. When the photoreduced ferredoxin was reoxidized by TPN (Table 1, line 3), the increase in optical density at 340 mμ included reduced TPN which absorbs strongly at this wavelength. From this increment it was possible to compute the amount of TPN reduced and to compare it with the amount of ferredoxin reoxidized. The amount of ferredoxin was computed from the changes in optical density at 420 and 463 mμ (Table 1).

The computations show that 1 mole of TPN reoxidized 2 moles of ferredoxin according to equation (1).

$$2\ \text{Ferredoxin}_{red} + \text{TPN}_{oxid} \xrightarrow{\text{flavoprotein}} \text{TPN}_{red} + 2\ \text{Ferredoxin}_{oxid} \qquad (1)$$

Discussion and Conclusions.—The experimental approach used here in isolating and separating the light and dark steps in TPN reduction was similar to that used

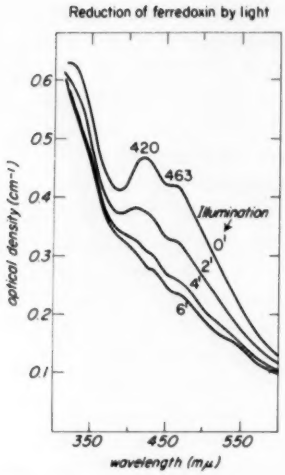

FIG. 1.—Reduction of ferredoxin by light. Spectral changes in oxidized ferredoxin on illumination. Spectral changes were recorded at 2 min intervals as a difference between a sample cuvette containing 1.75 mg (0.125 μmoles) ferredoxin and a reference cuvette without ferredoxin. Both cuvettes contained, in a final volume of 3 ml washed broken chloroplasts (P_{1s2}), heated at 55°C for 5 min, containing 5 μg chlorophyll and the following (μmoles): tris buffer pH 7.3, 100; sodium ascorbate, 10; and 2,6-dichlorophenolindophenol, 0.2. The reaction was carried out in Thunberg-type cuvettes in an atmosphere of argon at 20°C. Illumination was 10,000 lux.

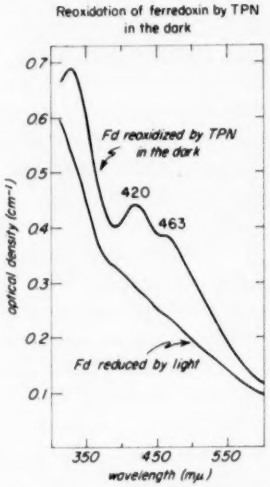

FIG. 2.—Reoxidation of ferredoxin by TPN in the dark. The initial spectrum for photoreduced ferredoxin is that shown at 6′ illumination in Figure 1. The spectrum of ferredoxin reoxidized by TPN in the dark was recorded as the difference between the sample cuvette containing 0.2 μmoles TPN (in 0.05 ml) tipped from the side arm, and the reference cuvette containing the same components except that TPN was replaced by 0.05 ml of water. Spectral change was recorded about 1 min after tipping.

TABLE 1

STOICHIOMETRY OF PHOTOREDUCTION OF SPINACH FERREDOXIN (Fd) AND ITS SUBSEQUENT REOXIDATION BY TRIPHOSPHOPYRIDINE NUCLEOTIDE (TPN) IN THE DARK

(Experimental conditions were as described in Figs. 1 and 2 except that the amount of chlorophyll was changed to 10 μg and that of TPN to 2 μmoles)

	Wavelength (mμ) →	Optical density 340	420	463
1.	Oxidized ferredoxin	0.547	0.434	0.383
2.	Photoreduced ferredoxin	0.461	0.257	0.196
3.	Ferredoxin reoxidized by TPN in the dark	0.644	0.440	0.337
4.	μmoles Fd photoreduced*	...	0.102	0.110
5.	μmoles Fd reoxidized by TPN in the dark*	...	0.106	0.108
6.	μmoles TPN reduced†	0.047		

* The provisional millimolar extinction coefficients for oxidized and reduced spinach ferredoxin (assuming a molecular weight of 14,000) are based on measurements of our purest preparation. Complete reduction was obtained with dithionite. The following values were obtained:

	Oxidized Fd	Reduced Fd	Δε(ox-red)
ϵ_{420} cm^{-1}, mM^{-1}	10.32	5.16	5.16
ϵ_{463} cm^{-1}, mM^{-1}	9.30	4.25	5.05

† The millimolar extinction coefficient used for $TPNH_2$ is $\epsilon_{340} = 6.22$ cm^{-1}, mM^{-1}.

earlier in the separation of the photochemical ATP and $TPNH_2$ formation from the dark CO_2 assimilation reactions in chloroplasts.[9] The photochemical reaction, which is "catalytic" under physiological conditions, has been isolated and transformed into a "substrate" reaction by supplying substrate amounts of the catalyst, and by preventing the product of the photochemical reaction (reduced ferredoxin) from reacting immediately with its normal physiological acceptor, TPN.

In the absence of TPN, reduced ferredoxin is rapidly oxidized by oxygen. It has also been our experience that the accumulation of photochemically reduced ferredoxin proceeds best with a chloroplast preparation that was heated at 55°C for 5 min and thus had lost its capacity for photoproduction of oxygen[14] and for reoxidizing ferredoxin anaerobically, but still retained its ability to use ascorbate as the electron donor for the photoreduction of ferredoxin.

Bleaching by light of photosynthetic pyridine nucleotide reductase (i.e., ferredoxin in our terminology), under apparently aerobic conditions, was observed by Chance and San Pietro (cf. ref. 15) and by Horio and Yamashita.[16] However, the light-induced spectral changes shown by Horio and Yamashita (see curve "L"–"D" in Fig. 2 of ref. 16) do not correspond to the spectrum of reduced ferredoxin (Figs. 1 and 2). Moreover, they report[16] that "the bleached PPNR is not restored to its original color by addition of TPN in darkness immediately after illumination"—a result that is contrary to ours (Fig. 2).

Equation (1) suggests that the photoreduction of ferredoxin occurs by single electron transfer which follows photon capture in the primary photochemical act. Ferredoxin thus replaces TPN as the first isolated electron acceptor in photosynthesis. The transfer of electrons from ferredoxin to TPN is a dark reaction catalyzed by the chloroplast flavoprotein TPN reductase.

The place assigned to ferredoxin in the noncyclic electron transport system of chloroplasts is shown in Figure 3. According to this scheme the photoreduction of ferredoxin would be a prerequisite for noncyclic photophosphorylation but only when it is coupled with TPN reduction. In this sequence of reactions ferredoxin is an electron carrier between the chlorophyll pigment system and TPN. Under nonphysiological conditions, when TPN is replaced by ferricyanide, noncyclic photophosphorylation occurs (in the cytochrome-chlorophyll region[17, 18]) without ferredoxin since the photoreduction of ferricyanide is independent of ferredoxin.

As for cyclic photophosphorylation, we have previously reported[10] that ferredoxin is not required for the nonphysiological type that is catalyzed by phenazine methosulfate. But, as will

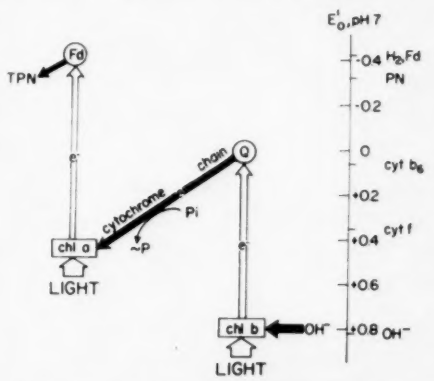

FIG. 3.—Diagrammatic representation of noncyclic electron flow in chloroplasts as a composite of two light reactions and associated dark reactions. The light reactions are indicated by open arrows, the dark reactions by black arrows. OH^- is the electron donor and TPN is the electron acceptor. "Fd" stands for ferredoxin; "Q" tentatively represents plastoquinone. Standard redox potentials of some of the intermediates are indicated on the adjoining redox scale.

be reported elsewhere, ferredoxin is required for physiological cyclic photophosphorylation where it is also a component of the electron transport chain. The involvement of ferredoxin (under the name PPNR) in photosynthetic phosphorylation has also been reported by Black *et al.*[19] and Horio and Yamashita.[16]

To recapitulate, reduced ferredoxin emerges as the most electro-negative, chemically identified substance that has been isolated following the photochemical events of photosynthesis. It is the physiological electron carrier in the reduction of TPN and in photosynthetic phosphorylation, cyclic and noncyclic.

* Aided by grants from the U.S. Public Health Service and the Office of Naval Research.

† Oxidized and reduced triphosphopyridine nucleotide are abbreviated, respectively, TPN and $TPNH_2$; adenosine triphosphate is abbreviated ATP.

[1] Priestley, J., *Experiments and Observations on Different Kinds of Air* (London: J. Johnson, 1777), vol. 3.

[2] Sachs, J., *Lectures on the Physiology of Plants* (Oxford: Clarendon Press, 1887).

[3] Benson, A. A., and M. Calvin, *Ann. Rev. Plant Physiol.*, **1**, 25 (1950).

[4] Vishniac, W., and S. Ochoa, *Nature*, **167**, 768 (1951).

[5] Tolmach, L. J., *Nature*, **167**, 946 (1951).

[6] Arnon, D. I., *Nature*, **167**, 1008 (1951).

[7] Arnon, D. I., M. B. Allen, and F. R. Whatley, *Nature*, **174**, 394 (1954).

[8] Arnon, D. I., F. R. Whatley, and M. B. Allen, *Science*, **127**, 1026 (1958).

[9] Trebst, A. V., H. Y. Tsujimoto, and D. I. Arnon, *Nature*, 182, **351** (1958).

[10] Tagawa, K., and D. I. Arnon, *Nature*, **195**, 537 (1962).

[11] Shin, M., K. Tagawa, and D. I. Arnon, *Fed. Proc.*, **22**, 100 (1963).

[12] Mortenson, L. E., R. C. Valentine, and J. E. Carnahan, *Biochem. Biophys. Res. Comm.*, **7**, 448 (1962).

[13] Valentine, R. C., R. L. Jackson, and R. S. Wolfe, *Biochem. Biophys. Res. Comm.*, **7**, 453 (1962).

[14] Arnon, D. I., and F. R. Whatley, *Arch. Biochem.*, **23**, 141 (1949).

[15] Goodwin, T. W., and O. Lindberg, eds. *Biological Structure and Function* (New York: Academic Press, 1961), vol. 2, p. 453.

[16] Horio, T., and T. Yamashita, *Biochem. Biophys. Res. Comm.*, **9**, 142 (1962).

[17] Arnon, D. I., *Nature*, **184**, 10 (1959).

[18] Arnon, D. I., in *Light and Life*, ed. W. D. McElroy and B. Glass (Baltimore: Johns Hopkins Press, 1961), p. 489.

[19] Black, C. C., C. A. Fewson, M. Gibbs, D. L. Keister, and A. San Pietro, *Fed. Proc.*, **21**, 398 (1962).

---

*INTERACTION OF GENOTYPES DETERMINING VIABILITY IN DROSOPHILA BUSCKII**

BY R. C. LEWONTIN AND YOSHIRO MATSUO†

DEPARTMENT OF BIOLOGY, UNIVERSITY OF ROCHESTER, NEW YORK

Communicated by Theodosius Dobzhansky, December 12, 1962

It is well known that the relative fitnesses of genotypes in a population are influenced by the physical factors of the environment. There is an increasing body of experimental evidence to show that the biotic components of the environment, especially the density and genotypic composition of the population, also may have effects on relative fitness. The literature on the effect of larval density on viabil-

ity in *Drosophila* is quite extensive.[1-5] The result of these experiments was that the relative viabilities of competing genotypes vary with density and that, in general, very high densities exaggerate differences between genotypes. Less work has been done, however, on the interesting question of how relative frequencies of different genotypes may affect the fitnesses. There is some indirect evidence that fitnesses of inversion types may be a function of frequency in natural populations.[6] In laboratory populations, there is clear evidence of changes in relative fitness of inversion with changing frequency.[7, 8] A specific test of whether genotypes may interact to give fitnesses not predictable from their performance in pure culture was made by Lewontin[1] and the lack of predictability was confirmed in those experiments.

This previous experiment was designed to survey a large number of genotypes to look for the phenomena of interaction. No genotype was really well studied, however. Of particular interest is the question of whether there are any regularities in the interaction between genotypes. The experiments reported in this paper are designed to take a closer look at interaction in a few genotypes by using a greater range of densities and a greater variety of mixture proportions than in previous experiments. In this way a norm of reaction for viability can be described with respect to two components of biotic environment: density and proportion.

Experimental Methods and Design.—Newly hatched first instar larvae varying in age from 1 to 7 hr were collected and placed in 25 mm × 45 mm shell vials containing 4 cc of Krivshenko's medium. This medium is made up in the following proportions: 1000 cc water, 10 gm agar, 80 gm corn meal, 50 gm dry brewers yeast, 100 gm white Karo sirup, and 6 gm linseed meal. No live yeast was added to the vials.

Five stocks of *D. busckii* were used. These were Acme-A (a wild-type stock) and four mutant strains white (w), claret (cl), cut (ct) and yellow (y). The experiments consisted in testing the viability of each mutant strain in pure culture and in various mixed proportions with the wild-type strain. The design for each of the mutant series was the same. The densities used were 2, 8, 32, 128, 256, and 512 *total* larvae per vial. At each *total* density the following series of mixtures were used: 100% Acme; 75% Acme: 25% mutant; 50% Acme:50% mutant; 25% Acme:75% mutant; 100% mutant. At a total density of 2 larvae only the pure cultures and the 50:50 mixture were possible.

The number of replicates for each density is given in Table 1. Because of the large size of the experiment it was not possible to make up all densities and all mixtures of a given mutant series on the same day. One fifth of all replicates of a given mutant series were made up on a given day. That is 5, 2, 2, 1, 1, and 1 vials respectively of the increasing densities were made up and this was repeated 5 times to make up the full set.

Emerging adults were counted and classified every day and the vials were kept until four successive days yielded no flies. The temperature was 25°C throughout.

Results of the Experiments.—The results are summarized in Figures 1, 2, 3, and 4. In each figure, part A shows the survival of the wild type, Acme-A, at each density for each of the mixture combinations. Part B of each figure shows the survival of the mutant. There are absolute, not relative survival proportions.

General effect of density: Every experiment shows the same general norm of reac-

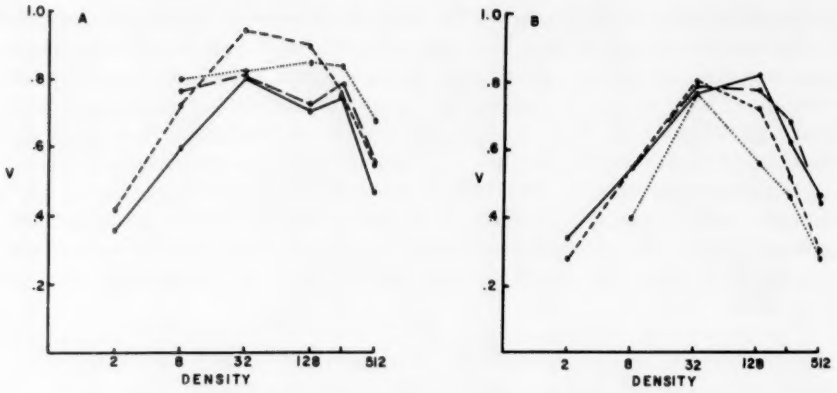

FIG. 1.—Absolute viabilities of Acme-A and *white*. A. solid line: 100% Acme; long dashes: 75% Acme; short dashes: 50% Acme; dots: 25% Acme. B. solid line: 100% *white*; long dashes: 75% *white;* short dashes: 50% *white;* dots: 25% *white*.

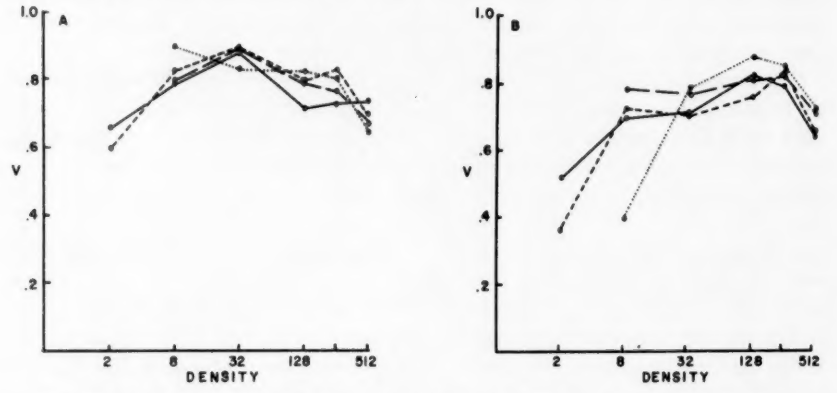

FIG. 2.—Absolute viabilities of Acme-A and *claret*. See Figure 1 for meaning of lines.

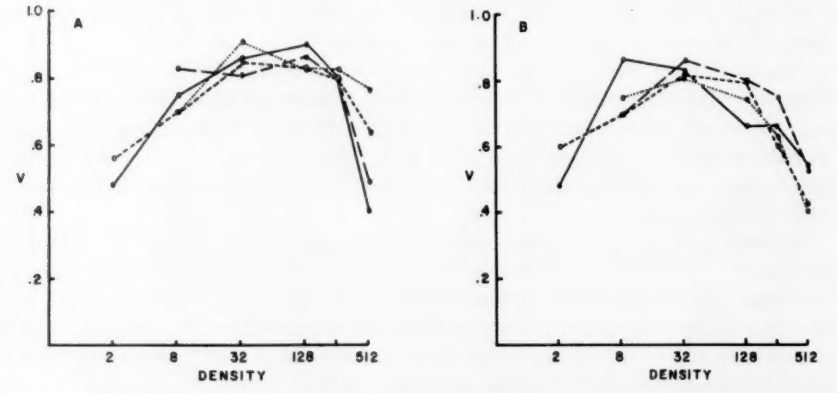

FIG. 3.—Absolute viabilities of Acme-A and *cut*. See Figure 1 for meaning of lines.

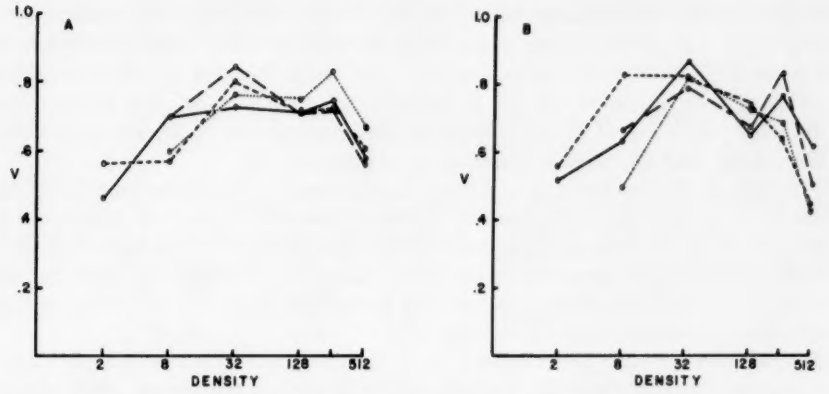

FIG. 4.—Absolute viabilities of Acme-A and *yellow*. See Figure 1 for meaning of lines.

TABLE 1

NUMBERS OF REPLICATES AND TOTAL NUMBERS OF LARVAE TESTED IN EACH MIXTURE AT DIFFERENT DENSITIES

Total density	Replicate vials per mixture	No. of mixtures	Total vials	Total larvae tested
2	25	3	75	150
8	10	5	50	400
32	10	5	50	1600
128	5	5	25	3200
256	5	5	25	6400
512	5	5	25	12800

tion of survival with respect to density. All the curves are concave downward with a peak of viability at intermediate densities. Both high and low densities result in lower survival. The mutant *claret* (Fig. 2) shows an optimum density shifted toward the high end, between 128 and 256 larvae per vial and an extremely low viability at low densities. The mutant *cut* (Fig. 3) is at the other extreme with an optimum density between 8 and 32 larvae per vial. Acme-A, *yellow* and *white* are intermediate between these two extreme types, but in all cases both high and low densities are deleterious. Thus, we have a very clear confirmation of the observations of Lewontin.[1] It has been pointed out[3] that the undercrowding effect in these earlier experiments may have been due to conditioning of the food for yeast growth by the action of the larvae since live yeast was used. It must be that the "cooperative" action of the larvae in the present experiments lies elsewhere than in conditioning the food for yeast growth, since no live yeast is added.

General effect of varying composition: The next question is whether the absolute viability of each mutant and Acme-A is altered at a given density by the presence of a different genotype in the same vial. From Figure 1*a* it is clear that the viability of *white* is lower at most densities when competing with Acme-A (broken lines) than it is in pure culture (solid line). The reverse is true for Acme-A (Fig. 1*b*). Here a mixture with *white* increases the viability of Acme-A. The increase in Acme-A viability in mixture is more consistent than the decrease in *white* viability. Sixteen out of sixteen mixed viabilities of Acme were greater than or equal to the pure viability at the comparable density. In the case of *white*, only eleven out of

sixteen values were lowered by mixture. On the other hand the viabilities of *white* show a kind of consistency lacking in the case of Acme. The viability curve for the 25% *white*: 75% Acme-A mixture lies below that for the 50:50 mixture, which in turn lies below the 75:25 mixture. The 75:25 mixture is not different from the pure *white* (Fig. 1*b*). Thus, as the proportion of white larvae increases, the absolute viability of *white* increases in a regular fashion.

In both the *yellow* series (Fig. 4) and the *claret* series (Fig. 2) the viability of Acme-A is generally shifted upward in mixtures from the viability of pure Acme-A, but this is not as striking or consistent as in the *white* series. In neither of these series is the mutant genotype consistently changed in viability by mixture. Finally, in the *cut* series there is no apparent general effect of composition on viability of either mutant or Acme-A genotypes.

Interaction of density and composition: It is, unfortunately, a very difficult matter to test statistically either the general effect of density or the general effect of composition in these experiments. This is because, by the very nature of the experiments, the replication variance of each determination is different. The replication variance at a density of 2 larvae per vial is on the average 20 times that for the highest density, 512 larvae per vial.

This difficulty of testing is not really a serious one in judging the results of the general effects of density and composition. The effect of density as seen in the previous section is so consistent, that there is not the slightest doubt of its reality. When we turn to the general effects of composition, there is no consistency over all experiments, but certain patterns are so clear as to leave no doubt as to their reality. In the *white* series, for example, there can be no doubt of the consistency of the general effect of composition on the viability of both mutant and wild-type genotypes. For the other mutants, there is no obvious general effect. What is possible, however, is to examine the effect of composition *within* each density and to test the reality of any observed differences by a conventional analysis of variance. For example, at a density of 512 larvae per vial both the *cut* genotype and the Acme-A genotype are affected by mixture (Fig. 3). The same applies to the *claret* series (Fig. 2) while for the *yellow* series only the mutant is consistently affected at the density of 512.

The result of tests for the effect of mixture on viability are shown in Table 2. The table gives the F values resulting from a series of one-factor analyses of variance testing whether the variation observed among the viabilities of different mixtures *within* each density is significantly greater than the variation among replicate vials. The upper figure of each pair refers to the viability of Acme-A in the series, the lower figure to the viabilities of mutants. Out of the 48 F values, 11 correspond to a probability of 5% or less, and 26 F values are greater than unity. Of the 11 significant F tests, 5 are at the density of 512 larvae per vial. Looked at in another way, at densities of 256 and 512, 15 out of 16 tests gave F values greater than unity and, of these, 7 were significant at the 5% level or better. All this points to the fact that there is a real effect of composition at the higher densities while there is none apparent at the lower densities by the criterion of the analysis of variance. The analysis is not very powerful at lower densities, however. Low densities have, *ipso facto*, a very large replication variance which makes detection of composition effects very difficult. For example, it is obvious that in the *white* series mixed

cultures were *consistently* different in viability of Acme-A from pure cultures at the lowest densities as well as the highest (Fig. 1*a*).

TABLE 2

F RATIOS FROM ANALYSES OF VARIANCE TESTING THE SIGNIFICANCE OF VARIATION IN VIABILITY DUE TO MIXTURE PROPORTIONS

Series		Density 2	8	32	128	256	512
White	A	0.240	1.080	2.445*	1.088	1.597	3.958‡
	w	0.274	0.547	0.171	4.140‡	2.781*	3.097†
Claret	A	0.244	0.809	0.452	0.685	1.645	1.042
	cl	1.535	2.453*	0.593	0.567	2.411*	1.392
Cut	A	0.663	0.654	2.369*	1.000	0.081	10.302‡
	ct	1.822	0.889	0.354	0.276	1.420	2.359*
Yellow	A	0.622	0.474	1.235	0.039	1.702	1.232
	y	0.092	1.512	0.404	0.171	1.656	3.846‡

* Prob ≅ 0.05.
† Prob ≅ 0.025.
‡ Prob ≅ 0.01.

In summary, then, at high densities there is a clear effect of mixture proportion on the viability of both components of the mixture; while at low densities there is a clear dependence in some cases, as in the *white* series, but the evidence is equivocal for other mutant series.

Relative Viabilities.—The real interest of these experiments is not in the absolute viabilities of the genotypes but in their relative viabilities.

For example, Figure 2 shows that, in pure culture at a density of 512 larvae per vial, Acme-A has a higher absolute viability (0.741) than *claret* (0.652). But all of the mixed cultures show a depression of Acme-A and an increase in *claret* to the extent that *claret* actually has a higher viability than Acme-A when these genotypes are in direct competition. The results of such comparisons for all the mutant series are shown in Figures 5, 6, 7, and 8. The heavy solid line, in each case, is the *predicted* relative viability of Acme-A calculated as the absolute viability of Acme-A in pure culture divided by the absolute viability of the mutant in pure culture. The broken lines show the *observed* relative viabilities of Acme-A calculated from the vials in which the two genotypes were actually in competition.

The most striking case is that of the *white* series (Fig. 5). The predicted relative viabilities of Acme-A show no particular trend with density and on the average over densities Acme-A has a slight predicted advantage ($\bar{V} = 1.038$). In actual competition, however, Acme-A was far superior to *white* and this superiority changed in a regular way with density and composition. At both high and low densities, Acme-A is far better in competition with *white* than was predicted from pure culture experiments, while at intermediate density, especially at 32 larvae per vial, the prediction and observation agree fairly closely. Moreover, at the three highest densities, the order of relative viabilities corresponds to the proportion of Acme-A in the mixture. Below the density of 32, however, the relationship is not consistent, although the 75% Acme-A mixture remains the best. It is interesting that this U-shaped curve of viability against density has its minimum at 32 larvae per vial which is the optimum density for survival of both Acme-A and *white*. That is, the relative viability curves are the inverse of the absolute viability curves.

The other mutant series show less dramatic but related phenomena. The *claret* series (Fig. 6) shows a downward slope of predicted relative viability with

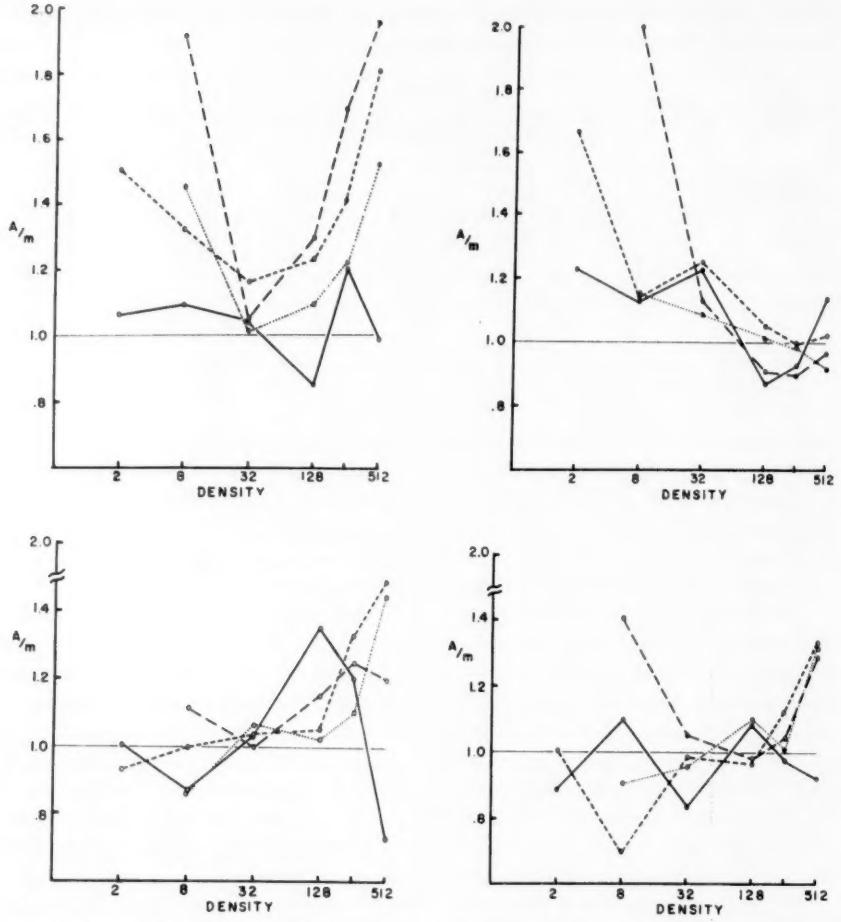

FIGS. 5–8.—*Solid lines:* predicted viability from pure cultures. *Long dashes:* observed viability in 75% Acme cultures. *Short dashes:* observed viability in 50% Acme cultures. *Dots:* observed viability in 25% Acme cultures.

density. The observed curves agree with the predicted curve except at the two lowest densities where Acme-A performs much better than predicted, while at the highest density the relative viabilities of Acme-A and *claret* are reversed by mixture. Again the deviation from prediction is most marked at an extreme, non-optimum density.

While the *claret* series shows the left limb of the *white* series U-shaped relationship, the *cut* series (Fig. 7) shows the right limb of this relation. Here, agreement with prediction from pure culture is again at a density of 32 and the only real deviation is at 512 larvae per vial.

Implications of the results: The supposition that one can predict the relative viabilities of genotypes from their absolute viabilities in pure culture is really a

supposition that there is no interaction between these genotypes in exploiting the resources; that is, that they are biologically independent of each other.

One kind of interaction is a result of direct interference of one genotype with another. In this case the viability of one genotype will decrease while that of the other either remains the same or increases. All of our cases of interaction are of this sort. What is particularly important is whether it is possible to predict from the results of pure culture experiments which will be the stronger competitor in such an interaction. In this case we expect the general form of the curve relating viability to density to be the same in all mixtures. This is the case for the *claret* series. It is as if one genotype were more efficient in using the resources available than another; this difference in efficiency shows up more clearly when the two genotypes are in active competition for the resource than when there is only intra-group competition.

The other three mutant series, however, show interactions that are not at all predictable from pure culture performance. Both *yellow* and *cut* series show a complete reversal of the relative predicted fitness in active competition at high densities. *White* shows no reversal but the unexpected appearance of drastic viability differences where no difference at all would have been predicted.

The general implications of these findings are several. First, it is not possible to make general statements about the relative viabilities of genotypes from a knowledge of those viabilities at a particular density of composition. However, predictability is reasonably good at *optimal* densities. Second, from a population genetic standpoint, the relative fitnesses of genotypes change as the frequencies of these genotypes change so that the course of natural selection cannot be predicted without a knowledge of the full norm of reaction of the genotypes with respect to density and composition.

Finally, from the evolutionary standpoint, such interactions as seen at high densities in the *cut* and *yellow* series raise the question of the relation between population fitness and genotype fitness. Since Acme-A in pure culture has a lower viability than the mutants in pure culture, a population of pure Acme-A is in some sense not as fit as a population of pure mutant individuals. At least the load of larval death is greater. Nevertheless, the presence of Acme-A and mutants in the same population results in a dramatic increase in Acme-A viability above that of the mutants. As a result the mutants will be eliminated. We then have the paradox that a population will evolve toward a lower *absolute* fitness, even though the value of intra-population fitness, $\overline{W}$, seems to be increasing. Thus, natural selection does not assure that the fitness of the population, as a whole, will be increased.

Summary.—The larval viability of four mutant strains and one wild-type strain of *Drosophila busckii* were tested over a range of densities and proportional mixtures of wild-type and mutant. Densities ranged from 2 to 512 larvae per vial and mixtures consisted of 100% mutant; 75% mutant; 25% wild type; 50%:50%, 25%:75% and 100% wild-type. The results were: (1) For all strains the highest viability is at an intermediate density, not at the lowest. (2) For a given density, especially at high density, the proportion of the two genotypes in the mixture was important in determining viability. (3) Relative viabilities observed in mixtures agreed with predicted viabilities from pure cultures at intermediate (optional den-

sities) but deviated strongly at high and low densities. (4) The genotype with higher viability in pure culture often had lower viability in mixed culture. The implication of this last observation is that the absolute fitness of a population may not have any relation to the direction of genetic change in that population, and that the population may evolve to a lower state of absolute fitness.

* This research was supported by Grant RG-6222 from the Division of Research Grants of the National Institutes of Health.

† Training Grant Fellow supported by National Institutes of Health Training Grant to the Department of Biology, University of Rochester.

[1] Lewontin, R. C., *Evolution*, **9**, 27–41 (1955).
[2] Birch, L. C., *Evolution*, **9**, 389–399 (1955).
[3] Boggild, O., and J. Keiding, *Oikos*, **9**, 1–21 (1958).
[4] Bakker, K., *Arch. Neerl. de Zool.*, **14**, 200–281 (1961).
[5] Moree, R., and J. R. King, *Genetics*, **46**, 1735–1752 (1961).
[6] Lewontin, R. C., and M. J. D. White, *Evolution*, **14**, 116–129 (1960).
[7] Levene, H., O. Pavlovsky, and Th. Dobzhansky, *Evolution*, **8**, 335–349 (1954)
[8] Spiess, E. B., *Evolution*, **11**, 84–93 (1957).

INFORMATION TO CONTRIBUTORS

THE PROCEEDINGS OF THE NATIONAL ACADEMY OF SCIENCES publishes promptly brief first announcements of the results of original research by members of the Academy or others. Articles are limited to 8 printed pages and no author may have more than 8 pages altogether in any one issue. Wherever practicable, results should be made clear without elaborate technical details; figures, tables, and formulae should be kept as simple as possible.

MANUSCRIPTS should be in the form of current numbers of the PROCEEDINGS, typewritten in duplicate with double spacing, the author retaining one copy, and addressed to THE PROCEEDINGS OF THE NATIONAL ACADEMY OF SCIENCES, 2101 Constitution Avenue, Washington 25, D. C. They will be accepted only from the members of the Academy who will assume responsibility for their propriety and scientific standards and for any printing costs in excess of those allowed them by the Academy.

GALLEY PROOF will be sent; as authors' corrections are charged to them, typewritten manuscripts should be letter-perfect. Original art work or figures will be returned if requested when the manuscript is submitted. Because of the time limitations, page proofs will not be sent. Reprints should be ordered when proof is returned on the reprint form enclosed therewith; they will be furnished at cost.

CONTENTS

Page

CHEMISTRY.—MECHANISM UNDERLYING THE EQUILIBRIUM REACTIONS BETWEEN IONS AND ION-PAIRS IN SOLUTIONS OF ELECTROLYTES, II. THE EFFECT OF TEMPERATURE . . . . . *By Lawrence C. Kenausis, E. Charles Evers, and Charles A. Kraus* 141

CHEMISTRY.—USE OF AN ULTRAMICROTOME FOR THE PREPARATION OF THIN SECTIONS OF SINGLE CRYSTALS FOR ABSORPTION SPECTROSCOPY . . . . . *By Robert F. Stewart and Norman Davidson* 146

GENETICS.—CHANGES IN MOLECULAR WEIGHT OF DNA ACCOMPANYING MUTATIONS IN PHAGE . . . . . *By Elizabeth Burgi* 151

GENETICS.—APPARENT CYTOPLASMIC STERILITY IN *Drosophila paulistorum* . *By Lee Ehrman* 155

GEOLOGY.—A DISCUSSION AND PROPOSALS CONCERNING FOSSIL DINOFLAGELLATES, HYSTRICHOSPHERES, AND ACRITARCHS, I . . . . . *By William R. Evitt* 158

MICROBIOLOGY.—THE PROGRAMMING OF HERPES VIRUS MULTIPLICATION IN DOUBLY-INFECTED AND IN PUROMYCIN-TREATED CELLS . . . . . *By Bernard Roizman* 165

MICROBIOLOGY.—STEPS IN THE NEOPLASTIC TRANSFORMATION OF HAMSTER EMBRYO CELLS BY POLYOMA VIRUS. . . . . *By Marguerite Vogt and Renato Dulbecco* 171

PHYSICS.—SPIN $^1/_2$ WAVE EQUATION IN DE-SITTER SPACE . *By F. Gürsey and T. D. Lee* 179

PHYSIOLOGY.—THE RELATIONSHIP OF BODY SIZE, NERVE CELL SIZE, AXON LENGTH, AND GLIAL DENSITY IN THE CEREBELLUM . . . . . *By Reinhard L. Friede* 187

PHYSIOLOGY.—FINE STRUCTURAL CHANGES IN HEART MUSCLE IN RELATION TO THE LENGTH-TENSION CURVE . . . . . *By E. H. Sonnenblick, D. Spiro, and T. S. Cottrell* 193

MATHEMATICS.—LYAPUNOV FUNCTIONS FOR THE PROBLEM OF LUR'E IN AUTOMATIC CONTROL . . . . . *By R. E. Kalman* 201

MATHEMATICS.—REGULARITY AT THE BOUNDARY OF THE $\bar{\partial}$-NEUMANN PROBLEM . . . . . *By J. J. Kohn* 206

MATHEMATICS.—ON THEORIES CATEGORICAL IN UNCOUNTABLE POWERS . *By Michael Morley* 213

MATHEMATICS.—BOUNDS OF ANALYTICAL FUNCTIONS OF TWO COMPLEX VARIABLES IN DOMAINS WITH THE BERGMAN-ŠILOV BOUNDARY . . . . . *By J. Śladkowska* 217

BIOCHEMISTRY.—THE EFFECT OF EXOGENOUS RNA AND DNA ON AMINO ACID INCORPORATION BY SUBCELLULAR FRACTIONS PREPARED FROM ERYTHROID TISSUES . . . . . *By Siegmund Fischer, Gail P. Bruns, Bertram A. Lowy, and Irving M. London* 219

BIOCHEMISTRY.—BASIS OF ACTINOMYCIN ACTION, II. EFFECT OF ACTINOMYCIN ON THE NUCLEOSIDE TRIPHOSPHATE-INORGANIC PYROPHOSPHATE EXCHANGE . . . . . *By I. H. Goldberg, M. Rabinowitz, and E. Reich* 226

BIOCHEMISTRY.—ON THE CHEMISTRY OF THE THYMUS GLAND . . . . . *By Andrew Hegyeli, Jane A. McLaughlin, and Albert Szent-Györgyi* 230

BIOCHEMISTRY.—GENESIS OF MITOCHONDRIA IN *Neurospora crassa* . . *By David J. L. Luck* 233

BIOCHEMISTRY.—DEMONSTRATION OF AN UNSTABLE RNA AND OF A PRECURSOR TO RIBOSOMAL RNA IN HeLa CELLS . *By Klaus Scherrer, Harriet Latham, and James E. Darnell* 240

BIOCHEMISTRY.—TRANSFER OF CHLOROPHYLL EXCITATION ENERGY IN GREEN PHOTOSYNTHETIC BACTERIA . . . . . *By Christiaan Sybesma and John M. Olson* 248

BIOCHEMISTRY.—AN IMIDAZOLE PUMP MODEL OF ELECTRON TRANSPORT . . . . . *By Dan W. Urry and Henry Eyring* 253

BIOCHEMISTRY.—INTERMEDIATE REACTIONS IN THE PHOSPHORYLATION COUPLED TO THE OXIDATION OF REDUCED CYTOCHROME *C* . . . . . *By George Webster, Archie L. Smith, and Marc Hansen* 259

BIOCHEMISTRY.—SEPARATION OF THE LIGHT AND DARK REACTIONS IN ELECTRON TRANSFER DURING PHOTOSYNTHESIS . . . . *By F. R. Whatley, K. Tagawa, and Daniel I. Arnon* 266

BIOCHEMISTRY.—INTERACTIONS OF GENOTYPES DETERMINING VIABILITY IN *Drosophila busckii* . . . . . *By R. C. Lewontin and Yoshiro Matsuo* 270